power spectral density function, representing the rocking response of the freight car, is then minimized using optimization techniques for an appropriate choice of the stiffness and damping elements. In all the cases considered, a practical solution to the freight car rocking problem can be recommended either by a choice of optimum suspension elements for a given vehicle or by introducing additional suspension elements with optimal parameters. Numerical results are given for a 100-ton freight car often used in service in North American rail transportation.

ACKNOWLEDGEMENTS

The author is deeply indebted to his supervisor, Dr. T.S. Sankar, for his continued guidance and encouragement throughout the course of this investigation.

The author is grateful to Miss L. Mikhail for her sincere effort in typing the manuscript.

Thanks are due to the Computer Centre at Concordia University and the staff of the Analog Laboratory of the National Research Council in Ottawa for their cooperation.

The financial support provided by the Department of Mechanical Engineering of Concordia University and the National Research Council is gratefully acknowledged.

Finally, the author would like to express his appreciation of the devotion and understanding of his wife, Nawal, during the course of this undertaking.

TABLE OF CONTENTS

LIST OF FIGURES

LIST OF TABLES

NOMENCLATURE

$\underset{\sim}{a}$	lower bound of the design variables defined as the suspension parameters
b_1	location of the car centre of gravity above the centre plate
b_2	location of the car centre of gravity above the side bearings
$\underset{\sim}{b}$	upper bound of the design variables defined as the suspension parameters.
$\underset{\sim}{b}(t)$	input forcing function in a vector form
C_1	location of the bolster centre of gravity below the centre plate
C_2	location of the bolster centre of gravity below the side bearings
C_c	viscous damping coefficient for the car
C_t	viscous damping coefficient for the truck
d	radius of the centre plate
e	distance from the king pin to the side bearings
f	distance from the king pin to the centre of the spring groups
g	gravitational acceleration
$\underset{\sim}{g}(\dot{\underset{\sim}{y}},\underset{\sim}{z})$	nonlinear forces vector (Chapter 7)
$\underset{\sim}{g}_1(\dot{\underset{\sim}{y}})$	nonlinear friction damper forces for the SCM (Chapter 7)
$\underset{\sim}{g}_2(\underset{\sim}{z})$	nonlinear spring forces for the SCM (Chapter 7)
h	distance from the bolster centre of gravity to the centre of friction shoes
n	number of independent generalized coordinates
q_i	the independent generalized coordinates of the system
$\underset{\sim}{q}$	state variable vector
r_1	wheel radius
r_2	distance between the bolster centre of gravity and wheel axle centre of gravity

s_1	sign of the truck friction force, right
s_2	sign of the truck friction force, left
s_3	sign of the car friction force, rotational
s_4	sign of the truck friction force in truck, lateral
$\underset{\sim}{u}$	filtered white noise input vector
$\underset{\sim}{y}$	friction damper displacement vector for the SCM (Chapter 7)
z_i	nonlinear spring displacements
$\underset{\sim}{z}$	nonlinear spring displacement for the SCM (Chapter 7)
$\underset{\sim}{A}^*$	a transformation matrix with constant coefficients
$\underset{\sim}{A}_F$	the system matrix corresponding to the filter equations
$\underset{\sim}{A}_V$	the equivalent linear system matrix for the vehicle
$\underset{\sim}{A}_0$	the overall system matrix (filter + vehicle)
$\underset{\sim}{B}_F$	the associated system matrix for the filter
$\underset{\sim}{B}_V$	the associated equivalent linear system matrix for the vehicle
$\underset{\sim}{B}_0$	the associated overall system matrix (filter + vehicle)
$\underset{\sim}{C}$	viscous damping matrix for the SCM (Chapter 7)
$\underset{\sim}{C}$	viscous damping matrix for the MCM (Chapter 4)
D_L	the car viscous damper force, left
D_R	the car viscous damper force, right
$\underset{\sim}{D}$	the input covariance matrix
$E[\ ]$	ensemble averaging
$\underset{\sim}{E}$	a transformation matrix with constant coefficients
F_c	friction damping force on the car
F_t	the friction damping force on truck
$F_k(z_k)$	nonlinear spring forces

$\underset{\sim}{F}_1$	a transformation matrix with constant coefficients
$\underset{\sim}{F}_c$	vector of constant gravitational forces in the MCM (Chapter 4)
$\underset{\sim}{G}$	constant forces vector in the MCM (Chapter 4)
H_1	distance of top of the side bearing above the rail
I_c	mass moment of inertia of the car
I_t	mass moment of inertia of the truck
I_w	mass moment of inertia of the wheelset
$\underset{\sim}{I}$	unit matrix
K	truck vertical spring constant
K_b	side bearing equivalent stiffness
K_G	gib stops equivalent stiffness
K_h	truck horizontal stiffness
K_p	centre plate equivalent stiffness
K_r	track equivalent stiffness, vertical
K_{pL}	centre plate equivalent stiffness, horizontal
K_{rL}	track equivalent stiffness, horizontal
$\underset{\sim}{K}$	stiffness matrix for the SCM (Chapter 7)
$\underset{\sim}{\hat{K}}$	stiffness matrix for the MCM (Chapter 4)
L_1	vertical centre plate force on extreme, right
L_2	vertical centre plate force on extreme, left
L_3	vertical side bearing force, right
L_4	vertical side bearing force, left
L_5	horizontal centre plate or side bearing force
MCM	the multiconfiguration model
M_c	mass of the car body

M_t	mass of the truck
M_w	mass of the wheelset
$\underset{\sim}{M}$	mass matrix for the SCM (Chapter 7)
$\underset{\sim}{M}$	mass matrix for the MCM (Chapter 4)
P_h	horizontal truck force
P_L	vertical truck force, left
P_R	vertical truck force, right
$\underset{\sim}{P}$	instantaneous covariance matrix of the response
$\underset{\sim}{Q}$	modified input-covariance matrix
$\underset{\sim}{R_h}$	horizontal wheelset force
R_L	vertical wheelset force, left
R_R	vertical wheelset force, right
SCM	the single configuration model
$S(\omega)$	power spectral density with appropriate subscript to denote particular cases
$S_k(z_k)$	nonlinearity terms associated with nonlinear spring forces $F_k(z_k)$
$S_{i_k}(\dot{y}_k, z_k)$	one of the nonlinear forces acting along the direction of the generalized coordinate X_i due to the velocity and displacement $\dot{y}_k$ and z_k of the nonlinear element k
W	weight of the two trucks excluding bolster
W_B	track gauge measured as Y_R-Y_L
$\underset{\sim}{W}$	input white noise vector
$\underset{\sim}{X}$	generalized coordinate vector
Y	track alignment measured as $(Y_R+Y_L)/2$
Y_c	lateral displacement of the car centre of gravity
Y_L	left rail profile in lateral direction
Y_R	right rail profile in lateral direction

Y_t	lateral displacement of the truck centre of gravity
Y_w	lateral displacement of the wheelset centre of gravity
$\underset{\sim}{Y}^{(1)}$	the nonlinear friction damping forces in the MCM (Chapter 4)
Z_c	vertical displacement of the car centre of gravity
Z_L	amplitude of the left rail profile as vertical displacement
Z_R	amplitude of the right rail profile as vertical displacement
Z_t	vertical displacement of the truck centre of gravity
Z_v	vertical track irregularities measured as $(Z_R+Z_L)/2$
Z_w	vertical displacement of the wheelset centre of gravity
Z_{cr}	track cross level measured as $(Z_R-Z_L)/2$
$\underset{\sim}{Z}$	design variables defined as the suspension parameters
ε	side bearing clearance
ε_G	gib clearance
θ_c	rotation of the car body
θ_t	rotation of the truck
θ_w	rotation of the wheelset
$\underset{\sim}{\eta}$	equivalent stiffness matrix
$\underset{\sim}{\Upsilon}$	equivalent damping matrix
$\underset{\sim}{\psi}$	state vector of the overall linear filter representing cross level, vertical and alignment inputs.

Dot above a letter indicates differentiation with respect to time.

CHAPTER 1

INTRODUCTION AND LITERATURE REVIEW

CHAPTER 1

INTRODUCTION AND LITERATURE REVIEW

1.1 General

Rail transportation systems provide a dependable, economical and comparatively rapid movement of all types of commodities especially those which fall under bulk freight class as well as other large volume shipping. Also the rail transportation system serves a useful purpose in the area of passenger movement. Railway industry is expected to play an increasingly important role in future, especially because of the severe energy limitation that is presently facing the world. During the past several years, a growing effort has been mounted to develop design concepts including analytical solutions, computer simulations, experimental data and operating strategies which will improve the performance of the mass transportation for now and for the future.

The introduction of new concepts in the design of suspension especially for large capacity freight cars in the railroad industry has not been without problems. Large capacity railroad freight vehicles when operating at low speeds, especially in the range of 10 to 25 mph (16.09 - 40.2 km/hr) are found to have a tendency to derail, as dramatically illustrated in Figs. 1.1 and 1.2, and these derailments are associated particularly with excessive rocking vibrations. The source of the input excitations to these vehicles, essentially arising from the wheel-rail relative motions, can be

Fig. 1.1: Derailed Freight Car During Canadian National Railway Test Study.

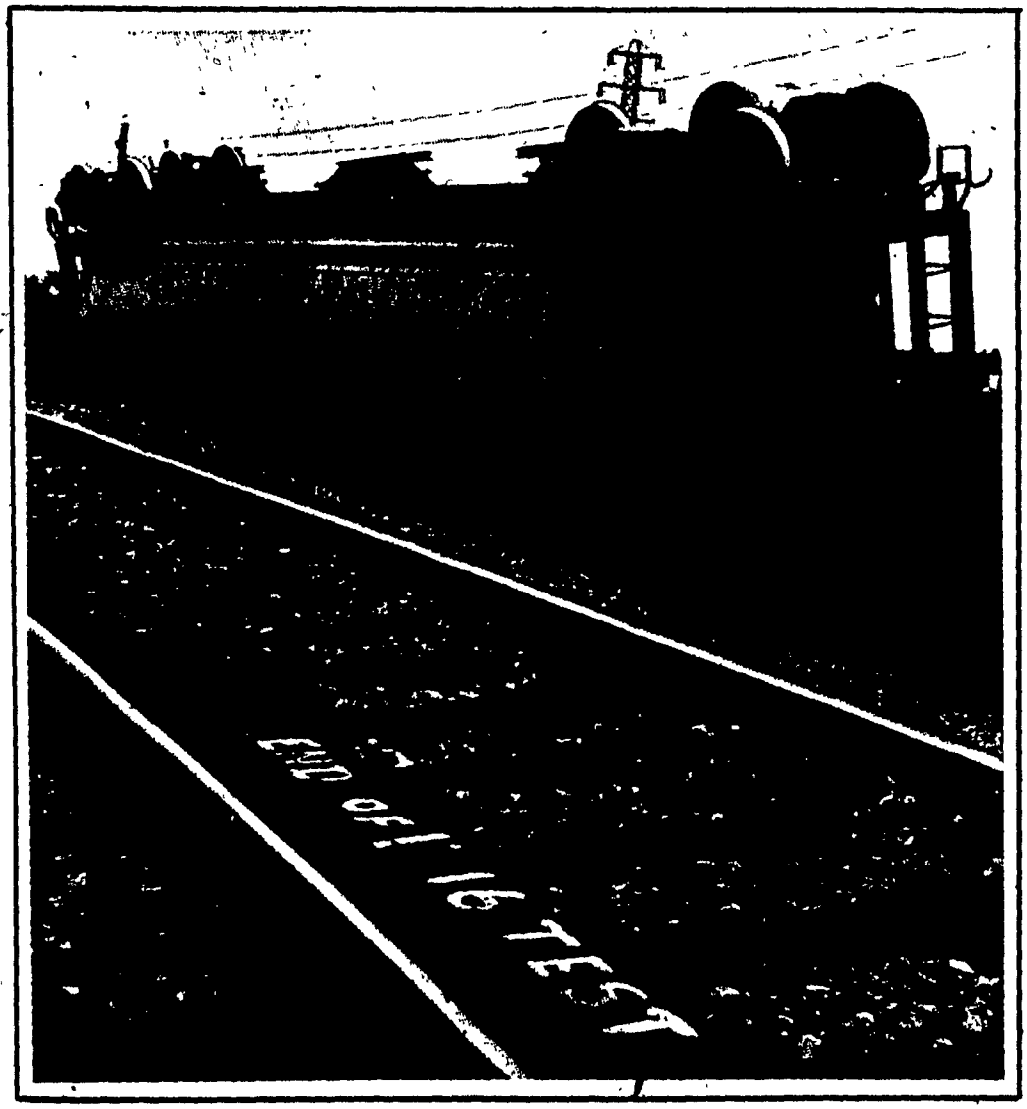

Fig. 1.2: Derailed Freight Car During Canadian National Railway Test Study. Another View.

classified as periodic when resulting purely from staggered rail joints, and additionally, nonperiodic or stochastic when resulting primarily from other random irregularities of the track. Severe car rocking produces excessive wheel-track dynamic forces, as much as two to three times the nominal static force levels, and also causes very high car body-bolster forces approaching three times the normal static levels. These large dynamic forces occurring during severe rocking resonance conditions lead to gradual degradation of both track and equipment performance over a period of time and thus directly influence vehicle operation and safety.

In this investigation, analytical techniques are employed for the determination of the dynamic responses of the rail vehicle and it is attempted to show how a solution to the derailing problem can be achieved by limiting the amplitude of the rocking motion within tolerable limits under service conditions. Such a control on the rocking vibrations of the vehicle can be implemented through appropriate modifications to the design specification of the entire suspension system.

1.2 Literature Review

Previous investigations in rail dynamic research include a diversity of subjects concerning the analytical and experimental determination of the dynamic responses of rail track structure [1,2,3], the wheel rail interface [4,5,6] car or truck stability and vehicle dynamics [7,8,9,10]. Since excessive rocking of freight

cars is a part of the recorded research in the field of vehicle dynamics, detailed literature review for the related experimental and analytical investigations in that area is given in the following Subsection 1.2.1. Review of the available multivariable optimization techniques as applied to the design of mechanical systems in general as well as to rail vehicle suspension in particular are described in Subsection 1.2.2. Finally, the study of the vehicle responses when subjected to stochastic excitation from the track demands a review of the few available techniques for solving nonlinear systems subjected to random inputs and this is given in Subsection 1.2.3.

1.2.1 Previous Investigations on the Rocking Problem

As early as 1926, the problem of excessive rocking of 70 ton hopper cars, which were at that time considered to be of high capacity, was encountered by Leffler [11]. In this paper the relation between car rocking and the rail-joint stagger is discussed along with a theoretical treatment and possible remedies to minimize excessive rocking of such high centre of gravity cars. Later, experimental field investigations were carried out by Pullman-Standard [12], American Association of Railroad (AAR) [13], Stuki Company [14,15], Canadian National Railways (CN) [16,17] and Southern Railway [18] with the objective of preventing 100 ton hopper cars from frequent derailing. The following four important dynamic phenomena can be summarized from these test results:

i) When travelling at certain low range of speeds, cars with

given truck centres 39.5 feet (12.04 m) will rock violently enough to lift the wheel off the tangent as well as curved tracks. That is, the track curvature does not affect significantly the rocking response of the vehicle.

ii) The cars described above in (i) will rock singly or as a series of cars. That is, rocking is independent of car to car coupling.

iii) When excessive rocking is taking place and if the train is slowed down, the amplitude of rocking tends to increase momentarily. This phenomenon will be later illustrated through the mathematical model developed in this investigation.

iv) Remedies such as long travel springs with additional damping, introduction of truck lateral motion, decreasing the side bearing distance by a certain amount etc, all tend to increase stability of the system. This will also be illustrated analytically through the mathematical model adopted.

A linear three dimensional model of a freight car was investigated by Manos and Shang [11]. The model is used for predicting the basic responses of rail vehicles due to track inputs. The rail inputs to this model are obtained using a graphical technique which shows the rail disturbances as a function of the truck-centre distance for any desired rail length, wheel base, track profile, and rail stagger. The simplified linear equations of motion suggested in this work can only be used for determining the car body rock or

roll frequency and its dependence on the roll amplitude. Such linear models are found not too reliable especially for describing the dynamic behavior of the vehicle that is associated with severe rocking conditions. During this rocking motion, the vehicle system nonlinearities arising from large vibratory motions cause separation of the car body from the centre plate and the wheels from the rails. Liepins [19] proposed the first nonlinear model for such problems. The only nonlinearity in the model proposed is due to the effect of separation of body from the centre plate and subsequent contact with side bearings and also the suspension friction damping effects. However, other important nonlinearities due to wheel lift, gib stops contact and spring bottoming are neglected in this work [19]. The type of input function used in the simulation solution given is not clearly defined in this paper, but it seems to be taken from previous experimental measurements on the track irregularities specified as a function of time. Mecham and Ahlbeck [20] studied a similar nonlinear model under periodic excitation and discussed the dynamic loads due to wheel-rail interactions and the manner in which the various parameters of the track structure affect these loads and the resulting stresses. However, this study does not emphasize the reasons for the nonlinearities proposed in the mathematical model and further does not describe the sensitivity of the vehicle responses to variation in the parameters of the suspension system, and consequently does not propose any design solutions to the vehicle rocking problem. Also a number of simplified mathematical models have been investigated

at Massachussetts Institute of Technology [21,22] assuming the vehicle to be either two or three degrees-of-freedom excited by periodic rail input without considering gib contact, bolster and wheelset inertias. These models are specifically investigated for the amount and duration of wheel lift and the values of the maximum loading exerted on the vehicle as a function of the vehicle speed. The effects of the suspension parameters on these loading conditions and on the overall vehicle responses are not investigated in this study.

Work at the AAR [13] and Illinois Institute of Technology [23], describe development of extremely complicated digital computer simulation programs to obtain the rocking responses in the time domain under cross-level track variations. These models and others [24,25] represent a high degree of modeling details and complexities and require evaluation of up 20 to 30 degrees-of-freedom system under harmonic or other periodic excitations. Because an accurate mathematical modeling of a complete railroad freight vehicle, allowing each mass for six degrees-of-freedom and including all nonlinearities, poses a formidable computer simulation problem, it is advisable for reasons of practicality to seek compromise solutions using slightly simpler model formulations. Therefore, emphasis will have to be on some reduction in the degrees-of-freedom of the system models appropriate to the specific dynamic performance under study. Nine degrees-of-freedom nonlinear planar model is utilized in the present investigation to describe all the main modes including the rocking

mode of vibration of the vehicle. The model proposed places only a reasonable demand on digital computer time and on the analog computer components needed to obtain simulation solution for the system equations of motion, consequently allowing for the implementation of appropriate optimization techniques to search for a practical solution to the rocking problem. A review of the optimization techniques applicable to the design of the rail car suspension systems are given in the following subsection.

1.2.2 Suspension Optimization

A survey of a few illustrative examples of the use of optimization techniques in the design of mechanical system is given by Seireg [26]. The cases discussed include gears, bearings, other machine dynamic elements, rotating discs, pressure vessels, shafts under bending and torsion, and problems of elastic contact and load distribution in an overall mechanical system. In the area of optimum design of the vibratory systems one of the earliest problems investigated is the optimum design of the dynamic absorbers for vibrating equipment. Den Hartog [27] gave functional relations for the absorber parameters which minimize the response of the main mass when subjected to simple sinusoidal excitation. Seireg and Howard [28] utilized a computer optimization technique to determine the absorber parameters which minimize the mean square response of the main mass when subjected to white noise or delta-correlated random excitation. Among other studies in design and optimization of multi degrees-of-freedom linear shock isolation systems in the literature include those of

Libre and Sevin [29], McMunn [30], and others [31-34]. Kemper [35] proposed means for finding optimum damping in nonlinear systems subjected to shock loads. This attempt to locate the near optimum damping parameters seem to have been done manually through plotting of the response curves for various combinations of the system as well as input parameters. McMunn [30] developed a more formal optimization technique for obtaining the multi-parameter optimum damping which minimizes the maximum of all the possible resonant responses for a linear dynamical system. Examples in this work include two discrete systems with three and five degrees-of-freedom with two and three dampers respectively and also the case of a continuous uniform column. Elmaraghy et al., [32] applied methods of multivariable optimization to a linear model of a locomotive to find the minimax response of the system in a critical frequency range of practical interest. Hedrick et al., [36] optimized vertical and lateral linear suspension systems of a high speed vehicle subjected to guide way and aerodynamic inputs. A topic which is not sufficiently discussed in the literature is that of minimizing the maximum dynamic response of nonlinear mathematical models representing railroad freight vehicles by appropriate adjustment of the vehicle damping (viscous and friction types) and the spring rates. The minimax principle together with available search algorithms [37,38] for multivariable optimization are utilized here to evaluate the optimum design variables for an existing freight vehicle suspension system or for specifying additional energy dissipation devices to be installed to reduce the risk of

derailing. The objective function, in this case, is the maximum car rocking response over the critical frequency range of interest and this objective function is minimized for the cases when the vehicle is subjected to inputs that are, purely periodic or a combination of periodic and random, generated from the rail track. Review of the previous investigations for identifying the two types of input processes due to track irregularities, the techniques for modeling these irregularities in a functional form, and the available closed form and numerical techniques that can be adopted to solve the non-linear vehicle system when subjected to such stochastic type of inputs are given in the following subsection.

1.2.3 Stochastic Excitation on the Nonlinear Freight Car System

Previous investigations [39,40] describe two distinct forms of track irregularities, in each homogeneous segment of rails, namely, a deterministic periodic input process and a stationary random input process. Power spectral density is an important statistical measurement technique well suited for describing both these types of irregularities. Though previous investigations have considered the excitation to the rail vehicle system only to be purely periodic, the study of the problem under both periodic and random irregularities is essential for a complete investigation in order to evaluate the contribution of each type of these irregularities to the dynamic response of the system. However, there are no previous studies, analytical or experimental, dealing with the dynamic response of freight vehicles under stochastic excitations from the track. The approaches

developed in this investigation for the solution of such problems considering both types of excitation utilizing the proposed stochastic nonlinear model is general enough for application to other nonlinear multi degrees-of-freedom mechanical systems subjected to similar type of random excitations. Examples of these applications vary from future high speed passenger vehicles (200-300 mph or 321.8-482.7 km/hr) under aerodynamic forces and guideway irregularities to machine tool systems excited by random cutting forces [41,42] and high rise buildings subjected to strong earthquake ground motions.

In the solution of a nonlinear system under periodic type deterministic input processes, methods of numerical integrations are often utilized [43,44]. However, the solution of a nonlinear stochastic model under previously mentioned types of excitations, represented in the form of filtered white noise power spectral density, requires an entirely different approach. The few available techniques to solve a multi degrees-of-freedom nonlinear systems under Gaussian white noise input are discussed in [45,46]. The first technique utilizes the stationary Fokker-Planck equation [47,48] which can be solved for the transitional probability density of the system responses. The main advantage of the Fokker Planck method over all others is that theoretically excact solutions may be obtained when the excitations are in the form of a Gaussian white noise. Unfortunately, the versatility of this approach is limited because of the severe restrictions that must be placed on the form of the nonlinearities present in the differential equation and on the spectral density matrix of

the excitation process. Since an exact solution giving the response probability is available only for limited statidnary cases, several other approximate approaches have been devised. Normal mode approach originated by Caughey [49] involves computational difficulties while the perturbation method first developed by Crandall [50] can be applied to dynamic systems having only weak nonlinearities and not to the problem under investigation here.

The statistical linearization technique [51,52,53] is found to be the best suited method for the present problem and therefore it is utilized in a modified form suitable for cases where the stochastic forcing function appears as nonlinear force vectors in the governing equations. The statistical linearization approach has been shown to generate acceptable solutions [52] even for systems with fairly strong nonlinearities. This method is essentially based on the idea of defining an equivalent linear system by minimizing certain measurable difference between the original nonlinear system and the equivalent linear system. Analytical procedures for obtaining the instantaneous correlation matrix for the response of the equivalent system are described in [54,55]. Generally, the solution requires an excessive amount of algebraic computation since it involves an inversion of $n^2 x n^2$ matrix when there exist n state variables for the system. A numerical technique developed by Davison and Man [56] and successfully used in [36] to solve a Liapunov system of equation is employed in this investigation to minimize the computer time and storage.

1.3 Scope of the Present Investigation

In this investigation, in addition to a general investigation of the transient and steady state dynamic responses of the freight car system, multivariable optimization techniques are employed to find the optimum suspension parameters of a modified nonlinear model of the freight vehicle. The optimum suspension elements are determined with an objective to minimize the maximum rocking response in the critical frequency range when the vehicle is under either periodic or a combination of periodic and random excitations from the track.

The mathematical models proposed in this investigation are constructed in such a way to describe the rock, sway and bounce modes of the car body, bolsters and wheelsets and also to account for most of the system nonlinearity effects. The equations of motion of the deterministic and stochastic models are solved by digital integration and/or by analog simulation for the state variables representing the system response. The deterministically computed responses are compared with the test data reported by the Canadian National Railways [16,17] for establishing validity of the model employed.

A study of the sensitivity of the system response to variation in the value of any one individual parameter is carried out to determine the near optimum suspension parameters which will minimize the amplitude of the car rocking response. This detailed study provides a valuable insight on the influence of each individual

suspension element on the reduction in rocking angle but does not yield an overall practical solution as to the optimal set of suspension parameters. Therefore, two different multivariable optimization approaches are used for determining the set of design parameters for the suspension system that minimizes an objective function representing the maximum rocking amplitude. Results obtained from the optimization procedures showed the existence of different local minima for the chosen objective function. Hence, for any particular choice of the optimization technique, the associated feasible region and the design variables, multiple solutions for the suspension parameters are obtained. From these results the designer can choose the optimum values for an existing suspension system or install additional energy dissipation devices with optimum values to produce minimum rocking.

In Chapter 2, the different physical models for representing the railroad freight vehicle are described after defining the purpose of each of the main components of the vehicle and the possible modes of vibrations of the system. The major assumptions and limitations of the model together with the sources of the system nonlinearities are discussed. Two distinct mathematical models are constructed to represent accurately the bounce, sway and rocking modes of vibration of the freight car. They are:

i) A multiconfiguration model utilized for obtaining a numerical solution on a digital computer to yield the transient response under periodic input from the track, and

ii) A single configuration model which is used for determining the analog solution giving the steady state response of the system and later when stochastic input forcing function is considered.

In Chapter 3, the types of excitation acting on the freight vehicle from the track irregularities are described. A Fourrier series is utilized for describing the periodic input process generated due to the segmented nature of the rails. Power spectral density in the form of a filtered white noise is used for specifying both periodic and random types of track excitation. This excitation spectral density is modeled as the output of a linear filter with a white noise input. The dynamic state equations of the filter are derived for solving the system response under stochastic input.

Chapter 4 describes the solution of the multiconfiguration deterministic model under periodic excitation. The equations of motion are developed using the Lagrange's technique. Transient responses are obtained using a numerical integration technique on a digital computer. Steady state responses using a single configuration model and using analog computer simulation are given in Chapter 5. The time responses obtained are utilized in examining the validity of the proposed models by comparing the numerical results with the experimental data obtained by the Canadian National Railways.

In Chapter 6 the frequency response information from the previous chapter is utilized to carry out a complete parametric sensitivity study. Some useful results are obtained from this

effort, however it showed that the solution to the problem requires further investigation through multivariable optimization techniques to determine the optimum set of suspension parameters. These parameters are evaluated to minimize the maximum transient response of the freight car rocking in the critical frequency range of interest.

In Chapter 7, the available methods for solving a strongly nonlinear system under random excitations are reviewed and the statistical linearization approach is found to be the appropriate technique for the problem under investigation. A scheme is described for solving the stochastic freight car model to evaluate the mean square value and power spectral density of the response process. Parametric study and multivariable optimization approaches are applied in Chapter 8 to the stochastic problem to minimize the maximum power spectral density of the rocking response. Finally, a discussion of the results, conclusions and recommendations for future work are presented in Chapter 9.

CHAPTER 2

THE PHYSICAL MODEL OF THE RAILROAD FREIGHT CAR

CHAPTER 2

THE PHYSICAL MODEL OF THE RAILROAD FREIGHT CAR

In this chapter, idealized models are formulated for a large capacity railroad freight vehicle. The essential features of the models are based on the proper representation of those major components of the vehicle which influence the system's dynamic response. The physical models are developed through identification of the mechanical characteristics of these major components by different idealized elements such as masses, springs and damping elements. Two ways of modeling the strong nonlinearities present in the system are formulated. The physical models developed describe the required dynamic responses of the system in a consistent manner when subjected to the identified input process. These models have either multi-configurations or a single configuration representations and each of them is chosen on the basis of the individual model's convenience in its application to derive the required type of responses. The system responses obtained through these models are used for illustrating certain dynamic phenomena which have not been previously identified and also to evaluate and optimize the parameters of the suspension system that yield a minimum rocking response.

2.1 Main Elements of the Vehicle

A typical railroad freight vehicle consists of two trucks and a car body. The car body has a high centre of gravity and is thus prone to severe rocking and bounce responses at vehicle critical

speeds. The trucks consist of two wheelsets, two side frames with springs and friction dampers; a typical truck configuration is shown in Fig. 2.1. The car body sits on the two bolsters (one on each truck) at a centre plate location. In this manner, a swivel movement can take place between the bolster and the car body. The main mechanical properties of the actual vehicle components and the corresponding idealized elements are described in detail in Table 2.1 for easy comparison. An improved physical representation of the system, described in Fig. 2.2, is now proposed to include adequately all the important dynamic characteristics of a large capacity railroad freight vehicle.

As the vehicle travels on the track, input excitations due to wheel-rail interactions produce vertical and lateral displacements of the right set of wheels with respect to the left wheels. The types of excitations on the system, essentially arising from such wheel-track relative motion, can be modeled either as purely periodic or random or a combination of periodic and random processes. These types of wheel-track excitation are discussed in detail in Chapter 3. The input displacements are transmitted through the suspension springs to the bolster and, in turn, through the centre plate and side bearings to the car body and can cause sway, bounce and rocking responses in the car system. Since rocking mode of vibration has been identified as a major phenomenon leading to derailment, three levels of rocking amplitude may be identified in terms of the importance of their magnitude.

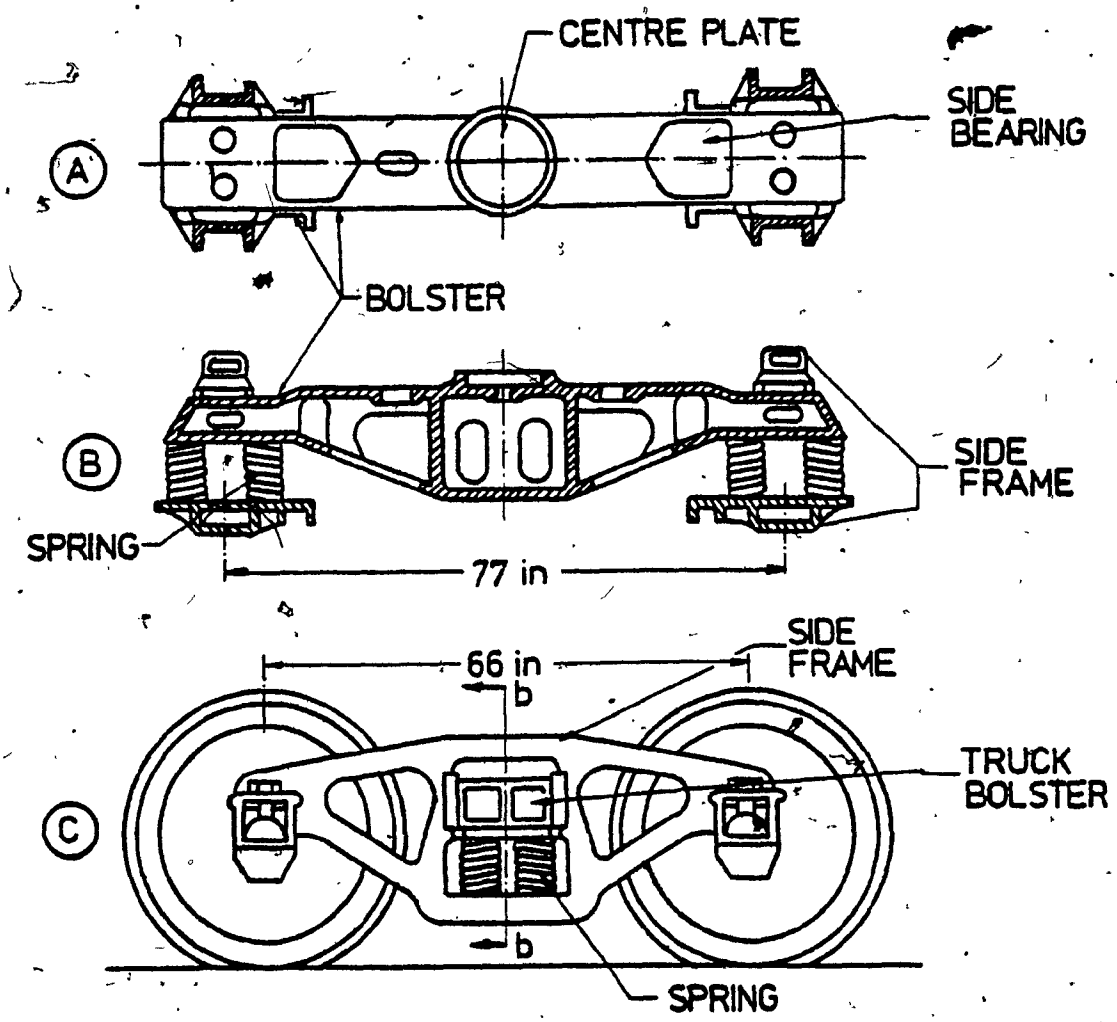

Fig. 2.1: Typical Double Truss Truck.

No.	Components of the Freight Car	Idealized Representation in the Model
1	Mass and mass moment of inertia of the car body	Represented by M_c, I_c respectively of a rigid body
2	Mass and mass moment of inertia of the two truck bolster systems	Represented by M_t, I_t respectively of a rigid body
3	Mass and mass moment of inertia of the wheelsets	Represented by M_w, I_w respectively of a rigid body
4	Vertical action of the truck suspension springs	Represented by two vertical springs each with stiffness K
5	Horizontal action of the truck suspension springs	Represented by a horizontal spring with stiffness K_h
6	The four friction shoes acting on the truck	Represented by vertical and horizontal friction dampers having friction forces F_t
7	Inherent structural damping present on the truck and other additional viscous damping devices	Represented by a pair of equivalent viscous dampers with a coefficient C_t
8	Stabilizing device composed of friction damper and shock absorber	Represented by a friction force F_c and viscous damping C_c acting between the car body and the side frames

Table 2.1: Comparison of Mechanical Properties of the Suspension Elements.

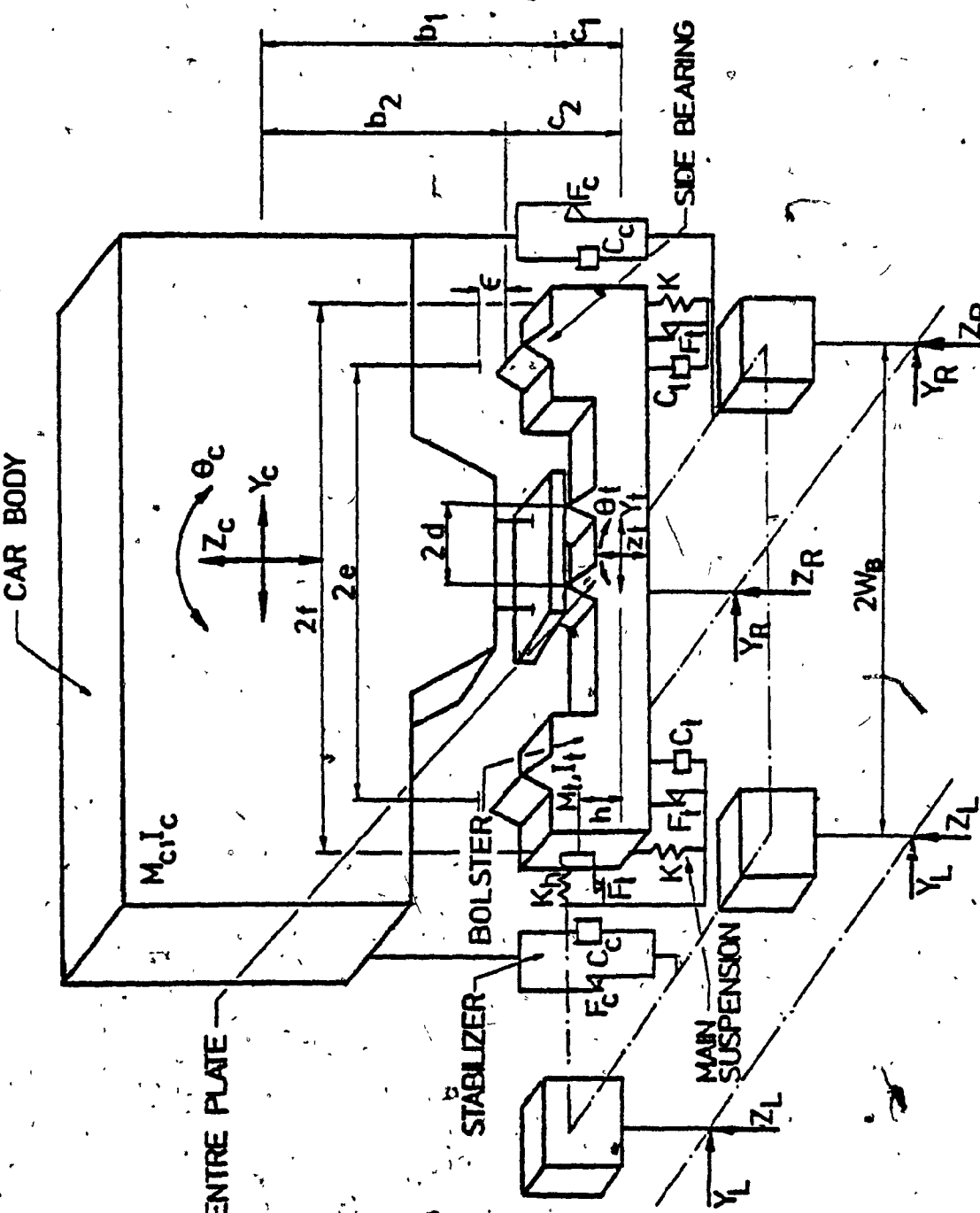

Fig. 2.2: Physical Model of a Railroad Freight Vehicle.

a) Light rocking when the wheels remain on and follow the tracks and the car body remains on the centre plate with no side bearing contact. This is shown as configurations 1, 2a, and 2b in Fig. 2.3(a).

b) Moderate rocking during when the car body rocks and makes contact with the side bearings but remains in contact with the centre plate. As the car body rocks onto push the side bearings, the bolster can move laterally into the gib stops. This is described as configurations 3a and 3b in Fig. 2.3(b).

c) Severe rocking when the car body rocks completely out of contact with the centre plate and forced onto the side bearings and drives the bolster into the gib stops. This can be seen from configurations 4a and 4b in Fig. 2.3(c). In this mode the wheel-track and the car body-bolster dynamic forces reach two to three times the nominal static force levels associated with the occurrence of large rocking angles approaching ±5 degrees and significant wheel lift from the rails. These large displacements and impact forces degrade both the track and the equipment performance and dramatically influence the freight car operation and safety.

To obtain the complete response characteristics in all the modes of vehicle vibration, a formulation of an accurate nonlinear model is required. Linear models [12] cannot predict accurately the dynamic behavior when dominant nonlinearities are present due to the car separation from the centre plate, contact with side bearings, wheel lift and gib stop contacts during moderate and

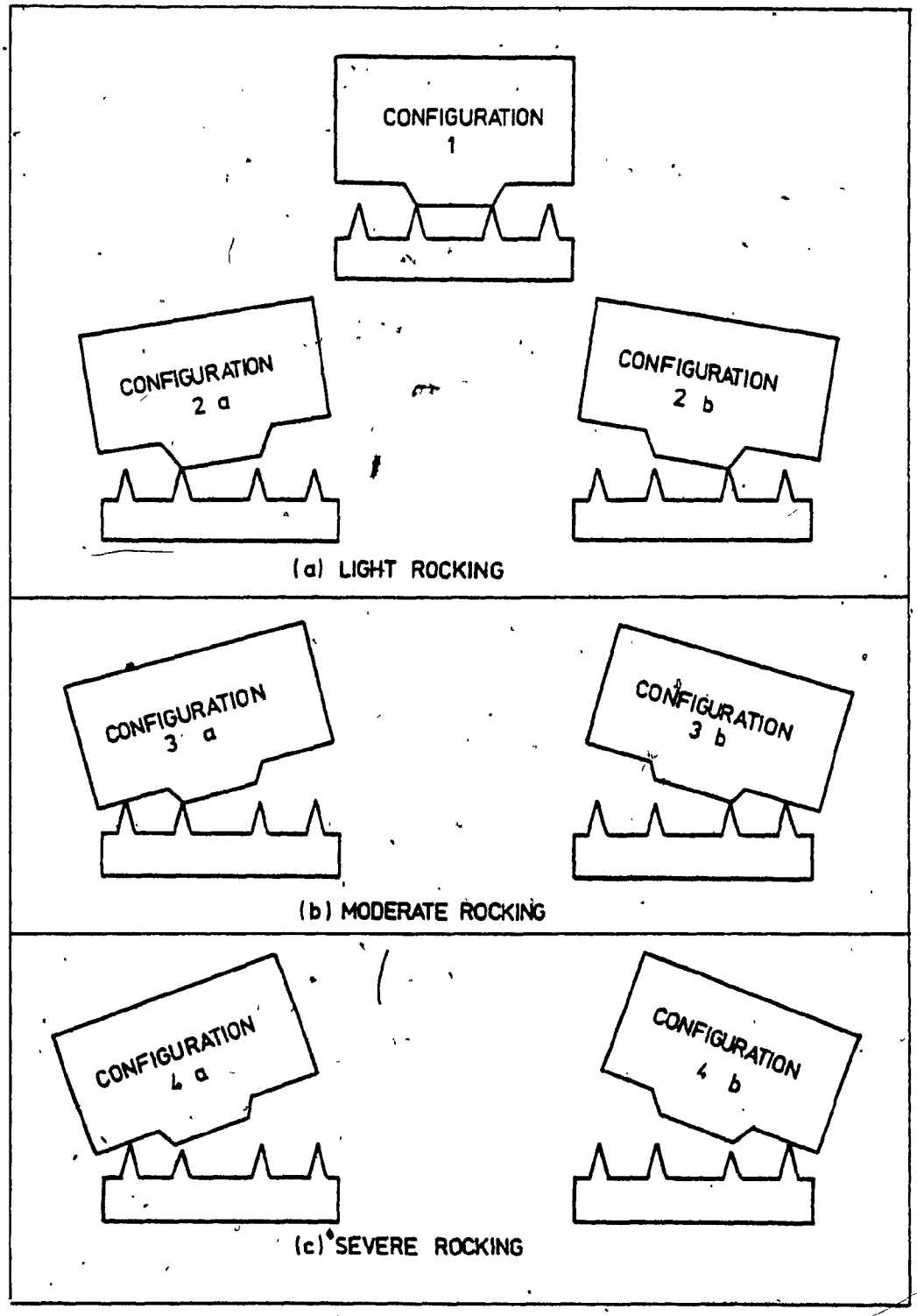

Fig. 2.3: The Model Configurations During Different Levels of Rocking.

severe rocking conditions. The proposed models, described in Fig. 2.4(a) and (b), representing the vehicle dynamics, take into consideration most of the nonlinearity effects present in the vehicle. The diagram describes two ways of modeling the system nonlinearities so that a choice of the model is available based on the suitability of the application. The multiconfiguration model, shown in Fig. 2.4(a), assumes that the nonlinearities produce different configurations, as discussed earlier in Fig. 2.3, which the vehicle can take depending on the severity of rocking. This model is found to be more efficient in solving for the vehicle transient responses on a digital computer when subjected to periodic excitations from the track. On the other hand, the single configuration model, shown in Fig. 2.4(b), describes these nonlinear separation effects using approximate bilinear stiffness elements having special properties described in a graphical form in Fig. 2.5. This model is found to be convenient for evaluating steady-state responses of the vehicle system on an analog computer and also for solving for the probabilistic response when stochastic excitation is considered.

The important vehicle nonlinearities included in the models may be summarized as follows:

i) The geometric nonlinearities: These result from the separation of car body from the centre plate with or without contact of the car on the side bearings. These nonlinearities are included in the multiconfiguration model (MCM) through the

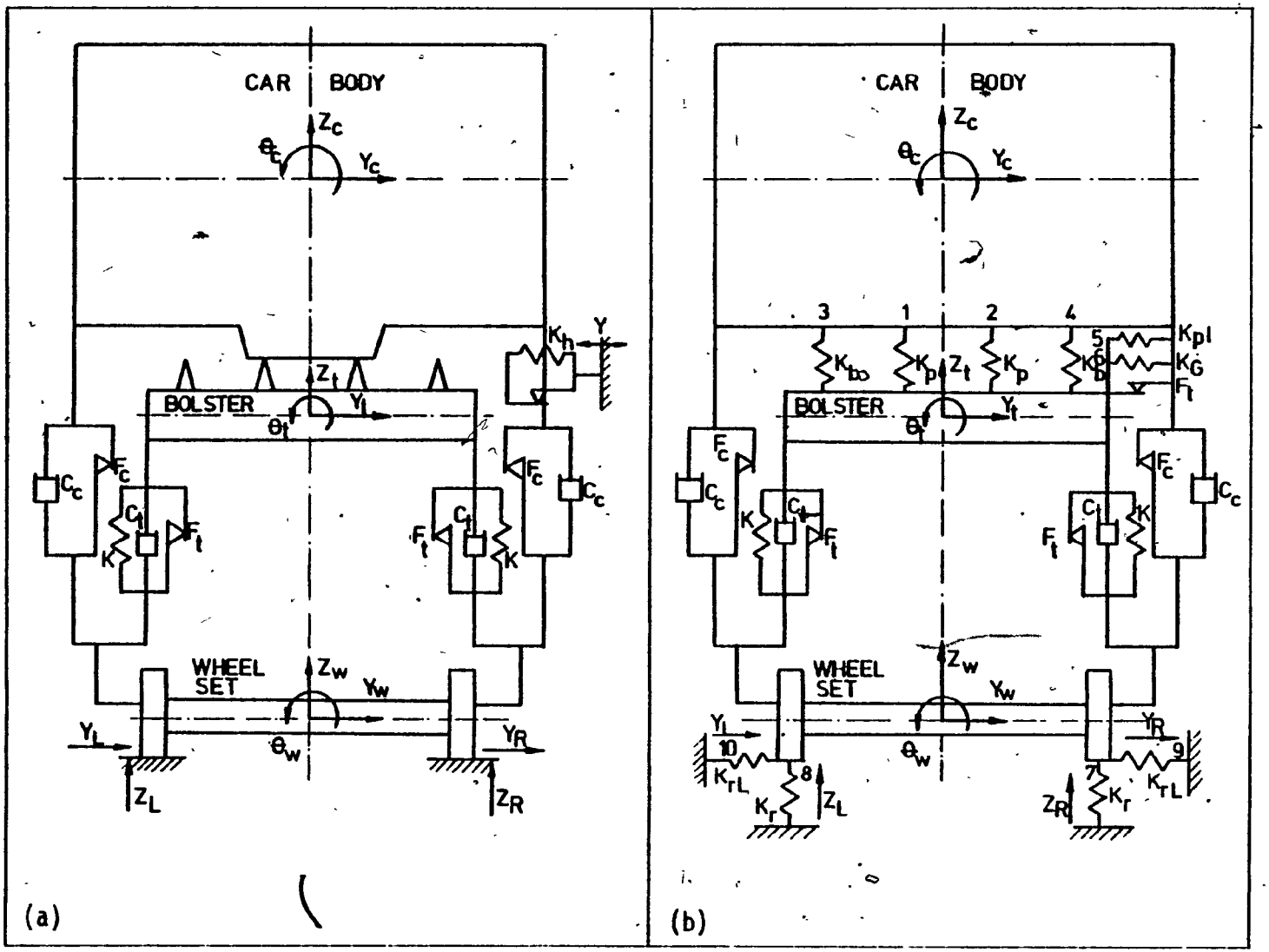

Fig. 2.4: (a) Multiconfiguration Model (MCM). (b) Single Configuration Model (SCM).

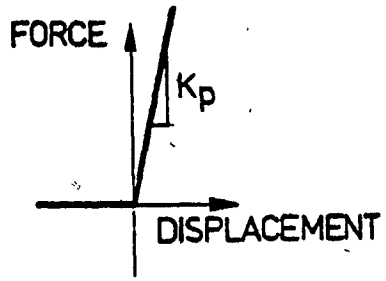

(a) CENTRE PLATE
SPRINGS # 1,2

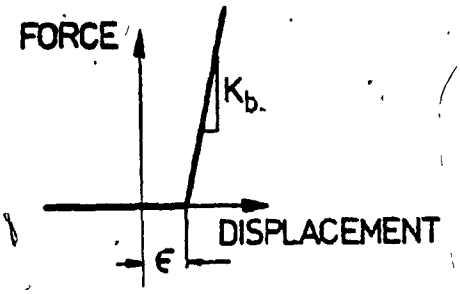

(b) SIDE BEARING
SPRINGS # 3,4

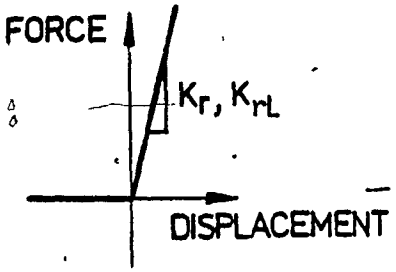

(c) WHEEL LIFT
SPRINGS # 7,8,9,10

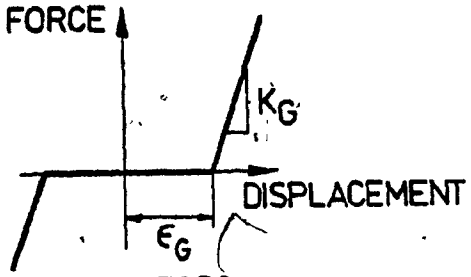

(d) GIB STOPS
SPRING # 6

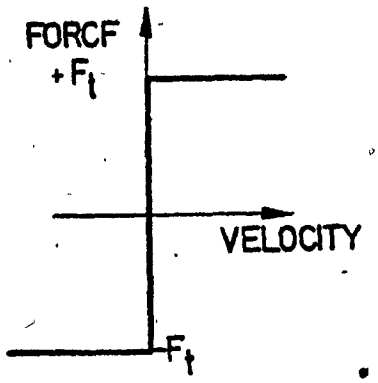

(e) FRICTION DAMPERS

Fig. 2.5: Representation of the Nonlinearities in the Single Configuration Model.

different configurations the vehicle can take according to Fig. 2.3. In the single configuration model (SCM), this is represented through bilinear springs number 1,2,3 and 4 in Fig. 2.4(b) which have the characteristics shown in Figs. 2.5(a) and (b).

ii) The separation due to wheel lift: This phenomenon occurring between the wheel and the rail during rocking is included in the model. The effect of this is indicated in the MCM by a momentary zero wheel force and gives rise to zero input forcing on that particular wheel at the instant of separation. In the SCM this phenomenon is modeled through the bilinear springs 7,8,9 and 10 shown in Fig. 2.4 with the corresponding properties given in Fig. 2.5(c).

iii) Nonlinear stiffness effects due to gib stop contact: This effect is included in the MCM by making K_h equal to the lateral stiffness of the side frames when zero gib clearance is found. In the SCM this is modeled using a bilinear spring 6 seen in Fig. 2.4 with a characteristic shown in Fig. 2.5(d).

iv) Friction damping: Coulomb type damping present in the suspension group for absorbing vertical and lateral motions is also properly incorporated both for the MCM and the SCM using ideal friction dampers with friction forces F_t and F_c as indicated in Fig. 2.4. The mechanical characteristics of these dampers are given in Fig. 2.5(e).

2.2 Assumptions and Limitations of the Model

Utilizing the results of the previous experimental investigations [12-18] described in Chapter 1, the main assumptions implied in the modeling process together with the limitations of the derived model may be stated in the following manner:

i) The input forcing function to the front and rear trucks are assumed to be identical. This assumption confines the significant motion of the car body and trucks in a plane perpendicular to the track. It is known that cars with truck centre distance equal to 39.5 feet (12 m.) experience severe rocking when operating on jointed rails with a standard rail length of 39 feet (11.9 m.). From the experimental investigations, the random input representing the track irregularities has been shown to be a stationary process [39]. Therefore, if the truck spacing is assumed equal to the rail length and the input random excitation to be stationary, a planar model can sufficiently describe the required vehicle responses under deterministic as well as stochastic inputs.

ii) It is assumed that the excitation acting on the vehicle is only due to track irregularities. This can be justified through previous experimental results [12] which state that the car to car coupling is insignificant in the rocking problem and therefore the coupler forces between cars need not be considered. Any aerodynamic force arising is generally neglected for low speeds such as the case considered in the present problem. Forces generated by the motion of freight within the car are also ignored as rocking has been observed

to occur irrespective of whether the cars are loaded or unloaded [22].

iii) Structural hysteretic damping inherent in the material of the system is represented through an equivalent linear viscous damper having a coefficient C_t as seen from Fig. 2.4 and represents both hysteretic material behavior as well as dissipation due to plastic deformation of the mechanical parts. Approximate value of the equivalent viscous damping coefficient C_t is obtained in Chapter 4 using a trial and error technique.

iv) The frictional dampers built into the side frames follow a simple Coulomb friction model whose static and dynamic friction coefficients have the same value. This assumption is well founded according to results obtained by the American Steel Foundries [60] from different test runs on freight car trucks.

v) In the multiconfiguration model, given in Fig. 2.4(a), the inertia forces of the wheelsets are not taken into consideration. This assumption is made to decrease the number of equations of motion to be integrated numerically for each time increment specified. Also the complexity of the model is reduced for carrying out the optimization analyses within reasonable computer time. The justification for this assumption is reflected by the validity of the overall model verified later from the analytical results obtained.

vi) Evidently the model cannot be used for detailed study of the longitudinal, pitch and yaw modes of vibrations because of the restriction on the features of the model to planar rocking motion only.

2.3 Formulation of the Mathematical Models

On the basis of the information available, a general modeling procedure for a given dynamic system is designed in order to produce the selected outputs under the action of certain identified system inputs. The models proposed in this work are chosen not only according to the above mentioned objectives but also to suit the analytical methods employed in the solution for the vehicle responses. In this section, general approaches for the development of the mathematical models and possible methods of solution are given.

For the MCM shown in Fig. 2.4(a), the complete set of equations of motion are to be derived to reflect the following points:

i) The equations of motion must represent all the seven configurations described in Fig. 2.3.

ii) The dynamic forces interacting between the car body and bolster and between the wheels and rail for each configuration must be included.

iii) The condition for transition from one configuration to another must be contained.

The number of differential equations of motion describing all the seven possible configurations can be reduced to three or four non-linear equations by incorporating the appropriate constraint equations associated with these configurations.

The second type of model proposed contains only a single configuration as shown in Fig. 2.4(b). This model is described

by a set of nine second order nonlinear differential equations corresponding to the nine generalized coordinates of motion. The solution for the response when subjected to periodic excitation from the track can be carried out numerically on a digital computer or by analog simulation. For digital computer solution, the multi-configuration model is preferable because of the reduced number (3 or 4) of simultaneous differential equations for successive integration corresponding to each time increment specified and thereby resulting in a decrease in the computer time required to obtain the transient response and for optimization of the suspension. It may be noted that if the SCM is used for digital integration, the entire system of nine equations has to be solved at each time increment to obtain the same results and require enormous computer time.

On the other hand, using the analog computer for obtaining the steady state response with the SCM requires much less number of analog components than those required for a similar solution utilizing the multiconfiguration model. The SCM is also useful for dealing with the system when subjected to stochastic excitations. The available methods of solution for this case dictate that the stochastic nonlinear equations are described in a single matrix form representing all possible motions of the system. This required form can be achieved only by utilizing the single configuration model as described later in Chapter 7.

2.4 Summary

In this chapter physical models for representing the freight vehicle dynamics are described. After defining the main components of the vehicle and the different modes of car vibrations, the sources of the nonlinear effects in the system are discussed. The major mechanical components are represented through idealized elements in the form of masses, springs, and damping elements. The assumptions and limitations implied in the modeling process are also summarized.

Two possible physical model representations are proposed which not only describe the desired system outputs under the action of identified inputs but are also suited for the proposed methods of solution. In the next chapter, the distortions in the track are modeled for use as the input forcing function to the freight vehicle system.

CHAPTER 3

REPRESENTATION OF THE INPUT EXCITATIONS FROM THE TRACK

CHAPTER 3

REPRESENTATION OF THE INPUT EXCITATION FROM THE TRACK

3.1 Basic Types of Track Irregularities

The four basic types of irregularities which are commonly used for defining the track geometry are described in Fig. 3.1. Gauge is the horizontal distance between the rails, cross level is the difference in elevation between the rails, alignment is the average lateral rail positions and the vertical profile is the average rail elevations. Alignment and cross level are known to be the major contributors to the rocking problem whereas the vertical profile affects mainly the bounce mode. Gauge is assumed constant throughout this investigation as there are no available measurements to describe it either in a deterministic or in a stochastic form.

Previous investigations [39,40] describe two distinct processes as the basis for defining the rail track irregularities. They are:

i) A periodic deterministic process.

ii) A stationary random process.

The periodic process describing the track distortion is principally due to the segmented nature of the rail. The profile distortion has been historically associated with a periodic form and is known commonly as a rectified sine wave (RSW), whose geometrical features are shown in Fig. 3.1(b). The maximum amplitude is defined as Z_{RO} and Z_{LO} for the right and left rails respectively and values as large as 3 inches (7.62 cm) have been reported [39]. Evidence of

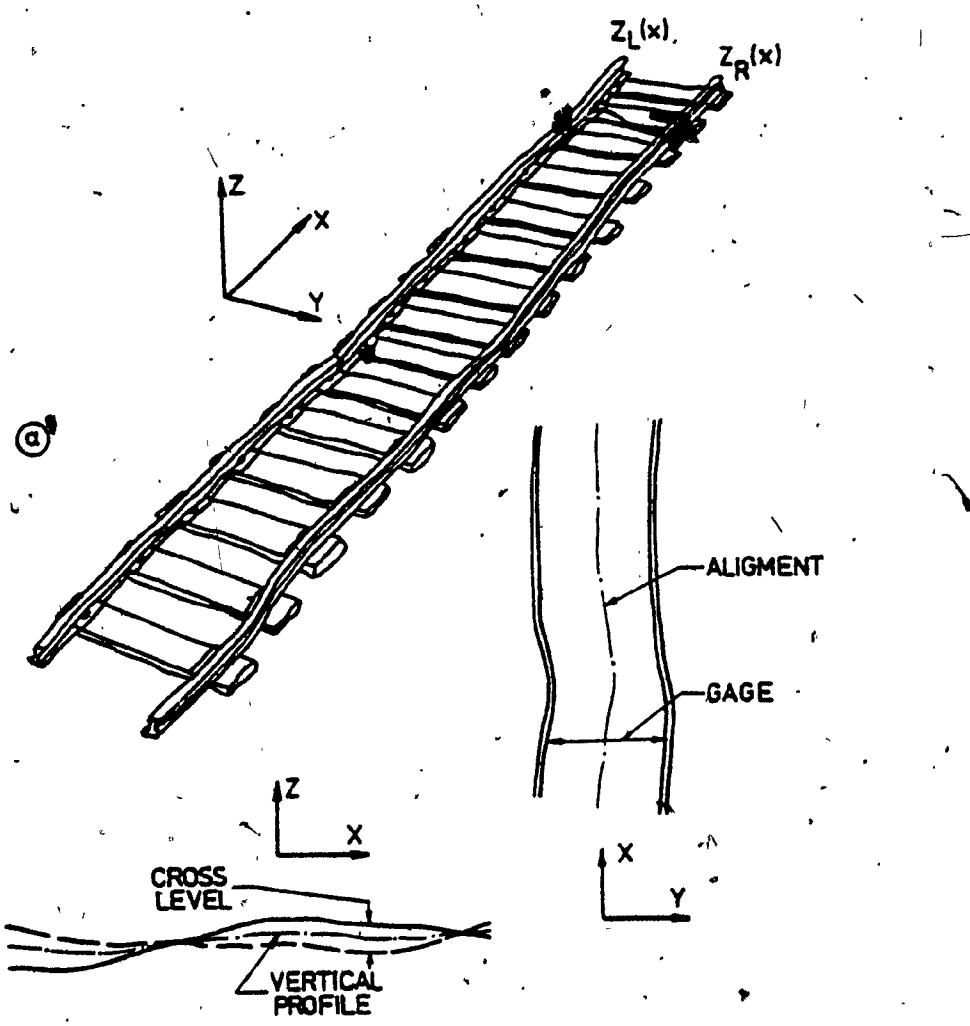

Fig. 3.1: Basic Track Irregularities.

such wave shape is found even on continuously welded rails. Measured alignment spectra of a jointed rail track also exhibit strong periodic components [40], although the physical reason for this has not yet been fully explained.

The other waveform representation of the track distortion is through a random process which is generated from a variety of sources [39]. Initially, when the track is laid, the reasons for the observed random surface roughness are due to imperfections in the rolling process and irregularities introduced in the rail during laying. Later on, these undulations combine with train dynamics in vertical and lateral directions and with the variations present in the flexibility of the track support medium, to introduce additional random disturbances to the system.

Different types of representations can be used for describing the above process in the track irregularities. They are:

i) Model as a purely periodic process only.

ii) Model as a purely random process only.

iii) Model as a combination of periodic and random processes.

From the experimental investigations available, the periodic process is found to be the dominant input that causes the rocking problem in the freight vehicle [11]. This means that in order to study the deterministic behavior of the vehicle, a purely periodic track input representation can be used. On the other hand, to study the stochastic responses of the vehicle, a realistic approach would be to combine

the periodic and the random processes for an acceptable analysis. To arrive at a proper presentation to include the two different excitation processes as the input to the model, a modified analytical form of an amplitude-frequency plot of the track irregularities is proposed in this work. Power spectral density (PSD) is such a statistical measure and is presently used for describing the combined effect of the periodic and random rail irregularities as described in Fig. 3.2. Introducing the input forcing function in the proposed PSD form to the vehicle model means that a stochastic excitation is also acting on the system and therefore the solution for the vehicle response can only be given in a probabilistic form. Therefore, this approach can be considered as a general case of the problem under investigation.

An analytical expression is proposed in Section 3.3 to approximate the available measured data in PSD form, the measured data being taken for the vertical profile, the alignment and the cross level irregularities [40] as given in Figs. 3.3, 3.4. The main characteristic of the PSD expression is that the periodic part of the track irregularity is approximated through a relatively large peak occurring at the track characteristic frequency Ω_0 in Fig. 3.2. The frequency Ω_0 is determined from the length of jointed rail and the speed of the vehicle.

3.2 Periodic Excitation from the Track

One way of representing the input forcing function to the system is to consider the periodic deterministic process representing

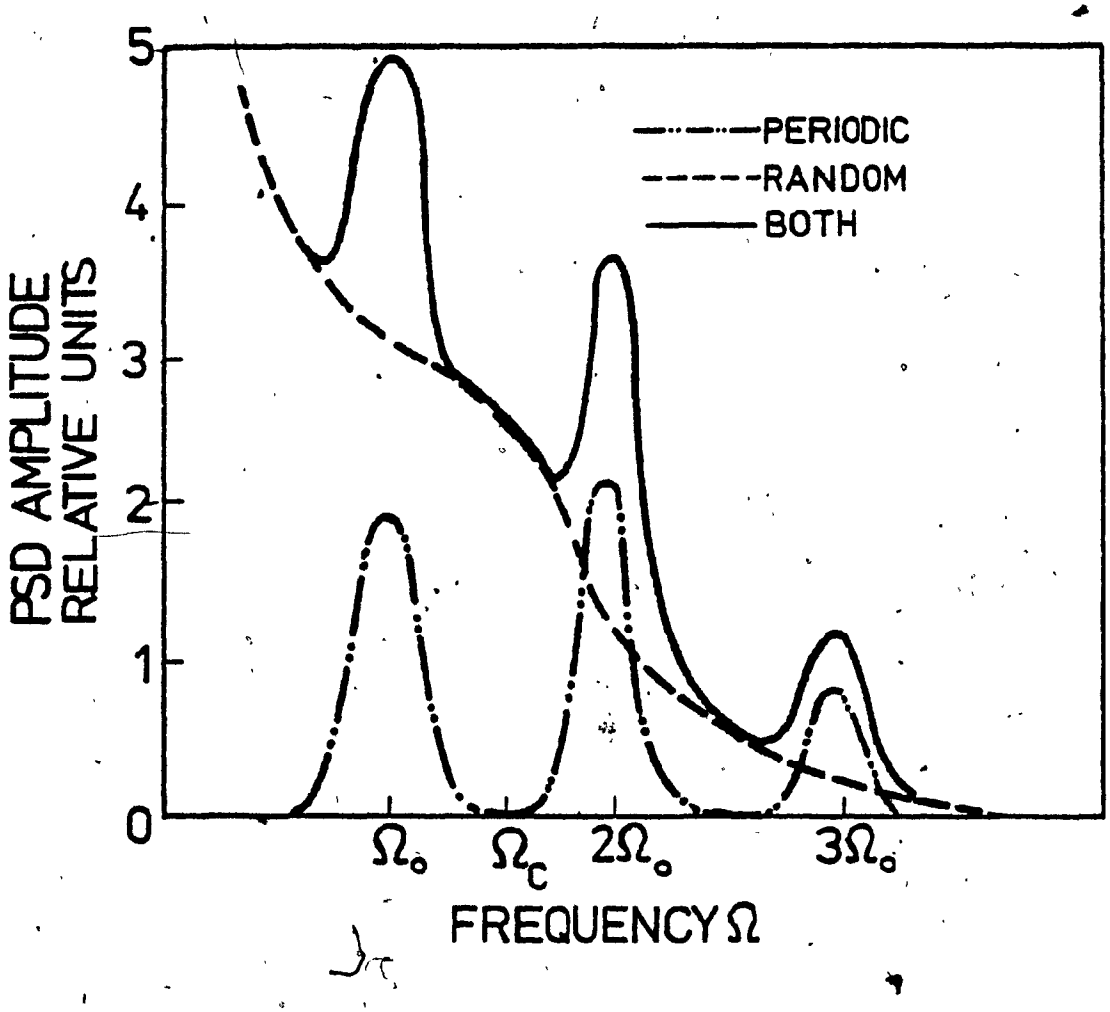

Fig. 3.2: Combination of Periodic and Random Spectra.

the track irregularities only and to neglect altogether the random effects. For such cases the forcing function can be described suitably as a spatial function and then transformed for analysis as a time function.

Periodic irregularities in the form of a rectified sine wave for a half-staggered rails are shown in Fig. 3.1(b) in the Z direction. These vertical irregularities can be expressed in terms of a series of harmonics employing a Fourier analysis in the following manner.

From Fig. 3.1(b), the right rail irregularity can be expressed as a function of the distance x in the form:

$$Z_R(x) = Z_{RO} \sin(\frac{\pi x}{2L}) \text{ for } 0 \leq x \leq 2L$$

where 2L is the standard rail length, 39 feet (11.9 m), and Z_{RO} is a constant depending on the track cross level and class.

$Z_R(x)$ is an even function with a period 2L and can be expanded as a Fourier cosine series in the form:

$$Z_R(x) = A_0 + \sum_{n=1}^{\infty} A_n \cos(\frac{n\pi x}{2L}) \qquad (3.1)$$

where A_0, A_n are the standard Fourier coefficients and are evaluated to be:

$$A_0 = \frac{1}{2L} \int_0^{2L} Z_R(x) \cdot dx = \frac{2}{\pi} Z_{RO}$$

$$A_n = \frac{2}{2L} \int_0^{2L} Z_R(x) \cos \frac{n\pi x}{2L} dx = \frac{2Z_{RO}(1 + \cos n\pi)}{\pi(1 - n^2)}, \quad n = 2,4,6...$$

Then Equation (3.1) becomes:

$$Z_R(x) = \frac{2Z_{R0}}{\pi}\left[1 - \frac{2}{3}\cos\frac{\pi x}{L} - \frac{2}{15}\cos\frac{2\pi x}{L} \ldots.\right] \qquad (3.2)$$

From Fig. 3.1(b), the left rail irregularity can be expressed similarly in the form:

$$Z_L(x) = \begin{cases} Z_{L0}\cos\left(\frac{\pi x}{2L}\right) & 0 \le x \le L \\ -Z_{L0}\cos\left(\frac{\pi x}{2L}\right) & L \le x \le 2L \end{cases} \quad \text{for}$$

$Z_L(x)$ is also an even function with a period 2L and therefore can be represented by:

$$Z_L(x) = B_0 + \sum_{n=1}^{\infty} B_n \cos\left(\frac{n\pi x}{2L}\right) \qquad (3.3)$$

B_0 and B_n are evaluated similar to A_0 and A_n as:

$$B_0 = \frac{2Z_{L0}}{\pi}, \quad B_n = \frac{4Z_{L0}\cos\left(\frac{n\pi}{2}\right)}{\pi(1 - n^2)}, \quad n = 2,4,6\ldots.$$

giving:

$$Z_L(x) = \frac{2Z_{L0}}{\pi}\left[1 + \frac{2}{3}\cos\left(\frac{\pi x}{L}\right) - \frac{2}{15}\cos\left(\frac{2\pi x}{L}\right) + \ldots\right] \qquad (3.4)$$

The input relations (3.2) and (3.4) can be expressed as time functions using the fact:

$$\frac{x}{2L} = \frac{t}{\tau} = \frac{\omega t}{2\pi}$$

or

$$\omega t = \frac{\pi x}{L}$$

where ω (rad/sec) is given by:

$$\omega = \frac{2\pi}{\tau} = \frac{2\pi}{2L/v} = \left(\frac{\pi}{L}\right) v$$

If v is given in mph as the vehicle speed, then for a standard rail length of 39 feet

$$\omega(\text{rad/sec}) = 0.2363\ v\ (\text{mph})\ (\text{or } 0.38\ v\ \text{km/hr})$$

Similar relations can be derived for representing the excitation due to alignment variations in the Y direction, shown in Fig. 3.1(a). Therefore the complete periodic deterministic excitation process acting on the system can be expressed through the following relations:

$$Z_R(t) = \frac{2Z_{R0}}{\pi}\left[1 - \frac{2}{3}\cos\omega t - \frac{2}{15}\cos 2\omega t - \frac{2}{35}\cos 3\omega t \ldots.\right]$$

$$Z_L(t) = \frac{2Z_{L0}}{\pi}\left[1 + \frac{2}{3}\cos\omega t - \frac{2}{15}\cos 2\omega t + \frac{2}{35}\cos 3\omega t \ldots.\right]$$

$$Y(t) = \frac{1}{2}\left[Y_R(t) + Y_L(t)\right] = \frac{2}{\pi} Y_0\left[1 - \frac{2}{15}\cos 2\omega t - \frac{2}{63}\cos 4\omega t + \ldots.\right]$$

3.3 Statistical Description of the Track Irregularities

The general description of the input forcing function which considers both periodic and random processes in track irregularities is achieved through an expression to approximate the available measured data giving the power spectral density (PSD) of the track derivations. Early measurements of PSD identifying a purely random waveforms for various types of road and track surfaces were approximated by the form:

$$S(\Omega) = \frac{A}{\Omega^2} \qquad (3.5)$$

where A is a constant depending on the type of the surface measured [39]. In dealing with railway track PSD, it was found that the above relationship is quite satisfactory for low frequencies but the spectral values over the higher frequencies are less than those predicted by Equation (3.5). More accurate expression for railroad track deviation spectra to cover larger range of frequencies can be given as:

$$S(\Omega) = \frac{\pi BA\ \Omega_c^2}{(\Omega^2 + \Omega_s^2)(\Omega^2 + \Omega_c^2)} \qquad (3.6)$$

where B is a constant depending upon the type of rail profile and Ω_c and Ω_s are the two critical frequencies calculated from the vehicle velocity and the rail length. Expression similar to (3.6) for the vertical and alignment inputs can be obtained by simply setting Ω_s to zero [40].

The expressions in (3.5) and (3.6) identify only the random aspects of the track surface irregularities. A modified expression is proposed here which takes into consideration also the effect of the rail surface periodicity by introducing and controlling a variable h in Equation (3.6) where $h \leq 1$. The modified expression for the spectra is defined by:

$$S(\Omega) = \frac{\pi BA\ \Omega_c^2(\Omega_c^2 + \Omega^2)}{(\Omega_s^2 + \Omega^2)(\Omega^4 - 2(1 - 2h^2)\Omega_c^2\Omega^2 + \Omega_c^4)} \qquad (3.7)$$

For $h = 1$, Equation (3.7) reduces to (3.6) describing the contribution due to random surface irregularity only, given in Figs. 3.3(a) and

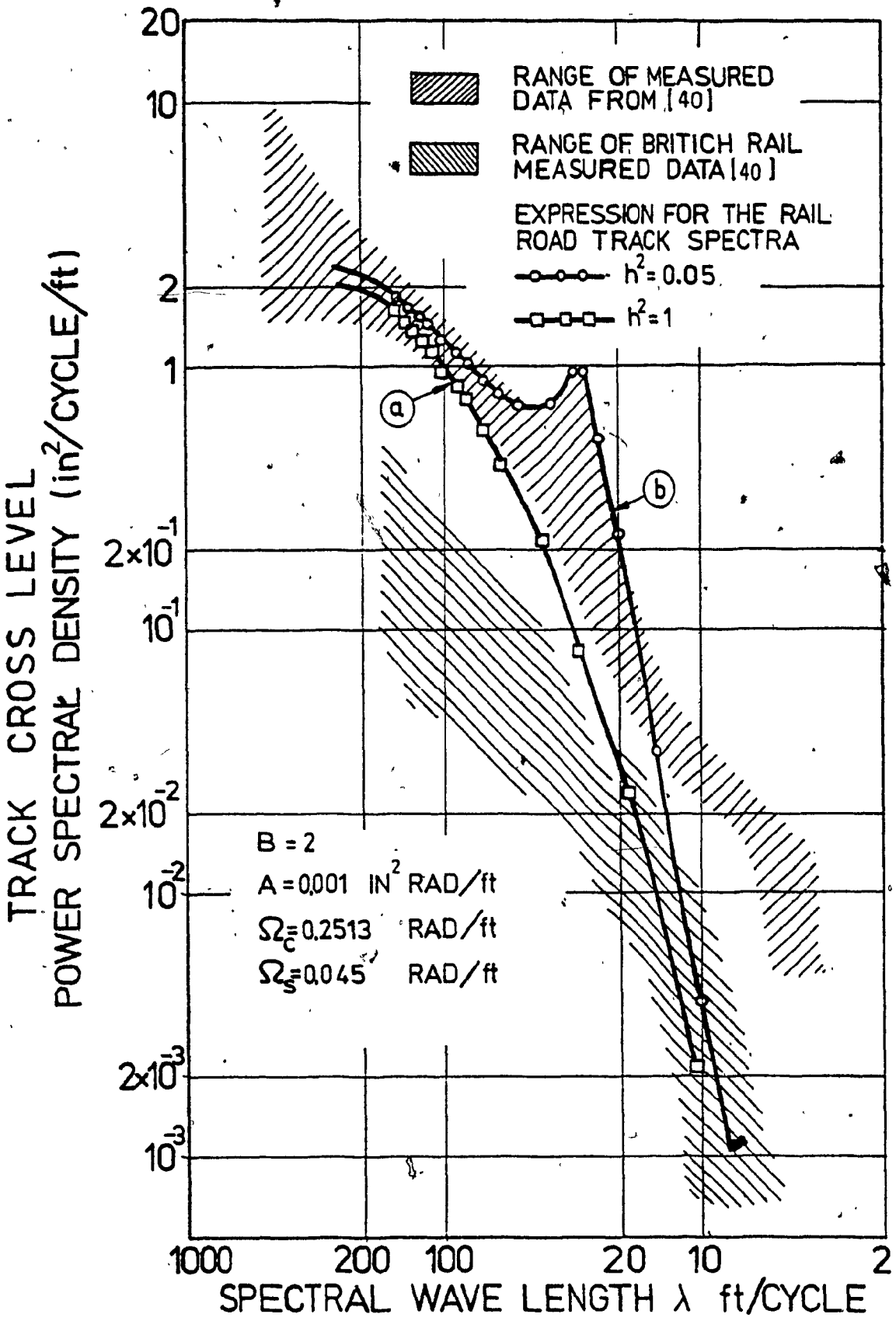

Fig. 3.3: Cross Level Spectral Density.

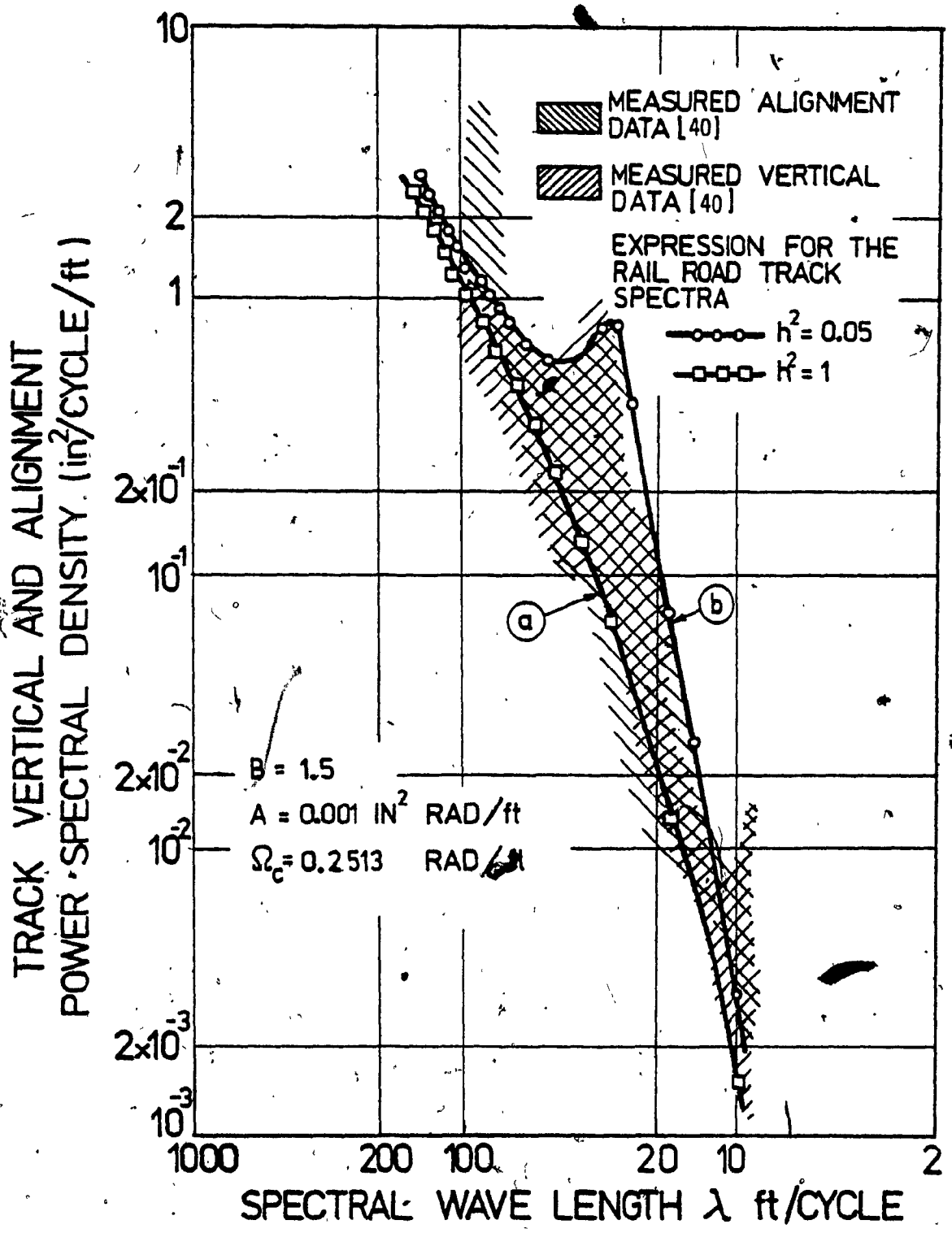

Fig. 3.4: Vertical and Alignment Spectral Density.

3.4(a). For smaller values of h, the PSD expressions indicate a relatively large amount of energy present at frequency Ω_c showing the presence of the periodic part of the track irregularity also. These can be seen in Figs. 3.3(b) and 3.4(b).

For analysis purposes, it is preferable to have the stochastic input to the system represented in terms of an equivalent white noise form. In order to achieve this, the PSD expression (3.7) is modeled as the output of a third order filter having a white noise input. The overall system equations, as given later in Chapter 7, is then considered to be composed of the filter dynamic equations together with the vehicle dynamic equations. In this manner, the system considered will have a white noise type input. To derive the transfer function H(s) of the filter and the corresponding filter dynamic equations, the following procedure is adopted.

Let, in Equation (3.7), $s = j\Omega$, where s is the Laplace transform variable. Therefore, for any one of the track irregularities, say the cross level,

$$S(s) = \frac{\pi BA\ \Omega_c^2(\Omega_c^2 - s^2)}{(\Omega_s^2 - s^2)(s^4 + 2(1 - 2h^2)\Omega_c^2 s^2 + \Omega_c^4)}$$

$$= \pi BA\ \Omega_c^2 \left| \frac{(\Omega_c + s)}{(\Omega_s + s)(s^2 + 2h\Omega_c s + \Omega_c^2)} \right|^2 \qquad (3.8)$$

For a linear system with a white noise input, shown in Fig. 3.5,

$$S(s) = S_w |H(s)|\,|H(-s)| = S_w |H(s)|^2 \qquad (3.9)$$

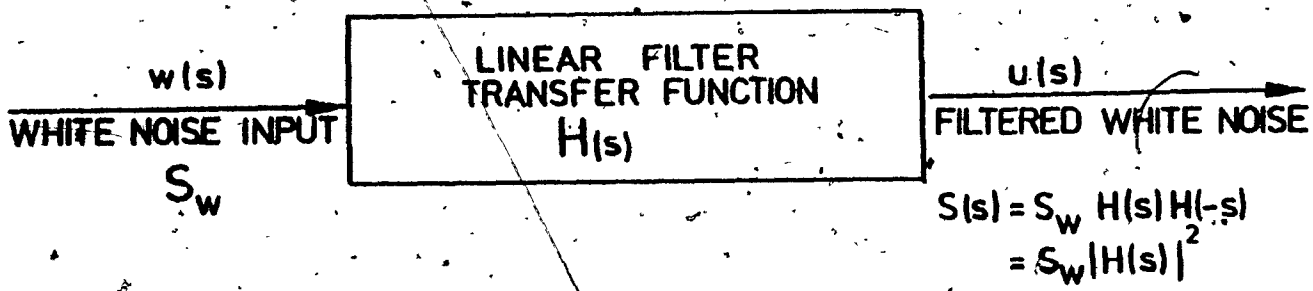

Fig. 3.5: Linear Filter with White Noise Input.

Comparing (3.8) and (3.9), the input white noise spectral density to the filter will then be:

$$S_w = \pi BA\ \Omega_c^2$$

with a delta correlation given by:

$$E[w(t)\ w(t+\tau)] = \pi BA\ \Omega_c^2\ \delta(\tau)$$

where $\delta(\tau)$ is the Dirac delta function.

The transfer function of the linear filter system is then:

$$H(s) = \frac{(\Omega_c + s)}{(\Omega_s + s)(s^2 + 2h\Omega_c s + \Omega_c^2)} = \frac{u(s)}{w(s)} \qquad (3.10)$$

To find from H(s) the filter equations of motion, Equation (3.10) is transformed into the time domain in the form:

$$\dddot{u}(t) + (2h\Omega_c + \Omega_s)\ddot{u}(t) + (\Omega_c^2 + 2h\Omega_c\Omega_s)\dot{u}(t) + \Omega_c^2\Omega_s u(t) = \dot{w}(t) + \Omega_c w(t) \qquad (3.11)$$

Equation (3.11) can be realized in terms of state variables with the following set of equations.

The state equations being

$$\begin{bmatrix}\dot{\psi}_1\\ \dot{\psi}_2\\ \dot{\psi}_3\end{bmatrix} = \begin{bmatrix}0 & 0 & -\Omega_s\Omega_c^2\\ 1 & 0 & -(\Omega_c^2 + 2h\Omega_c\Omega_s)\\ 0 & 1 & -(2h\Omega_c + \Omega_s)\end{bmatrix}\begin{bmatrix}\psi_1\\ \psi_2\\ \psi_3\end{bmatrix} + \begin{bmatrix}\Omega_c\\ 1\\ 0\end{bmatrix} w(t)\ ,$$

the output equation is:

$$[u(t)] = [0 \quad 0 \quad 1]\begin{bmatrix}\psi_1\\ \psi_2\\ \psi_3\end{bmatrix} \tag{3.12}$$

The equations (3.12) above represent completely the dynamic equations that describe the filter representing the cross level PSD with a white noise input w(t).

Similarly, two other dynamic equations can also be constructed to represent the other two irregularities, namely the vertical profile and the alignment. Hence, the dynamic equations for the overall shaping filter will have the form:

$$\begin{aligned}\dot{\underset{\sim}{\psi}}_{(9x1)} &= \underset{\sim}{A}_{F(9x9)}\,\underset{\sim}{\psi}_{(9x1)} + \underset{\sim}{B}_{F(9x3)}\,\underset{\sim}{W}_{(3x1)}\\ \underset{\sim}{u}_{(3x1)} &= \underset{\sim}{C}_{F(3x9)}\,\underset{\sim}{\psi}_{(9x1)} + \underset{\sim}{D}_{F(3x3)}\,\underset{\sim}{W}_{(3x1)}\end{aligned} \tag{3.13}$$

where

$\underset{\sim}{\psi}$ is state vector for the overall linear filter,

$\underset{\sim}{W}$ is white noise Gaussian disturbance vector,

$\underset{\sim}{u}$ is the vector specifying the input forcing functions to the system,

and

$$\underset{\sim}{u}^T = [Z_{cr} \quad Z_v \quad Z_A].$$

Here,

$Z_{cr} = \dfrac{Z_R - Z_L}{2}$, the cross level input to the vehicle.

$Z_v = \dfrac{Z_R + Z_L}{2}$, the vertical profile input to the vehicle.

$Z_A = Y$, the alignment input to the vehicle.

Further,

$$\underset{\sim}{A}_{F(9x9)} = \begin{bmatrix} \underset{\sim}{A}_{F_{cr}} & \underset{\sim}{0} & \underset{\sim}{0} \\ \underset{\sim}{0} & \underset{\sim}{A}_{F_V} & \underset{\sim}{0} \\ \underset{\sim}{0} & \underset{\sim}{0} & \underset{\sim}{A}_{F_A} \end{bmatrix}, \quad \underset{\sim}{B}_{F(9x3)} = \begin{bmatrix} \underset{\sim}{B}_{F_{cr}} & \underset{\sim}{0} & \underset{\sim}{0} \\ \underset{\sim}{0} & \underset{\sim}{B}_{F_V} & \underset{\sim}{0} \\ \underset{\sim}{0} & \underset{\sim}{0} & \underset{\sim}{B}_{F_A} \end{bmatrix}$$

$$\underset{\sim}{C}_{F(3x9)} = \begin{bmatrix} \underset{\sim}{C}_{F_{cr}} & \underset{\sim}{0} & \underset{\sim}{0} \\ \underset{\sim}{0} & \underset{\sim}{C}_{F_V} & \underset{\sim}{0} \\ \underset{\sim}{0} & \underset{\sim}{0} & \underset{\sim}{C}_{F_A} \end{bmatrix}, \quad \underset{\sim}{D}_{F(3x3)} = \underset{\sim}{0}$$

and

$$E[\underset{\sim}{W}(t)\ \underset{\sim}{W}(t+\tau)] = \underset{\sim}{D}\ \delta(\tau).$$

$\underset{\sim}{D}$ is the constant covariance matrix for an equivalent white noise input and is given by:

$$\underset{\sim}{D} = \begin{bmatrix} 2\pi A_{cr}\Omega_{c_{cr}}^2 & 0 & 0 \\ 0 & 1.5\pi A_V \Omega_{c_V}^2 & 0 \\ 0 & 0 & 1.5\pi A_A \Omega_{c_A}^2 \end{bmatrix} \qquad (3.14)$$

The dynamic equations of the filter given in (3.13) are utilized in Chapter 7 together with the vehicle dynamic equations to form the overall system equations. The overall system will then be subjected to the specified stochastic input in the form of an equivalent white noise spectrum and further analysis can be carried out employing available probabilistic methods.

3.4 Proposed Analytical Investigation for the Vehicle Dynamic Responses

In the following chapters, the solution for the vehicle

responses when subjected to different forms of track irregularities is attempted using digital and analog computers. First, the excitation is assumed to be a purely periodic process and the vehicle's transient as well as steady state responses are evaluated. The MCM is used for evaluating and optimizing the system transient response using a digital computer. The steady state response of the system is calculated using the SCM on an analog computer. Finally, the determination of the system response and subsequent optimization, when subjected to a combination of periodic and random inputs, are presented in Chapters 7 and 8 using the SCM on a digital computer.

3.5 Summary

In this chapter, different types of representation of the track distortions are given. The basic types of track irregularities are defined as a purely periodic process and a stationary random process. A Fourier series is utilized to model the periodic part arising due to the segmented nature of the rail. More general model of the track input which describes a combination of periodic and random process is obtained in the form of an equivalent white noise passing through a third order linear filter. The dynamic equations of filter are derived for use in Chapter 7 to investigate the vehicle responses under stochastic excitation. In the next two chapters, the transient and steady state responses of the system are evaluated when the input from the track is in the form of a purely periodic process.

CHAPTER 4

TRANSIENT RESPONSES IN THE TIME AND FREQUENCY DOMAINS BASED ON THE MULTICONFIGURATION MODEL

CHAPTER 4

TRANSIENT RESPONSES IN THE TIME AND FREQUENCY DOMAINS BASED ON THE MULTICONFIGURATION MODEL

In the following chapters the rocking response of the vehicle when subjected to purely periodic excitation from the tracks is investigated. The transient response is the part of the system behavior influenced essentially by the initial conditions before reaching a steady state. The transient behavior is useful in showing the way the rocking response builds up to a maximum value and then decays to form a sequence of beating cycles. The maximum value in each of the response beating cycle indicates the occurrence of severe rocking causing vehicle instability associated with wheel lift and excessive side bearing forces. During the steady state part, a nonlinear jump can be shown to occur between one value of car rocking amplitude to another at the same frequency along with a few other dynamic phenomena associated with the system nonlinearities.

Closed form analytical solutions for the nonlinear models described in Chapter 2 are very difficult to achieve and therefore interest is turned to numerical integration techniques and can be applied to the multiconfiguration as well as single configuration models. The multiconfiguration model is more reliable in checking the correct vehicle configuration that satisfies both forces and geometry appropriate to the response obtained. Moreover the number of independent generalized coordinates corresponding to each of its different configurations are less than that for the single configu-

ration model. Due to these reasons, the MCM is chosen for solution by numerical integration on a digital computer. However, because of the computer time limitations, the numerical values of the response can be evaluated only for a limited time period. Hence, the results obtained are termed as the transient response of the freight car system since they cannot be utilized to show accurately the jump in amplitude. This phenomenon is later described through the steady state solution on an analog computer.

In this chapter, the transient response of the system is evaluated by numerical integration of the equations of motion on a digital computer. The equations of motion for the MCM are derived using Lagrange's technique. The solution gives the system's time response, from which the response characteristics in the frequency domain can be obtained. The time response curves include the car rocking angle, lateral displacements, the forces acting between the car and the side bearing and between the wheels and rails. The validity of the model employed is checked by comparing the numerical results with the reported field test results both in the time as well as frequency domains. Transient response results in the frequency domain is utilized in Chapter 6 to carry out the optimization of the suspension system.

4.1 The Equations of Motion of the Multiconfiguration Model

The multiconfiguration model shown in Figs. 4.1(a) and (b) was described in detail in Chapter 2. The derivation of the complete equations of motion consists of the following steps:

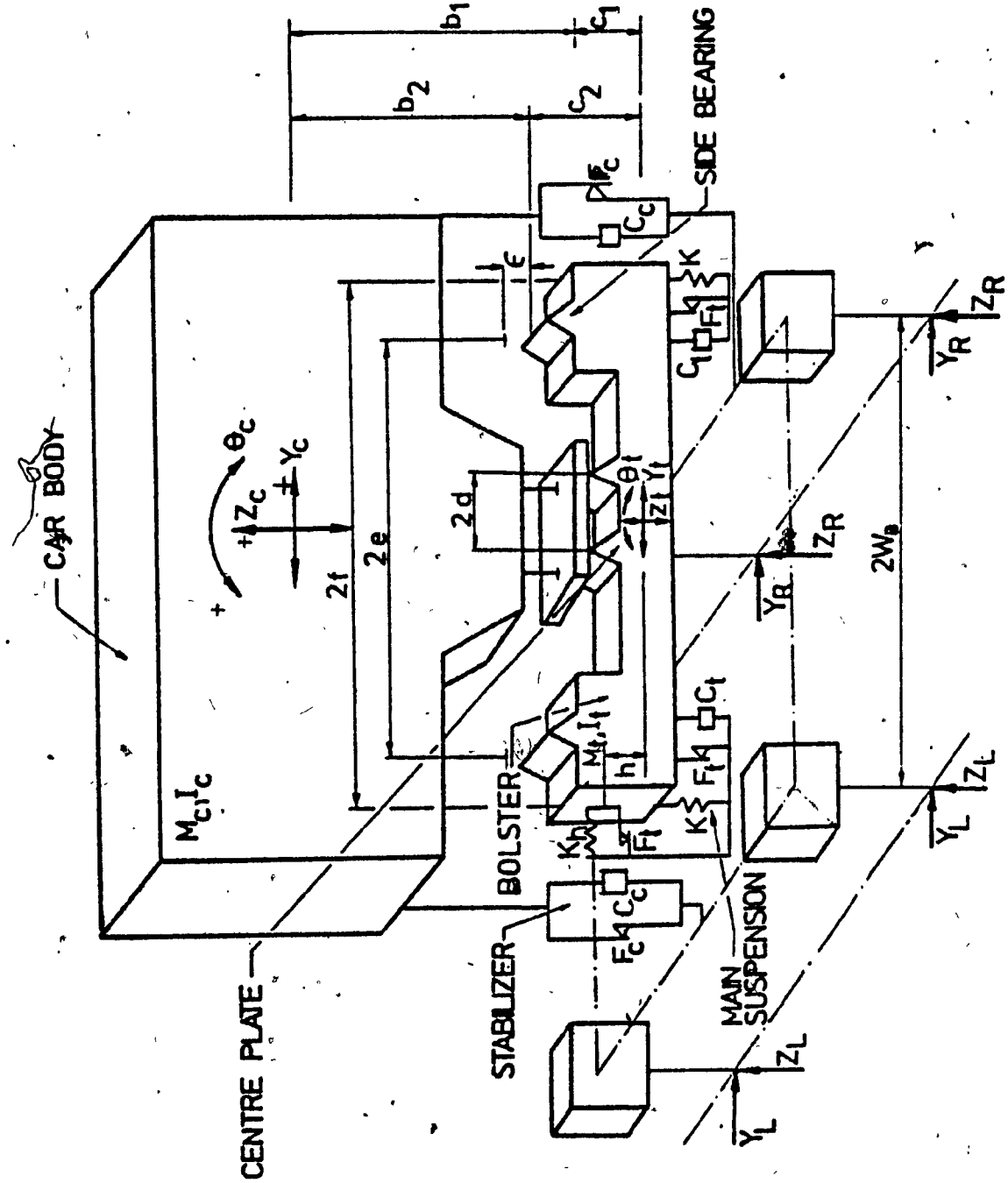

Fig. 4.1(a): The Freight Vehicle Model.

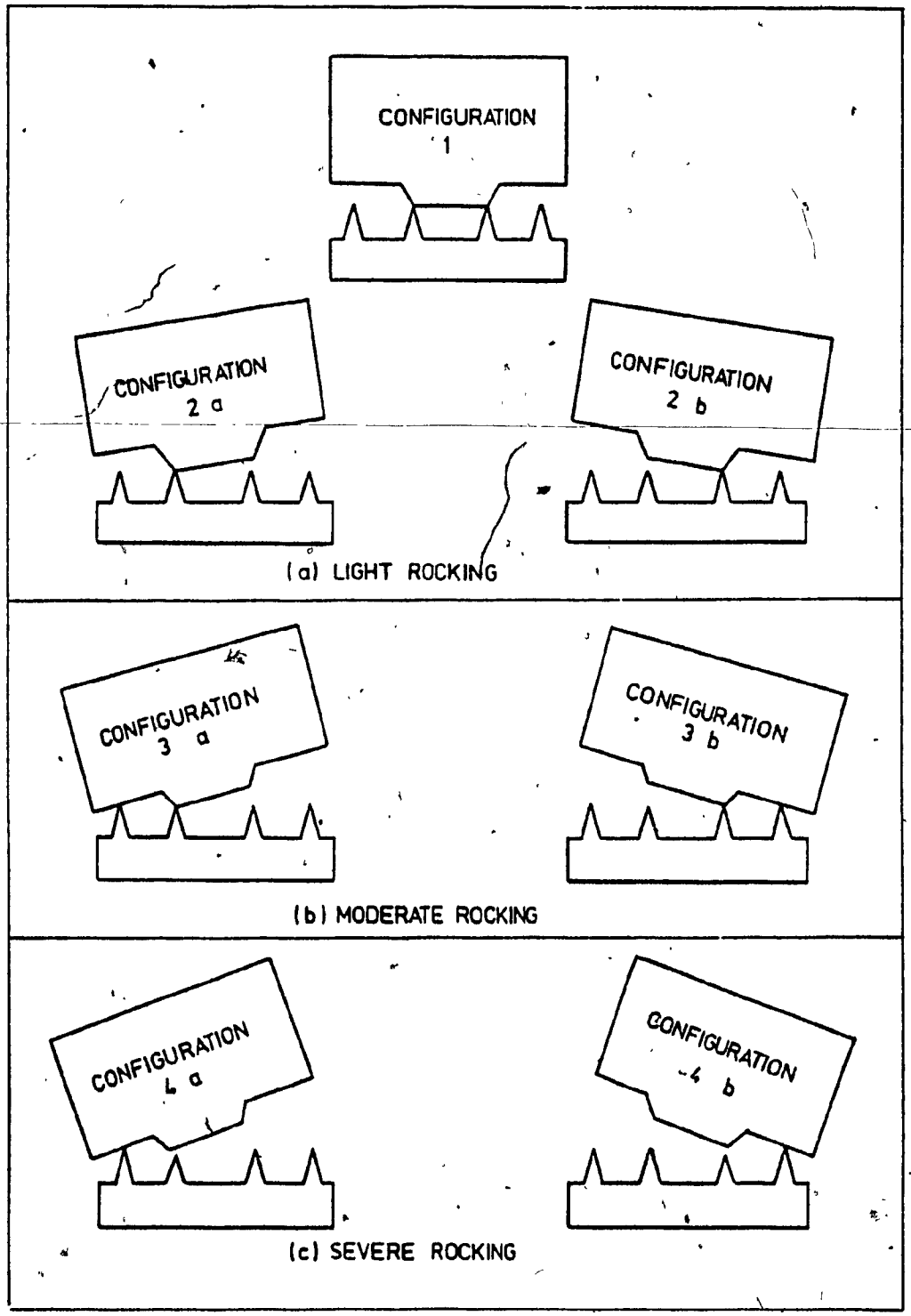

Fig. 4.1(b): Car Body-Bolster Relative Positions.

i) The equations of motion associated with all the possible configurations given in Fig. 4.1(b) are derived using Lagrange's technique. This is done in Subsection 4.1.1. The equations are independently checked by rederiving them using the force analysis method.

ii) The expressions for the forces acting between the bolster and the car body and between the wheels and rails for each configuration are derived. These forces can be computed utilizing the solution of the configuration equations of motion, that is employing the car and bolster displacements and velocities. This is given in detail in Subsection 4.1.2.

iii) The conditions for transition from one configuration to another are set up. These utilize the solution of the equations of motion given in (i) together with the force relationships in (ii) to specify the configuration of the system corresponding to each time increment of the solution and are detailed in Subsection 4.1.3.

The complete set of equations of motion are then solved on a digital computer to yield the vehicle time responses under the action of the periodic excitation. In the following section, the equations of motion pertinent to each of the different configurations of the system are derived.

4.1.1 The Equations of Motion

The equations of motion applicable to the nonlinear MCM model of the freight car corresponding to each configuration are derived

using Lagrange's equation by the following procedure:

i) The vector representing the generalized coordinates required for describing the motion of the system in Fig. 4.1(a) are given by $[Z_c, Y_c, \theta_c, Z_t, Y_t, \theta_t]$.

ii) The energy expressions for the system are formulated. They are the kinetic energy, T, of the system:

$$T = \frac{1}{2} M_c \dot{Z}_c^2 + \frac{1}{2} M_c \dot{Y}_c^2 + \frac{1}{2} I_c \dot{\theta}_c^2 + \frac{1}{2} M_t \dot{Z}_t^2 + \frac{1}{2} M_t \dot{Y}_t^2 + \frac{1}{2} I_t \dot{\theta}_t^2,$$

the potential energy, V,

$$V = \frac{1}{2} K(Z_t + f\theta_t - Z_R)^2 + \frac{1}{2} K(Z_t - f\theta_t - Z_L)^2 + \frac{1}{2} K_h(Y_t - h\theta_t - Y)^2,$$

Rayleigh's dissipation function, D, of the system,

$$D = \frac{1}{2} C_t(\dot{Z}_t + f\dot{\theta}_t - \dot{Z}_R)^2 + \frac{1}{2} C_t(\dot{Z}_t - f\dot{\theta}_t - \dot{Z}_L)^2 + \frac{1}{2} C_c(\dot{Z}_c + f\dot{\theta}_c - \dot{Z}_R)^2 + \frac{1}{2} C_c(\dot{Z}_c - f\dot{\theta}_c - \dot{Z}_L)^2.$$

The virtual work, δW, due to gravitational and friction forces, is given by:

$$\delta W = - M_c g \delta Z_c - M_t g \delta Z_t - F_t s_1 \delta(Z_t + f\theta_t - Z_R) - F_t s_2 \delta(Z_t - f\theta_t - Z_L) - F_c s_3 \delta(2f\theta_c - Z_R + Z_L) - F_t s_4 \delta(Y_t - h\theta_t - Y)$$

Here,

$$s_1 = \mathrm{Sgn}(\dot{Z}_t + f\dot{\theta}_t - \dot{Z}_R), \quad s_2 = \mathrm{Sgn}(\dot{Z}_t - f\dot{\theta}_t - \dot{Z}_L)$$

$$s_3 = \mathrm{Sgn}(2f\dot{\theta}_c - \dot{Z}_R + \dot{Z}_L), \quad s_4 = \mathrm{Sgn}(\dot{Y}_t - h\dot{\theta}_t - \dot{Y})$$

iii) The constraint equations for each of the configuration of the model, shown in Fig. 4.1(b), are derived based on the points of contact between the car body and the bolster. The number of equations describing these holonomic constraints determines automatically the remaining number of independent equations of motion. The constraints for each of the configuration, in Fig. 4.1(b), are expressed in the following manner:

Configuration 1: $Z_t = Z_c$, $\theta_t = \theta_c$, $Y_t = Y_c + (C_1+b_1)\theta_c$ (4.1.1)

Configuration 2a: $Z_t = Z_c + d(\theta_c-\theta_t)$, $Y_t = Y_c + b_1\theta_c + C_1\theta_t$ (4.1.2a)

Configuration 2b: $Z_t = Z_c - d(\theta_c-\theta_t)$, $Y_t = Y_c + b_1\theta_c + C_1\theta_t$ (4.1.2b)

Configuration 3a: $Z_t = Z_c - d\varepsilon/(e-d)$, $\theta_t = \theta_c + \varepsilon/(e-d)$
$Y_t = Y_c + (b_1+C_1)\theta_c + C_1\varepsilon/(e-d)$ (4.1.3a)

Configuration 3b: $Z_t = Z_c - d\varepsilon/(e-d)$, $\theta_t = \theta_c - \varepsilon/(e-d)$
$Y_t = Y_c + (b_1+C_1)\theta_c - C_1\varepsilon/(e-d)$ (4.1.3b)

Configuration 4a: $Z_t = Z_c + e\theta_c + e\theta_t + \varepsilon$,
$Y_t = Y_c + b_2\theta_c + C_2\theta_t$ (4.1.4a)

Configuration 4b: $Z_t = Z_c - e\theta_c + e\theta_t + \varepsilon$,
$Y_t = Y_c + b_2\theta_c + C_2\theta_t$ (4.1.4b)

iv) The energy equations given in (ii) are modified by substituting the constraint equations (iii) in (ii) to express them in terms of completely independent generalized coordinates.

v) Employing Lagrange's equation in the form:

$$\frac{d}{dt}\left(\frac{\partial T}{\partial \dot{q}_i}\right) + \frac{\partial V}{\partial q_i} + \frac{\partial D}{\partial \dot{q}_i} = \frac{\delta W}{\delta q_i}, \quad i = 1,2,3 \text{ or } 4$$

where q_i's are the independent generalized coordinates. Using the energy expressions given in (iv), the equations of motion corresponding to each of the different configuration of the system are derived. These equations can be expressed in a matrix form as:

$$\underset{\sim}{M}\ddot{\underset{\sim}{X}} + \underset{\sim}{C}\dot{\underset{\sim}{X}} + \underset{\sim}{K}\underset{\sim}{X} + \underset{\sim}{S}(\dot{\underset{\sim}{Y}}^{(1)}) + \underset{\sim}{G} = \underset{\sim}{F}(t)$$

where

$\underset{\sim}{X}$ is a vector associated with the n independent generalized coordinates,

$\underset{\sim}{M}, \underset{\sim}{C}, \underset{\sim}{K}$ are nxn symmetric matrices representing mass, damping and stiffness,

$\underset{\sim}{S}(\dot{\underset{\sim}{Y}}^{(1)})$ represents the n nonlinear friction damping forces,

$\underset{\sim}{G}$ represents the n constant forces vector,

and $\underset{\sim}{F}(t)$ represents the n forcing functions.

Further,

$$\dot{\underset{\sim}{Y}}^{(1)} = \underset{\sim}{A}^{(1)}\dot{\underset{\sim}{X}} - \dot{\underset{\sim}{b}}(t)$$

where $\underset{\sim}{b}(t)$ is a vector function representing the input periodic excitations.

The complete set of equations including all the derivations of the expressions associated with each configuration and are presented in Appendix I.

4.1.2 Force and Moment Analysis for the Vehicle Configurations

A detailed force analysis is carried out to obtain the relationships for the forces acting between the car body and bolster and for those acting between the wheels and the rails. From these force

relations three sets of equilibrium conditions can be developed.

i) By considering the free body equilibrium of the car body for the different configurations shown in Fig. 4.2, the centre plate and side bearing forces are expressed in terms of the other known forces. These relationships are necessary to establish the conditions for transition from one configuration to another and are given in Subsection 4.1.3.

ii) By considering the equilibrium of the bolster for the different configurations shown in Fig. 4.3, equations of motion are separately derived as a check against those given using Lagrange's technique in Subsection 4.1.1.

iii) By considering the equilibrium of the wheelset in Fig. 4.3 the wheel-rail interacting forces can also be evaluated. These forces are used for checking the wheel lift conditions. Wheel lift is indicated by a zero wheel force at that particular wheel at the instant of its separation from the rail.

All the forces mentioned above are described in the free body diagrams in Figs. 4.2 and 4.3 and are defined by the following expressions:

the car viscous damper force at left $D_L = - C_c(\dot{Z}_c - f\dot{\theta}_c - \dot{Z}_L)$,

the car viscous damper force at right $D_R = - C_c(\dot{Z}_c + f\dot{\theta}_c - \dot{Z}_R)$,

the suspension force at left $P_L = - K(Z_t - f\theta_t - Z_L) - C_t(\dot{Z}_t - f\dot{\theta}_t - \dot{Z}_L) - F_t s_2$,

the suspension force at right $P_R = -K(Z_t + f\theta_t - Z_R) - C_t(\dot{Z}_t + f\dot{\theta}_t - \dot{Z}_R) - F_t s_1$,

and the horizontal suspension force $P_h = -K_h(Y_t - h\theta_t - Y) - F_t s_4$.

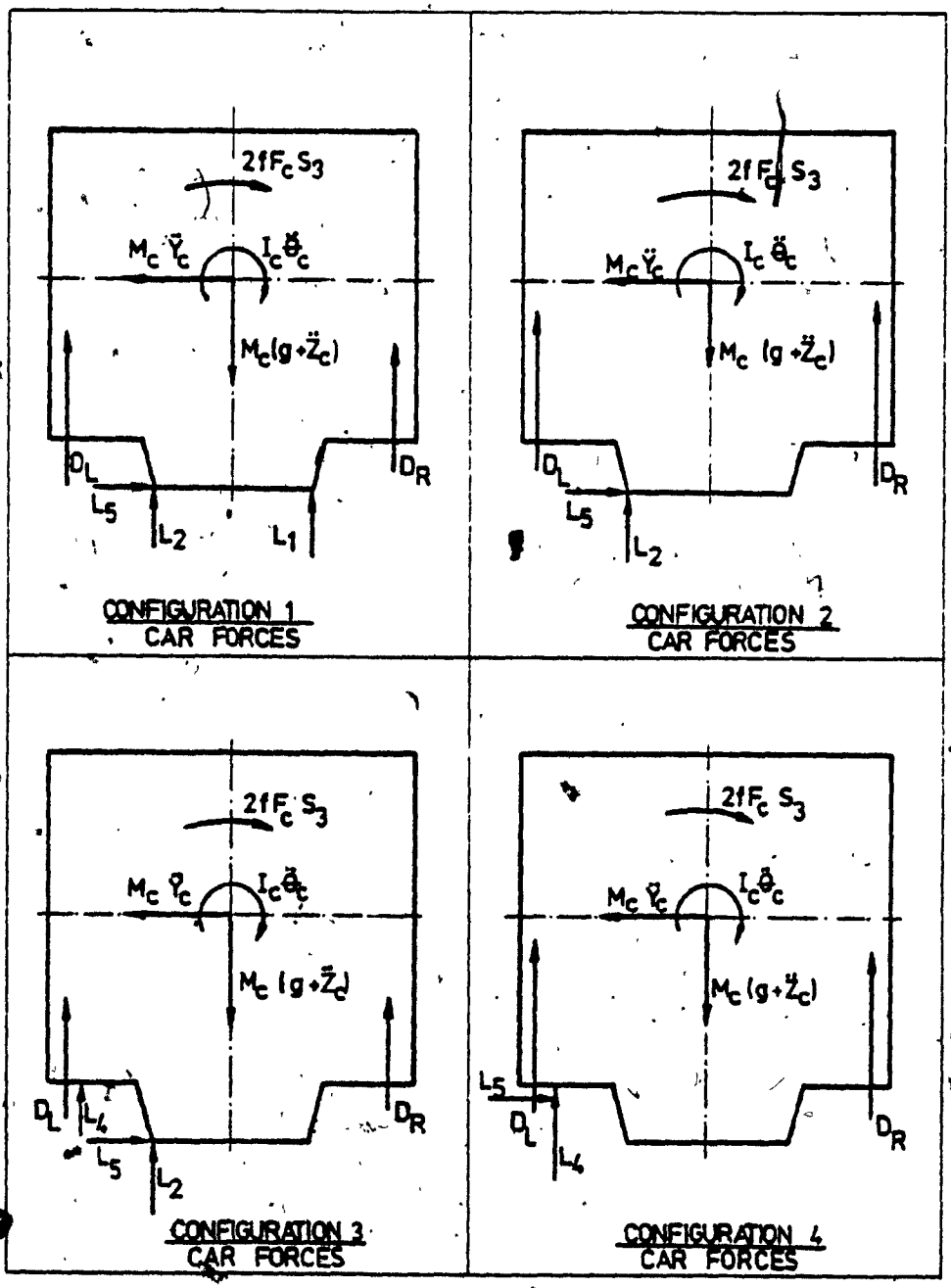

Fig. 4.2: Free Body Diagrams of the Car Body.

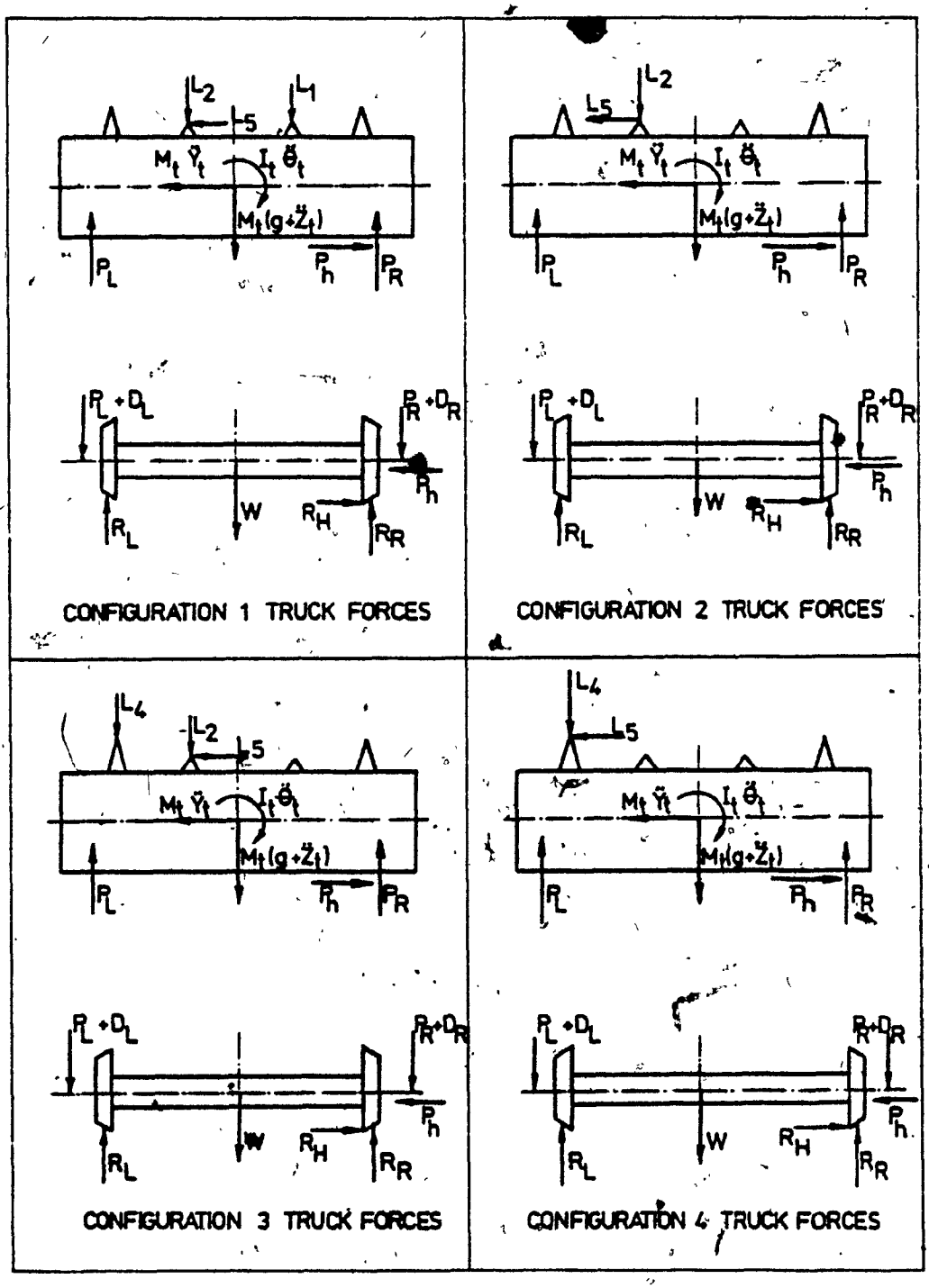

Fig. 4.3: Free Body Diagrams of the Bolster and Wheelset.

Further,

R_L is the wheel force at left and R_R the wheel force at right.

R_h, the horizontal wheel force.

And

L_1, L_2 are the right and left centre plate forces,

L_3, L_4 are the right and left side bearing forces, and

L_5 is the horizontal centre plate or the side bearing force.

Considering the equilibrium of the car in Fig. 4.2 expressions for the side bearing and centre plate forces L_1, L_2, L_3, L_4 and L_5 for the different configurations are derived in the following manner:

Configuration 1:

$$\begin{aligned} L_1 &= [D_L(f-d) + M_c(\ddot{Z}_c+g)d + I_c\ddot{\theta}_c - D_R(f+d) - M_c\ddot{Y}_c b_1 + 2fF_c s_3]/2d \\ L_2 &= M_c(\ddot{Z}_c+g) - (D_R+D_L) - L_1 \\ L_3 &= L_4 = 0 \\ L_5 &= M_c\ddot{Y}_c \end{aligned} \qquad (4.2.1)$$

Configuration 2a:

$$L_1 = 0 \ , \ L_2 = M_c(\ddot{Z}_c+g) - (D_L+D_R) \qquad (4.2.2a)$$

$$L_3 = L_4 = 0 \ , \ L_5 = M_c\ddot{Y}_c$$

$$I_c\ddot{\theta}_c = [D_R(f+d) - D_L(f-d) - M_c(\ddot{Z}_c+g)d + M_c\ddot{Y}_c b_1 - 2F_c f s_3]$$

Configuration 2b:

$$L_2 = 0 \ , \ L_1 = M_c(\ddot{Z}_c+g) - (D_L+D_R) \qquad (4.2.2b)$$

$$L_3 = L_4 = 0 \ , \ L_5 = M_c\ddot{Y}_c$$

$$I_c\ddot{\theta}_c = D_R(f+d) - D_L(f-d) - M_c(\ddot{Z}_c+g)d + M_c\ddot{Y}_c b_1 - 2F_c f s_3 + 2L_1 d$$

Configuration 3a:

$$L_1 = 0\ ,\quad L_2 = M_c(\ddot{Z}_c+g) - (D_L+D_R) - L_4$$

$$L_3 = 0\ ,\quad L_5 = M_c\ddot{Y}_c \qquad (4.2.3a)$$

$$L_4 = [D_R(f+d) - D_L(f-d) + M_c\ddot{Y}_c b_1 - I_c\ddot{\theta}_c - M_c(\ddot{Z}_c+g)d - 2fF_c s_3]/(e-d)$$

Configuration 3b:

$$L_1 = M_c(\ddot{Z}_c+g) - (D_L+D_R) - L_3,\quad L_2 = 0$$

$$L_3 = [D_L(f+d) + I_c\ddot{\theta}_c - M_c\ddot{Y}_c b_1 - M_c(g+\ddot{Z}_c)d - D_R(f-d) + 2F_c f s_3]/(e-d)$$

$$L_4 = 0\ ,\quad L_5 = M_c\ddot{Y}_c \qquad (4.2.3b)$$

Configuration 4a:

$$L_1 = L_2 = L_3 = 0$$

$$L_4 = M_c(g+\ddot{Z}_c) - (D_L+D_R)\ ,\quad L_5 = M_c\ddot{Y}_c \qquad (4.2.4a)$$

$$I_c\ddot{\theta}_c = D_R(f+e) - D_L(f-e) - M_c(\ddot{Z}_c+g)e + M_c\ddot{Y}_c b_2 - 2F_c f s_3$$

Configuration 4b:

$$L_1 = L_2 = L_4 = 0$$

$$L_3 = M_c(g+\ddot{Z}_c) - (D_L+D_R)\ ,\quad L_5 = M_c\ddot{Y}_c \qquad (4.2.4b)$$

$$I_c\ddot{\theta}_c = D_R(f+e) - D_L(f-e) - M_c(\ddot{Z}_c+g)e + M_c\ddot{Y}_c b_2 - 2F_c f s_3 + 2L_3 e$$

As the next step, the bolster equilibrium is considered from Fig. 4.3. A set of equations of motion for the bolster can be derived as follows:

$$M_t\ddot{Y}_t = P_h - L_5$$

$$M_t\ddot{Z}_t = P_L + P_R - (L_1+L_2+L_3+L_4) - M_t g \qquad (4.3)$$

$$I_t\ddot{\theta}_t = (P_R-P_L)f + (L_2-L_1)d + (L_4-L_3)e + L_5 C_1 - P_h h$$

Now the equations of motion for all configurations of the system in terms of a set of independent generalized coordinates $\underset{\sim}{X}$.

can also be found by incorporating the set of Equation (4.3) into the set (4.2) and further substituting the constraint Equations (4.1). These set of equations are useful to check the equations of motion derived using the Lagrange's equation in Subsection 4.1.1.

The force and moment equilibrium of the wheelset shown in Fig. 4.3 leads to different set of independent conditions that are necessary for checking whether a wheel lift has occurred. These conditions can be stated in the following manner:

i) If there is no wheel lift, then:

$$R_h = P_h$$

$$R_R = [(D_R+P_R)(f+W_B) - (P_L+D_L)(f-W_B) - P_h r_1 - 2fF_c s_3 + WW_B]/2W_B$$

$$R_L = [D_R+P_R+D_L+P_L+W-R_R]$$

ii) If right wheel lift occurs,

$$R_h = P_h \, , \; R_R = 0 \, , \; R_L = P_R+P_L+W+D_L+D_R$$

iii) If left wheel lift occurs,

$$R_h = P_h \, , \; R_L = 0, \; R_R = P_R+P_L+W+D_L+D_R$$

4.1.3 Conditions for Transition from One Configuration to Another

The conditions for transition from one configuration to another are described as a series of sequential checks on the geometry corresponding to equations of motion. These checks are derived mainly from the centre plate and side bearing forces computed in Subsection 4.1.2. These conditions are essential at each time increment

of the numerical solution of the system to find the configuration which satisfies both the force and geometric compatibilities. The series of configuration checks are described in the form of a flow chart in Fig. 4.4 and can be stated in the following manner:

i) Check the magnitude of the centre plate forces L_1, L_2 computed using the velocities and displacements obtained at the previous time instant t_{i-1}. If $L_1>0$ and $L_2>0$, then the vehicle is in Configuration 1, at t_i, according to Fig. 4.1(b).

ii) If $L_1>0$ and $L_2<0$, check the magnitude of the force L_3 in Configuration 3b. If $L_3>0$, then go to Configuration 3b in Fig. 4.1(b). If $L_3<0$ then go to Configuration 2b.

iii) If $L_1<0$ and $L_2<0$, check if θ_C is positive. If positive, go to Configuration 4a in Fig. 4.1(b). If θ_C is negative, go to Configuration 4b.

iv) If $L_1<0$ and $L_2>0$, then check the force L_4 in Configuration 3a. If $L_4>0$, go to Configuration 3a. If $L_4<0$, go to Configuration 2a.

v) For each one of the chosen configurations check whether the associated geometric constraints given in Equations (4.1) are satisfied.

vi) If none of the configurations satisfies both the force and the geometric compatibilities, then the configurations used at t_{i-1} is used again for the next time instant t_i.

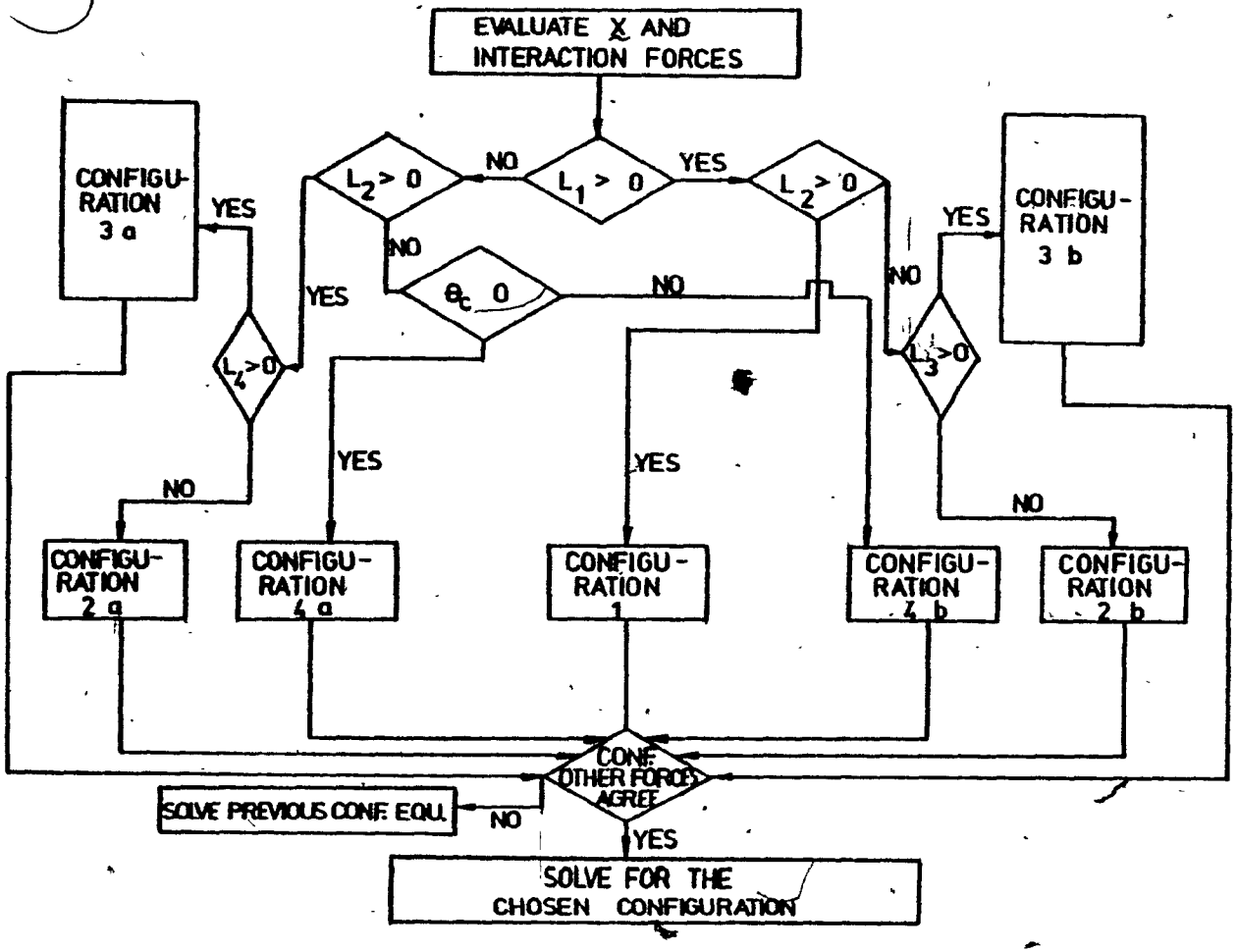

Fig. 4.4: Search Procedure for the System Configuration Transition.
[Refer to Fig. 4.1(b) for Configurations].

The rocking response of the multiconfiguration model requires a solution of the complete set of equations of motion. This set of equations would then consist of the configuration equations derived in Subsection 4.1.1 plus the conditions for possibility of transition from one configuration to another as stated above. The method of solving these equations is given in detail in the next section.

4.2 The Method of Solution

The complete equations of motion derived in Section 4.1 to describe the dynamics of the freight car is solved for the time response. The procedure followed for finding the time response of the system is described in a flow chart in Fig. 4.5 and can be summarized in the following manner:

i) The coupled equations of motion of the chosen model configuration are first solved simultaneously to get expressions for the accelerations in an explicit form. Equations associated with Configuration 1 with zero initial conditions are used for starting the numerical integration.

ii) The accelerations are integrated for the velocities employing a fourth order Runge-Kutta technique for time instants t_i's. The velocities and displacements obtained at t_{i-1} are used as the initial conditions at t_i.

iii) The forces and moments acting on the system are calculated at the time instants t_i utilizing the information obtained in the previous step (ii).

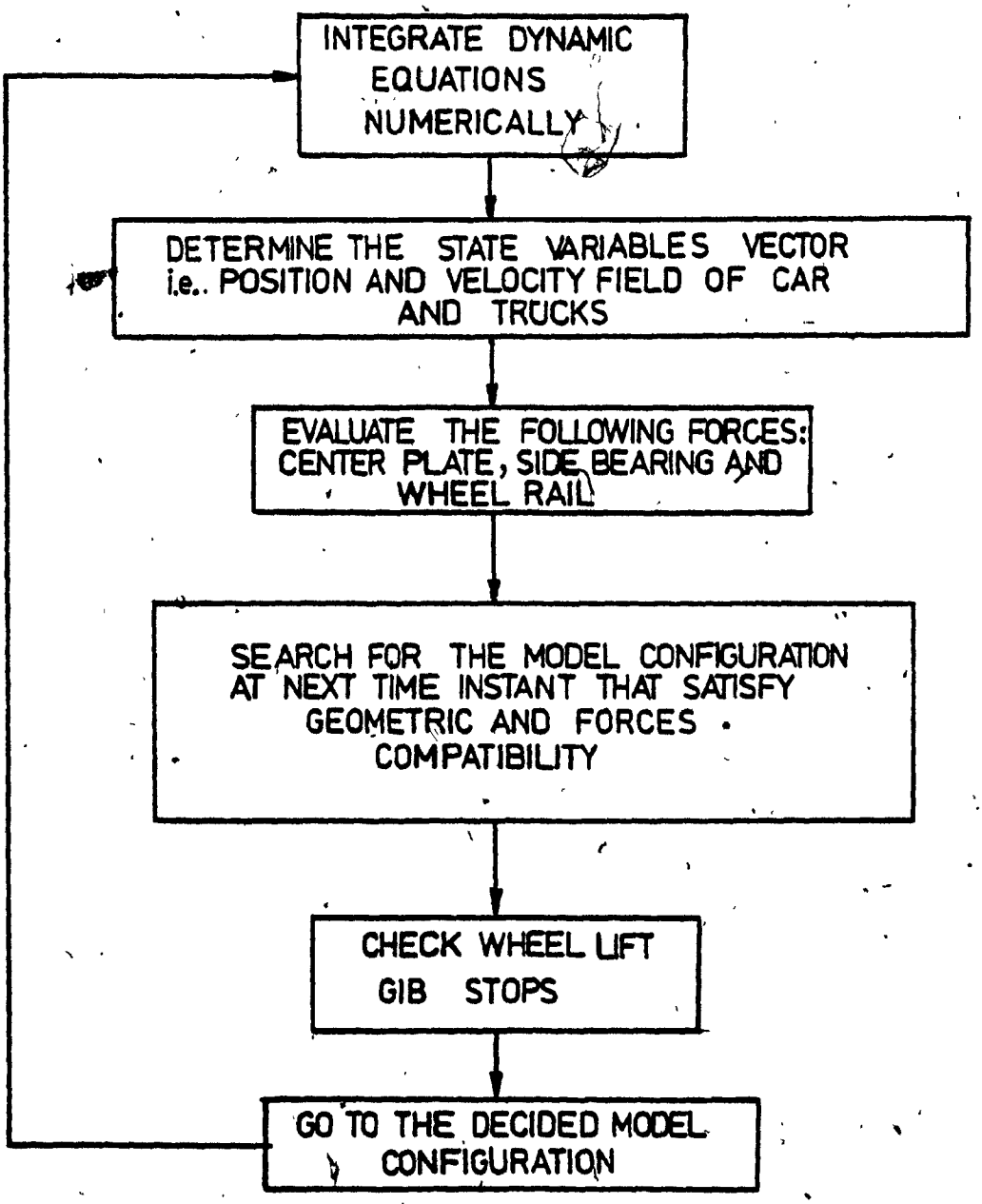

Fig. 4.5: The Numerical Procedure for Obtaining the Time Response.

iv) The series of checks described in Subsection 4.1.3 is then applied to determine the actual system configuration that satisfies the geometric and force compatibilities. Also checks for the wheel lift and gib stop contact are carried out at this stage.

The procedure described is repeated for successive t_i's and the process is terminated when t_i reach a certain predetermined final time t_f, essentially from the maximum computer time available. In this work, t_f is fixed at 15 seconds. This value is chosen to allow for describing at least some of the interesting aspects of the response that illustrate some of the dynamic phenomena associated with severe rocking in the time domain.

A listing of the computer program to execute the above procedure is given in Appendix II. Also given in this Appendix is the computer output in the form of a plot describing the car rocking response in the time domain.

4.3 System Response in the Time Domain

Typical examples of the time response obtained in this analysis are reproduced and compared with the test results reported by the Canadian National Railways [16,17]. These are given in Figs. 4.6, 4.7, 4.8 and 4.9 for an input excitation from a track cross level variation of 0.75 inch (1.905 cm). Plotted in these figures are respectively the car body rocking angle, the lateral displacement, the side bearing forces and the right wheel force. In general, it may be seen that the time responses grow from the given initial

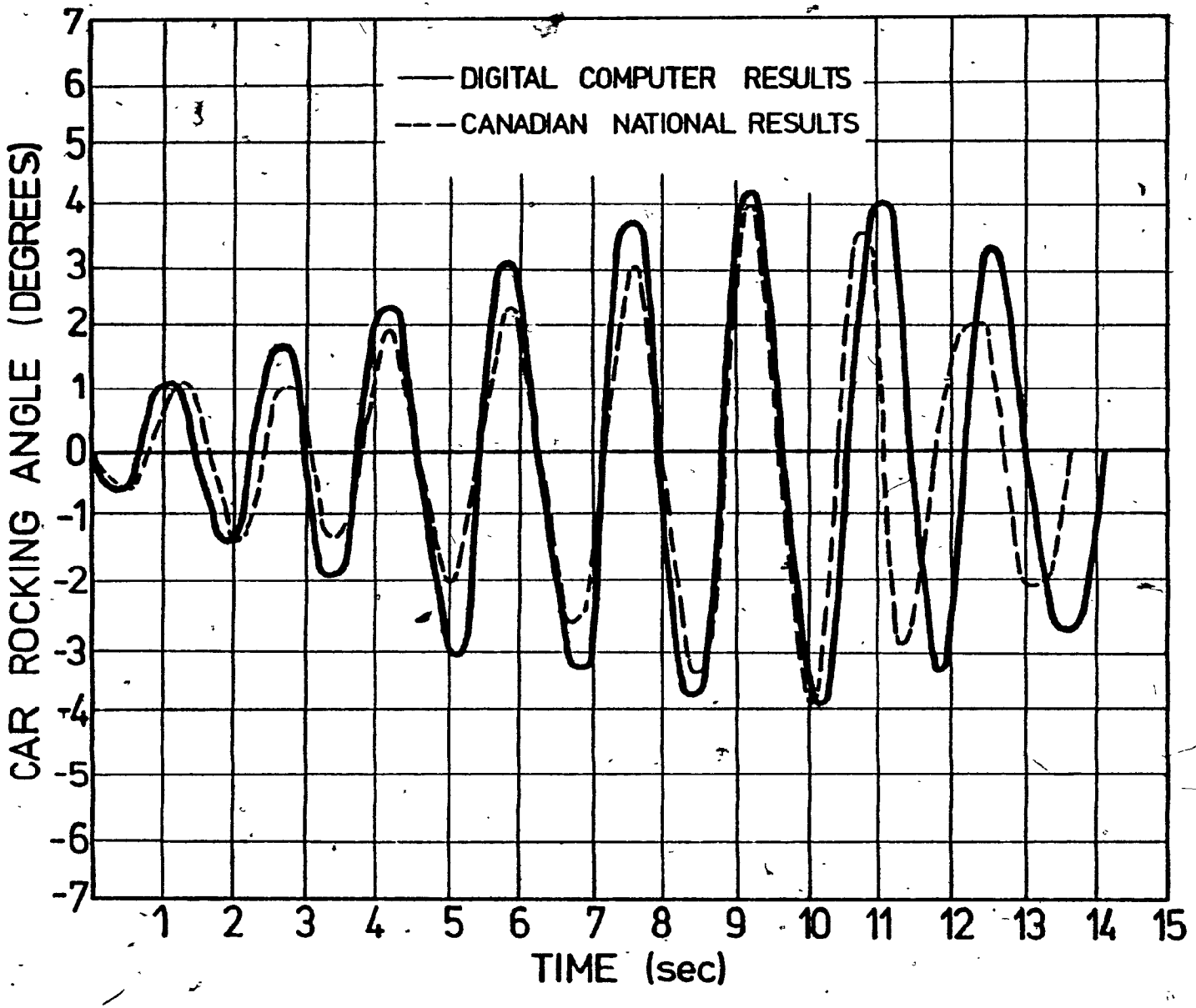

Fig. 4.6: Car Body Rocking Response at 17.5 mph (28.15 km/hr).

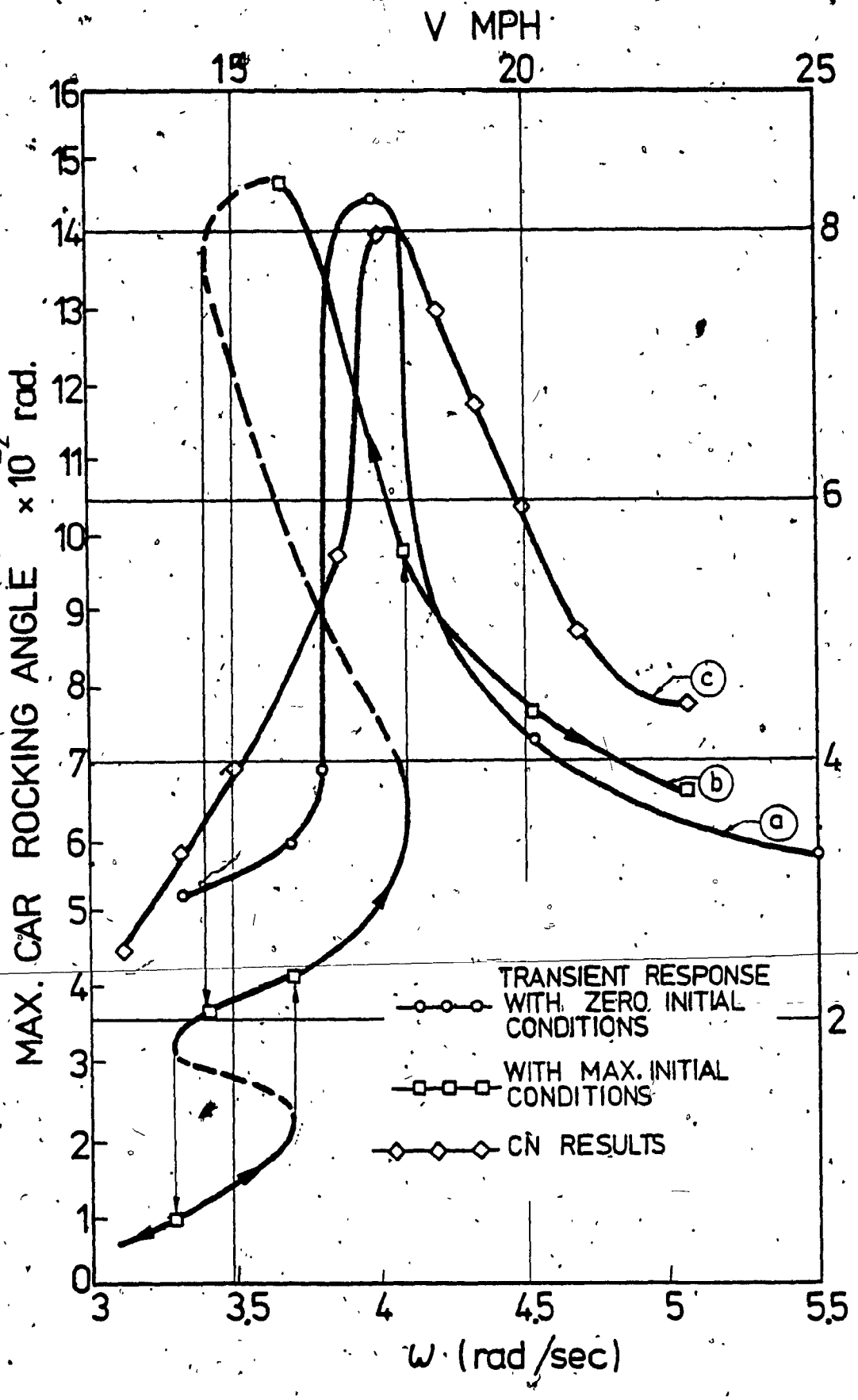

Fig. 4.10: Frequency Response of a 100-Ton Freight Car for a Track Cross Level of 0.75 in.(1.905 cm).

and analytical results. This again amply justifies the use of multiconfiguration model for this part of investigation.

4.5 Summary

In this chapter, the rocking responses of the system represented by a multiconfiguration model are evaluated in time as well as in the frequency domains. The equations of motion for the system, under a purely periodic excitation from the tracks, are derived. Utilizing a numerical integration technique, the equations are solved on a digital computer. The solution yields the vehicle time response curves which are then transformed to the frequency domain. Both time and frequency responses compare well with the measured data obtained by Canadian National. An attempt to study the vehicle steady state responses by this approach was not fully possible because of the computer time limitations. Both the steady state responses as well as transient responses can be obtained through an analog simulation of the system as given in the next chapter.

CHAPTER 5

STEADY STATE RESPONSES BASED ON THE SINGLE CONFIGURATION MODEL

CHAPTER 5

STEADY STATE RESPONSES BASED ON THE SINGLE CONFIGURATION MODEL

5.1 Introduction

In this chapter, the steady state responses of the railroad freight vehicle when subjected to purely periodic excitation from the track are studied. The steady state responses are obtained by solving the system equations of motion using analog simulation. As stated earlier, the equations of motion can be derived using the multiconfiguration model or the single configuration model, the difference being the ease of application depending on the technique used for the solution of response. For the steady state response evaluation, the single configuration model described in Chapter 2 is used. The single configuration model requires a much smaller number of components for the simulation study on the analog computer than that required for the multiconfiguration model. Though this is true in comparison, still the SCM requires a very large capacity analog computer. A simplified system consisting of only Configuration 1 in Fig. 4.1(b) had to be used to carry out a preliminary study to investigate the required computer capacity for the problem. This was done in the Analog Laboratory of Concordia University. Even this simplified model required the use of almost the full capacity of this computer. This means that the original problem requires a capacity of at least three times and therefore it was decided to use the Analog Laboratory of the National Research Council of Canada in

Ottawa. At that time, it was also intended to simulate the system when subjected to a combination of periodic and random inputs to evaluate the accuracy of the statistical linearization technique applied in Chapter 7. However, the demand on analog components for patching was so large that even at NRC this was not possible. Therefore, analog solutions are obtained for evaluating the steady state responses under periodic track excitation only.

In this chapter, the equations of motion of the single configuration model is derived using the Lagrange's technique. Analog simulation is utilized to solve the nonlinear equation of motion under periodic input from the track. From the analog solution, both the transient and the steady state parts of the responses, as defined in the previous chapter, are determined. The transient response in time domain is compared with the measured data reported by CN. From this comparison, it is evident that the single configuration model is also acceptable for a valid representation of the freight car dynamic behavior. The system behavior in time domain shows the occurrence of the sequence of beating cycles in the transient state and a harmonic rocking motion in the steady state. The steady state frequency responses are important because they can show clearly the effects of the nonlinearities in the system, especially the occurrence of the jump phenomenon between different levels of car rocking amplitude.

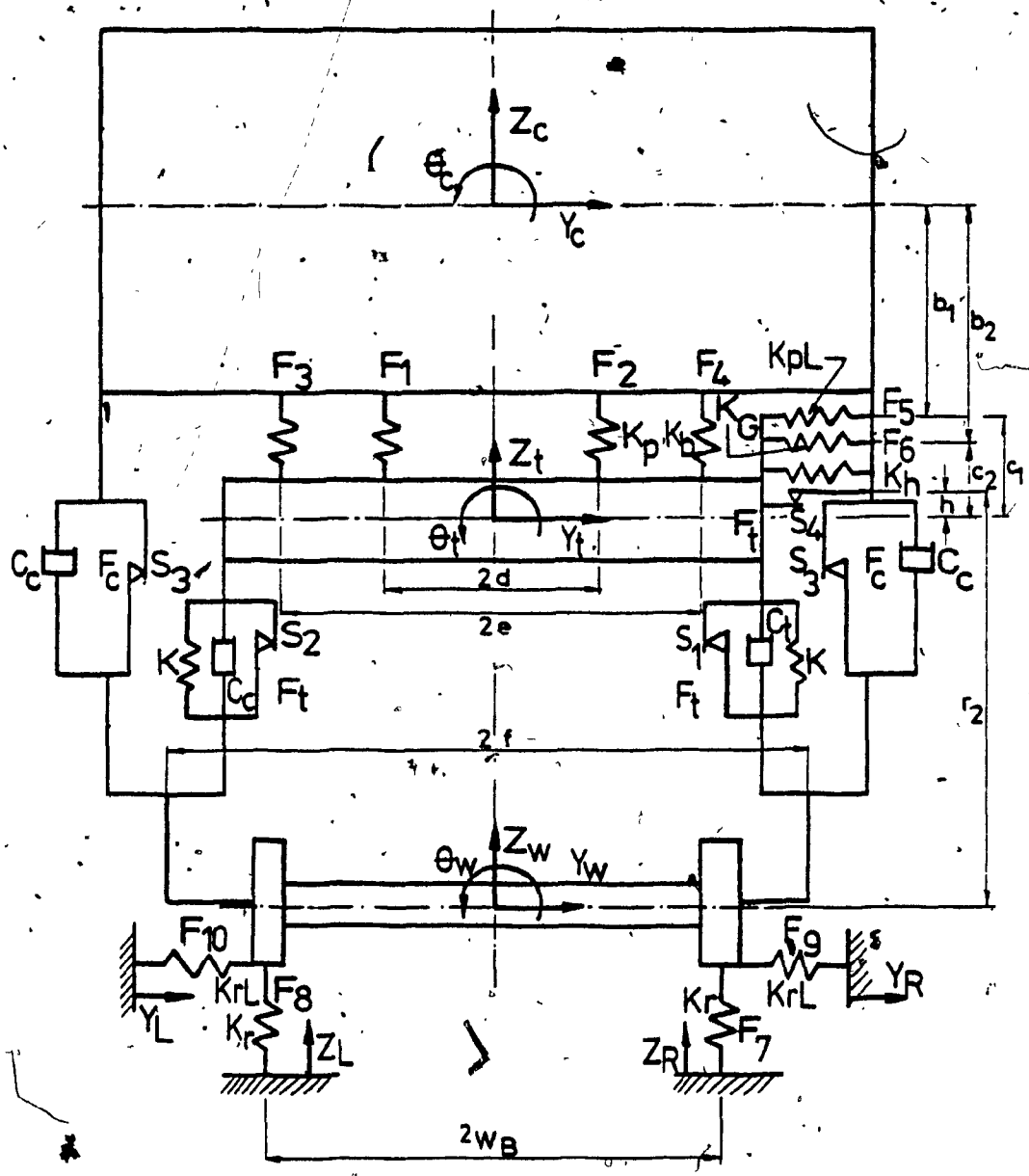

Fig. 5.1: Single Configuration Model of the Freight Vehicle.

5.2 The Equations of Motion for the Single Configuration Model

The equations of motion applicable to the nonlinear single configuration model of the railroad freight vehicle are derived in this section using the Lagrange's technique. The single configuration model shown in Fig. 5.1 was earlier described in detail in Chapter 2. The nine independent generalized coordinates required to describe the motion of this system completely are the elements of the vector $\underset{\sim}{X}$ where

$$\underset{\sim}{X}^T = [Z_c, Y_c, \theta_c, Z_t, Y_t, \theta_t, Z_w, Y_w, \theta_w]$$

The energy expressions needed for the Lagrange's equations are derived and expressed in the following manner:

The kinetic energy, T, of the system is given by

$$T = \frac{1}{2} M_c \dot{Z}_c^2 + \frac{1}{2} M_c \dot{Y}_c^2 + \frac{1}{2} I_c \dot{\theta}_c^2 + \frac{1}{2} M_t \dot{Z}_t^2 + \frac{1}{2} M_t \dot{Y}_t^2 + \frac{1}{2} I_t \dot{\theta}_t^2 + \frac{1}{2} M_w \dot{Z}_w^2 + \frac{1}{2} M_w \dot{Y}_w^2 + \frac{1}{2} I_w \dot{\theta}_w^2 \quad (5.1)$$

The total potential energy, V, of the system is

$$V = V_L + \sum_{i=1}^{10} \frac{1}{2} F_i z_i \quad (5.2)$$

where V_L is the potential energy due to the linear elements in the system alone, and $\sum_{i=1}^{10} \frac{1}{2} F_i z_i$ is the work done by the nonlinear spring forces, F_i, undergoing deflections, z_i, respectively. V_L is obtained in the form:

$$V_L = \frac{1}{2} K(Z_t + f\theta_t - Z_w - f\theta_w)^2 + \frac{1}{2} K(Z_t - f\theta_t - Z_w + f\theta_w)^2 + \frac{1}{2} K_h(Y_t - h\theta_t - Y_w + r_2\theta_w)^2 \quad (5.3)$$

by recalling the different nonlinear spring characteristics in Fig. 2.5. Derived expressions for all F_i and Z_i are given in Table 5.1.

Rayleigh's dissipation function, D, of the system is:

$$D = \frac{1}{2} C_t(\dot{Z}_t+f\dot{\theta}_t-\dot{Z}_w-f\dot{\theta}_w)^2 + \frac{1}{2} C_t(\dot{Z}_t-f\dot{\theta}_t-\dot{Z}_w+f\dot{\theta}_w)^2 + \frac{1}{2} C_c(\dot{Z}_c+f\dot{\theta}_c-\dot{Z}_w-f\dot{\theta}_w)^2 + \frac{1}{2} C_c(\dot{Z}_c-f\dot{\theta}_c-\dot{Z}_w+f\dot{\theta}_w)^2 \quad (5.4)$$

The virtual work, δW, done by the gravitational and the friction forces of the system is calculated as:

$$\delta W = - M_c g\delta Z_c - M_t g\delta Z_t - M_w g\delta Z_w - F_t s_1 \delta(Z_t+f\theta_t-Z_w-f\theta_w) - F_t s_2 \delta(Z_t-f\theta_t-Z_w+f\theta_w) - F_c s_3 \delta(2f\theta_c-2f\theta_t) - F_t s_4 \delta(Y_t-h\theta_t-Y_w+r_2\theta_w) \quad (5.5)$$

Employing the Lagrange's equation in the form:

$$\frac{d}{dt}\left(\frac{\partial T}{\partial \dot{q}_i}\right) + \frac{\partial V}{\partial q_i} + \frac{\partial D}{\partial \dot{q}_i} = \frac{\delta W}{\delta q_i}, \quad i = 1,2,3,\ldots.9 \quad (5.6)$$

where q_i's are the independent generalized coordinates (i.e. the elements of $\underset{\sim}{X}$) and using the energy expressions given above, the equations of motion are derived. The set of equations of motion are solved by analog simulation to yield the vehicle responses in the time domain. Details of the method of solution are presented in the next section.

5.3 Method of Solution

The programming procedure for the analog simulation can be summarized as follows:

i) Each of the differential equations is rewritten to give

Description	Force	Deflection	Presentation	Nonlinear Term
Left Centre Plate	$F_1(z_1)=K_p z_1 S_1(z_1)$	$z_1=Z_c-d\theta_c-Z_t+d\theta_t$		$S_1(z_1)=\begin{cases}0 & \text{if } z_1>0\\ 1 & \text{if } z_1<0\end{cases}$
Right Centre Plate	$F_2(z_2)=K_p z_2 S_2(z_2)$	$z_2=Z_c+d\theta_c-Z_t-d\theta_t$	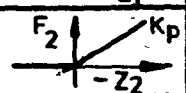	$S_2(z_2)=\begin{cases}0 & \text{if } z_2>0\\ 1 & \text{if } z_2<0\end{cases}$
Left Side Bearing	$F_3(z_3)=K_b(z_3+z_{30})S_3(z_3)$	$z_3=Z_c-e\theta_c-Z_t+e\theta_t$	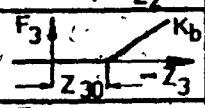	$S_3(z_3)=\begin{cases}0 & \text{if } (z_3+z_{30})>0\\ 1 & \text{if } (z_3+z_{30})<0\end{cases}$
Right Side Bearing	$F_4(z_4)=K_b(z_4+z_{40})S_4(z_4)$	$z_4=Z_c+e\theta_c-Z_t-e\theta_t$	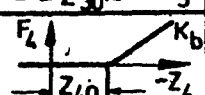	$S_4(z_4)=\begin{cases}0 & \text{if } z_4+z_{40}>0\\ 1 & \text{if } z_4+z_{40}<0\end{cases}$
Lateral Side Bearing	$F_5(z_5)=K_{pL} z_5 S_5(z_5)$	$z_5=Y_c+b_1\theta_c-Y_t+C_1\theta_t$	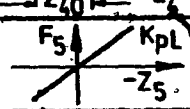	$S_5(z_5)=1$
Gib Stop	$F_6(z_6)=K_G(z_6-z_{60}\cdot Sgnz_6)S_6(z_6)$	$z_6=Y_c+b_2\theta_c-Y_t+C_2\theta_t$		$S_6(z_6)=\begin{cases}0 & \text{if } z_{60}>z_6>-z_{60}\\ 1 & \text{if } -z_{60}>z_6>z_{60}\end{cases}$
Right Rail Vertical	$F_7(z_7)=K_r z_7 S_7(z_7)$	$z_7=Z_w+W_B\theta_w-Z_R$	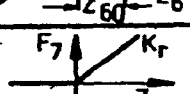	$S_7(z_7)=\begin{cases}0 & \text{if } z_7>0\\ 1 & \text{if } z_7<0\end{cases}$
Left Rail Vertical	$F_8(z_8)=K_r z_8 S_8(z_8)$	$z_8=Z_w-W_B\theta_w-Z_L$	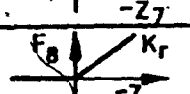	$S_8(z_8)=\begin{cases}0 & \text{if } z_8>0\\ 1 & \text{if } z_8<0\end{cases}$
Right Rail Lateral	$F_9(z_9)=K_{rL} z_9 S_9(z_9)$	$z_9=Y_R-Y_w-r_1\theta_w$	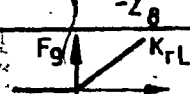	$S_9(z_9)=\begin{cases}0 & \text{if } z_9>0\\ 1 & \text{if } z_9<0\end{cases}$
Left Rail Lateral	$F_{10}(z_{10})=K_{rL} z_{10} S_{10}(z_{10})$	$z_{10}=Y_L-Y_w-r_1\theta_w$	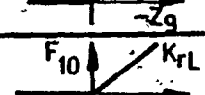	$S_{10}(z_{10})=\begin{cases}0 & \text{if } z_{10}>0\\ 1 & \text{if } z_{10}<0\end{cases}$

Table 5.1. The Nonlinear Spring Forces F_i, and the Corresponding Deflections z_i.

an expression for its highest order derivative. The resulting equations give the system accelerations in terms of the subsequent lower order derivatives and the dependent variables.

ii) A sketch of the unscaled circuit diagram is drawn from the acceleration equations in (i). The diagram shows the operational amplifiers, potentiometers, nonlinear components, auxiliary equipment and interconnections necessary to form the computer circuits analogous to the equations in (i). These steps are given in detail in Subsection 5.3.1.

iii) The maximum anticipated values of the physical parameters and the state variables appearing in the problem are estimated. From these maxima, appropriate scale factors are introduced into the equations in (i) and the circuit elements in (ii) to form the scaled circuit diagram. The scaling procedures are given in detail in Subsection 5.3.2.

iv) The standard static checks are carried out on the scaled circuit after it has been patched onto the analog computer. From these static checks, the programming errors and component malfunctions can be detected and corrected. This is also described in detail in Subsection 5.3.3.

5.3.1 Rearrangement of the Equations of Motion

The equations of motion derived in Section 5.2 can be restated in a form suitable for analog simulation by solving for the highest order derivatives. The expressions for the different

accelerations for the car are given in the following manner:

Car vertical acceleration, $\ddot{Z}_c = [-(F_1+F_2+F_3+F_4) - 2C_c\dot{Z}_c + 2C_c\dot{Z}_w]/M_c - g$

Car lateral acceleration, $\ddot{Y}_c = -[F_5+F_6]/M_c$

Car rocking acceleration, $\ddot{\theta}_c = [(F_1-F_2)d + (F_3-F_4)e - F_5b_1 - F_6b_2 - 2C_tf^2\dot{\theta}_c + 2C_cf^2\dot{\theta}_w - 2F_cfs_3]/I_c$

Bolster vertical acceleration, $\ddot{Z}_t = [-2KZ_t + 2KZ_w - 2C_t\dot{Z}_t + 2C_t\dot{Z}_w + F_1+F_2+F_3+F_4 - F_ts_1 - F_ts_2]/M_t - g$

Bolster lateral acceleration, $\ddot{Y}_t = [-K_hY_t + hK_h\theta_t + k_hY_w - r_2K_h\theta_w + F_5 + F_6 - F_ts_4]/M_t$

Bolster rotational acceleration, $\ddot{\theta}_t = [-2Kf^2\theta_t + 2Kf^2\theta_w + K_hhY_t - K_hh^2\theta_t - K_hhY_w + K_hr_2h\theta_w - F_1d + F_2d - F_3e + F_4e - F_5C_1 - F_6C_2 - 2C_tf^2(\theta_t-\theta_w) - F_ts_1f + F_ts_2f + F_ts_4h]/I_t$

Wheelset vertical acceleration, $\ddot{Z}_w = [-2KZ_w + 2KZ_t - F_7 - F_8 - 2C_t\dot{Z}_w - 2C_c\dot{Z}_w + 2C_t\dot{Z}_t + 2C_c\dot{Z}_c + F_ts_1 + F_ts_2]/M_w - g$

Wheelset lateral acceleration, $\ddot{Y}_w = [-K_hY_w + K_hY_t - K_hh\theta_t + F_ts_4 + K_hr_2\theta_w + F_9 + F_{10}]/M_w$

Wheelset rotational acceleration, $\ddot{\theta}_w = [-2Kf^2\theta_w + 2Kf^2\theta_t - F_7W_B + F_8W_B - 2C_tf^2\dot{\theta}_w - 2C_cf^2\dot{\theta}_w + 2C_tf^2\dot{\theta}_t + 2C_cf^2\dot{\theta}_c + F_ts_1f - F_ts_2f + 2F_cfs_3 + F_ts_4r_2 - r_2K_hY_t + r_2K_hh\theta_t + r_2K_hY_w + r_2^2K_h\theta_w + F_9r_1 + F_{10}r_1]/I_w$

In these expressions

$$s_1 = \mathrm{Sgn}(\dot{Z}_t + f\dot{\theta}_t - \dot{Z}_w - f\dot{\theta}_w) ,$$
$$s_2 = \mathrm{Sgn}(\dot{Z}_t - f\dot{\theta}_t - \dot{Z}_w + f\dot{\theta}_w) , \qquad (5.7)$$
$$s_3 = \mathrm{Sgn}(2f\dot{\theta}_c - 2f\dot{\theta}_t) ,$$
$$s_4 = \mathrm{Sgn}(\dot{Y}_t - h\dot{\theta}_t - \dot{Y}_w + r_2\dot{\theta}_w)$$

and the forcing functions in the form of rectified harmonic waves are given by

$$Z_R = Z_{RO}\left|\sin\frac{\omega t}{2}\right|, \quad Z_L = Z_{LO}\left|\cos\frac{\omega t}{2}\right| \qquad (5.8)$$
$$Y_R = Y_{RO}\left|\sin\frac{\omega t}{2}\right|, \quad Y_L = Y_{LO}\left|\cos\frac{\omega t}{2}\right| .$$

The above equations are used for drawing the unscaled computer diagram using the Kelving feedback method [59]. The linear parts of the equations are modeled by linear components like potentiometers, invertors, summers and integrators as shown in Fig.5.2. The nonlinear friction damper forces are modeled through diode or bang-bang circuits (amplifiers 11,21,31 and 41 in Fig. 5.3). The forces due to nonlinear springs are modeled through limiters or relay dead-zone circuits with limiters [59] as indicated in Fig. 5.3. The forcing function in the form of rectified harmonic waves are modeled through explicit function generators and limiters [59] seen in Fig. 5.3.

5.3.2 Computer Scaling

Before setting the above equations on the computer circuit, it is convenient to scale each of the dependent variables in terms of voltage. For example, the vertical car displacement $Z_c(t)$ may be scaled such that 10 volts equal 10 inch (25.4 cm) of displacement.

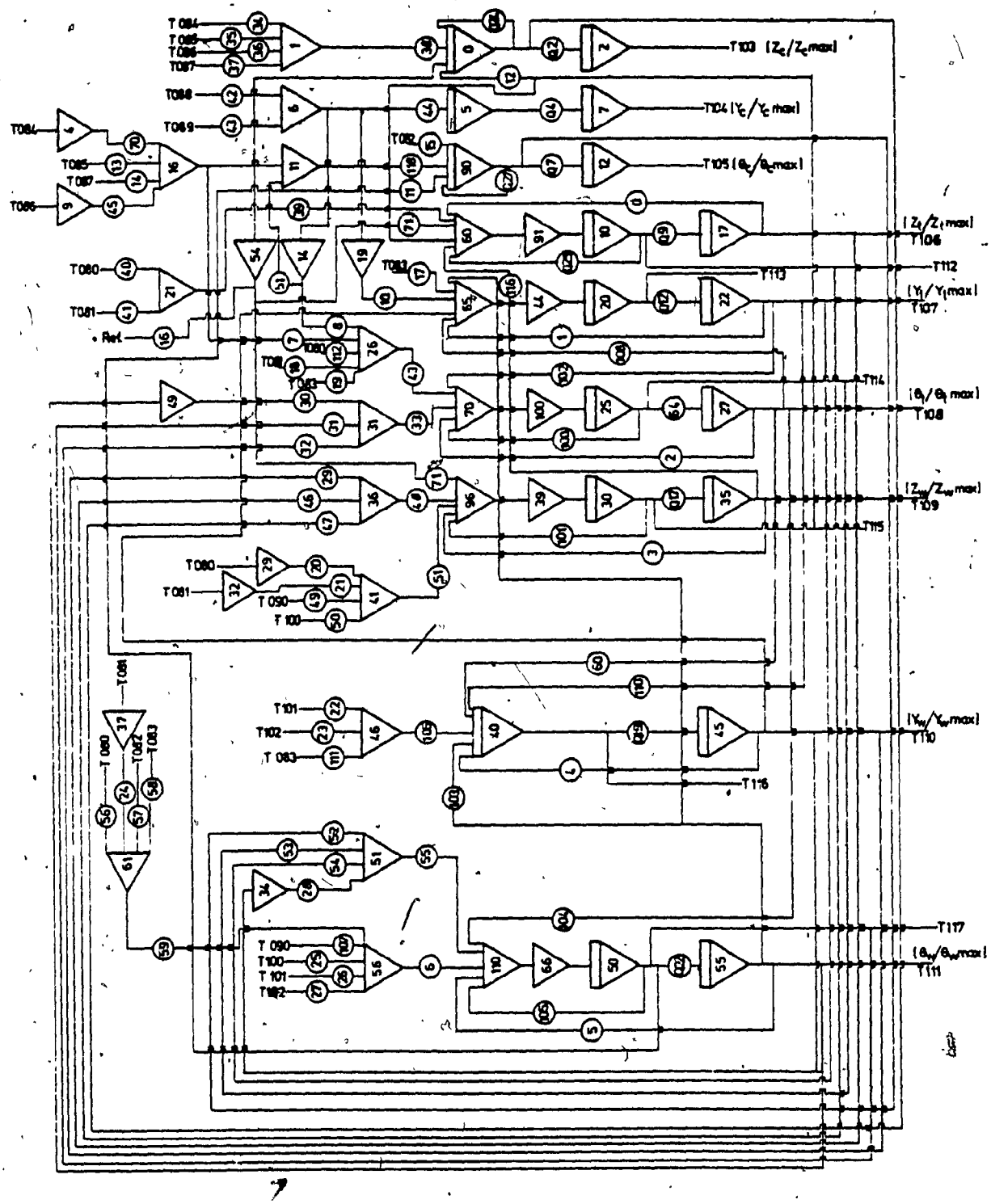

Fig. 5.2: The Scaled Circuit Diagram Representing the Linear Part of the Equations of Motion.

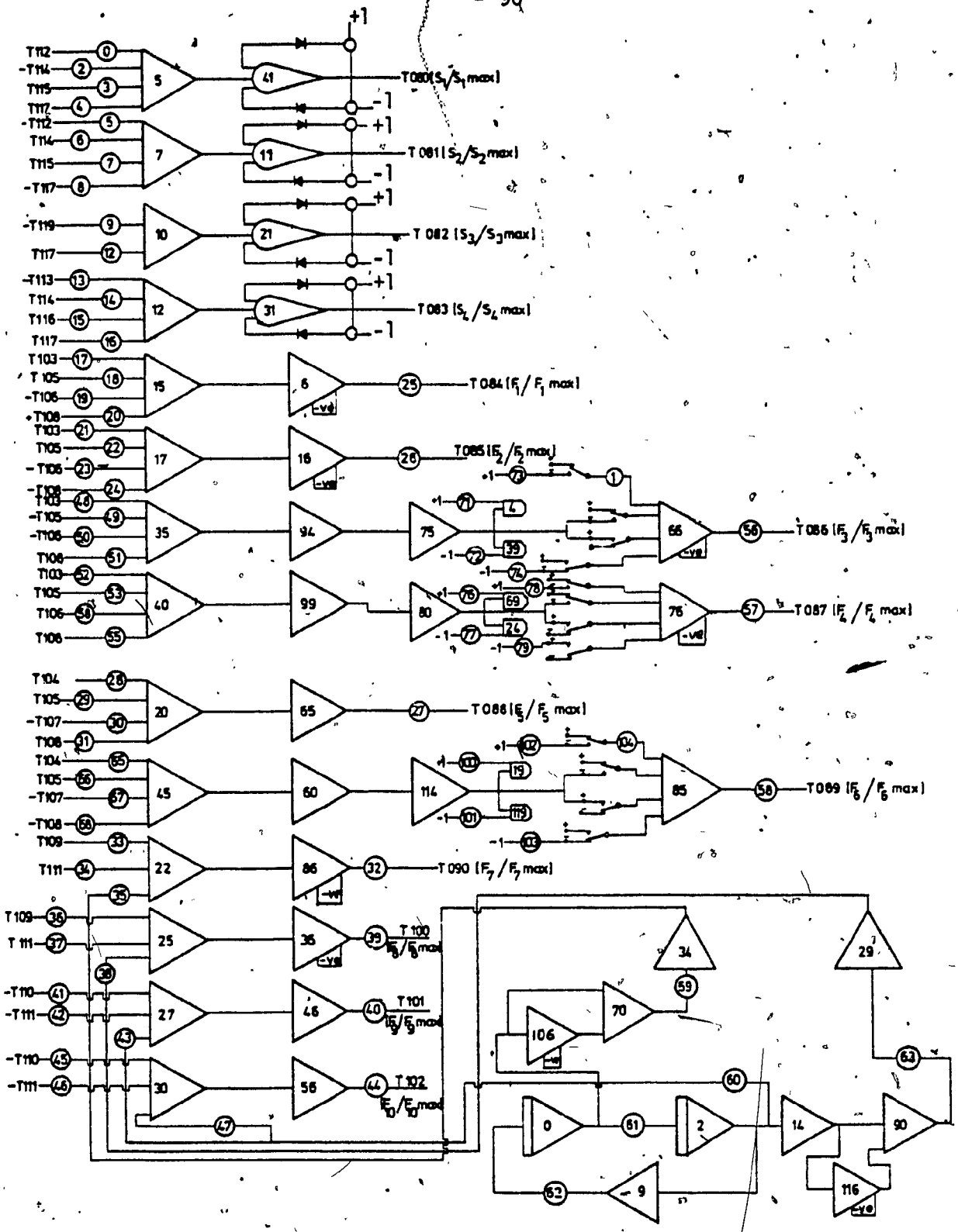

Fig. 5.3: The Scaled Circuit Diagram Representing the Friction Damper Forces, Nonlinear Spring Forces and Forcing Function in the Form of Rectified Harmonic Waves.

The scaling factors to be used will depend on the given problem and the voltage limit of the computer (10 volts in this case). The amplitude scaling of the system is carried out through the following steps:

i) all the physical model parameters are defined and listed as given in Computer Program Appendix III.

ii) maxima of the system variables (velocities and displacements) are estimated to permit a suitable scaling transformation,

iii) the values of the computer variables that are always less than 10 volts are estimated from the maxima of the problem variables in (ii),

iv) from the computer variables in (iii) the system equations are rewritten to account for the scale factors.

It is also necessary to perform a proper time scaling. For the problem under investigation, it was found convenient to utilize a scale factor of 100, that is, the dynamics of the railroad vehicle is slowed down 100 times. This factor makes most of the integrator gains reasonable (either 1 or 10). The scaled computer circuit representing the complete system is given in detail in Figs. 5.2 and 5.3. The scaled circuit diagram is written in terms of the problem parameters instead of the numerical values to allow for an easy variation of any parameter while carrying out a parametric sensitivity study. Because of the large number of potentiometers employed in the scaled circuit in Figs 5.2 and 5.3, a digital computer program is used to set these potentiometers automatically. A listing of this

digital computer program is given in Appendix- III. The listing includes the values of the system parameters, the potentiometer settings and the gains of each amplifier in the circuit diagram shown in Figs. 5.2 and 5.3.

The scaled circuit was patched on an EAI 680 analog computer in the Analog Laboratory of the National Research Council of Canada. The patching required the use of almost all the analog components available for this large computer.

5.3.2 Static Check

Two standard checks are used for detecting any programming errors and component malfunctions. They are:

i) a program check, to determine whether the program, i.e. the circuit diagram and the digital computer program for setting the potentiometers, actually represents the original equations given in Subsection 5.3.1.

ii) a circuit check, to determine whether the actual computer set up corresponds to the program formulated. The circuit check should detect sources of error like mis-patching, faulty components, etc.

In the program check, the first step is to assume a set of arbitrary values for all the integrator outputs (velocities and displacements) and to use these as the problem variables. The corresponding computer variables are obtained by scaling these problem variables. Appendix III lists the scaling factors used in the check. Using these, two sets of calculations for the values of

Variable	$\ddot{Z}_c$	$\ddot{Y}_c$	$\ddot{\theta}_c$	$\ddot{Z}_t$	$\ddot{Y}_t$	$\ddot{\theta}_t$	$\ddot{Z}_w$	$\ddot{Y}_w$	$\ddot{\theta}_w$
Calculated from the problem	+793.5	-3.92×10^3	-92.4	-1.49×10^5	$+3.65 \times 10^5$	-1.8×10^3	-384.75	$+6.5 \times 10^3$	-151.27
Calculated from the program	+796.48	-3.66×10^3	-87.45	-1.42×10^5	$+3.56 \times 10^5$	-1.46×10^3	-384.00	$+6.8 \times 10^3$	-149.04

Table 5.2. Program Check - Results of Two Sets of Calculations

Amplifier No.	Output Variable	Calculated Derivative	Measured Derivative
D00	$[\ddot{Z}_c/75]$	0.1158	0.1133
D02	$[-\dot{Z}_c/10]$	-0.0249	-0.0251
D05	$[\ddot{Y}_c/150]$	-0.157	-0.157
D07	$[-\dot{Y}_c/20]$	-0.0249	-0.0249
D90	$[\ddot{\theta}_c/3.5]$	-0.163	-0.163
D12	$[-\dot{\theta}_c/0.25]$	-0.0399	-0.04
D10	$[\ddot{Z}_t/75]$	+0.1995	+0.1975
D17	$[-\dot{Z}_t/10]$	-0.0249	-0.025
D20/10	$[\ddot{Y}_t/150]$	-0.985	-0.983
D22	$[-\dot{Y}_t/20$	-0.015	-0.0148
D25	$[\ddot{\theta}_t/3.5]$	+0.0505	+0.0500
D27	$[-\dot{\theta}_t/0.25]$	-0.02998	-0.0296
D30	$[\ddot{Z}_w/75]$	-0.0513	-0.0512
D35	$[-\dot{Z}_w/10]$	-0.0249	-0.0249
D40/10	$[\ddot{Y}_w/150]$	-0.3126	-0.3188
D45	$[-\dot{Y}_w/20]$	-0.00499	-0.0049
D50/10	$[\ddot{\theta}_w/3.5]$	-0.3678	-0.3670
D55	$[-\dot{\theta}_w/0.25]$	-0.0199	-0.0199

Table 5.3. The Circuit Check Results (Refer to Fig. 5.2 for Amplifier Numbers).

the acceleration are made; the first one from the original equations given in Subsection 5.3.1 and the other from the program. The results of the two sets of calculations are compared after correcting for all the detected errors as seen from Table 5.2. The close agreement reflects the program accuracy of the simulation program.

After the program check is completed, the list of amplifier outputs and integrator derivatives are used for the circuit check. This is made on the computer by establishing the appropriate initial conditions, measuring all amplifier outputs, and comparing the measured values with the previously calculated values.

Table 5.3 shows this comparison after correcting for all the circuit errors detected and the good agreement between the values shows the accuracy of the circuit.

5.4 System Response in the Time Domain

Time responses of the system were recorded before at and after the critical speed. The resonance frequency, ω_{cr}, of the system is found to be 3.5 rad/sec which corresponds to a vehicle speed of 15 mph (24.14 km/hr). At each exciting frequency specified, the vertical and lateral displacements of the car body and the rocking angles of the car and truck are recorded. Setting the initial conditions for the system to be zero a set of transient time response plots were obtained as shown in Fig. 5.4 ($\omega < \omega_{cr}$), Fig. 5.5 ($\omega = \omega_c$) and Fig. 5.7 ($\omega > \omega_c$). These graphs also include the left rail periodic excitation and the track cross level waveform.

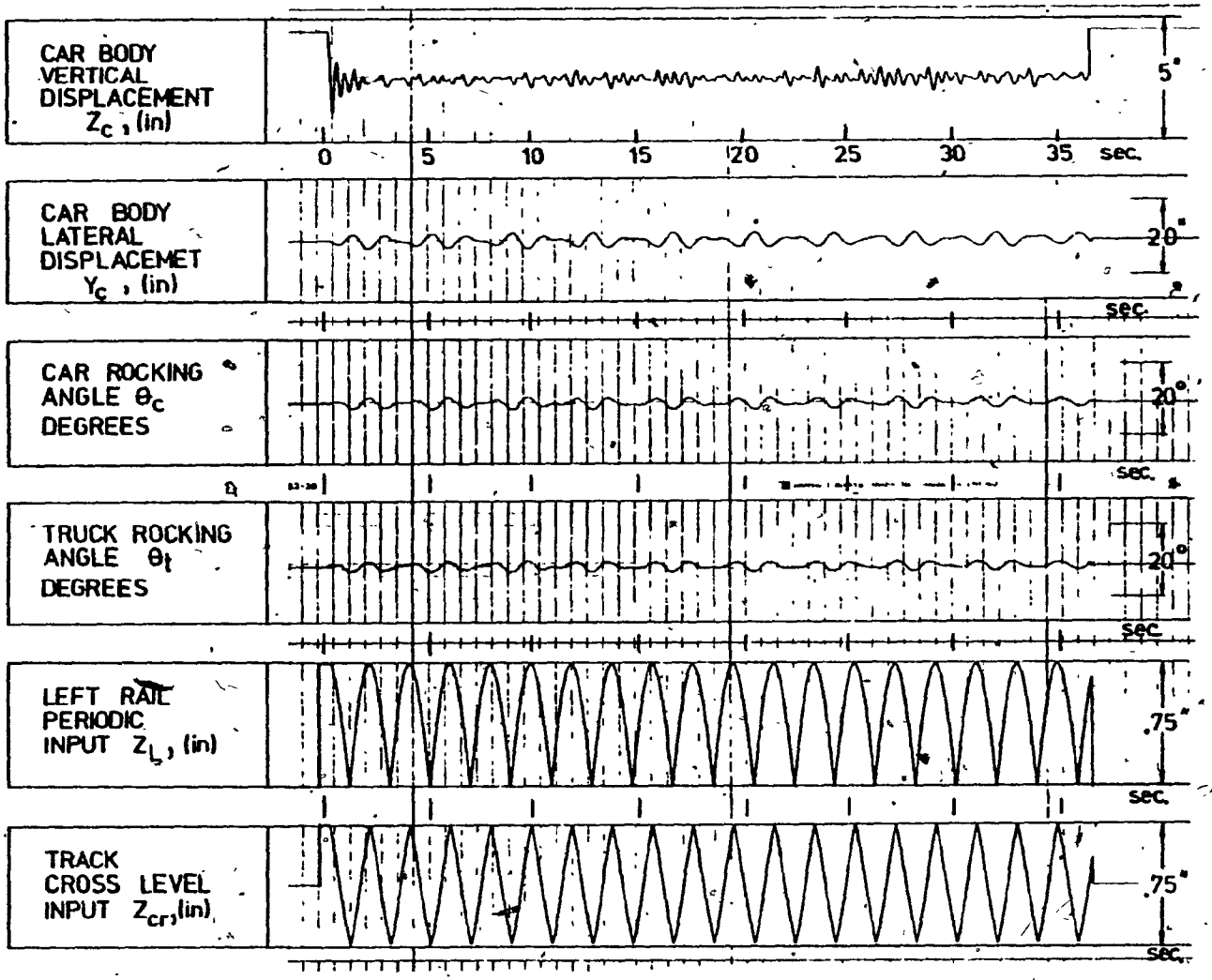

Fig. 5.4: Time Responses (Before Resonance) at 10 mph (16.09 km/hr).

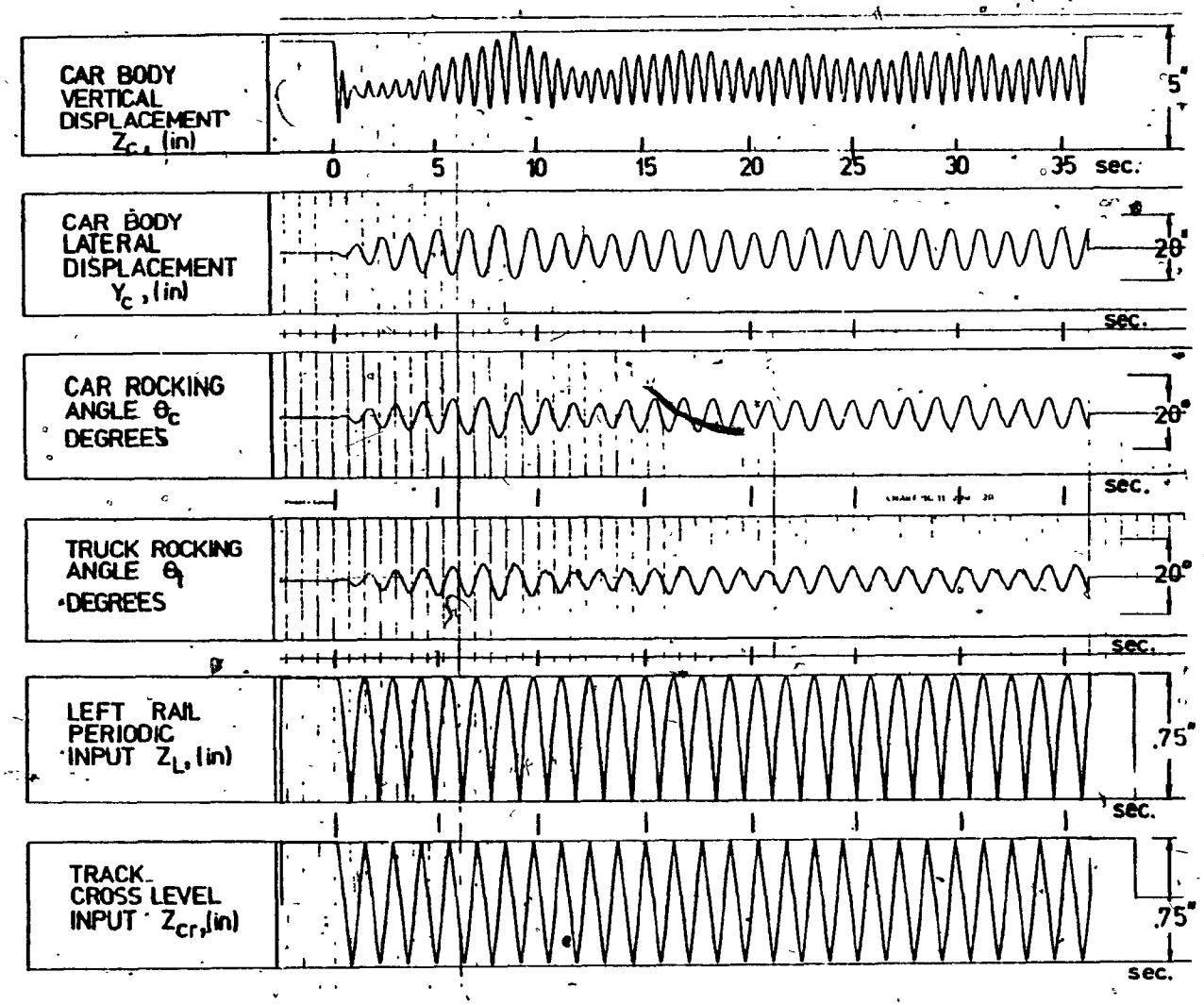

Fig. 5.5: Time Responses (At Resonance) at 15 mph (24.13 km/hr).

In addition, sample records indicating the variation of the forces transmitted by the centre plate and the side bearing are also obtained for critical speed and shown in Fig. 5.6.

Figure 5.4 shows a typical time response of the system at a vehicle speed of 10 mph (16 km/hr) which corresponds to an exciting frequency of 2.4 rad/sec. This represents the response before the system enters the resonance condition, when a small rocking amplitude of the order of ±1.4 degrees occurs. It can be seen from Fig. 5.4 that the car rocking response is in phase with the input track cross level excitation. From the record of the forces at that frequency, it is found that there is no occurrence of either wheel lift or gib contact. The nature of the car responses for all the speeds before entering into the resonance speed are similar to those described here and also previously as light rocking in Chapter 2.

In Fig. 5.5, the system responses are given for the resonance speed 15 mph (24.14 km/hr). Generally, it can be seen that all the responses are built up reaching maximum values after about 9 seconds from the start, and then decay indicating a sequence of beating action. This beating action repeats itself for at least ten cycles and then the vehicle enters a steady state. At the resonant speed, the car angular displacement reaches a maximum aplitude of ±5.5 degrees and has a phase shift of $\pi/2$ radians with respect to the input track cross level. The magnitude of the car vertical displacement reaches ±1.5 inch (3.81 cm), and the lateral displacement increases up to ±8 inches (20.3 cm).

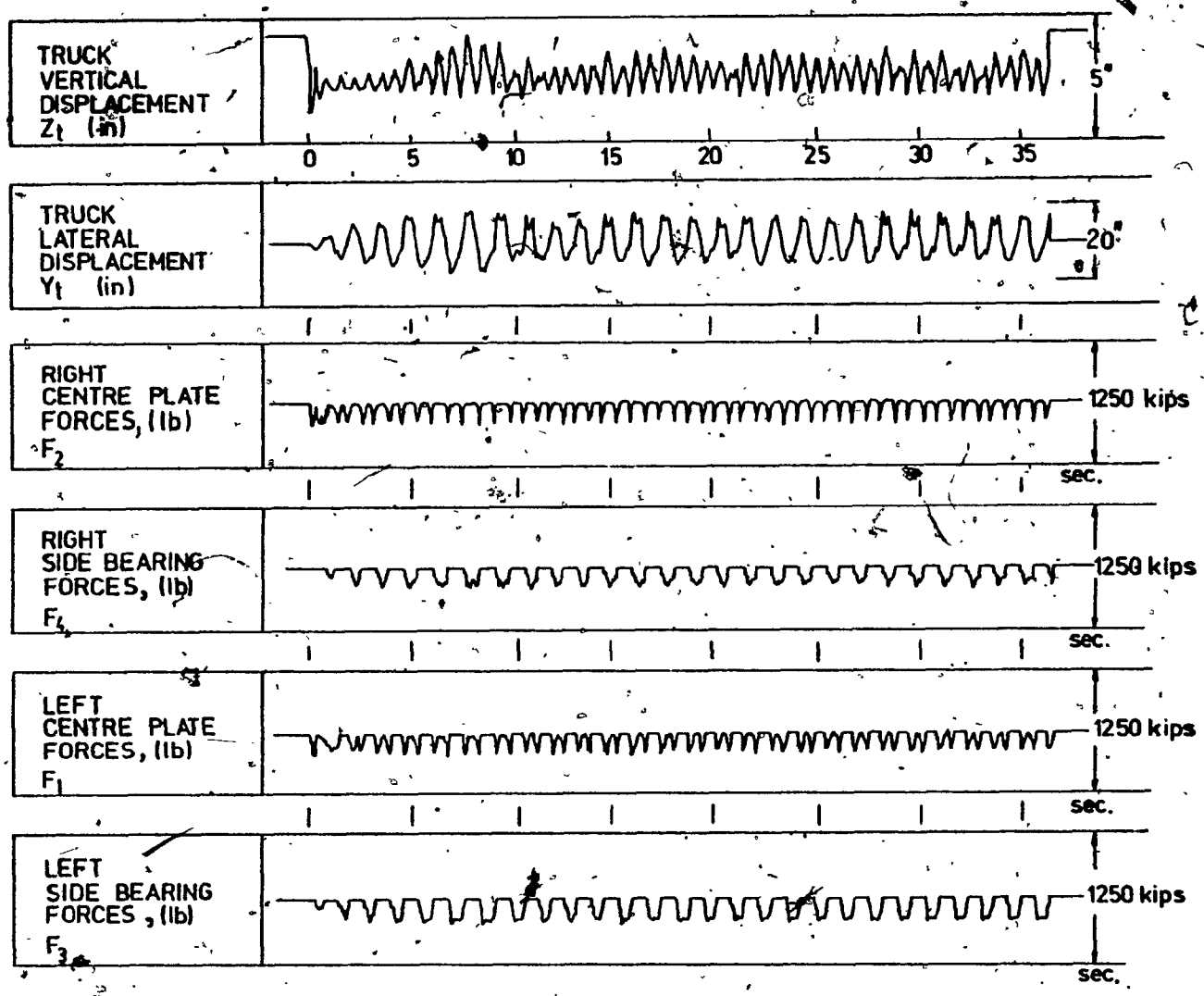

Fig. 5.6: Time History of the Car Body-Bolster Interaction Forces at Resonance Speed 15 mph (24.13 km/hr).

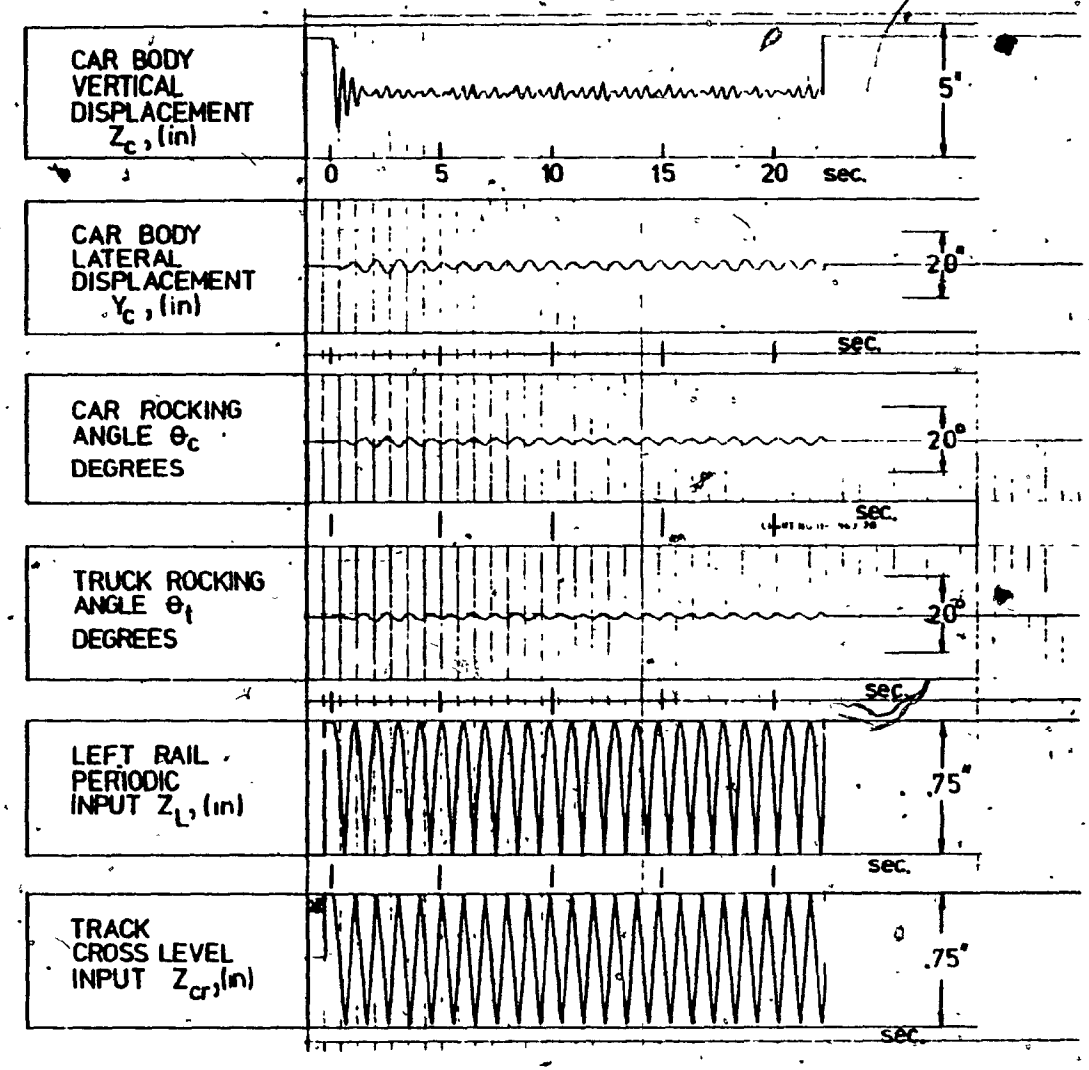

Fig. 5.7: Time Responses (After Resonance) at 20 mph (32.18 km/hr).

The forces interacting between the car body and the bolster, at the critical frequency ω_{cr}, are recorded and shown in Fig. 5.6. The plots describe the effect of the geometric nonlinearities present in the system due to separation of the car body from the centre plate and contact with the side bearings at each rocking cycle. The centre plate dynamic forces shown in the figure approach 2.5 times the nominal static force levels and the side bearing forces grow to 220 kips (978.5 kN). Figure 5.7 shows the vehicle responses at 20 mph (32.2 km/hr) after passing the critical speed. The responses here show evidently light rocking condition with no side bearing contact or centre plate separation.

The experimental records obtained in the field by the Canadian National Railways [16] are given in Fig. 5.8 so that a comparison with the present results can be made. The vehicle used in the CN test has a resonance speed of 17.5 mph (28.1 km/hr) which is higher than the critical speed 15 mph (24.1 km/hr) for the analytical model. This may be due to the introduction of the additional stiffness elements in the single configuration model to simulate the different nonlinear separation effects. These additional stiffnesses make the overall system stiffness softer and therefore lead to a lower resonance frequency for the system. Since the response of the system is highly sensitive to the initial conditions and to the frequency of excitation specified, a one to one comparison between points on the plots and the CN results is difficult to establish because the initial conditions for the CN findings are not known. However, a comparison

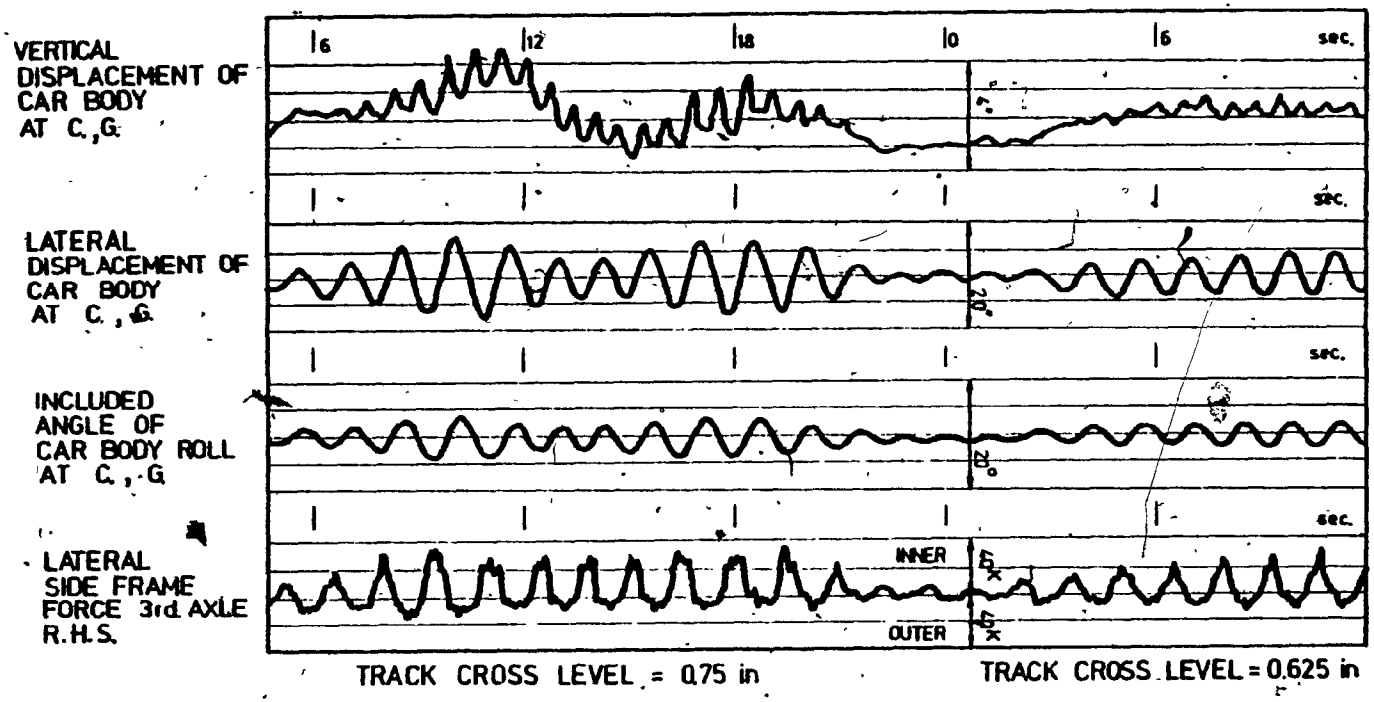

Fig. 5.8: Experimental Results Obtained by the Canadian National Railways at Resonant Speed [16].

of the general trend of the waveform of the responses as well as their maximum values shows a close agreement.

5.5 The Frequency Response

A complete information on the behavior of the vehicle at the critical range of speed from 8.5 to 25 mph (13.6 to 40.2 km/hr) can be obtained only through the steady state frequency response plots for the system. In order to obtain this, it is necessary to have the time records of the response with initial conditions corresponding to the maximum car rocking amplitude for every exciting frequency within the range mentioned above. This range of speed has been chosen in order to cover the range of frequencies at which excessive rocking has been previously reported. In this procedure, the input frequency is fixed at the lowest value of the critical range and the time response record is obtained until a steady state is reached. The maximum amplitude of the car rocking θ_c is obtained and the values of all the other parameters of the system for that instant are obtained and used as initial conditions for the next input frequency increment. This procedure is repeated for all the frequency increments until the upper limit of the critical speed range is reached. In order to investigate all the stable regions of the response curve, the input frequency had to be adjusted in both the directions through the entire frequency range of interest, i.e. by both increasing and decreasing the input frequency values. Sample records obtained through this process are shown in Figs. 5.9 and 5.10. In all the cases, the maximum amplitude of the steady state car rocking was recorded and

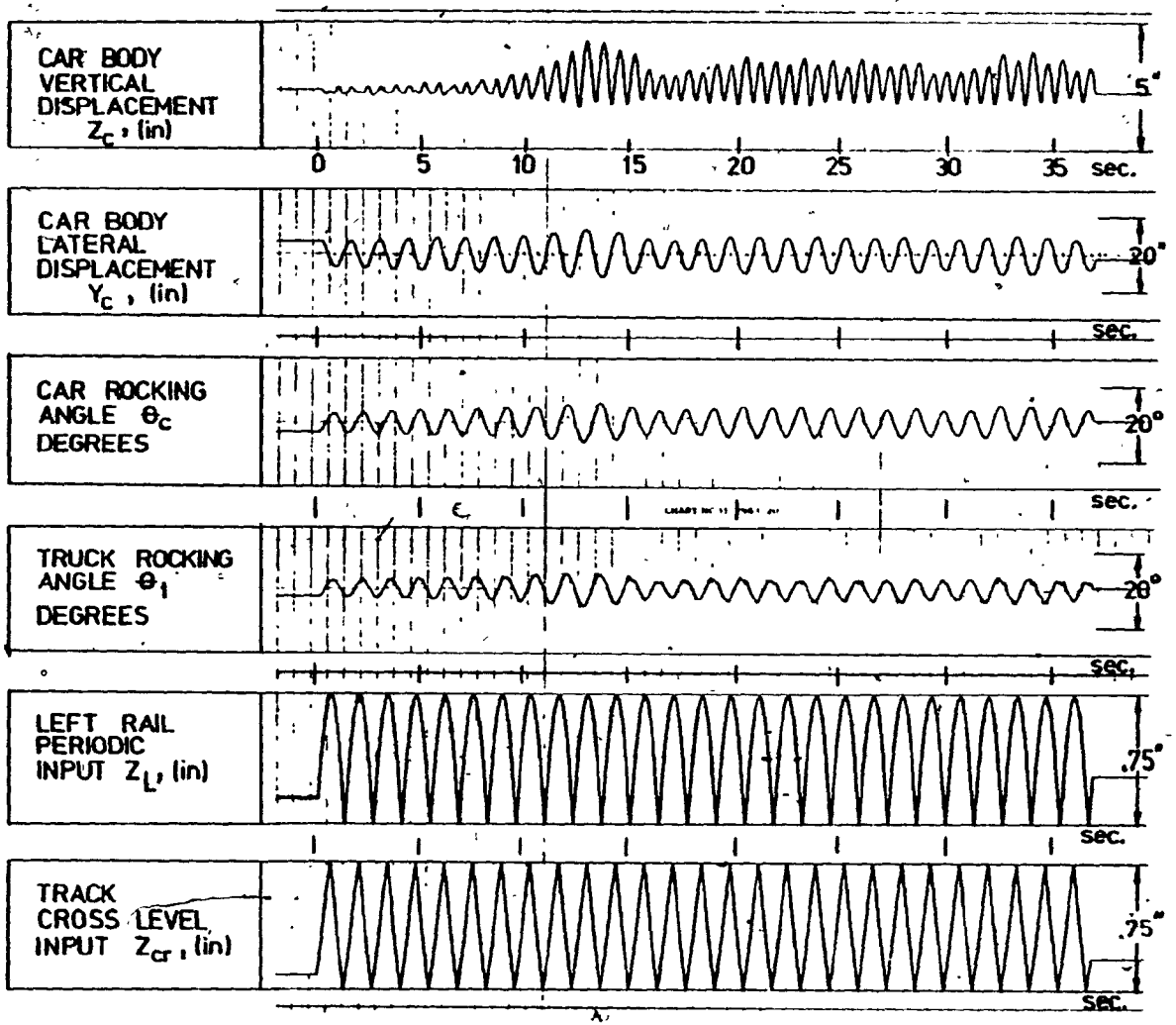

Fig. 5.9: Time Responses While the Vehicle Speed is Decreased from 15 mph (24.13 km/hr).

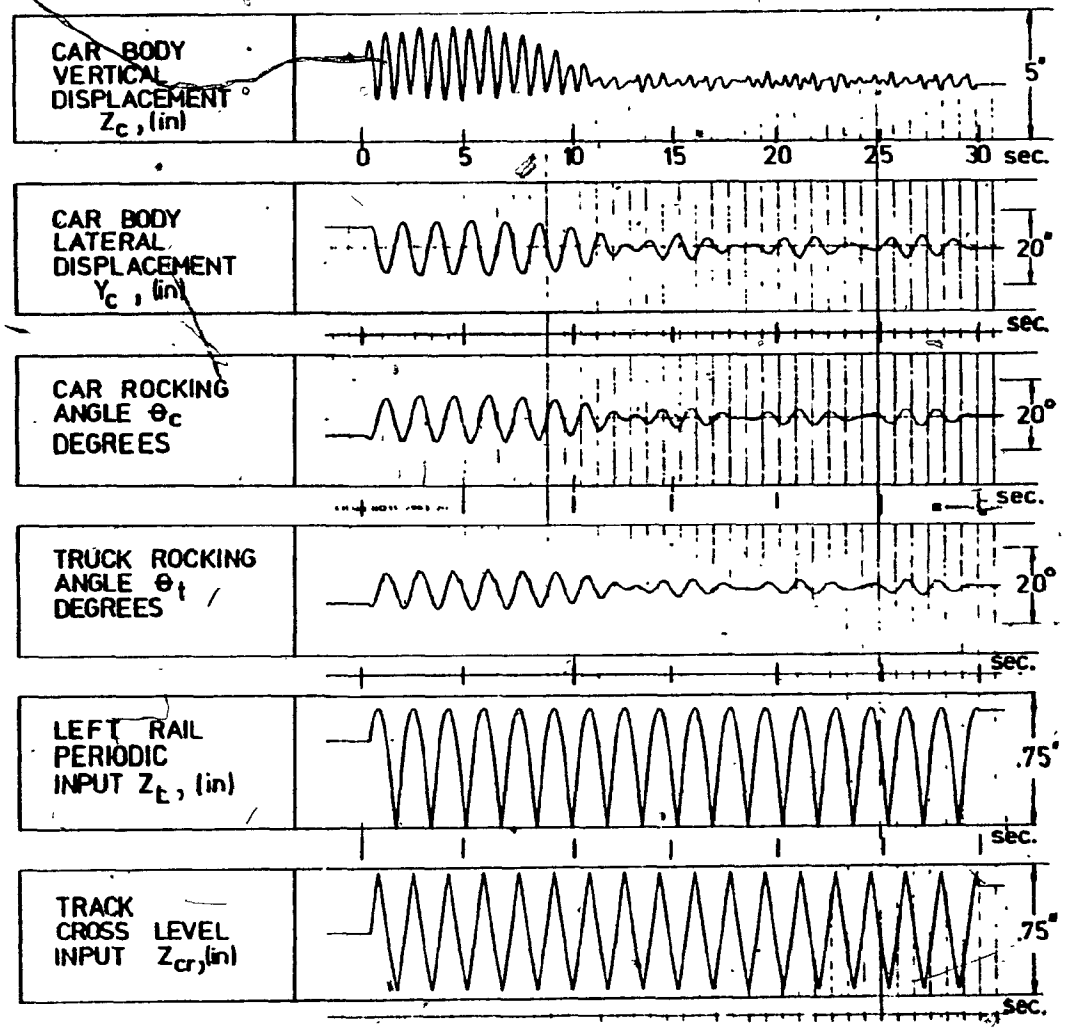

Fig. 5.10: Time Responses While the Vehicle Speed is Decreased from 12 mph (19.3 km/hr).

plotted against the input frequency, as shown in Fig. 5.11.

Figure 5.11 shows a typical steady state frequency response of the system describing the different levels of car rocking in the frequency domain. While light rocking of the car body takes place, the bolster and the wheelset all move together in phase. As the frequency increases, say to 2.6 rad/sec, a sudden jump in the amplitude occurs to moderate rocking level, at which a phase shift of $\pi/4$ radians between the car body angular displacement and input cross level may be noticed. When the frequency is further increased to 3.5 rad/sec, another jump in amplitude to severe rocking levels takes place. During this, the response is $\pi/2$ radians out of phase with the cross level input. Further, increase in the speed produces a decrease in the rocking angular displacement. When the frequency reaches 4.4 rad/sec, light rocking reoccurs with a phase angle of π radians. Most importantly, decreasing the vehicle speed from resonance state only increases the vehicle rocking response momentarily. This phenomenon was also observed in the experimental investigations reported in [12]. The reason for this phenomenon, as shown in Fig. 5.11, is due to the softening type spring action arising from the geometric nonlinearities of the vehicle.

The frequency response plots of the freight vehicle show clearly a strong peak characterizing excessive rocking occurring at a vehicle speed range of 10 to 20 mph (16.1 to 32.2 km/hr). Such severe rocking as known to degrade both the track and equipment performance over a period of time, and thus directly affect the reliability of car

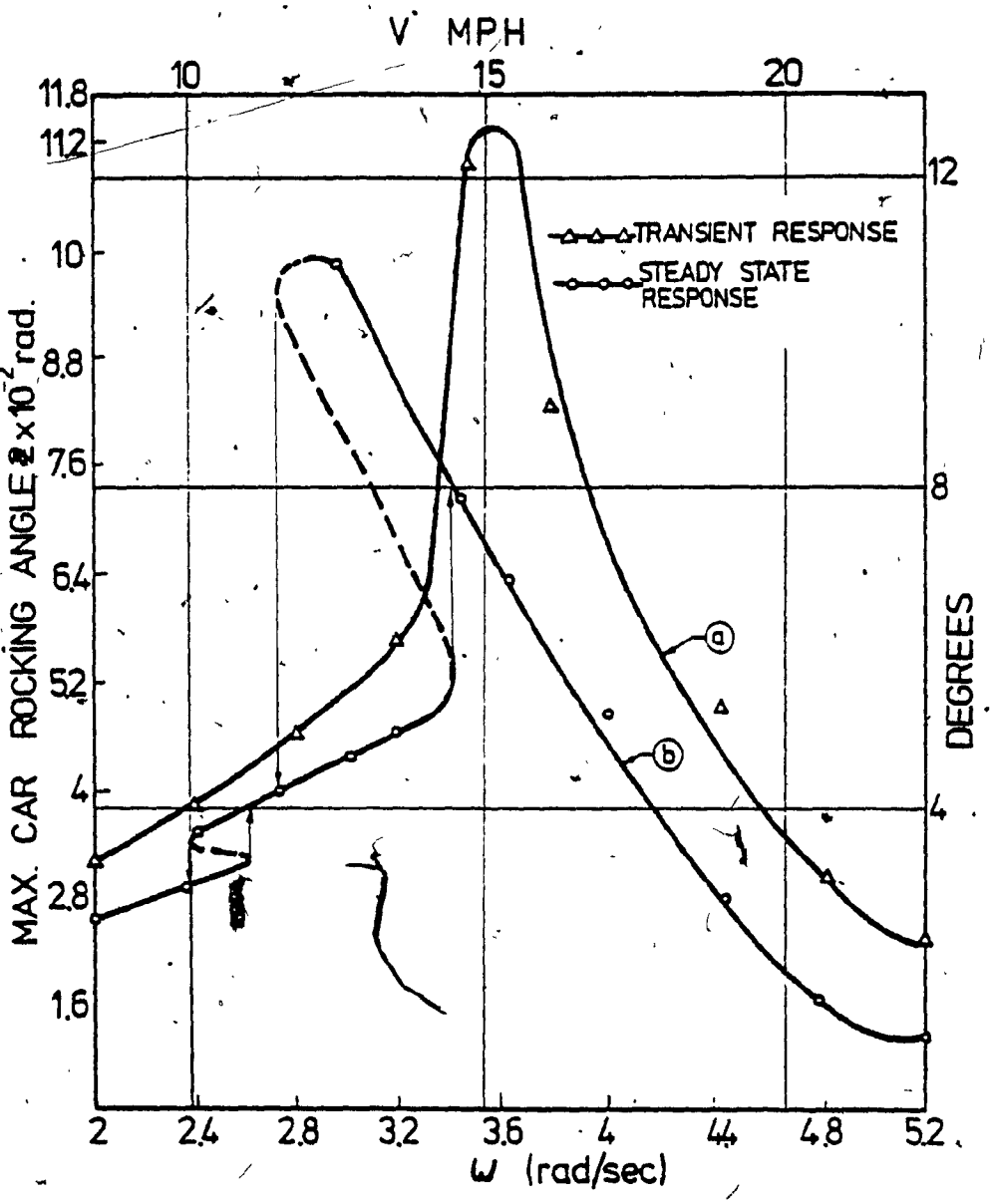

Fig. 5.1†: Frequency Response of a 100-Ton Freight Car for a Track Cross Level of 0.75 in. (1.905 cm).

operation and safety. A better understanding of the system behavior under such conditions and methods of reducing such occurrences can be obtained only through a detailed parameter sensitivity study for the system suspension. Such study is carried out in the next chapter utilizing the information obtained thus far.

Summary

In this chapter the steady state frequency response of a railroad freight vehicle is presented. The vehicle is described through the single configuration mathematical model. The equations of motion of the system are derived using Lagrange's procedure. Analog computer is employed for solving the nonlinear differential equations to obtain the response in time domain. The vehicle steady state frequency response is derived from sequences of these time responses. In the next chapter the frequency response plots are utilized to carry out a detailed parametric study. The results of this study show that a more realistic search for an optimal solution to the problem can be achieved using multivariable optimization.

CHAPTER 6

PARAMETRIC STUDY AND OPTIMIZATION OF THE SUSPENSION SYSTEM

CHAPTER 6

PARAMETRIC STUDY AND OPTIMIZATION OF THE SUSPENSION SYSTEM

6.1 Introduction

The frequency response plots of the freight car given in Chapters 4 and 5 show a strong peak characterizing excessive rocking occurring at a vehicle speed range of 10 to 20 mph (16.1 to 32.2 km/hr). This severe rocking motion has been known to result in serious degradation of both the track and the suspension system and thus directly affect car operation and safety. A better understanding of the system behavior under such conditions and methods of reducing such occurrences can be obtained only through a parameter sensitivity study for the suspension. Such a study would describe the sensitivity of the car rocking response to variations in the different suspension parameters.

In order to conduct a parametric study, certain function of the rocking response should be chosen to represent truly the performance of the system. This objective function may be chosen either as the maximum value of the transient rocking response in the frequency domain, as given in Fig. 4.10, obtained from solving the multiconfiguration model on the digital computer or as the maximum value of the transient or the steady state rocking responses in the frequency domain obtained from the solution of the single configuration model on the analog computer as given in Fig. 5.11. Chapters 4 and 5 give the system response in the time domain from which the frequency response

was obtained. The transient responses in the frequency domain was established assuming that the car enters a frequency ω_i with zero initial conditions corresponding to a stationary position at the previous frequency ω_{i-1}. This behavior was utilized in Figs. 4:10 and 5.11 to show the critical frequency range and to give the corresponding maximum car rocking angle as a single value for each input frequency considered. This type of representation provides a better basis for comparing the system performance at the required range of frequencies independent of the initial conditions or the time required to reach steady state conditions and therefore it is more suitable than the steady state response for use in carrying out the parametric study. Moreover, the single configuration model is slightly less accurate than the multiconfiguration model in satisfying all the possible conditions for transition from one configuration to another. Therefore, the parametric sensitivity is determined from the transient frequency response information reported in Chapter 4.

6.2 Objectives

A detailed parametric study is presented in this chapter utilizing the transient frequency response obtained from the solution of the multiconfiguration model with an objective to minimize the maximum value of the car rocking response. The study involves finding the effect of variation of a single suspension parameter on the vehicle performance when subjected to purely periodic excitation from the tracks. The parametric study results in the form of trial solutions show that the problem requires further investigation using

classical multivariable optimization techniques. Through such optimization procedures, it would be possible to find the optimum combination of the suspension elements that would minimize the maximum car rocking response in the critical frequency range of interest. The optimum parameters could then be presented in different forms suitable for application; either for the existing suspension elements or for additional stabilizers to be introduced.

6.3 Parametric Study of the Suspension

In this study, sensitivity of the system responses to variations in a single parameter at a time is carried out in order to determine the near optimum suspension parameters which would produce a minimum of the maximum car rocking angle. Specifically, the effect on the response due to variation in the values of the coefficient of the viscous dampers, forces in friction dampers, stiffness of springs, and changes in track cross level are studied in detail and presented in the following subsections.

6.3.1 Viscous Dampers - Shock Absorbers

Figure 6.1 shows all the suspension elements of the vehicle consisting of the existing (K, K_h, F_t) and the stabilizing components (C_t, C_c, F_c). In the figure, it may be seen that these additional stabilizing shock absorbers can be introduced either by mounting between the truck bolster and the side frame (C_t) or between the car body and the side frame (C_c).

The effect on the vehicle frequency response of varying the

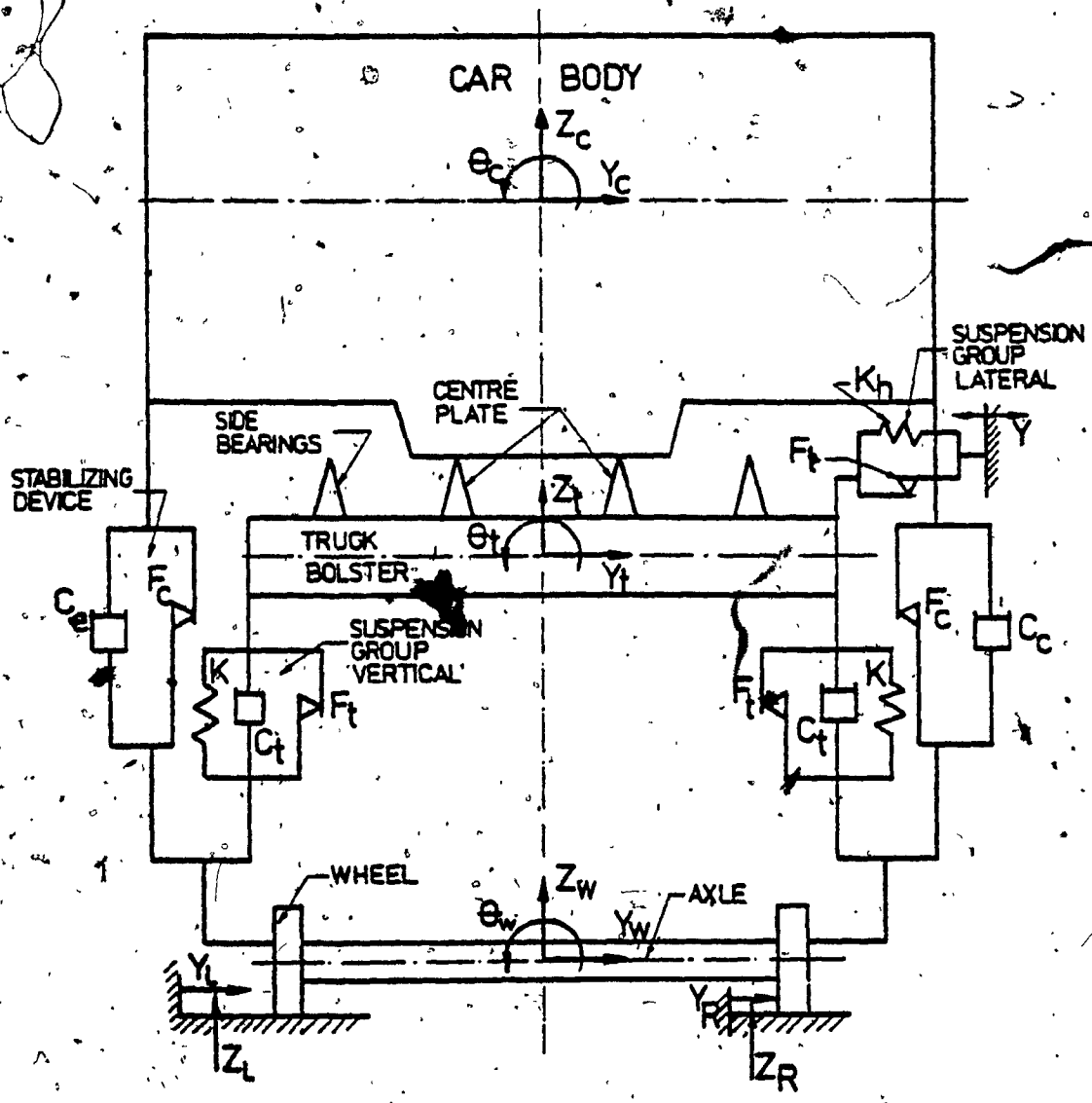

Fig. 6.1: The Freight Vehicle Suspension Elements.

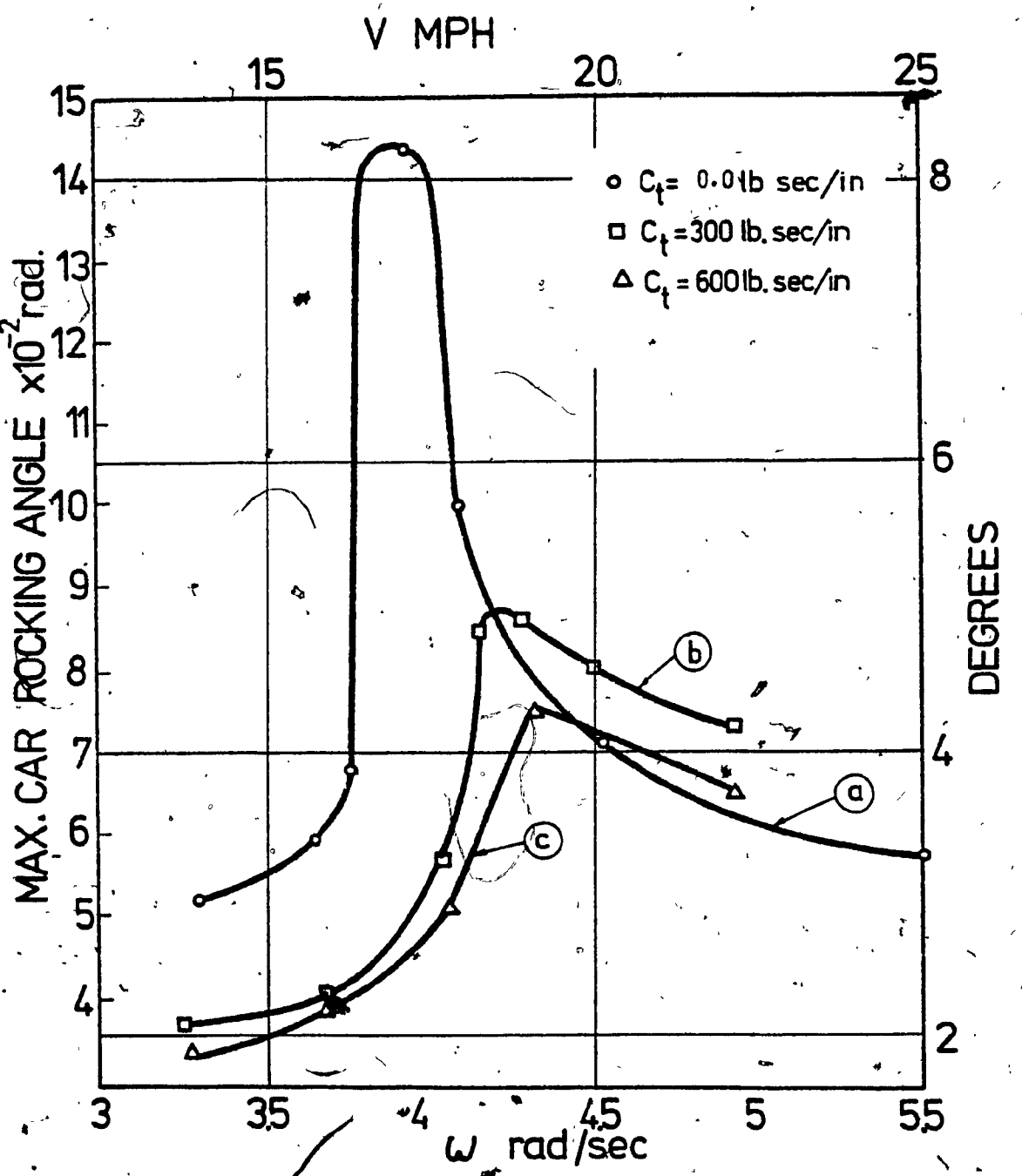

Fig. 6.2: The Effect of Varying the Viscous Damping of Shock Absorbers Mounted Between the Truck Bolster and the Side Frame.

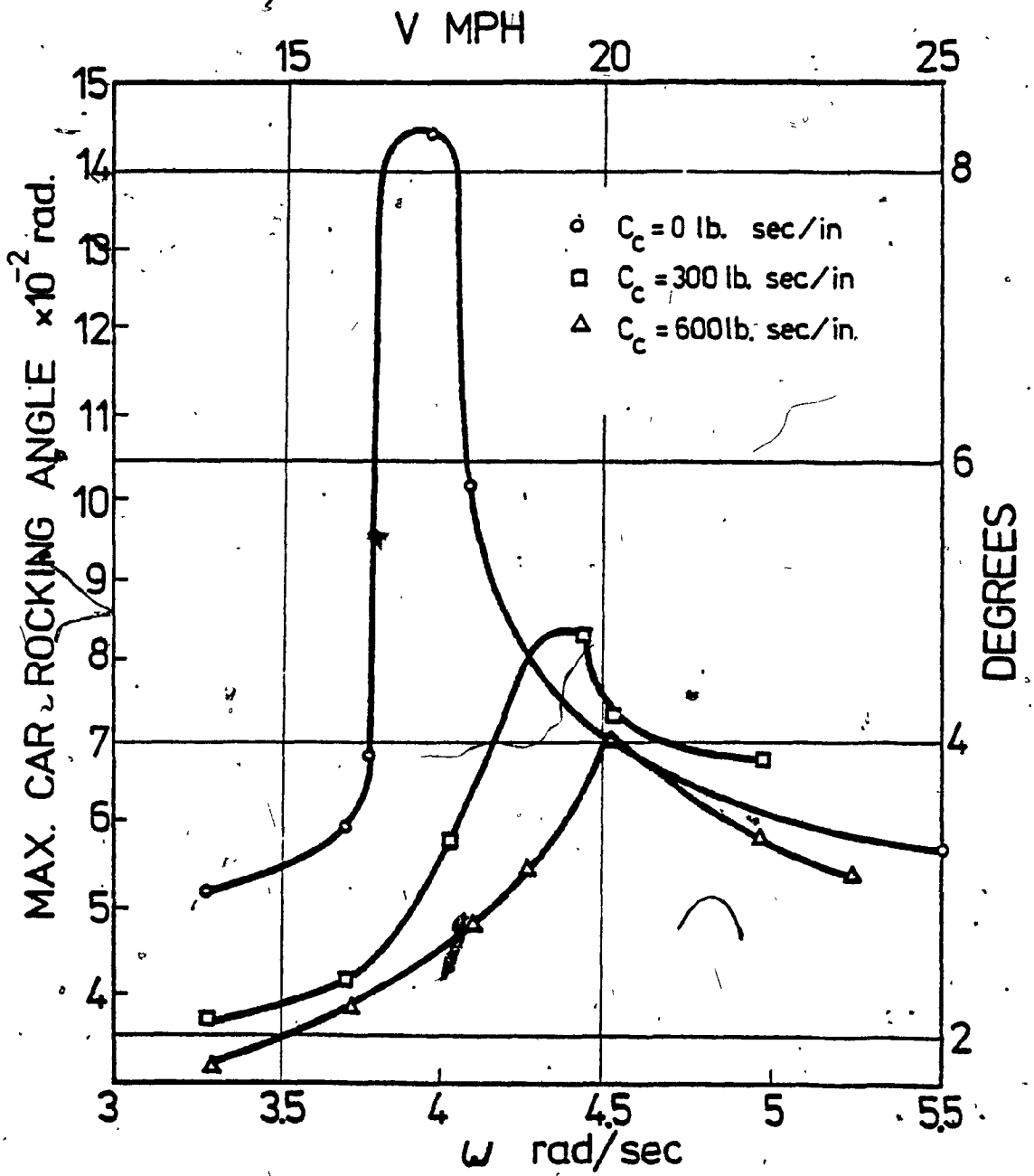

Fig. 6.3: The Effect of Varying the Viscous Damping of Shock Absorbers Mounted Between the Car Body and the Side Frame.

viscous damper coefficients, C_t, of the shock absorbers mounted between the truck bolster and the side frame is shown graphically in Fig. 6.2. Increasing viscous damping coefficient certainly increases the vehicle stability. The results obtained in Fig. 6.2 are for two sets of shock absorbers one with a soft setting and the other with a hard setting. Figure 6.2(a) shows how the system behaves without any damping included in the suspension. Shock absorber with a soft setting decreases the car rocking response by about 39.6% as seen in Fig. 6.2(b), while for a hard setting, shown in Fig. 6.2(c), the response is reduced by about 46.55%. Same results are obtained when the shock absorbers are installed between the car body and the side frame, indicated by C_c, instead of between the bolster and the side frame, as seen from Fig. 6.3. From Figs. 6.2 and 6.3 it may be seen that hard settings for these shock absorbers give a reasonable reduction in the rocking response provided that the associated maintenance problems can be taken care of.

6.3.2 Friction Dampers

Figures 6.4 and 6.5 show the effect of increasing the car and truck friction damping forces, F_c and F_t, on minimizing the car rocking angle. Increasing the original vehicle friction damping force F_t from 8000 lb to 10000 lb (35.6 to 44.48 kN) reduces the rocking angle from 8.5 to 5.44 degrees as seen from Fig. 6.4(b). Further increase in F_t to 12000 lb (53.37 kN) as in Fig. 6.4(c) reduces the rocking to 4.87 degrees. The effect of operating instead a friction damper mounted between the car body and the side frame and having a

force F_c is given in Fig. 6.5 and this also produces a decrease in the rocking response. As a trial, the additionally installed car friction damper, F_c, is set equal to the original truck damping, F_t, and it is noted that the response decreases significantly as seen from Fig. 6.5(d). Increasing the car friction damping to such large values may appear to be a fair solution to the problem. However, large values of car friction damping force would tend to lock the car body to the side frames, thereby eliminating entirely the required action of the suspension system.

6.3.3 Stiffness Elements

Figures 6.6 and 6.7 show the effect of variations in the stiffness of the vertical and lateral suspension springs on the car rocking response. Stiff springs are generally recommended in practice to prevent high initial deflections under loaded cars relative to unloaded cars at points of coupling. But, the sensitivity curve shows clearly that stiff springs in Fig. 6.6(a) affect badly the car rocking response. Soft spring, shown in Fig. 6.6(c), produce limited rocking but, on the other hand, would cause large initial deflections in fully loaded cars that may result in separation of two adjacent cars, if one is loaded and the other is not.

6.3.4 Track Cross Level

It is also possible to reduce excessive rocking by controlling the input from the rails such as the track cross level. The effect of track cross level on the response is separately shown in Fig. 6.8.

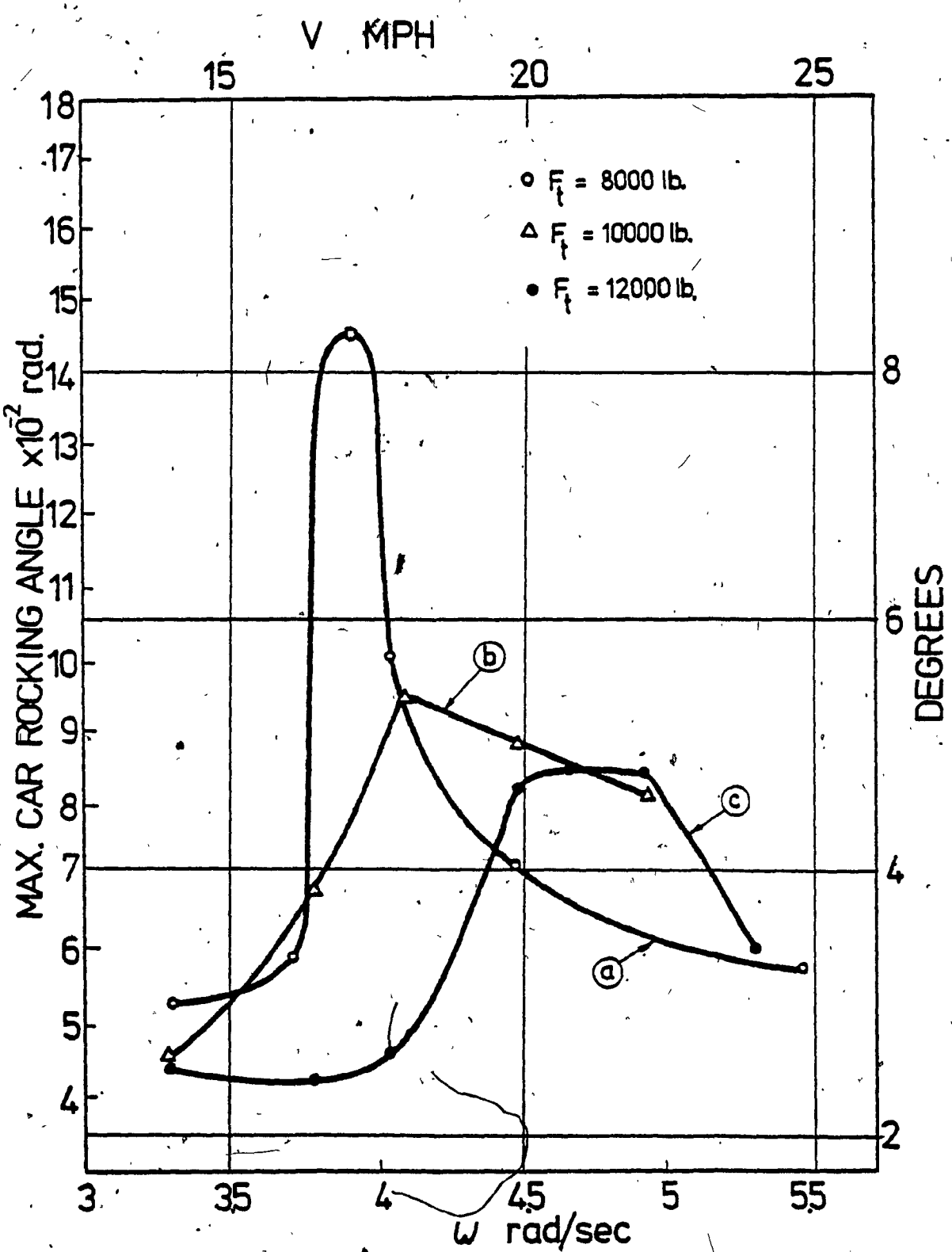

Fig. 6.4: The Effect of Varying the Truck Friction Damper Force.

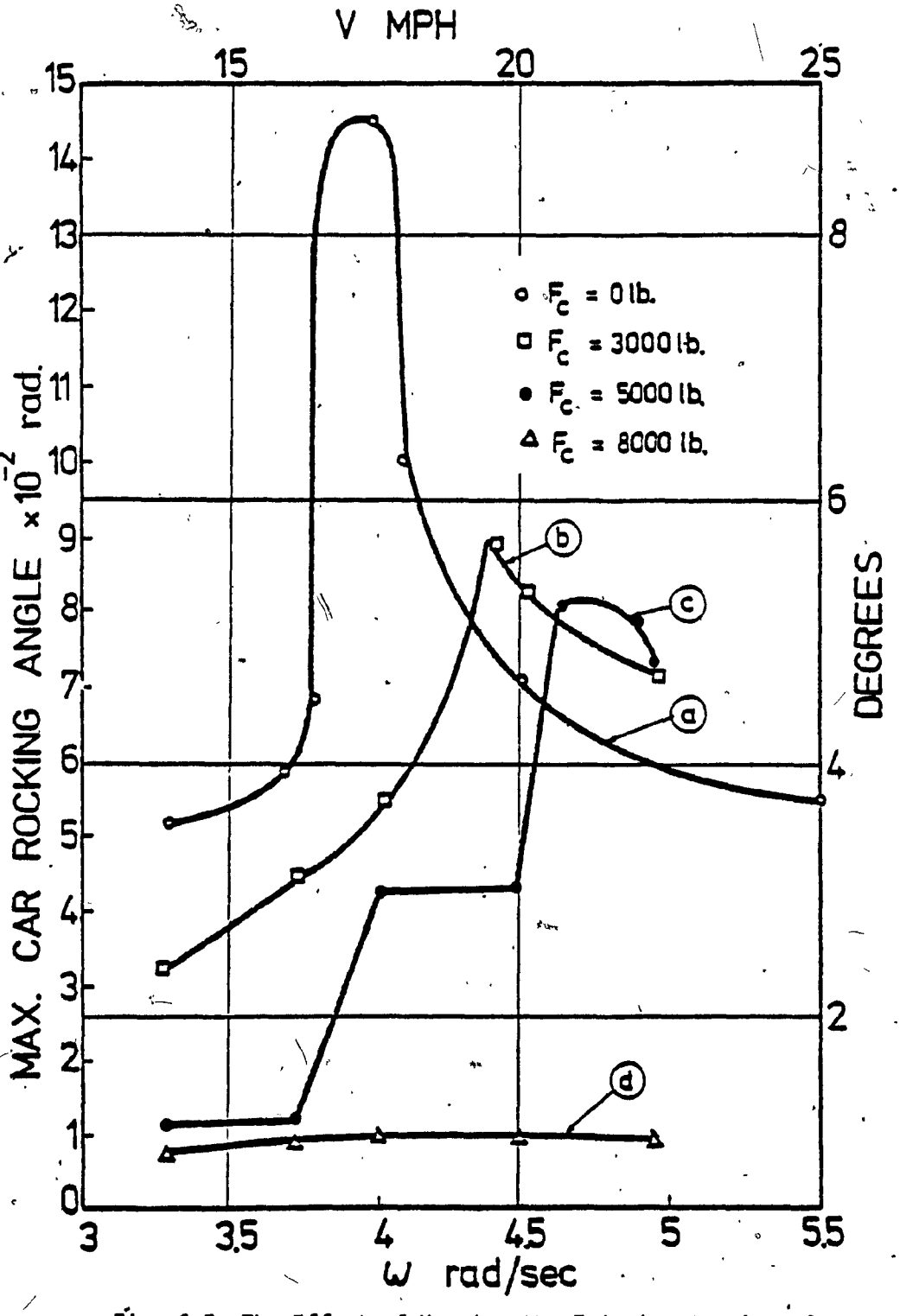

Fig. 6.5: The Effect of Varying the Friction Damping of a Stabilizer Mounted Between the Car Body and the Side Frame.

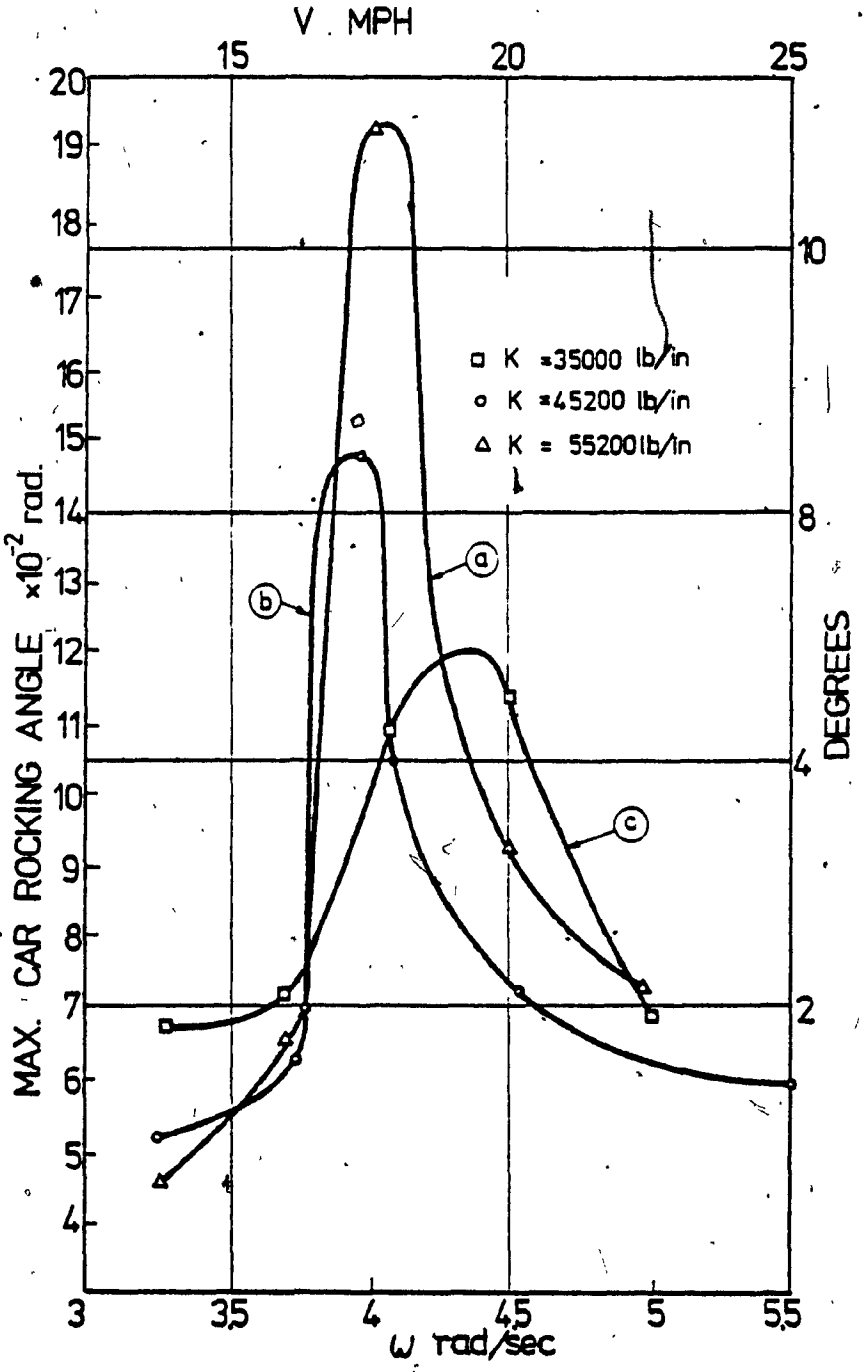

Fig. 6.6: The Effect of Varying the Vertical Stiffness of the Truck Suspension.

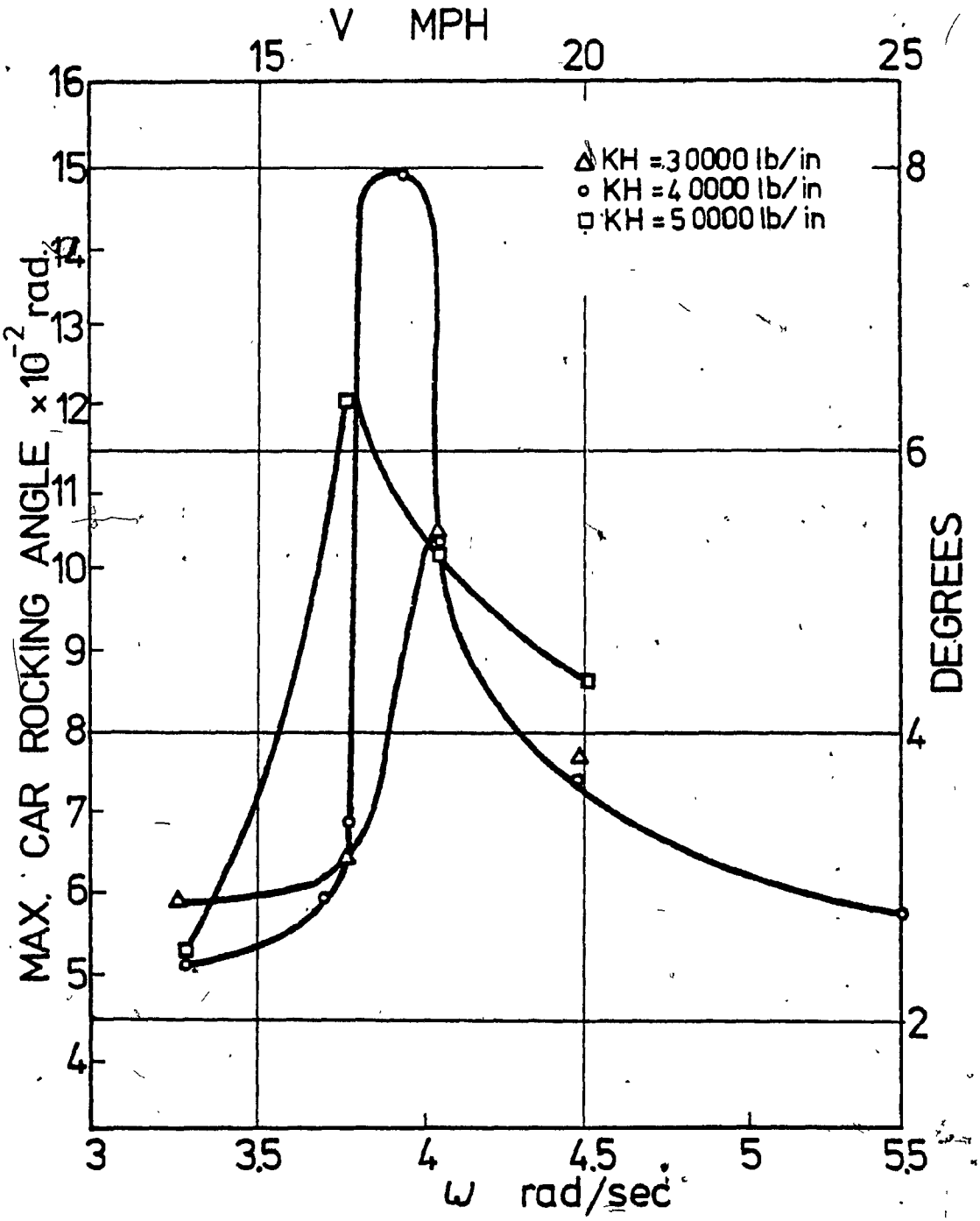

Fig. 6.7: The Effect of Varying the Lateral Stiffness of the Truck Suspension.

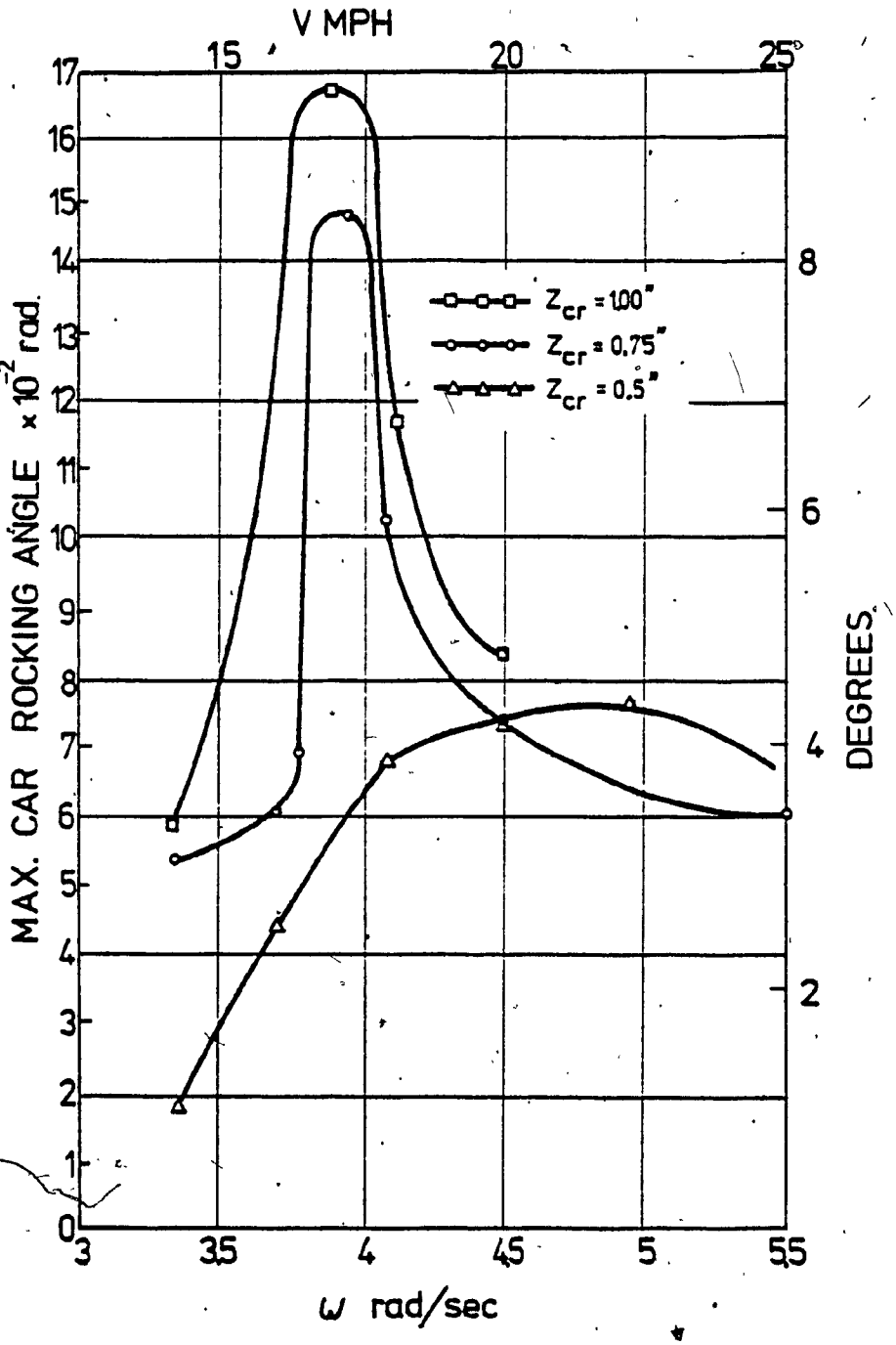

Fig. 6.8: The Effect of Varying the Track Cross Level.

A decrease in the track cross level to about 0.5 inch (1.27 cm) decreases the maximum rocking response to about 4.46 degrees. Though desired reduction in rocking amplitude is obtained, this cannot be considered as a realistic solution to the rocking problem, since an accurate control of the track cross level within such small values like 0.5 inch (1.27 cm) is not feasible in actual field applications.

In summary, the maximum car rocking response can be minimized by:

i) Using shock absorbers with hard settings provided their maintenance problem can be overcome.

ii) Increasing the system friction damping forces; but large values of car friction damping forces would eliminate altogether the suspension action.

iii) Using soft springs; but this would create large initial deflections in loaded cars.

Due to the above contradictions in the recommendations in the case of soft springs and in the case of friction dampers, the solution to the problem demands further investigation utilizing multivariable optimization techniques, as given in the next section.

6.4 Suspension Optimization

As stated earlier, the transient rocking response in the frequency domain using the solution of the multiconfiguration model provides the most suitable basis for comparing the system performance. This type of behavioral representation is used again for carrying out

a multivariable optimization which is defined in the following Subsection 6.4.1. The groups of the suspension parameters used as design variables are given in Subsection 6.4.2. The optimization procedure and the methods utilized in solving the problem are given in Subsections 6.4.3 and 6.4.4 respectively. Finally, a discussion of the optimization results is given in Subsection 6.4.5.

6.4.1 Definition of the Optimization Problem

From the viewpoint of mathematical programming, a statement of the min-max problem for the railroad freight vehicle is achieved as following:

Given the multiconfiguration mathematical model, defined in Subsection 4.1.1, to be:

$$\underset{\sim}{M}\ddot{\underset{\sim}{X}} + \underset{\sim}{C}\dot{\underset{\sim}{X}} + \underset{\sim}{K}\underset{\sim}{X} + \underset{\sim}{S}(\dot{\underset{\sim}{Y}}^{(1)}) + \underset{\sim}{G} = \underset{\sim}{F}(t)$$

where $\underset{\sim}{X}$ is the set of independent generalized coordinates, the problem is to find the suspension parameters $\underset{\sim}{Z}$ that minimize the objective function E which is defined to be the maximum value of an arbitrary function $f(\underset{\sim}{X}(\underset{\sim}{Z}))$ of the transient response of the vehicle in the range of input frequency of interest. That is, it is required to find the suspension elements $\underset{\sim}{Z}$ that gives:

$$\min E = \min_{\omega_i} \max f[\underset{\sim}{X}(\omega_i(\underset{\sim}{Z}), \underset{\sim}{Z})] .$$

subjected to constraints of the form

$$\underset{\sim}{a} \leq \underset{\sim}{Z} \leq \underset{\sim}{b} \quad \text{where } \underset{\sim}{a}, \underset{\sim}{b} \in R^n,$$

$\underset{\sim}{a}$ and $\underset{\sim}{b}$ defining the feasible or practical region in which the search for the optimum $\underset{\sim}{Z}$ takes place.

6.4.2 Suspension Groups for Optimization

The following three groups of suspension parameters $\underset{\sim}{Z}$ are chosen for optimization.

i) The first group consists of the original suspension without the stabilizer system, in Fig. 6.1, operating. Therefore:

$$\underset{\sim}{Z}_1 = [K, K_h, F_t]$$

ii) The second group consists of the stiffness elements with the stabilizer in operation assuming F_t and C_t, in Fig. 6.1, are fixed. This gives:

$$\underset{\sim}{Z}_2 = [K, K_h, C_c, F_c]$$

iii) The third group consists of the damping elements of the original suspension with the stabilizer in operation assuming K, K_h, in Fig. 6.1, are fixed and therefore:

$$\underset{\sim}{Z}_3 = [C_t, F_t, C_c, F_c]$$

The transient response function $f(\underset{\sim}{X}(\underset{\sim}{Z}))$ is chosen as the true representation of the performance of the suspension and therefore it can be either an element or a combination of elements of the vector $\underset{\sim}{X}$ and its derivatives. The transient rocking response in the frequency domain shows a strong peak occurring in the critical speed range of the vehicle. Thus, it is proposed that this car rocking response be chosen as $f(\underset{\sim}{X}(\underset{\sim}{Z}))$.

6.4.3 The Optimization Procedure

The optimization scheme for the given car rocking response function and the design variables $\underset{\sim}{Z}$ can be carried out as indicated in the flow chart in Fig. 6.9 using the following step by step procedure.

i) An initial guess for the vector $\underset{\sim}{Z}$ is used to start the optimization program. The original parameters of the 100 ton vehicle [19] are used for this purpose.

ii) A frequency in the range $\omega_{min} \leq \omega \leq \omega_{max}$ is chosen where ω_{min} and ω_{max} are the limits of the critical frequency range already identified in this problem.

iii) For the given input frequency, the system equations of motion are solved and the response vector $\underset{\sim}{X}$ is determined as a time function.

iv) The maximum of the function $f(\underset{\sim}{X}(\underset{\sim}{Z}))$ is evaluated for that given frequency.

v) Steps (iii) and (iv) are repeated for the entire frequency range of interest and the maximum value of the response maxima is evaluated. This is then the objective function E.

vi) Direct search methods of multivariable optimization, as described in the following subsection, are applied to minimize E.

6.4.4 Optimization Methods

The direct search methods utilized in optimization problems are based on sequential examination of trial solutions which by simple

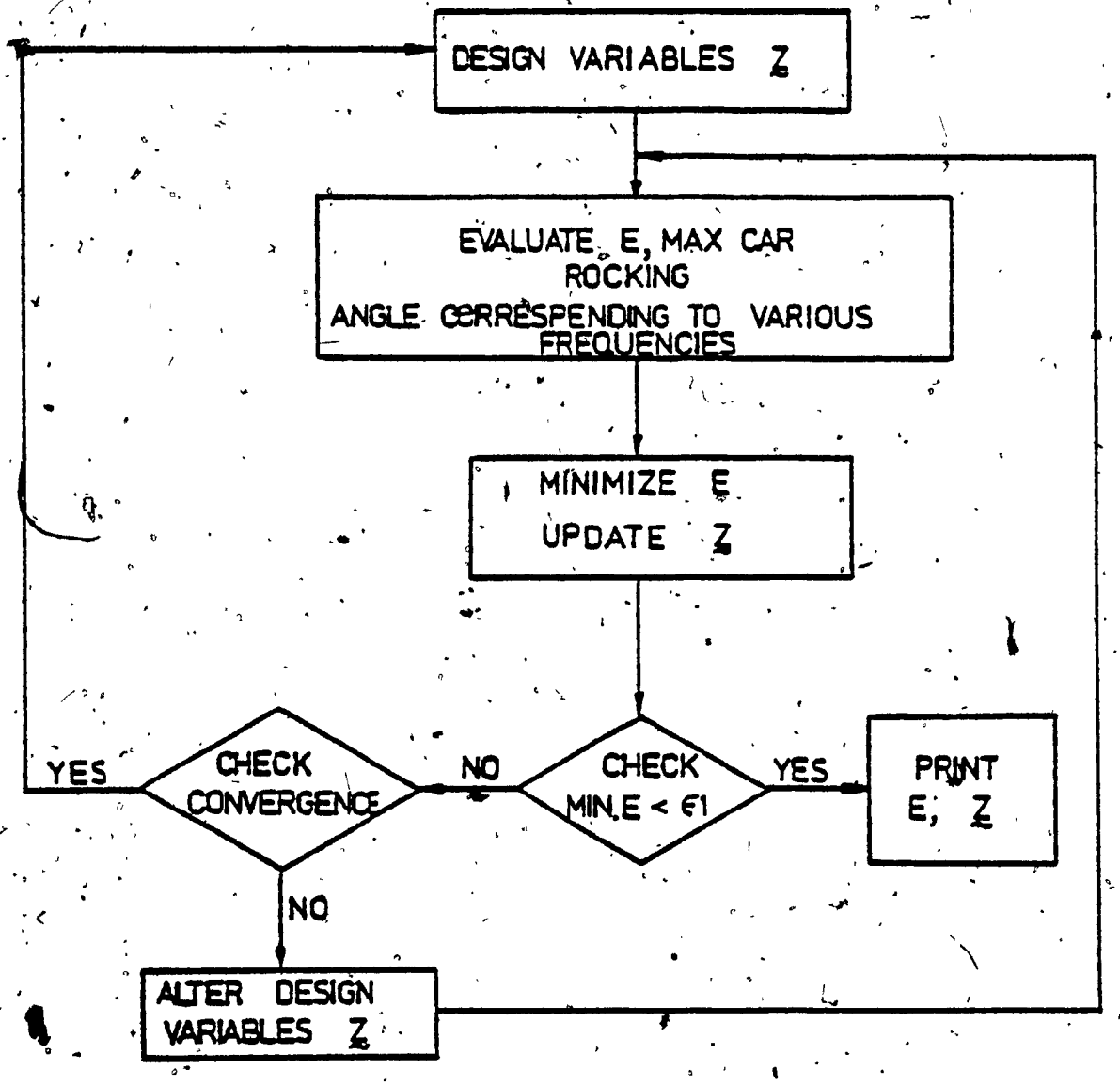

Fig. 6.9: The Optimization Scheme.

comparisons give an indication for further searching procedure. These methods are often preferred because they require only the ability to evaluate the value of the functions at a given point. Two methods are used in this investigation. The first one changes the parameters of $\underset{\sim}{Z}$ one by one at a time starting from an initial point, but once the full series of perturbations has been completed, it takes a step along the direction joining the last and the initial point. This method is due to Hooke and Jeeves [37] and is referred to as the pattern search method (PS) as it comprises of two kinds of moves, namely, exploratory and pattern. A considerable improvement in the computing time over such pattern search was achieved using a second method suggested by Rosenbrock [38]. In this technique, known as the rotating coordinates method (RC), lower values of the objective function are sought along certain mutually orthogonal directions. This set of directions is then rotated in the functional space so that it adopts itself to the directions of the most rapid decrease of the objective function:

6.4.5 Optimization Results

The objective function, which is now the maximum transient response of the freight car rocking amplitude, is plotted against varying input frequencies, before and after optimization, in Figs. 6.10, 6.11 and 6.12. The responses before optimization are computed with the existing system parameters for a 100 ton car described in Appendix IV.

Suspension Description	Method Used	Optimum Design Variables Z for						Objective Function. E in rads.
		Existing Suspension			Additional Energy Dissipators			
		K	K_h	F_t	C_t	C_c	F_c	
Group 1 Soft	PS	33000	33000	12000	200*	0*	0*	0.0526
Group 1 Hard	PS	49200	40000	11500	200*	0*	0*	0.0634
Group 1 Hard	RC	58000	39500	12775	200*	0*	0*	0.0664
Group 2	PS	51200	39000	8000*	200*	300	4000	0.0742
Group 2	RC	45200	39968	8000*	200*	500	4875	0.0374
Group 3	PS	45200*	40000*	9000	300	300	4000	0.0634
Group 3	RC	45200*	40000*	8062	400	100	6000	0.0474

*Fixed Parameters.

Table 6.1: Optimum Suspension Parameters.

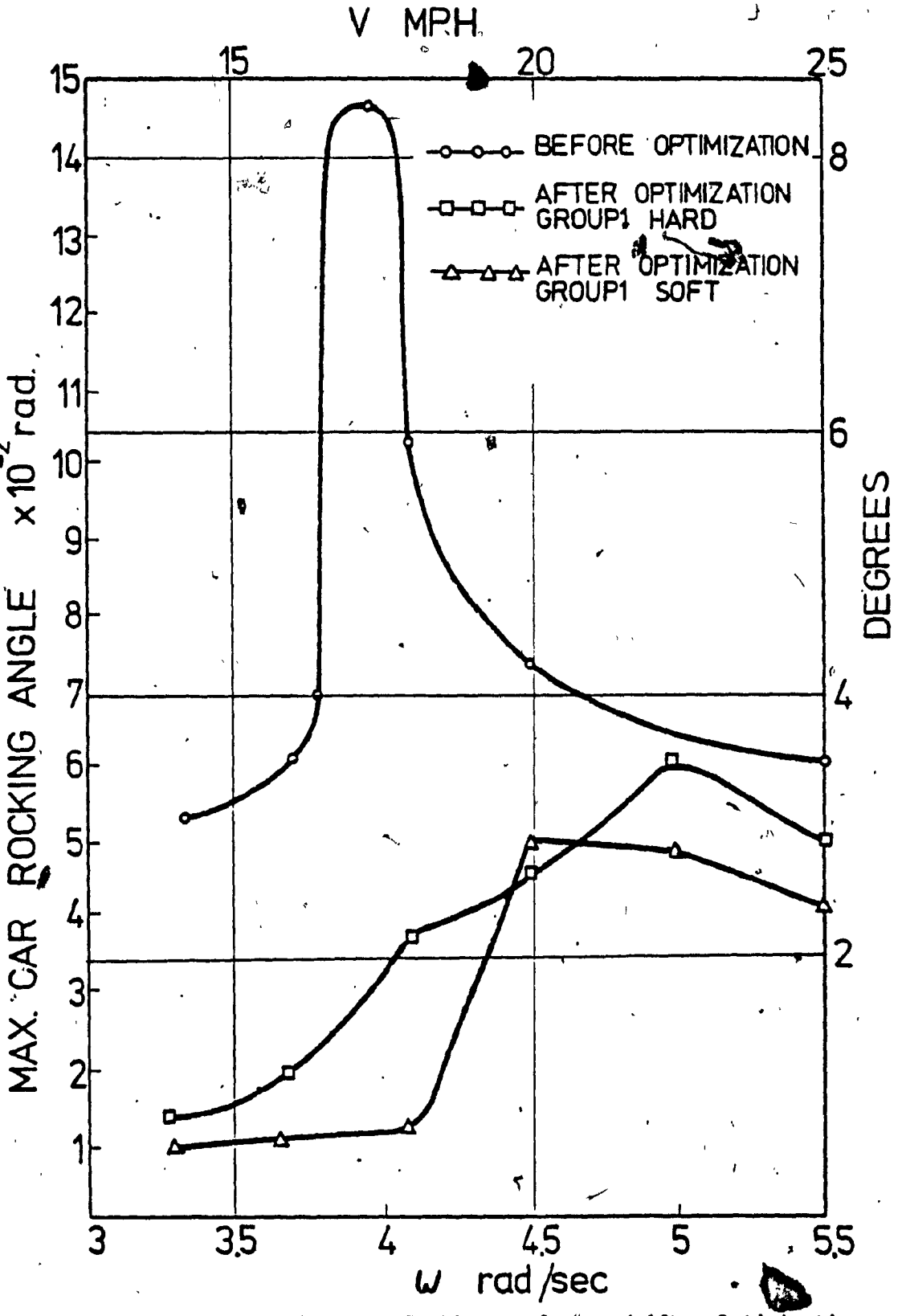

Fig. 6.10: Maximum Car Rocking, Before and After Optimization for Suspension Group 1 (PS Method).

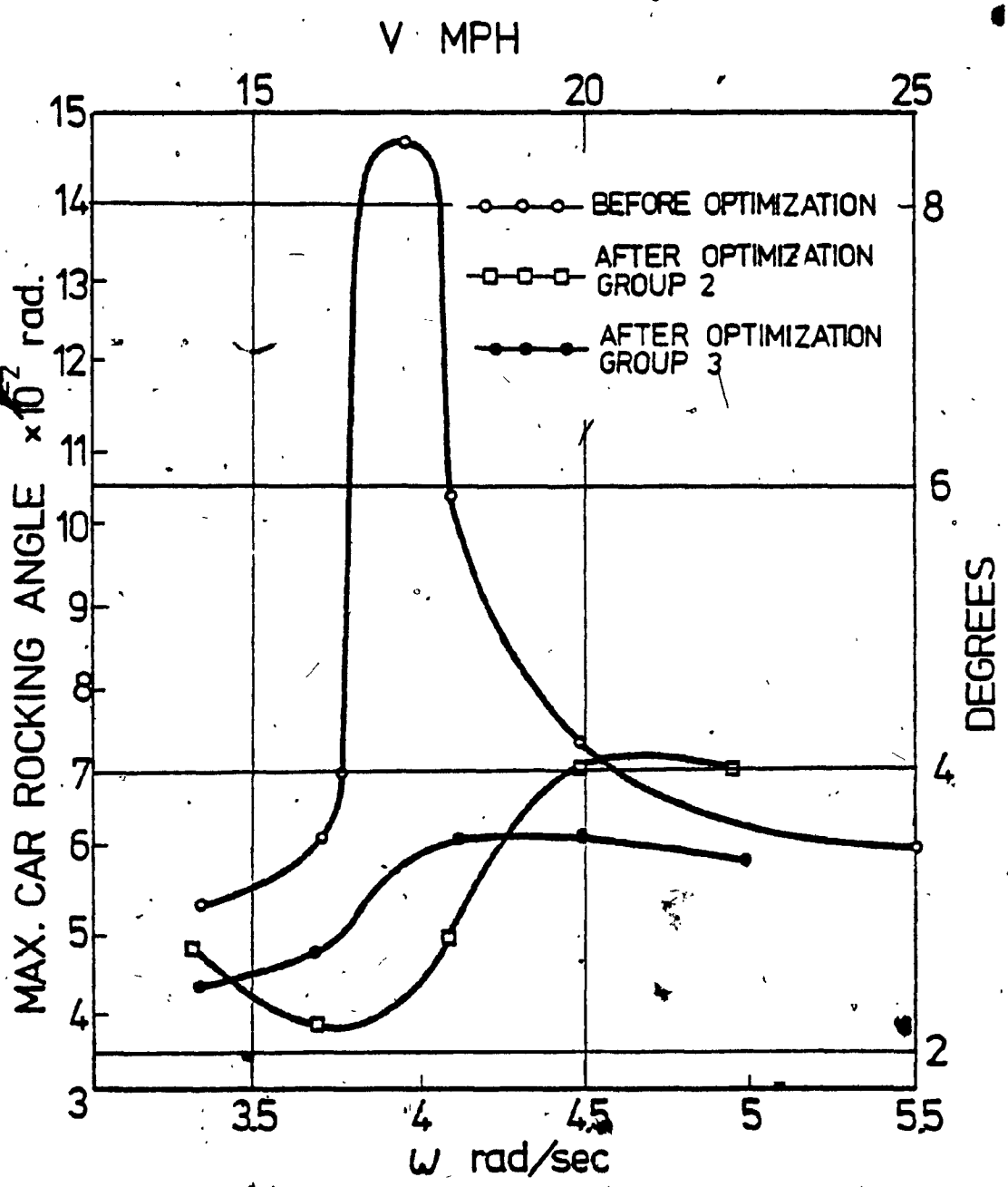

Fig. 6.11: Maximum Car Rocking, Before and After Optimization for Suspension Groups 2 and 3 (PS Method).

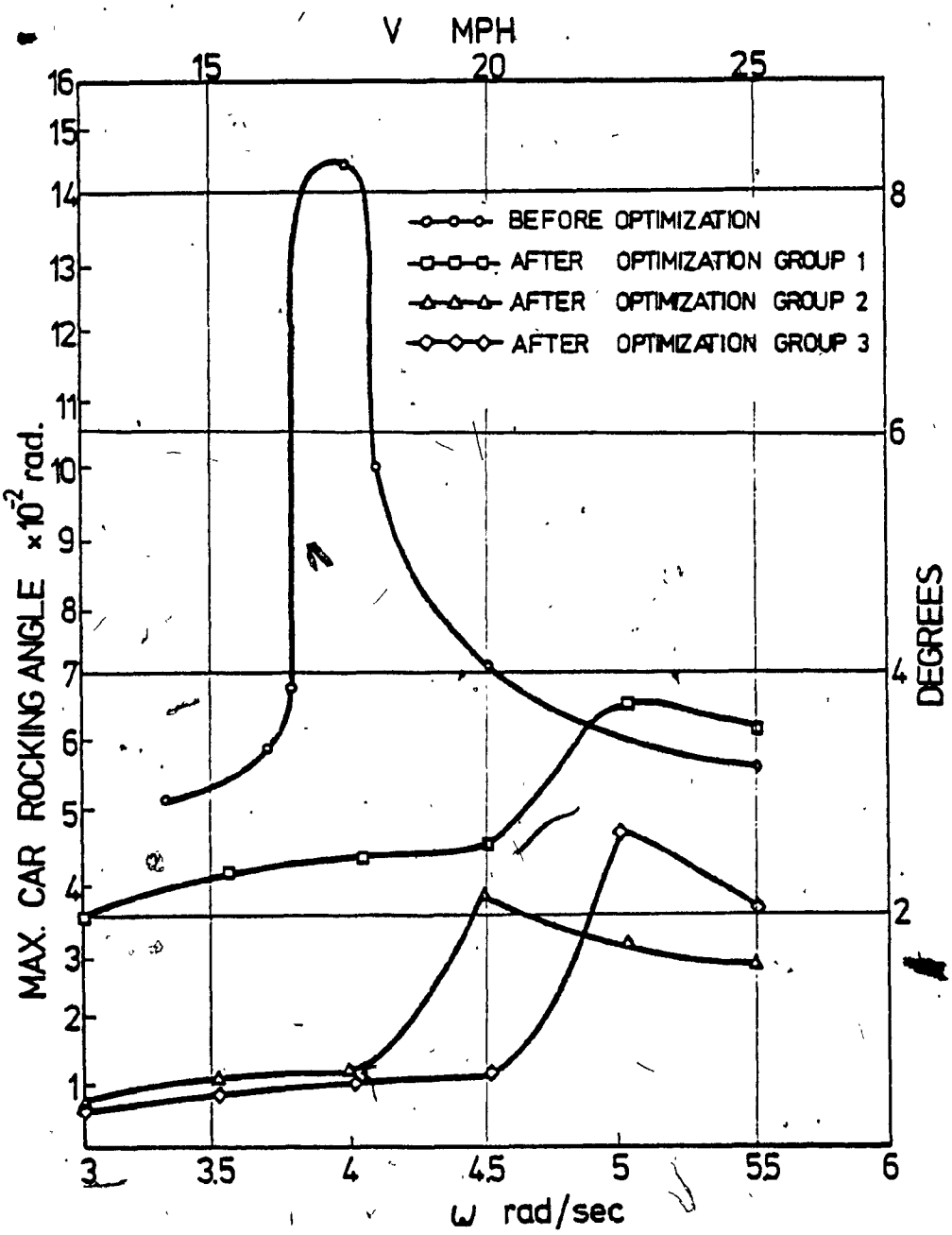

Fig. 6.12: Maximum Car Rocking, Before and After Optimization for Suspension Groups 1, 2 and 3 (RC Method).

The values of the suspension parameters given for the 100 ton car were used to start the search procedure for a min-max response of the system using both the optimization techniques described in Subsection 6.4.4. The results obtained for the three groups of suspension parameters, defined in Subsection 6.4.2, are presented in Table 6.1 and are summarized as follows:

Group 1: $\underset{\sim}{Z}_1 = [K, K_h, F_t]$

Through control of the constraint vectors $\underset{\sim}{a}$ and $\underset{\sim}{b}$, the elements of $\underset{\sim}{Z}_1$ can lead to different suspension designs. The first set of results are obtained by controlling the search toward an optimum soft suspension while the second leads to an optimum hard suspension. The two optimum suspension groups are given in Table 6.1. The use of the pattern search method (PS) reduced the car maximum rocking, in the case of soft suspension, by 63.29%, while for the hard group by 55.69%. Rotating coordinates method (RC) failed in obtaining an optimal soft suspension group while for the hard type, it reduced the objective function by 53.57%.

Group 2: $\underset{\sim}{Z}_2 = [K, K_h, C_c, F_c]$

The application of the optimization scheme to the stiffness elements with the stabilizer in operation, assuming the truck suspension coefficients C_t, F_t in Fig. 6.1 are fixed, leads to results shown in Figs. 6.11 and 6.12. A suspension design based on these values decreases the objective function by about 48.1% using the PS technique and 73.79% using the RC method.

Group 3: $\underset{\sim}{Z}_3 = [C_t, F_t, C_c, F_c]$

Here a search is made for the damping elements of the original suspension with the stabilizer in operation, assuming that the values of the elements K, K_h are fixed. The results obtained are presented in Figs 6.11 and 6.12. The optimum suspension parameters determined using the PS method reduced the objective function by 55.69% while application of the RC method gave a reduction of 66.8%.

The above results of optimization showed different local minima for the chosen objective function. For any given choice of the optimization technique, the associated feasible region, and the design variable $\underset{\sim}{Z}$, multiple solutions for the suspension parameters are obtained as shown in Table 6.1. From these results, the designer can either:

(i) choose optimal values of the stiffness elements K, K_h and the truck friction damper with a dissipating force F_t for an already existing car suspension group, or

(ii) choose additional energy dissipation devices in the form of shock absorbers C_t, C_c and car friction damper F_c.

Although the second choice produces a better reduction in the objective function (by RC method), this is balanced by the extra installation and maintenance costs of adding this stabilizing group. Therefore, the first choice is recommended as a more practical solution.

6.5 Summary

In this chapter, a detailed parametric study is carried out to find the near-optimum suspension parameters of a large capacity freight vehicle. The parametric study shows the sensitivity of the car rocking response to variation in a single suspension parameter at a given time. Though useful results were obtained from this sensitivity, a solution to the problem is attempted using multivariable optimization techniques because of the conflict in the recommendations. The results of the optimization show that possible solutions to excessive rocking could be achieved either by using optimal values for the original suspension configuration or by installing new stabilizing devies with optimum parameters. Up to this point, the problem considered had an input excitation in a purely periodic form. The more general problem which considers the input forcing function to the vehicle as a combination of periodic and random processes is discussed in the following chapters.

CHAPTER 7

THE STOCHASTIC ROCKING RESPONSE OF THE FREIGHT CAR SYSTEM

CHAPTER 7

THE STOCHASTIC ROCKING RESPONSE OF THE FREIGHT CAR SYSTEM

7.1 Introduction

In the previous chapters the rocking response of the freight car was treated using a deterministic approach. Although it was recognized that the track irregularities generated a random component in addition to the periodic forces, the effect of the random process in the track irregularities was ignored. For the freight car rocking problem such an assumption for the excitation process is reasonable since the investigation is concerned only with low vehicle speeds. However, for an accurate and complete investigation, the input excitation on the model should be described stochastically to include both the random and the periodic irregularities and the responses described probabilistically. The stochastic approach may be regarded as the general solution to the overall problem while the previous approach using a deterministic analysis becomes an important special case.

7.2 Statement of the Problem

The problem of excessive rocking responses of the freight vehicle is treated in this chapter utilizing a previously established nonlinear model subjected to a stochastic forcing function. For this, the equations of motion of the system should be described in a certain matrix form in order to suit the methods available for

solving such problems. This required form, for the equations of motion, can be obtained only by using the single configuration model described earlier in Chapters 2 and 5. The excitation on the model due to the wheel track interaction will then consist of the periodic and the random processes in the form of a filtered white noise power spectral density according to expressions developed in Chapter 3.

The available techniques for solving nonlinear systems subjected to stochastic excitation are reviewed in Section 7.3. The statistical linearization technique was found to be the most suitable for the present problem and therefore it is described in detail in Section 7.4. The equations of motion of the single configuration model derived earlier in Section 5.2 are stated again in the proper matrix form suitable for application of the statistical linearization technique in Section 7.5. The numerical method adopted for solving the equivalent linear system is described in Section 7.6 and finally a discussion of the results, in the form of mean square and power spectral density of the vehicle responses, is included in Section 7.7.

7.3 Available Analytical Techniques

At present, there are four basic methods which can be employed for the study of a stochastically excited, nonlinear, multidegree-of-freedom system. These are the Fokker-Planck equation approach, the normal mode technique, the perturbation method and the statistical linearization approach. The major advantages and limitations of these methods are reviewed briefly in this section in order that a suitable

technique can be adopted in solving the stochastic equations of motion of the freight car system.

7.3.1 The Fokker-Planck Equation Approach [47,48]

The Fokker-Planck equation approach has one great advantage over all the other approaches considered here including the one which has been eventually chosen for solving the problem under discussion; it gives an exact solution for the problem of response. However, this advantage is compromised by the fact that such solutions have been found only for certain restricted class of problems.

For a system under a Gaussian white noise excitation, the transitional probability density of the response process is known to be governed by the Fokker-Planck equation [47]. This transitional probability density can completely define all the required statistics of the response process. However, the complete nonstationary Fokker-Planck equation has not been solved until now. Even the solution of the stationary Fokker-Planck equation, which corresponds to the steady state type solution in the deterministic case, is available only for a few limited cases.

The most general extensions of this approach to date to problems involving mechanical systems are due to Coughy [47] and Ariaratnam [48]. They showed that a stationary form of the Fokker-Planck equation can be solved and the first probability density of the Markovian response process can be obtained, provided:

i) the only energy dissipation in the system arises from

viscous damping forces which are proportional to the system velocity,

ii) the excitation is a Gaussian white noise or delta-correlated, and

iii) the correlation matrix of the excitation is proportional to the damping matrix of the system.

It is easily seen that the present problem does not satisfy any of the above stated conditions. The freight car system contains a nonlinear friction damping vector which evidently has no linear variation with the velocity vector and this violates the first condition stated under (i). Further, the excitation on the system is a filtered white noise and its correlation matrix is not proportional to the damping matrix of the system. Since the problem cannot be reformulated, without loss of reality, to suit the Fokker-Planck technique for an exact solution, attention is now given to other approaches to obtain the response statistics.

7.3.2 The Normal Mode Approach [49]

The normal mode approach [49] has been developed for obtaining only the stationary random responses and this method is based on the idea of reducing a given set of coupled nonlinear second order differential equations to a set of equations containing coupling only in the nonlinear terms and having statistically uncorrelated excitations. The reduced equations can then be solved by technique such as the method of equivalent linearization. For successful application of this method to a given dynamical system, two conditions

must be satisfied. First, the linear system, which is obtained by neglecting all the system nonlinearities, must possess normal modes and secondly, the correlation matrix of the excitation must be diagonalized by the same transformation matrix that diagonalizes the mass, damping, and the stiffness matrices. The second condition is quite restrictive and imposes rather a severe limitation on the usefulness of this approach for the present problem.

7.3.3 The Perturbation Method [50]

In this application, the stochastically excited nonlinear system is treated in the same way as a deterministically excited system. The solution is assumed as an expansion in powers of some small parameter which corresponds to the magnitude of the nonlinearity. Substituting the power series solution into the original equations of motion and equating the coefficients of like powers of the nonlinearity parameter, a set of linear differential equations can be obtained for the terms in the expansion of the solution. This leads to a first order approximation which can be obtained by solving two sets of linear differential equations. The first set of differential equations is obtained by assuming all nonlinearities equal to zero, and the second is a system of equations having an excitation which is a function of the solution of the first system. The major limitations of this approach are that the system analyzed should possess only weak nonlinearities and that the system must contain some finite amount of linear viscous dissipation so that the solution of the linearized equations would be in a bounded form. In the

present case, the system has strong nonlinearities and the viscous damping matrix is especially a null matrix when the stabilizer is not in operation. Therefore, the mean square responses of the linearized vehicle equations based on the perturbation method will tend to infinity and simply indicate an instability of the solutions obtained.

7.3.4 The Statistical Linearization Technique [51,52]

The technique of statistical linearization overcomes many of the previously stated limitations and difficulties encountered in the earlier discussed methods for studying the stationary random response of a multidegree-of-freedom stochastic system. This technique is based on the concept of replacing the nonlinear system by a related linear system in such a way that the difference in behavior between the two systems is minimized as much as possible. This concept has been widely employed in the study of multidegree-of-freedom nonlinear systems with deterministic excitations. The application of this concept to nonlinear multidegree-of-freedom systems under stochastic excitations has been discussed by Foster [51], Iwan and Yang [52] and recently by Atalik and Utku [46]. The only limitation for this approach is that the excitation should possess basically a Gaussian distribution. This condition is well satisfied in the case of track irregularities [58]. The statistical linearization procedure is discussed in detail in the following section and is applied to the present problem for obtaining probabilistic measure of the rocking response.

7.4 The Application of Statistical Linearization

Let the n degree-of-freedom nonlinear system be described by the equation of motion

$$\underset{\sim}{M}\ddot{\underset{\sim}{X}} + \underset{\sim}{C}\dot{\underset{\sim}{X}} + \underset{\sim}{K}\underset{\sim}{X} + \underset{\sim}{g}(\dot{\underset{\sim}{y}},\underset{\sim}{z}) = \underset{\sim}{F}_c \qquad (7.1)$$

Here,

$\underset{\sim}{X}$ is the generalized displacement vector,

$\underset{\sim}{g}(\dot{\underset{\sim}{y}},\underset{\sim}{z})$ is the generalized nonlinear force vector containing the stationary Gaussian forcing function acting on the system

where $\dot{\underset{\sim}{y}}$ is a vector representing the rate of displacements of the velocity dependent nonlinear elements,

$\underset{\sim}{z}$ is a vector representing the displacements of the displacement-dependent nonlinear elements.

Further,

$\underset{\sim}{y}$ and $\underset{\sim}{z}$ are linear functions of the generalized coordinates vector $\underset{\sim}{X}$ and

$\underset{\sim}{F}_c$ is a constant vector representing the deviation of the input forcing function from a zero mean.

In order to obtain an approximate solution of Equation (7.1), consider an auxiliary system which is described by a set of linear differential equations of the form.

$$\underset{\sim}{M}\ddot{\underset{\sim}{X}} + \underset{\sim}{C}\dot{\underset{\sim}{X}} + \underset{\sim}{K}\underset{\sim}{X} + \underset{\sim}{\gamma}\dot{\underset{\sim}{y}} + \underset{\sim}{\eta}\underset{\sim}{z} = \underset{\sim}{F}_c \qquad (7.2)$$

where $\underset{\sim}{\gamma}$ and $\underset{\sim}{\eta}$ are two arbitrary matrices. The elements of $\underset{\sim}{\gamma}$ and $\underset{\sim}{\eta}$ are represented by γ_{ij} and η_{ij} respectively. Equation (7.2) is assumed to

possess a known stationary Gaussian solution which may be represented in the form:

$$\underset{\sim}{X} = \underset{\sim}{X}(\gamma_{ij}, \eta_{ij}, t) \tag{7.3}$$

The difference between the vector equation describing the actual system and that of the auxiliary system may be expressed as $\underset{\sim}{e}$ so that

$$\underset{\sim}{e} = \underset{\sim}{g}(\dot{\underset{\sim}{y}}, \underset{\sim}{z}) - \underset{\sim}{\gamma}\dot{\underset{\sim}{y}} - \underset{\sim}{\eta}\underset{\sim}{z} \tag{7.4}$$

The magnitude of the vector $\underset{\sim}{e}$, representing the error, is clearly a function of the auxiliary system parameters γ_{ij} and η_{ij}. An approximate solution for the original Equation (7.1) can be generated by selecting γ_{ij} and η_{ij} in such a way that some measure of the difference $\underset{\sim}{e}$ is minimized. As a minimization criterion on $\underset{\sim}{e}$, it is taken that the mean value of the scalar product $\underset{\sim}{e}^T\underset{\sim}{e}$ be a minimum. That is:

$$E[\underset{\sim}{e}^T\underset{\sim}{e}] \text{ is a minimum} \tag{7.5}$$

where the operator E denotes the statistical average or the mathematical expectation of the process.

The necessary conditions for the criterion (7.5) are then:

$$\begin{aligned} \frac{\partial E[\underset{\sim}{e}^T\underset{\sim}{e}]}{\partial \gamma_{ij}} &= 2E[\underset{\sim}{e}^T \frac{\partial \underset{\sim}{e}}{\partial \gamma_{ij}}] = 2E[e_i \dot{y}_j] = 0 \\ \frac{\partial E[\underset{\sim}{e}^T\underset{\sim}{e}]}{\partial \eta_{ij}} &= 2E[\underset{\sim}{e}^T \frac{\partial \underset{\sim}{e}}{\partial \eta_{ij}}] = 2E[e_i z_j] = 0 \end{aligned} \tag{7.6}$$

Using the definition of $\underset{\sim}{e}$ in Equation (7.4) into the conditions (7.6) above:

$$E[\underset{\sim}{e}\dot{\underset{\sim}{y}}^T] = E[\underset{\sim}{g}(\dot{\underset{\sim}{y}},\underset{\sim}{z})\dot{\underset{\sim}{y}}^T] - \underset{\sim}{\gamma}E[\dot{\underset{\sim}{y}}\dot{\underset{\sim}{y}}^T] - \underset{\sim}{\eta}E[\underset{\sim}{z}\dot{\underset{\sim}{y}}^T] = 0$$

$$E[\underset{\sim}{e}\underset{\sim}{z}^T] = E[\underset{\sim}{g}(\dot{\underset{\sim}{y}},\underset{\sim}{z})\underset{\sim}{z}^T] - \underset{\sim}{\gamma}E[\dot{\underset{\sim}{y}}\underset{\sim}{z}^T] - \underset{\sim}{\eta}E[\underset{\sim}{z}\underset{\sim}{z}^T] = 0 \qquad (7.7)$$

In all of these equations $\underset{\sim}{X}$, $\underset{\sim}{y}$ and $\underset{\sim}{z}$ correspond to the approximate solution of Equation (7.2).

In order to determine analytically the coefficients of $\underset{\sim}{\eta}$ and $\underset{\sim}{\gamma}$ in Equation (7.2), the nonlinear forces vector $\underset{\sim}{g}(\dot{\underset{\sim}{y}},\underset{\sim}{z})$ in Equation (7.1) must be decomposed into a sum of simpler nonlinear forces, each of which depending solely on the velocity and displacement of a single nonlinear element. To accomplish the above decomposition, a function $S_{ik}(\dot{y}_k,z_k)$ is employed to denote one of the nonlinear forces acting along the direction of the generalized coordinate X_i due to the velocity and displacement $\dot{y}_K$ and z_k of the nonlinear element k. Therefore, the nonlinear force in the direction X_i will have the summation form:

$$g_i(\dot{\underset{\sim}{y}},\underset{\sim}{z}) = \sum_k S_{ik}(\dot{y}_k,z_k) \qquad (7.8)$$

and the summation is taken over all the nonlinear elements associated with the ith generalized coordinate.

Multiplying the expression (7.8) by $\dot{y}_j$ and averaging both sides and then repeating the same for z_j,

$$E[g_i(\dot{\underset{\sim}{y}},\underset{\sim}{z})\dot{y}_j] = \sum_k E[S_{ik}(\dot{y}_K,z_K)\dot{y}_j]$$

$$E[g_i(\dot{\underset{\sim}{y}},\underset{\sim}{z})z_j] = \sum_k E[S_{ik}(\dot{y}_k,z_k)z_j] \qquad (7.9)$$

Since $\underset{\sim}{X}$ is Gaussian, it follows that the quantities $\dot{y}_k$, z_k, $\dot{y}_j$ and z_j will also be Gaussian distributed. Hence it may be shown that

$$E[S_{ij}(\dot{y}_k,z_k)\dot{y}_j] = E[S_{ik}(\dot{y}_k,z_k)\dot{y}_k]\cdot E[\dot{y}_k\dot{y}_j]/E[\dot{y}_k^2] + E[S_{ik}(\dot{y}_k,z_k)z_k]\cdot E[z_k\dot{y}_j]/E[z_k^2] \tag{7.10}$$

and

$$E[S_{ik}(\dot{y}_k,z_k)z_j] = E[S_{ik}(\dot{y}_k,z_k)\dot{y}_k]\cdot E[\dot{y}_k z_j]/E[\dot{y}_k^2] + E[S_{ik}(\dot{y}_k,z_k)z_k]\cdot E[z_k z_j]/E[z_k^2]$$

The details of the derivation of the above expressions is given in Appendix V.

Now the coefficients of the matrices $\underset{\sim}{\gamma}$ and $\underset{\sim}{\eta}$ given in Equation (7.2) can be defined in a probabilistic form as follows:

$$\gamma_{ik} = E[S_{ik}(\dot{y}_k,z_k)\dot{y}_k]/E[\dot{y}_k^2]$$
$$\eta_{ik} = E[S_{ik}(\dot{y}_k,z_k)z_k]/E[z_k^2] \tag{7.11}$$

Using the above in Equation (7.10):

$$E[S_{ik}(\dot{y}_k,z_k)\dot{y}_j] = E[(\gamma_{ik}\dot{y}_k + \eta_{ik}z_k)\dot{y}_j]$$
$$E[S_{ik}(\dot{y}_k,z_k)z_j] = E[(\gamma_{ik}\dot{y}_k + \eta_{ik}z_k)z_j] \tag{7.12}$$

The parameters γ_{ik} and η_{ik} defined in Equation (7.11) may therefore be thought of as defining an associated linear system which will have the same expected values $E[\underset{\sim}{g}(\underset{\sim}{\dot{y}},\underset{\sim}{z})\underset{\sim}{\dot{y}}^T]$ and $E[\underset{\sim}{g}(\underset{\sim}{\dot{y}},\underset{\sim}{z})\underset{\sim}{z}^T]$ as that of the given nonlinear system. It may be noted that, up to this point, no condition has been placed on the associated linear system that it should be such that $E[\underset{\sim}{e}^T\underset{\sim}{e}]$ is a minimum.

Substitution of Equation (7.12) into Equation (7.9) gives

$$E[g_i(\dot{\underset{\sim}{y}},\underset{\sim}{z})\dot{y}_j] = E[\sum_k(\gamma_{ik}\dot{y}_k + \eta_{ik}z_k)\dot{y}_j]$$
$$E[g_i(\dot{\underset{\sim}{y}},\underset{\sim}{z})z_j] = E[\sum_k(\gamma_{ik}\dot{y}_k + \eta_{ik}z_k)z_j] \qquad (7.13)$$

Let the stiffness matrix and the damping matrix of the equivalent linear system defined through Equation (7.11) be denoted by $\underset{\sim}{K}_e$ and $\underset{\sim}{C}_e$. Then Equation (7.13) can also be written as:

$$E[\underset{\sim}{g}(\dot{\underset{\sim}{y}},\underset{\sim}{z})\dot{\underset{\sim}{y}}^T] = \underset{\sim}{C}_e E[\dot{\underset{\sim}{y}}\dot{\underset{\sim}{y}}^T] + \underset{\sim}{K}_e E[\underset{\sim}{z}\dot{\underset{\sim}{y}}^T]$$
$$E[\underset{\sim}{g}(\dot{\underset{\sim}{y}},\underset{\sim}{z})\underset{\sim}{z}^T] = \underset{\sim}{C}_e E[\dot{\underset{\sim}{y}}\underset{\sim}{z}^T] + \underset{\sim}{K}_e E[\underset{\sim}{z}\underset{\sim}{z}^T] \qquad (7.14)$$

Equation (7.7) may now be solved for the values of $\underset{\sim}{\gamma}$ and $\underset{\sim}{\eta}$ which would yield a minimum of $E[\underset{\sim}{e}^T\underset{\sim}{e}]$. Substitution of Equation (7.14) into Equation (7.7) results in:

$$(\underset{\sim}{\eta} - \underset{\sim}{K}_e)E[\underset{\sim}{z}\dot{\underset{\sim}{y}}^T] + (\underset{\sim}{\gamma} - \underset{\sim}{C}_e)E[\dot{\underset{\sim}{y}}\dot{\underset{\sim}{y}}^T] = \underset{\sim}{0}$$
$$(\underset{\sim}{\eta} - \underset{\sim}{K}_e)E[\underset{\sim}{z}\underset{\sim}{z}^T] + (\underset{\sim}{\gamma} - \underset{\sim}{C}_e)E[\dot{\underset{\sim}{y}}\underset{\sim}{z}^T] = \underset{\sim}{0}$$

This set of equations may also be written in the form:

$$[(\underset{\sim}{\eta}-\underset{\sim}{K}_e) \quad (\underset{\sim}{\gamma}-\underset{\sim}{C}_e)]\begin{bmatrix} E[\underset{\sim}{z}\dot{\underset{\sim}{y}}^T] & E[\underset{\sim}{z}\underset{\sim}{z}^T] \\ E[\dot{\underset{\sim}{y}}\dot{\underset{\sim}{y}}^T] & E[\dot{\underset{\sim}{y}}\underset{\sim}{z}^T] \end{bmatrix} = \underset{\sim}{0} \qquad (7.15)$$

If the square matrix in Equation (7.15) is non singular, the only solution to these equations is given by:

$$\underset{\sim}{\eta} = \underset{\sim}{K}_e$$
$$\underset{\sim}{\gamma} = \underset{\sim}{C}_e \qquad (7.16)$$

If the square matrix in Equation (7.15) is singular, Equation (7.16) is not necessarily the only solution [52]. Since no other

specific criterion is available to indicate that any of the solutions, other than the one in Equation (7.16), is better, the solution (7.16) is taken as the appropriation solution [52].

Consider now an important special case when the displacement-dependent nonlinear forces $\underset{\sim}{g}_2(\underset{\sim}{z})$ are independent of the velocity-dependent nonlinear forces $\underset{\sim}{g}_1(\dot{\underset{\sim}{y}})$. In this case, the nonlinear forces vector in (7.1) will take the form:

$$\underset{\sim}{g}(\dot{\underset{\sim}{y}},\underset{\sim}{z}) = \underset{\sim}{g}_1(\dot{\underset{\sim}{y}}) + \underset{\sim}{g}_2(\underset{\sim}{z})$$

This actually corresponds to the problem of the freight car system that is presently investigated. For such problems, the force vector $S_{ik}(\dot{y}_k, z_k)$, introduced in Equation (7.8), becomes:

$$S_{ik}(\dot{y}_k, z_k) = S_{ik}^{(1)}(\dot{y}_k) + S_{ik}^{(2)}(z_k) \tag{7.17}$$

as shown in detail in Appendix V. The expression in (7.17) results from the fact that variables z_k and $\dot{y}_k$ can be shown to be completely uncorrelated. This implies that expressions (7.11) can be reduced to the form:

$$\gamma_{ik} = E[S_{ik}^{(1)}(\dot{y}_k)\cdot\dot{y}_k]/E[\dot{y}_k^2] \tag{7.18}$$

$$\eta_{ik} = E[S_{ik}^{(2)}(z_k)\cdot z_k]/E[z_k^2] \tag{7.19}$$

When expressions for γ_{ik} and η_{ik} given in (7.18) and (7.19) are used in the system Equations (7.2), the original nonlinear stochastic system (7.1) is reduced to an equivalent linear system. In summary, the nonlinear equations of motion given by (7.1) have

been reduced to a set of Equations (7.2) of an associated linear problem. The parameters required to define the equivalent linear system are the elements of the matrices $\underset{\sim}{\gamma}$ and $\underset{\sim}{\eta}$ through expressions (7.18) and (7.19). The elements of $\underset{\sim}{\gamma}$ and $\underset{\sim}{\eta}$ are in turn functions of the mean square response of the linearized system.

The linear stochastic equations given in (7.2) may be solved on a digital computer by means of an iterative procedure. A set of initial values for $\underset{\sim}{\gamma}$ and $\underset{\sim}{\eta}$ are assumed and the instantaneous covariance matrix $\underset{\sim}{P}$ is calculated from which the mean square responses are defined. Using these responses more accurate values for the elements of $\underset{\sim}{\gamma}$ and $\underset{\sim}{\eta}$ are recalculated and the process is repeated until the desired accuracy of the mean square responses of the given system is achieved. The step by step procedure is explained in the form of a flow chart in Fig. 7.1. In the following section the procedure for evaluating the elements of the equivalent linear freight car system is described.

7.5 The Equivalent Linear Freight Car System

As mentioned earlier the freight car equations of motion should be described in a certain matrix form in order to conform to the methods available for solving such nonlinear systems under random excitation. This form for the equations of motion can be obtained using the single configuration model described in Chapter 2. The equations of motion of this system were presented in Section 5.2. Expressed in a matrix form, these equations of motion become:

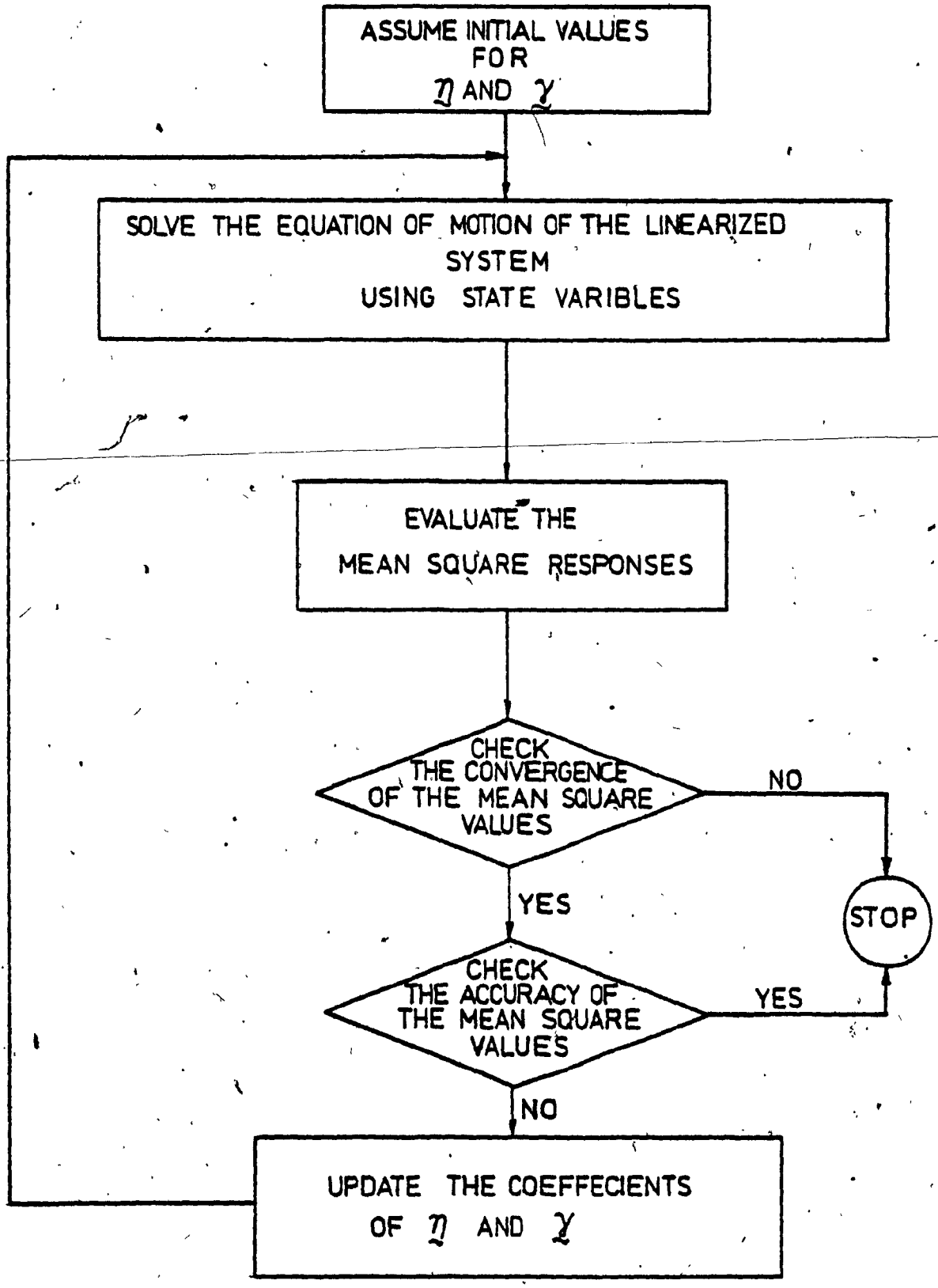

Fig. 7.1: Procedure for Solving for the Mean Square Response.

$$\underset{\sim}{M}\ddot{\underset{\sim}{X}} + \underset{\sim}{C}\dot{\underset{\sim}{X}} + \underset{\sim}{K}\underset{\sim}{X} + \underset{\sim}{g}_1(\dot{\underset{\sim}{y}}) + \underset{\sim}{g}_2(\underset{\sim}{z}) = \underset{\sim}{F}_c \tag{7.20}$$

where

$\underset{\sim}{M}$, $\underset{\sim}{C}$ and $\underset{\sim}{K}$ are the (9x9) mass, damping and stiffness matrices,

$\dot{\underset{\sim}{y}}$ is the friction damper velocities, given by:

$$\dot{\underset{\sim}{y}} = \underset{\sim}{A}^*\dot{\underset{\sim}{X}} = \begin{bmatrix} \dot{y}_1 \\ \dot{y}_2 \\ \dot{y}_3 \\ \dot{y}_4 \\ \dot{y}_5 \\ \dot{y}_6 \end{bmatrix} = \begin{bmatrix} \dot{Z}_c \\ \dot{Y}_c \\ 2f\dot{\theta}_c - 2f\dot{\theta}_w \\ \dot{Z}_t + f\dot{\theta}_t - \dot{Z}_w - f\dot{\theta}_w \\ \dot{Y}_t - h\dot{\theta}_t - \dot{Y}_w + r_2\dot{\theta}_w \\ \dot{Z}_t - f\dot{\theta}_t - \dot{Z}_w + f\dot{\theta}_w \end{bmatrix} \tag{7.21}$$

Futher, $\underset{\sim}{g}_1(\dot{\underset{\sim}{y}})$ represents the nonlinear friction damper forces which can be expressed in the form

$$\underset{\sim}{g}_1(\dot{\underset{\sim}{y}}) = \begin{bmatrix} 0 \\ 0 \\ 2F_c f s_3 \\ F_t(s_1 + s_2) \\ F_t s_4 \\ F_t s_1 f - F_t s_2 f - F_t s_4 h \\ -F_t(s_1 + s_2) \\ -F_t s_4 \\ -F_t s_1 f - F_t s_2 f - 2F_c f s_3 - F_t s_4 r_2 \end{bmatrix} \tag{7.22}$$

where s_1, s_2, s_3 and s_4 are defined in Equation (5.7) to be:

$$s_1 = \mathrm{Sgn}(\dot{y}_4), \qquad s_2 = \mathrm{Sgn}(\dot{y}_6)$$
$$s_3 = \mathrm{Sgn}(\dot{y}_3), \qquad s_4 = \mathrm{Sgn}(\dot{y}_5) \tag{7.23}$$

Also $\underset{\sim}{z}$ are the nonlinear spring deflections, given in Table 7.1, having the form:

$$\underset{\sim}{z} = \underset{\sim\sim}{E}\underset{\sim}{X} - \underset{\sim}{b}(t) = \begin{bmatrix} z_1 \\ z_2 \\ z_3 \\ z_4 \\ z_5 \\ z_6 \\ z_7 \\ z_8 \\ z_9 \\ z_{10} \end{bmatrix} = \begin{bmatrix} Z_c - d\theta_c - Z_t + d\theta_t \\ Z_c + d\theta_c - Z_t - d\theta_t \\ Z_c - e\theta_c - Z_t + e\theta_t \\ Z_c + e\theta_c - Z_t - e\theta_t \\ Y_c + b_1\theta_c - Y_t + C_1\theta_t \\ Y_c + b_2\theta_c - Y_t + C_2\theta_t \\ Z_w + W_B\theta_w - Z_R \\ Z_w - W_B\theta_w - Z_L \\ Y_R - Y_w - r_1\theta_w \\ Y_L - Y_w - r_1\theta_w \end{bmatrix} \qquad (7.24)$$

and $\underset{\sim}{g}_2(\underset{\sim}{z})$ represents the force vector due to the nonlinear stiffness elements, expressed in the form:

$$\underset{\sim}{g}_2(\underset{\sim}{z}) = \begin{bmatrix} F_1(z_1) + F_2(z_2) + F_3(z_3) + F_4(z_4) \\ F_5(z_5) + F_6(z_6) \\ -(F_1(z_1)-F_2(z_2))d-(F_3(z_3)-F_4(z_4))e+F_5(z_5)b_1+F_6(z_6)b_2 \\ -F_1(z_1) - F_2(z_2) - F_3(z_3) - F_4(z_4) \\ -F_5(z_5) - F_6(z_6) \\ -(F_1(z_1)-F_2(z_2))d+(F_3(z_3)-F_4(z_4))e+F_5(z_5)C_1+F_6(z_6)C_2 \\ F_7(z_7) + F_8(z_8) \\ -F_9(z_9) - F_{10}(z_{10}) \\ (F_7(z_7) - F_8(z_8))W_B - (F_9(z_9) - F_{10}(z_{10}))r_1 \end{bmatrix} \qquad (7.25)$$

Description	Force	Deflection	Presentation	Nonlinear Term
Left Centre Plate	$F_1(z_1)=K_p z_1 S_1(z_1)$	$z_1=Z_c-d\theta_c-Z_t+d\theta_t$	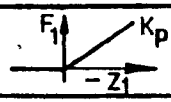	$S_1(z_1)=\begin{cases}0 & \text{if } z_1>0\\ 1 & \text{if } z_1<0\end{cases}$
Right Centre Plate	$F_2(z_2)=K_p z_2 S_2(z_2)$	$z_2=Z_c+d\theta_c-Z_t-d\theta_t$	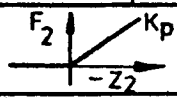	$S_2(z_2)=\begin{cases}0 & \text{if } z_2>0\\ 1 & \text{if } z_2<0\end{cases}$
Left Side Bearing	$F_3(z_3)=K_b(z_3+z_{30})S_3(z_3)$	$z_3=Z_c-e\theta_c-Z_t+e\theta_t$	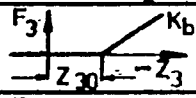	$S_3(z_3)=\begin{cases}0 & \text{if } (z_3+z_{30})>0\\ 1 & \text{if } (z_3+z_{30})<0\end{cases}$
Right Side Bearing	$F_4(z_4)=K_b(z_4+z_{40})S_4(z_4)$	$z_4=Z_c+e\theta_c-Z_t-e\theta_t$	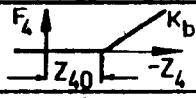	$S_4(z_4)=\begin{cases}0 & \text{if } z_4+z_{40}>0\\ 1 & \text{if } z_4+z_{40}<0\end{cases}$
Lateral Side Bearing	$F_5(z_5)=K_{pL} z_5 S_5(z_5)$	$z_5=Y_c+b_1\theta_c-Y_t+C_1\theta_t$	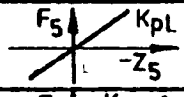	$S_5(z_5)=1$
Gib Stop	$F_6(z_6)=K_G(z_6-z_{60}\cdot \mathrm{Sgn} z_6)S_6(z_6)$	$z_6=Y_c+b_2\theta_c-Y_t+C_2\theta_t$	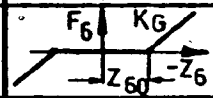	$S_6(z_6)=\begin{cases}0 & \text{if } z_{60}>z_6>-z_{60}\\ 1 & \text{if } -z_{60}>z_6>z_{60}\end{cases}$
Right Rail Vertical	$F_7(z_7)=K_r z_7 S_7(z_7)$	$z_7=Z_w+W_B\theta_w-Z_R$	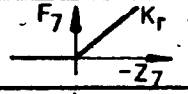	$S_7(z_7)=\begin{cases}0 & \text{if } z_7>0\\ 1 & \text{if } z_7<0\end{cases}$
Left Rail Vertical	$F_8(z_8)=K_r z_8 S_8(z_8)$	$z_8=Z_w-W_B\theta_w-Z_L$	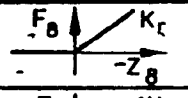	$S_8(z_8)=\begin{cases}0 & \text{if } z_8>0\\ 1 & \text{if } z_8<0\end{cases}$
Right Rail Lateral	$F_9(z_9)=K_{rL} z_9 S_9(z_9)$	$z_9=Y_R-Y_w-r_1\theta_w$	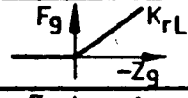	$S_9(z_9)=\begin{cases}0 & \text{if } z_9>0\\ 1 & \text{if } z_9<0\end{cases}$
Left Rail Lateral	$F_{10}(z_{10})=K_{rL} z_{10} S_{10}(z_{10})$	$z_{10}=Y_L-Y_w-r_1\theta_w$	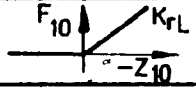	$S_{10}(z_{10})=\begin{cases}0 & \text{if } z_{10}>0\\ 1 & \text{if } z_{10}<0\end{cases}$

Table 7.1. The Nonlinear Spring Forces F_i, and the Corresponding Deflections z_i.

and $F_i(z_i)$ are the nonlinear spring forces undergoing respective deflections, z_i. Expressions for F_i and the appropriate z_i for different nonlinear springs are given in Table 7.1. Also, $\underset{\sim}{A}^*$ in (7.21) and $\underset{\sim}{E}$ in (7.24) are the transformation matrices of constant coefficients, and are given in Appendix VI. Further $\underset{\sim}{b}(t)$ in (7.24) is a vector function representing the input stochastic excitations, and $\underset{\sim}{F}_c$ represents the constant gravitational forces.

Now the elements of the matrices $\underset{\sim}{\gamma}$ and $\underset{\sim}{\eta}$ in Equation (7.2) can be evaluated to reduce the original nonlinear stochastic system (7.20) to an equivalent linear system. First, the elements of $\underset{\sim}{\gamma}$ are computed utilizing the elements of the force vector $\underset{\sim}{g}_1(\dot{\underset{\sim}{y}})$ in Equation (7.22).

As described earlier, that in order to apply the expression derived for the elements γ_{ik} in Equation (7.18), the elements of the force vector $\underset{\sim}{g}_1(\dot{\underset{\sim}{y}})$ in Equation (7.22) associated with the generalized coordinate i should be decomposed into a sum of simpler nonlinear forces $S_{ik}^{(1)}(\dot{y}_k)$. Each of these forces depend solely on the velocity $\dot{y}_k$ of a single nonlinear element. The required decomposed form of $\underset{\sim}{g}_1(\dot{\underset{\sim}{y}})$ is given by:

$$\underset{\sim}{g}_1(\dot{\underset{\sim}{y}}) = \begin{bmatrix} 0 \\ 0 \\ S_{33}(\dot{y}_3) \\ S_{44}(\dot{y}_4) + S_{46}(\dot{y}_6) \\ S_{55}(\dot{y}_5) \\ S_{64}(\dot{y}_4) + S_{65}(\dot{y}_5) + S_{66}(\dot{y}_6) \\ S_{74}(\dot{y}_4) + S_{76}(\dot{y}_6) \\ S_{85}(\dot{y}_5) \\ S_{93}(\dot{y}_3) + S_{94}(\dot{y}_4) + S_{95}(\dot{y}_5) + S_{96}(\dot{y}_6) \end{bmatrix} \tag{7.26}$$

The elements of the γ matrix in Equation (7.18) was defined earlier to be of the form:

$$\gamma_{ik} = E[S_{ik}^{(1)}(\dot{y}_k)\cdot\dot{y}_k]/E[\dot{y}_k^2] \qquad (7.27)$$

with $i = 1,2,\ldots 9$, $k = 1,2,\ldots 6$

Let the terms of the friction forces $S_{ik}^{(1)}(\dot{y}_k)$ above be expressed in terms of a magnitude F_{ik} and appropriate sign. Then:

$$S_{ik}^{(1)}(\dot{y}_k) = F_{ik}\,\mathrm{Sgn}(\dot{y}_k)$$

$$= \begin{bmatrix} F_{ik} \\ 0 \\ -F_{ik} \end{bmatrix} \quad \text{if} \quad \dot{y}_k \quad \begin{bmatrix} +(ve) \\ 0 \\ -(ve) \end{bmatrix} \qquad (7.28)$$

Substituting (7.28) into (7.27)

$$\gamma_{ik} = F_{ik}\cdot E[\mathrm{Sgn}(\dot{y}_k)\cdot\dot{y}_k]/E[\dot{y}_k^2] \qquad (7.29)$$

In order to generate the expected values in (7.29), the probability density of $\dot{y}_k$ should be given. $\dot{y}$ is a linear function of the response vector X. Since X is a stationary Gaussian process, $\dot{y}$ can also be shown to be stationary and Gaussian. Therefore, the probability density $p(\dot{y}_k)$ is given by:

$$p(\dot{y}_k) = \frac{1}{\sqrt{2\pi}\,\sigma_{\dot{y}_k}} \exp[-\dot{y}_k^2/2\sigma_{\dot{y}_k}^2] \qquad (7.30)$$

Now using expressions for the expectations in (7.29) in terms of $p(\dot{y}_k)$,

$$\gamma_{ik} = [F_{ik}\int_{-\infty}^{\infty} \mathrm{Sgn}(\dot{y}_k)\cdot\dot{y}_k\cdot p(\dot{y}_k)d\dot{y}_k]/E[\dot{y}_k^2] \qquad (7.31)$$

Substituting the normal probability density (7.30) in Equation (7.31):

$$\gamma_{ik} = \frac{F_{ik}}{\sqrt{2\pi}\,\sigma_{\dot{y}_k}^{3}}\left[-\int_{-\infty}^{0}\dot{y}_k\,\exp\left[\frac{-\dot{y}_k^{2}}{2\sigma_{\dot{y}_k}^{2}}\right]d\dot{y}_k + \int_{0}^{\infty}\dot{y}_k\,\exp\left[\frac{-\dot{y}_k^{2}}{2\sigma_{\dot{y}_k}^{2}}\right]d\dot{y}_k\right]$$

Carrying out the integration, the above expression simplies to:

$$\gamma_{ik} = \sqrt{\frac{2}{\pi}}\,\frac{F_{ik}}{\sigma_{\dot{y}_k}} \tag{7.32}$$

Substituting the values of the forces F_{ik} in Equation (7.22) into Equation (7.32) for all values of i from 1 to 9 and k from 1 to 6, the γ matrix in Equation (7.2) has the final form:

$$\underset{\sim}{\gamma} = \begin{bmatrix}
0 & 0 & 0 & 0 & 0 & 0 \\
0 & 0 & 0 & 0 & 0 & 0 \\
0 & 0 & 2\sqrt{\frac{2}{\pi}}\frac{F_c f}{\sigma_{\dot{y}_3}} & 0 & 0 & 0 \\
0 & 0 & 0 & \sqrt{\frac{2}{\pi}}\frac{F_t}{\sigma_{\dot{y}_4}} & 0 & \sqrt{\frac{2}{\pi}}\frac{F_t}{\sigma_{\dot{y}_6}} \\
0 & 0 & 0 & 0 & \sqrt{\frac{2}{\pi}}\frac{F_t}{\sigma_{\dot{y}_3}} & 0 \\
0 & 0 & 0 & \sqrt{\frac{2}{\pi}}\frac{F_t f}{\sigma_{\dot{y}_4}} & -\sqrt{\frac{2}{\pi}}\frac{F_t h}{\sigma_{\dot{y}_5}} & -\sqrt{\frac{2}{\pi}}\frac{F_t f}{\sigma_{\dot{y}_6}} \\
0 & 0 & 0 & -\sqrt{\frac{2}{\pi}}\frac{F_t}{\sigma_{\dot{y}_4}} & 0 & -\sqrt{\frac{2}{\pi}}\frac{F_t}{\sigma_{\dot{y}_6}} \\
0 & 0 & 0 & 0 & -\sqrt{\frac{2}{\pi}}\frac{F_t}{\sigma_{\dot{y}_5}} & 0 \\
0 & 0 & -2\sqrt{\frac{2}{\pi}}\frac{F_c f}{\sigma_{\dot{y}_3}} & \sqrt{\frac{2}{\pi}}\frac{F_t f}{\sigma_{\dot{y}_4}} & -\sqrt{\frac{2}{\pi}}\frac{F_t r_2}{\sigma_{\dot{y}_5}} & \sqrt{\frac{2}{\pi}}\frac{F_t f}{\sigma_{\dot{y}_6}}
\end{bmatrix} \tag{7.33}$$

Now a procedure, similar to that applied for evaluating the elements of $\underset{\sim}{\gamma}$ matrix from the nonlinear forces vector $\underset{\sim}{g}_1(\underset{\sim}{y})$, is used for obtaining the elements of the $\underset{\sim}{\eta}$ matrix from the nonlinear force vector $\underset{\sim}{g}_2(\underset{\sim}{z})$ in Equation (7.25). In order to achieve this, it is necessary that the elements of the nonlinear force vector $\underset{\sim}{g}_2(\underset{\sim}{z})$ in Equation (7.25) associated with the generalized coordinate i be decomposed into a sum of simpler forces $S_{ik}^{(2)}(z_k)$. Each of these forces should then depend solely on the displacements of each single nonlinear element z_k. Such a decomposed form of $\underset{\sim}{g}_2(\underset{\sim}{z})$ is given:

$$\underset{\sim}{g}_2(\underset{\sim}{z}) = \begin{bmatrix} S_{11}(z_1) + S_{12}(z_2) + S_{13}(z_3) + S_{14}(z_4) \\ S_{25}(z_5) + S_{26}(z_6) \\ S_{31}(z_1)+S_{32}(z_2)+S_{33}(z_3)+S_{34}(z_4)+S_{35}(z_5)+S_{36}(z_6) \\ S_{41}(z_1) + S_{42}(z_2) + S_{43}(z_3) + S_{44}(z_4) \\ S_{55}(z_5) + S_{56}(z_6) \\ S_{61}(z_1)+S_{62}(z_2)+S_{63}(z_3)+S_{64}(z_4)+S_{65}(z_5)+S_{66}(z_6) \\ S_{77}(z_7) + S_{78}(z_8) \\ S_{89}(z_9) + S_{8,10}(z_{10}) \\ S_{97}(z_7) + S_{98}(z_8) + S_{99}(z_9) + S_{9,10}(z_{10}) \end{bmatrix} \qquad (7.34)$$

The elements of the $\underset{\sim}{\eta}$ matrix in Equation (7.19) were defined earlier to be of the form:

$$\eta_{ik} = E[S_{ik}^{(2)}(z_k)\, z_k]/E[z_k^2] \qquad (7.35)$$

with $i = 1,2,\ldots.9$, and $k = 1,2,\ldots.10$

The terms $S_{ik}^{(2)}(z_k)$ in Equation (7.34) are the same nonlinear spring forces $F_k(z_k)$ given in Table 7.1 earlier. These forces $S_{ik}^{(2)}(z_k)$ can be expressed in terms of the stiffness elements K_{ik}, displacements z_k, and the nonlinearity terms $S_k(z_k)$ as in Table 7.1.

Then, for all values of k = 1,2,...10, except k = 5,6

$$S_{ik}^{(2)}(z_k) = F_k(z_k) = K_{ik}(z_k + z_{k0})S_k(z_k) \qquad (7.36a)$$

where $S_k(z_k) = \begin{cases} 0 & \text{for } (z_k + z_{k0}) > 0 \\ 1 & \text{for } (z_k + z_{k0}) < 0 \end{cases}$

For k = 5,6

$$S_{ik}^{(2)}(z_k) = F_k(z_k) = K_{ik}(z_k - z_{k0}\,\mathrm{Sgn}(z_k))S_k(z_k) \qquad (7.36b)$$

where $S_6(z_6) = \begin{cases} 0 & \text{for } (z_6)_0 > z_6 > -(z_6)_0 \\ 1 & \text{for } -(z_6)_0 < z_6 < (z_6)_0 \end{cases}$

and $S_5(z_5) = 1$

Using (7.36) in (7.35):

$$\eta_{ik} = K_{ik}\, E[(z_k + z_{k0})S_k(z_k)z_k]/E[z_k^2]$$

for k = 1,2,3,4,7,8,9,10 (7.37)

$$\eta_{ik} = K_{ik}\, E[(z_k - z_{k0}\,\mathrm{Sgn}(z_k))S_k(z_k)z_k]/E[z_k^2]$$

for k = 5,6

In order to generate the expected values in (7.37) the probability density of z_k should also be known. Since $\underset{\sim}{z}$ is a linear function of the response vector $\underset{\sim}{X}$ and $\underset{\sim}{X}$ is stationary Gaussian process, $\underset{\sim}{z}$ can also be shown to be a stationary Gaussian. Therefore,

the probability density $p(z_k)$ is:

$$p(z_k) = \frac{1}{\sqrt{2\pi}\,\sigma_{z_k}} \exp[-z_k^2/2\sigma_{z_k}^2] \qquad (7.38)$$

Now, expressions of the expectation in (7.37) is evaluated as:

$$\eta_{ik} = \frac{K_{ik}}{\sigma_{z_k}^2}\left[\int_{-\infty}^{-z_{k0}} z_k(z_k + z_{k0})p(z_k)dz_k\right]$$

for $k = 1,2,3,4,7,8,9,10$ (7.39)

$$\eta_{ik} = \frac{K_{ik}}{\sigma_{z_k}^2}\left[\int_{-\infty}^{-z_{k0}} z_k(z_k + z_{k0})p(z_k)dz_k + \int_{z_{k0}}^{\infty} z_k(z_k - z_{k0})p(z_k)dz_k\right]$$

for $k = 5,6$

Substituting for the probability density and evaluating the resulting integration, the above expressions simplify to:

$$\eta_{ik} = \frac{K_{ik}}{2}\left[1 + \text{erf}\left(\frac{-z_{k0}}{\sqrt{2}\,\sigma_{z_k}}\right)\right]$$

for $k = 1,2,3,4,7,8,9,10$ (7.40)

$$\eta_{ik} = K_{ik}\left[1 + \text{erf}\left(\frac{-z_{k0}}{\sqrt{2}\,\sigma_{z_k}}\right)\right]$$

for $k = 5,6$

Using the values of the stiffness elements K_{ik} from Equation (7.25) and Table 7.1 in the above expressions for all values of i from 1 to 9 and k from 1 to 10, the η matrix, in Equation (7.2), has the form:

$$\underset{\sim}{\eta} = \begin{bmatrix}
\frac{K_p}{2} & \frac{K_p}{2} & \frac{K_b}{2}+I_{13} & \frac{K_b}{2}+I_{14} & 0 & 0 & 0 & 0 & 0 & 0 \\
0 & 0 & 0 & 0 & K_{pL} & K_G+2I_{26} & 0 & 0 & 0 & 0 \\
\frac{-K_p d}{2} & \frac{K_p d}{2} & \frac{-K_b e}{2}+I_{33} & \frac{K_b e}{2}+I_{34} & K_{pL}b_1 & K_G b_2+2I_{36} & 0 & 0 & 0 & 0 \\
\frac{-K_p}{2} & \frac{-K_p}{2} & \frac{-K_b}{2}+I_{43} & \frac{-K_b}{2}+I_{44} & 0 & 0 & 0 & 0 & 0 & 0 \\
0 & 0 & 0 & 0 & -K_{pL} & -K_G+2I_{56} & 0 & 0 & 0 & 0 \\
\frac{K_p d}{2} & \frac{-K_p d}{2} & \frac{K_b e}{2}+I_{63} & \frac{-K_b e}{2}+I_{64} & K_{pL}C_1 & K_G C_2+2I_{66} & 0 & 0 & 0 & 0 \\
0 & 0 & 0 & 0 & 0 & 0 & \frac{K_r}{2} & \frac{K_r}{2} & 0 & 0 \\
0 & 0 & 0 & 0 & 0 & 0 & 0 & 0 & \frac{-K_L}{2} & \frac{-K_L}{2} \\
0 & 0 & 0 & 0 & 0 & 0 & \frac{K_r}{2} & \frac{-K_r}{2} & \frac{-K_{rL}}{2} & \frac{K_{rL}}{2}
\end{bmatrix} \tag{7.41}$$

where

$$I_{ik} = \frac{K_{ik}}{2}\left[\operatorname{erf}\left(\frac{-z_{k0}}{\sqrt{2}\,\sigma_{z_k}}\right)\right]$$

By using the $\underset{\sim}{\gamma}$ and $\underset{\sim}{\eta}$ matrices, (7.33) and (7.41), the original nonlinear problem in (7.20) is reduced to the solution of a related linear system (7.2). The numerical method utilized for solving the equivalent linear stochastic Equations (7.2) is described in detail in the following section.

7.6 Stochastic Response of the Equivalent Linear System

In this section, the solution of the equivalent linear stochastic system, defined by Equation (7.2), is described. The linear stochastic equations can be solved by any number of analytical

technique available in the literature [54,55]. These techniques are used for calculating the mean response vector and the instantaneous correlation matrix of the response process. However, since the input is Gaussian, the response process must also be Gaussian for a linear system and therefore the mean and the instantaneous correlation matrix completely define the first probability density of the process and therefore the response process is completely specified in the statistical sense.

Several techniques are available to calculate the mean and instantaneous correlation matrix, the most commonly used methods use either the impulse response or the frequency response approaches. In the first approach, the impulse response function and the principle of superposition are used to express the response vector in terms of stochastic integrals. Then, all of the instantaneous correlation matrices of the response process have to be deduced from the response integral. This involves evaluation of complex double integrals which may not possess simple closed-form solutions. In the second approach, the complex frequency response function matrix of the system is first determined. From this, the spectral density matrix of the response process is derived which is then integrated to yield the instantaneous correlation matrix. It is known that the difficulty of determining the complex frequency response matrix and performing the required integration increases rapidly with increasing number of degrees-of-freedom of the system. Hence, for a complex system such as the one under investigation both approaches involve fairly

serious computational problems.

To overcome this difficulty, a numerical approach is presented here which provides a particularly direct way of determining the instantaneous correlation matrix of the stationary random response of multidegree-of-freedom linear systems. In order to apply this approach, the system equations of motion should be expressed in terms of state variables as described in Subsection 7.6.1. The instantaneous correlation matrix $\underset{\sim}{P}$ is then described through a set of algebraic equations evaluated from these system state equations. Numerical solution of these equations yields the system mean square responses.

7.6.1 Representation of the System in State Space

To obtain the stochastic response of the equivalent linear system, the equations of motion are to be expressed in terms of state variables with a white noise input. First, the system stochastic Equation (7.2), is represented in state space and then the filter dynamic Equations (3.13) derived earlier, are incorporated into Equation (7.2) to arrive at the state equation of the complete system subjected to pure white noise input. This procedure is given in the following mathematical form.

Neglecting the effect of the gravitational forces, $\underset{\sim}{F}_c$, equations of motion (7.2) can be restated in the form:

$$\underset{\sim\sim}{M}\ddot{\underset{\sim}{X}} + \underset{\sim\sim}{C}\dot{\underset{\sim}{X}} + \underset{\sim\sim}{K}\underset{\sim}{X} + \underset{\sim\sim}{\gamma}\dot{\underset{\sim}{y}} + \underset{\sim\sim}{\eta}\underset{\sim}{z} = \underset{\sim}{0} \tag{7.42}$$

or in an alternate form, using the expressions for $\underset{\sim}{y}$ in Equation

(7.21) and $\underset{\sim}{z}$ in Equation (7.24), as:

$$\underset{\sim}{M}\ddot{\underset{\sim}{X}} + (\underset{\sim}{C} + \gamma\underset{\sim}{A}^*)\dot{\underset{\sim}{X}} + (\underset{\sim}{K} + \eta\underset{\sim}{E})\underset{\sim}{X} = \eta\underset{\sim}{b}(t) \qquad (7.43)$$

Premultiplying by $\underset{\sim}{M}^{-1}$ and using the identity $\dot{\underset{\sim}{X}} = \underset{\sim}{I}\dot{\underset{\sim}{X}}$, the above equation can be written in the form:

$$\begin{bmatrix} \ddot{\underset{\sim}{X}} \\ \dot{\underset{\sim}{X}} \end{bmatrix}_{(18x1)} = \begin{bmatrix} -\underset{\sim}{M}^{-1}(\underset{\sim}{C}+\gamma\underset{\sim}{A}^*) & -\underset{\sim}{M}^{-1}(\underset{\sim}{K}+\eta\underset{\sim}{E}) \\ \underset{\sim}{I} & \underset{\sim}{0} \end{bmatrix}_{(18x18)} \begin{bmatrix} \dot{\underset{\sim}{X}} \\ \underset{\sim}{X} \end{bmatrix}_{(18x1)} + \begin{bmatrix} \underset{\sim}{M}^{-1}\eta\underset{\sim}{F}_1 \\ \underset{\sim}{0} \end{bmatrix}_{(18x3)} \left[\underset{\sim}{F}_1^{-1}\underset{\sim}{b}(t)\right]_{(3x1)} \qquad (7.44)$$

where $\underset{\sim}{F}_1$ represents (10x3) transformation matrix with constant coefficients.

Then the equivalent linear system under filtered white noise in Equation (7.44) has the following state variable representation,

$$\dot{\underset{\sim}{q}} = \underset{\sim}{A}_V\underset{\sim}{q} + \underset{\sim}{B}_V\underset{\sim}{u} \qquad (7.45)$$

where

$\underset{\sim}{q}^T = [\dot{\underset{\sim}{X}}, \underset{\sim}{X}]$ is the state vector,

$\underset{\sim}{A}_V$ is the system matr

$\underset{\sim}{B}_V$ is the sys ed matrix,

and $\underset{\sim}{u}$ is the forcing functions in the form of

a fi

t), to the system consists of

the pe and was modeled in Chapter 3

as a th e noise input. The filter dynamic

Equations

$$\dot{\underset{\sim}{\psi}} = \underset{\sim}{A}_F\underset{\sim}{\psi} + \underset{\sim}{B}_F\underset{\sim}{W}$$
$$\underset{\sim}{u} = \underset{\sim}{C}_F\underset{\sim}{\psi} + \underset{\sim}{D}_F\underset{\sim}{W} \qquad (7.46)$$

Incorporating the filter Equations (7.46) into the system state Equations (7.45), the state equation of the complete system with a white noise input can be obtained:

$$\dot{\underset{\sim}{q}} = \underset{\sim}{A}_v\underset{\sim}{q} + \underset{\sim}{B}_v\underset{\sim}{C}_F\underset{\sim}{\psi} + \underset{\sim}{B}_v\underset{\sim}{D}_F\underset{\sim}{W}$$
$$\dot{\underset{\sim}{\psi}} = \underset{\sim}{A}_F\underset{\sim}{\psi} + \underset{\sim}{B}_F\underset{\sim}{W} \qquad (7.47)$$

or in an alternate form:

$$\begin{bmatrix}\dot{\underset{\sim}{q}}\\ \dot{\underset{\sim}{\psi}}\end{bmatrix} = \begin{bmatrix}\underset{\sim}{A}_v & \underset{\sim}{B}_v\underset{\sim}{C}_F\\ \underset{\sim}{0} & \underset{\sim}{A}_F\end{bmatrix}\begin{bmatrix}\underset{\sim}{q}\\ \underset{\sim}{\psi}\end{bmatrix} + \begin{bmatrix}\underset{\sim}{B}_v\underset{\sim}{D}_F\\ \underset{\sim}{B}_F\end{bmatrix}\underset{\sim}{W} \qquad (7.48)$$

Equation (7.48) can be restated to represent the complete linear system in a state variable form:

$$\dot{\underset{\sim}{q}}_0 = \underset{\sim}{A}_0\underset{\sim}{q}_0 + \underset{\sim}{B}_0\underset{\sim}{W} \qquad (7.49)$$

where $\underset{\sim}{W}$ is the input white noise vector having a covariance matrix $\underset{\sim}{D}$ given in Equation (3.14).

7.6.2 The Instantaneous Response Covariance Matrix

As mentioned earlier, the input white noise vector $\underset{\sim}{W}(t)$ to the complete system in Equation (7.49) is stationary and Gaussian, and therefore, the response process will also be stationary and Gaussian. Hence, the mean response vector and the instantaneous correlation matrix are sufficient to specify completely the response process. The procedure for obtaining the mean response vector is derived in

Appendix VII. The instantaneous covariance matrix for the system given by Equation (7.49) is defined by:

$$\underset{\sim}{P} = E[\underset{\sim}{q}_0(t)\ \underset{\sim}{q}_0{}^T(t)] \tag{7.50}$$

where the diagonal elements of $\underset{\sim}{P}$ are the mean square values of the vector $\underset{\sim}{q}_0$.

Following the procedure described by Gersch [54], a solution to the system given by the state equation (7.49) may now be proposed. Let:

$$\underset{\sim}{q}_0(t) = e^{\underset{\sim}{A}_0(t-t_0)}\underset{\sim}{q}_0(t_0) + \int_{t_0}^{t} e^{\underset{\sim}{A}_0(t-\tau)}\underset{\sim}{B}_0\underset{\sim}{W}(\tau)d\tau \tag{7.51}$$

Using Equation (7.51) in the definition for $\underset{\sim}{P}$ in Equation (7.50), letting $t_0 \to \infty$ and averaging,

$$\underset{\sim}{P} = E[\underset{\sim}{q}_0(t)\ \underset{\sim}{q}_0{}^T(t)] = \int_{\infty}^{0} e^{-\underset{\sim}{A}_0\tau}\underset{\sim}{B}_0\underset{\sim}{D}\underset{\sim}{B}_0{}^T e^{-\underset{\sim}{A}_0{}^T\tau}d\tau \tag{7.52}$$

Instead of the integral relationship (7.52), an algebraic expression for $\underset{\sim}{P}$ can be developed following Gersch [54] by defining

$$\underset{\sim}{\xi}(\tau) = e^{-\underset{\sim}{A}_0\tau}\underset{\sim}{B}_0\underset{\sim}{D}\underset{\sim}{B}_0{}^T e^{-\underset{\sim}{A}_0{}^T\tau}, \tag{7.53}$$

and

$$\frac{d\underset{\sim}{\xi}(\tau)}{d\tau} = -\underset{\sim}{A}_0\underset{\sim}{\xi}(\tau) - \underset{\sim}{\xi}(\tau)\underset{\sim}{A}_0{}^T \tag{7.54}$$

Equation (7.54) can be integrated between the limits $(0, \infty)$ yielding directly the algebraic matrix equation:

$$\underset{\sim}{A}_0\underset{\sim}{P} + \underset{\sim}{P}\underset{\sim}{A}_0{}^T = -\underset{\sim}{B}_0\underset{\sim}{D}\underset{\sim}{B}_0{}^T = -\underset{\sim}{Q} \tag{7.56}$$

where $\underset{\sim}{Q}$ is a modified constant input covariance matrix.

A numerical solution of the Equation (7.56) for the unknown elements of $\underset{\sim}{P}$, in terms of the elements of the matrices $\underset{\sim}{A}_0$ and $\underset{\sim}{Q}$, is demonstrated in the following subsection.

7.6.3 Numerical Solution for the Response

The set of linear algebraic Equations (7.56), classically referred to as the Lyapunov's equation [56], appears in many engineering applications and an efficient solution for $\underset{\sim}{P}$ has often been sought. A numerical method suggested by Davison and Man [56] is employed in the present problem. The method assumes a solution for $\underset{\sim}{P}$ by a limiting process. That is:

$$\underset{\sim}{P} = \lim_{k\to\infty} \underset{\sim}{P}_k \qquad (7.57)$$

where

$$\underset{\sim}{P}_{k+1} = (\underset{\sim}{\Gamma}^T)^{2^k} \underset{\sim}{P} (\underset{\sim}{\Gamma})^{2^k} + \underset{\sim}{P}_k \ , \ k = 0,1,2,3..,$$

and

$$\underset{\sim}{P}_0 = h_0 \underset{\sim}{Q}$$

where h_0 is suggested to be 10^{-4} to 10^{-6}. Here, $\underset{\sim}{\Gamma}$ is a state transition matrix and a good approximation for it is given in [56] as:

$$\underset{\sim}{\Gamma} \doteq (\underset{\sim}{I} - \frac{h_0}{2}\underset{\sim}{A}_0 + \frac{h_0^2}{12}\underset{\sim}{A}_0^2)^{-1}(\underset{\sim}{I} + \frac{h_0}{2}\underset{\sim}{A}_0 + \frac{h_0^2}{12}\underset{\sim}{A}_0^2)$$

The algorithm is said to be numerically stable for all values of h since

$$\mathrm{Re}[\lambda_i(\underset{\sim}{A}_0)] < 0 \ , \quad i = 1,2,\ldots n$$

This property is checked in the computer program during the solution by evaluating the eigenvalues λ_i of the matrix $\underset{\sim}{A}_0$ using a library

value of the rocking power spectral density $S_{\theta_c}(\omega)$. The first function was plotted earlier in Fig. 7.2. To obtain such a plot, the nonlinear equations of motion (7.20) at a certain vehicle speed, v, were reduced to an associated linear problem (7.2) and then solved through iterative procedure to obtain values of $E[\theta_c^2]$ against v. This process demands excessive computer time and therefore it is not suitable for carrying out the parametric study. In the second type of representation using the spectral density plot, the linearization technique is applied only once, after which the power spectral density values are evaluated from expression (7.58). The function $S_{\theta_c}(\omega)$ has been plotted in Fig. 7.3 at a vehicle speed of 17 mph (27.3 km/hr). The maximum value of this function is a suitable measure of the vehicle performance over the critical range of exciting frequencies. Minimizing the maximum value of $S_{\theta_c}(\omega)$ over all the range of frequencies can then be undertaken.

The parametric study employed in this section utilizes the spectral density of the rocking response obtained from the solution of the single configuration model under stochastic excitation. Specifically, the effect on the responses in the rocking and sway modes due to installation of stabilizing device and due to track periodicity are studied as described in the following subsections.

8.2.1 Effect of the Stabilizer

Figures 8.1 and 8.2 show the effect of operating the stabilizing devices mounted between the car body and the side frame, shown in

Fig. 6.1, on minimizing the spectral density of the rocking and sway responses. The stabilizing device consists of a friction damper having a force F_c and shock absorber with a damping coefficient C_c. As a trial, the friction damper F_c is set equal to 8000 lb (35.58 kN) which is the original truck damping force and the shock absorber, C_c, is used with a soft setting.

It is seen from Figs. 8.1 and 8.2 that the stabilizer device reduces the system responses in the rocking mode as well as in the sway mode. The maximum value of the power spectral density of the rocking response is decreased by 42.01% when stabilizer is in operation. However, as mentioned earlier, large values of car friction damping force is not recommended because it would tend to lock the car body to the side frames, thereby eliminating the action of the suspension system entirely.

8.2.2 Effect of the Track Periodic Process

The effect of the rail periodicity on the rocking problem can be investigated from Figs. 8.3 and 8.4 shown. It can then be deduced that by eliminating the periodic input due to the rail joints from the total forcing function to the system, the car rocking response can be reduced significantly. This result can be obtained by equating the factor h in the input spectral density expression (3.7) to unity. However, such a conclusion cannot be considered a realistic solution to the problem, since the object of this study is to find the suspension parameters that minimize the rocking response while the

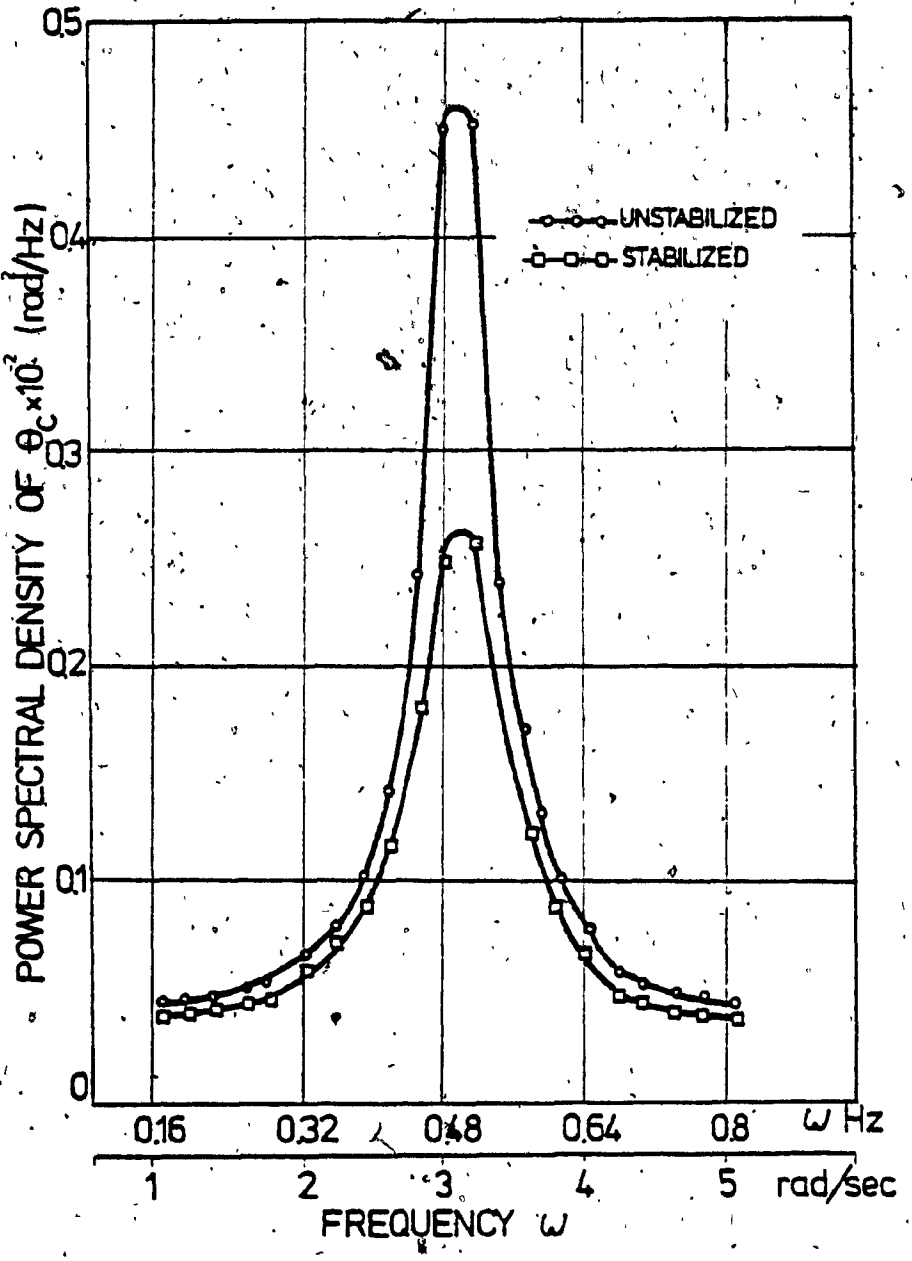

Fig. 8.1: The Power Spectral Density of the Rocking Response for Stabilized and Unstabilized Cars.

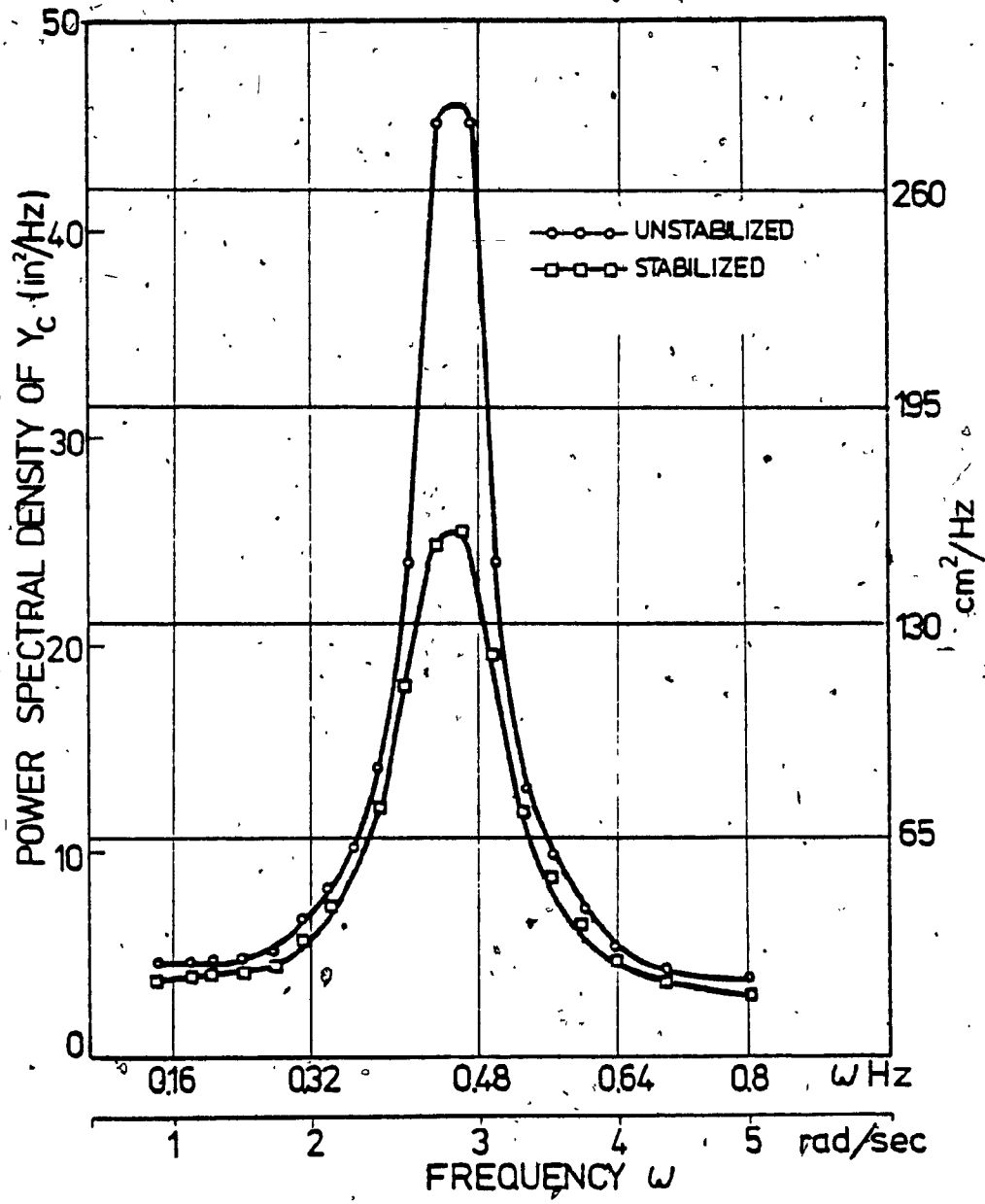

Fig. 8.2: The Power Spectral Density of the Car Lateral Displacement for Stabilized and Unstabilized Cars.

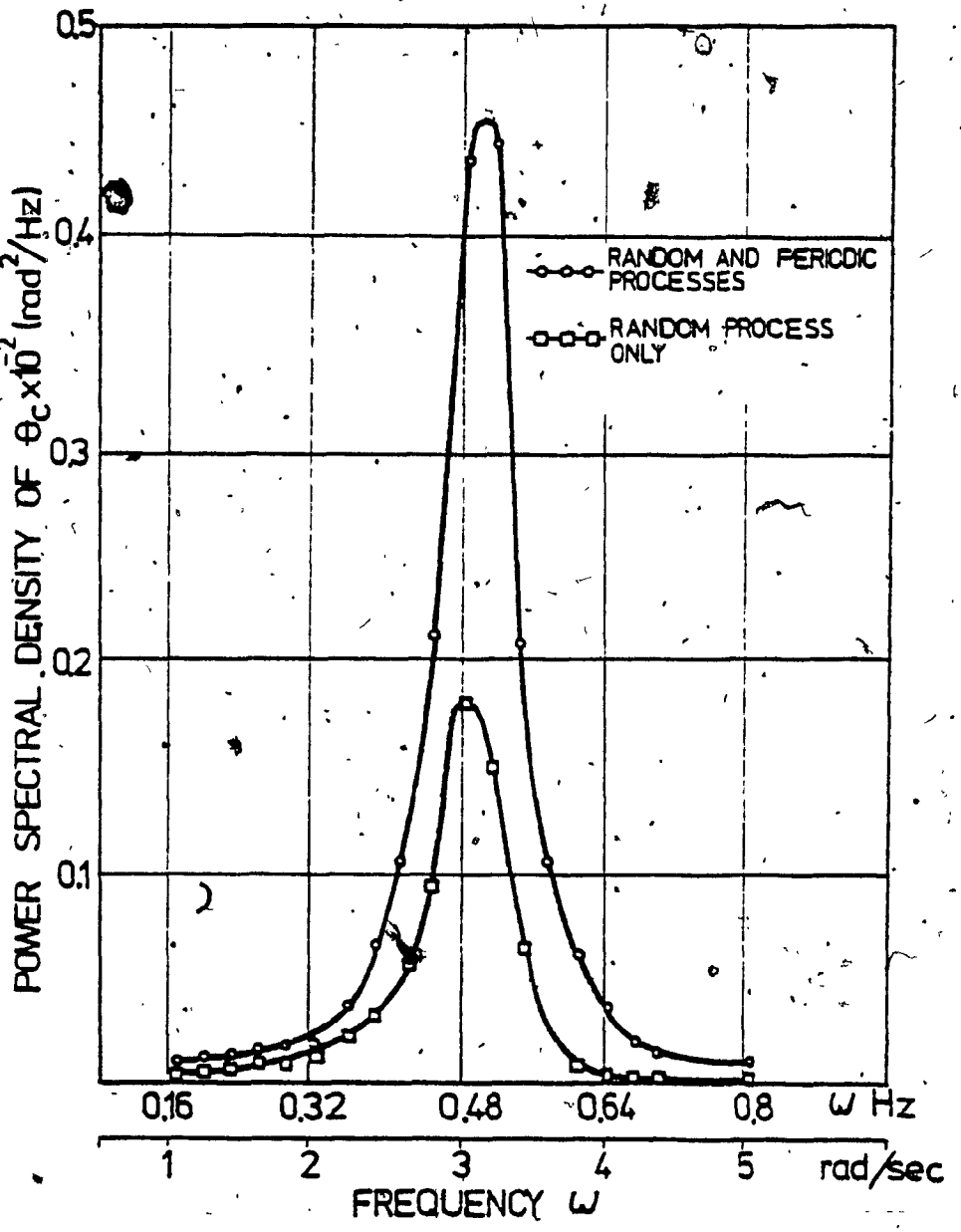

Fig. 8.3: Effect of the Track Periodicity on the Car Rocking Power Spectral Density.

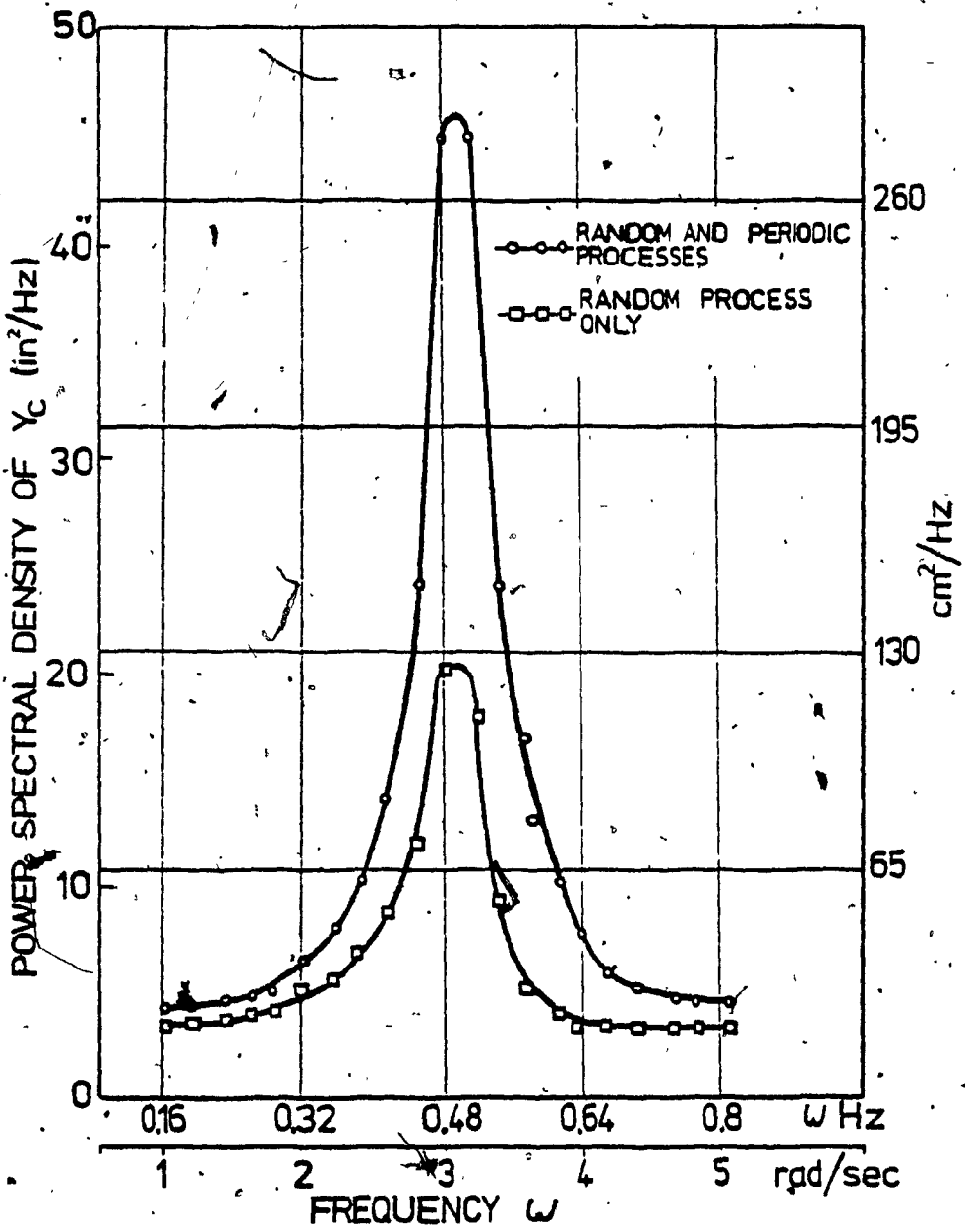

Fig. 8.4: Effect of the Track Periodicity on the Car Lateral Displacement Power Spectral Density.

track remains as it is. Hence, a practical solution to this problem requires further investigation utilizing multivariable optimization techniques, as described in the next section.

8.3 Suspension Optimization

As stated earlier, the spectral density of the rocking response shows a strong peak characterizing excessive rocking occurring in the region of the rocking mode natural frequency. This results in degradation of the track and deterioration of the suspension system over a period of time and thus directly affecting freight car operation and safety. Evidently, a solution for this is through a choice of optimum suspension parameters that would produce a minimum of car rocking power spectral density.

The objective function E of the minimax problem is defined in this case as the maximum value of the power spectral density of the car rocking response $S_{\theta_c}(\omega)$ in the range of frequencies ω of interest. It is then required to find the suspension elements $\underset{\sim}{Z}$ that give:

$$\min E = \min_{\omega_i} \max [S_{\theta_c}(\omega_i(\underset{\sim}{Z}), \underset{\sim}{Z})] \qquad (8.1)$$

subjected to constraints of the form:

$$\underset{\sim}{a} \leq \underset{\sim}{Z} \leq \underset{\sim}{b} \quad \text{where} \quad \underset{\sim}{a}, \underset{\sim}{b} \in R^n$$

The design variables vector $\underset{\sim}{Z}$ represents the group of suspension parameters chosen for carrying out the optimization. Since $S_{\theta_c}(\omega)$ is derived for the equivalent linear system given in Equation

(7.2), then $\underset{\sim}{Z}$ can only consist of the original linear elements of the suspension and the stabilizer device shown in Fig. 6.1. Therefore, $\underset{\sim}{Z}$ is given by

$$\underset{\sim}{Z} = [K, K_h, C_t, C_c]$$

The optimization scheme for the given function $S_{\theta_c}(\omega)$ and the design variables $\underset{\sim}{Z}$ can be carried out, as indicated earlier in the flow chart in Fig. 6.9, using the following procedure:

i) An initial guess for the vector $\underset{\sim}{Z}$ is used for starting the optimization cycle. The original parameters of the 100 ton vehicle [19] are used for this purpose.

ii) The frequency range $\omega_{min} \leq \omega \leq \omega_{max}$ is chosen.

iii) The linear system in Equation (7.2), that approximates closely the original nonlinear system in Equation (7.20), is determined.

iv) The power spectral density $S_{\theta_c}(\omega)$ for the equivalent linear system is evaluated using expression (7.58) over the frequency range.

v) The maximum of $S_{\theta_c}(\omega)$ is then the objective function E.

vi) Direct search method is applied, as in Chapter 6, to find $\underset{\sim}{Z}_{opt}$ that minimizes E.

vii) If the minimum of E is less than certain predetermined required value, calculation is termined. If not, $\underset{\sim}{Z}$ is updated and the steps (iv) onwards repeated.

The rotating coordinates (RC) method of search is used in this case since this technique demanded considerably less computer time than

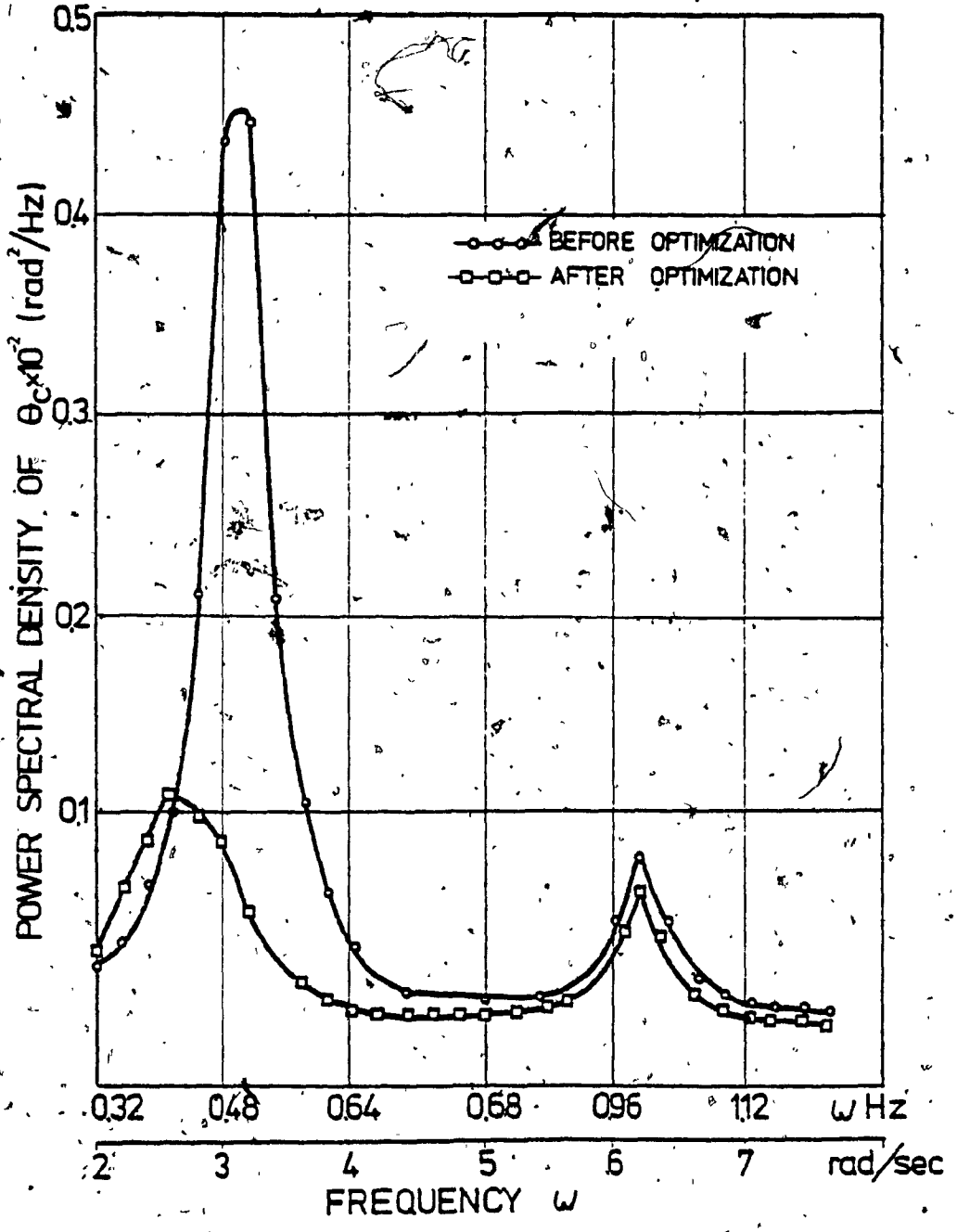

Fig. 8.5: Power Spectral Density of Car Rocking - Before and After Optimization.

the pattern search (PS) method in the earlier optimization cases reported in Subsection 6.4.4.

The objective function, i.e. the maximum $S_{\theta_c}(\omega)$, is plotted before and after optimization in Fig. 8.5 and it can be seen that it reduced from 0.00465 to 0.00112 rad^2/Hz. The corresponding Z_{opt} values are found to be:

K = 27200 lb/in(47600 N/cm), K_h = 20500 lb/in(35875 N/cm)

C_t = 400 lb.sec/in(700 N.sec/cm), C_c = 600 lb.sec/in(1050 N.sec/cm)

This shows that the optimum stiffness elements in both vertical and lateral directions are essentially soft springs. Optimum damping in the system can be achieved through the two shock absorbers C_t and C_c; C_t is mounted between the truck bolster and the side frame and has a soft setting and the other, C_c, is mounted between the car body and the side frame and has a hard setting. These results are consistent with those optimum values obtained for the system under purely periodic track excitation given in Section 6.4 and also with the recommendations of Pullman Standard [12] from their field tests.

8.4 Summary

The spectral density plot of the freight vehicle rocking response shows a strong peak characterizing excessive rocking at a frequency equal to the car rocking natural frequency. Optimal suspension parameters to reduce this are found through a parameter sensitivity study and classcial optimization techniques. The sensi-

tivity study describes the effect of operating the stabilizer consisting of viscous and friction dampers mounted between the car body and the side frame. It is found that the response spectral density is reduced only when large values of friction damping are used. The effect of the periodic input due to the rail joints on the vehicle performance is also investigated. Though a reduction in the rocking response can be obtained by eliminating the periodic component of the input, this is not really a practical solution. Multivariable optimization techniques are then applied to determine a set of optimum suspension elements that minimizes the car rocking power spectral density in the critical range of frequencies.

CHAPTER 9

CONCLUSIONS AND RECOMMENDATIONS

CHAPTER 9

CONCLUSIONS AND RECOMMENDATIONS

9.1 Highlights of the Investigation

This investigation attempts to show that certain practical solutions to the vibration problems of railroad freight vehicles can be achieved, prior to full scale testing and hardware developments, utilizing analytical and computer simulation techniques. The analytical approaches used in this thesis can also be extended to the design and development of locomotives, high speed trains, etc.

Based on a modified nonlinear mathematical model, the dynamic responses of a large capacity railroad freight vehicle are derived when the vehicle is subjected to either a purely periodic or a combination of periodic and random track inputs. Particular attention is given to the response of the vehicle in its rocking mode which has been identified as an important problem experienced in many of the earlier investigations in this field. The equations of motion of the system under deterministic and stochastic inputs are solved for the state variables representing the system response. The results obtained show a close agreement with the available test data and also illustrate certain new dynamic phenomena which have not been previously identified. Further, parameter sensitivity analysis and multivariable optimization techniques are applied for determining the optimal design parameters of the suspension system that minimize an objective function which represents the maximum car rocking response over the critical frequency

range of practical interest.

The original aspects of the investigation presented in this thesis can be summarized in terms of the following set of statements:

i) A compromise but an effective nonlinear physical model is developed for describing the freight vehicle mathematically, containing both adequate accuracy and complexity, to reflect the actual dynamic behavior. The accuracy of the model is sustained by considering most of the system nonlinearities and by also including both the periodic and the random types of track irregularities as input to the system. In order to generate a reasonably analyzable system, for investigating the rocking responses, the complexity is reduced by considering an effective planar model of nine degrees-of-freedom. Provision is made for including a stabilizing device in the model for investigating the possibilities of increasing the vehicle stability at critical speeds.

ii) The mathematical model is chosen in such a way to eliminate excessive computer time for performing the numerical integration of the equations of motion to obtain the responses and for carrying out the optimization process. Similarly, when the analog simulation is employed for obtaining the steady state response, the model is so constructed to demand only a reasonable number of analog components. Also the particular choice of the mathematical model was made appropriate to the solution techniques employed when dealing with the case under the additional random input.

iii) Available multivariable optimization techniques are judiciously applied to the nonlinear freight car system under periodic input to specify the optimal stiffness and damping parameters that would minimize the maximum car rocking transient response.

iv) The nonlinear freight car system is solved for the case when it is acted on by stochastic excitations from the track by employing the method of statistical linearization. But, the system contains both static and damping coupling in the equations of motion. In order to decouple these effects, a representation of the governing equations through an auxiliary coordinate system is proposed so that the nonlinear forces corresponding to each of the independent coordinates is separated and expressed in a form of summation of certain nonlinear terms, each term being a function of the displacement or velocity of only one of the nonlinear elements. This operation simplifies significantly the computational difficulties experienced when evaluating the equivalent damping and stiffness coefficients for the associated linear system.

v) The stochastic response of the equivalent linear system is optimized to determine the stiffness and damping elements that would minimize the maximum car rocking response process expressed as a power spectral density function.

9.2 Discussion of the Results

Comparison of the solutions obtained from the nonlinear mathematical models with the measured time and frequency data available

from the Canadian National Railways [16], leads to the following observations.

Both the digital and analog simulation of the system under deterministic track input showed a close agreement with the field results of Canadian National Railways. Because of the strong non-linearities present in the system, multiple solutions exist for a specified frequency (or vehicle speed) under different initial conditions. Therefore, a straight one to one comparison between points on the plots is difficult to establish since the initial conditions applicable for the Canadian National Railways test results are not known. However, a comparison of the trend of the waveform of the responses as well as the maximum amplitudes show a good agreement. This justifies amply the validity of the mathematical model employed in this investigation.

The response data recorded as time functions illustrates the occurrence of a beating action at the critical speed. During severe rocking conditions, the car rocking angle is shifted by $\pi/2$ radians in phase from the input track cross level. At this state, the car body experiences a maximum rocking amplitude of ±5.5 degrees and a lateral displacement of ±8 inch (±20.3 cm). The different system forces indicating wheel lift, centre plate separation, side bearing contact and gib contact are observed at the critical speed for each rocking cycle. During such resonance conditions, it is observed that the wheel forces reach almost 2 1/2 times the nominal static force level. Maximum centre plate forces grow to 175 kips (778.4 kN), and

large side bearing dynamic forces of about 220 kips (978.5 kN) occur.

The frequency response curves obtained can be used for illustrating some of the dynamic phenomena associated with the rocking problem. For example, the different levels of rocking and the sudden increase in its magnitude at the critical frequencies reported in [12] are found mainly because of the strong nonlinearities present in the system. At 11.5 mph (18.5 km/hr), an amplitude jump from light to moderate rocking takes place. A second jump from moderate to severe rocking occurs at 15 mph (24.13 km/hr). Decreasing the vehicle velocity from this resonance speed of 15 mph (24.13 km/hr) only produces a higher vehicle rocking. This strange phenomenon was further investigated and it was found that this is due to the softening spring characteristics of the vehicle behavior. The conclusions arrived at, as identified above, show that the strong nonlinearities present in the railway freight vehicles are essential for describing accurately all the important dynamic phenomena associated with severe rocking vibrations.

The study of the system's sensitivity to variations in a single suspension or track parameter at a given time shows that the vehicle's stability against rocking can be increased by either increasing the coefficients of the damping elements, or by decreasing the suspension spring stiffness or by decreasing the track cross level. Multivariable optimization techniques proved to be an effective tool for determining those suspension parameters that minimize the maximum rocking amplitude in the critical frequency range. As a result, the

maximum rocking angle reduced by 63.29% when a soft suspension group with additional friction damping is introduced. Operating the stabilizer at these speeds can reduce the rocking response by 66.8% and this does not affect the existing system stiffness elements. The results show that the solution to the rocking problem can be achieved either through optimal parameters for the original suspension or by additionally installing new elements with optimum values.

An important extension of the analysis, that describes the probabilistic response of the vehicle under a stationary Gaussian excitation process from the rails, gives the mean square and power spectral density of the rocking response. The random track irregularities are modeled as a stationary, stochastic, filtered, white noise that consists of both the periodic and random inputs. The investigation of the stochastic case showed that the statistical linearization technique can be effectively used for such nonlinear systems which have coupling terms in the equations of motion. The method utilizes an auxiliary coordinate system to separate the nonlinear forces to express them as a function of the displacement or velocity of only one of the nonlinear element. The root mean square rocking response is derived and plotted as a function of the vehicle speed in the 5 to 20 mph (8 to 32.18 km/hr) range. A comparison of the maximum value of the mean square response is made with the maximum steady state response obtained from the deterministic model in the time domain. The comparison shows a good agreement between the two results implying that the effect of the additional random input on the system is small

especially when investigating low speed problems like the present case. Also this agreement establishes the validity of the stochastic model used in this work. The power spectral density curve obtained shows that the response is essentially a narrow-band process with a central frequency equal to that of the car rocking natural frequency. The periodic component of the total input process is found to affect car rocking so significantly that its elimination will reduce the rocking response power spectral density by almost 60%. Result of optimization indicates that the maximum response power spectral density can be reduced from 0.0045 to 0.0011 rad^2/HZ. This minimax response is obtained by employing again a combination of high viscous damping elements and low stiffness springs.

9.3 Recommendations for Future Work

The investigation presented in this thesis provides new information on the dynamics of the railway freight vehicle-track interaction phenomenon. The nonlinear mathematical models and the analytical methods used for the solutions presented here may be easily extended to study the vibratory response of the freight car in other modes such as sway, bounce, pitch and yaw besides the rocking motion. The approaches developed can also be extended to other dynamic problems including an analysis of the transient responses of the vehicle under types of inputs such as impulsive forces due to sudden accelerations and braking actions. Although the mathematical models developed here refer only to the dynamics of a single car, the problem can be reinvestigated by including the coupling effects between the

freight cars by taking into account the lateral and vertical forces generated by such coupling. It is expected that the results reported in this investigation would not change considerably since it has been shown that the planar model neglecting the coupling effects is valid for analysing the rocking responses. However, for studying the other modes of car vibrations, the coupling arising from a series of cars might prove to be important. Similarly, the influence of the motion of the freight within the vehicle could also be included in any overall investigation for all modes of vibrations.

One of the dynamic phenomena associated with high vehicle speeds, is the problem of wheel hunting which corresponds to a tendency for the system to become unstable due to the wheel taper. An analytical investigation of this important phenomenon requires a detailed study of the different modes of vibrations of the truck bolster-wheelset system. This can also be achieved through an extension of the present investigation by removing the car body from the nonlinear dynamic model and then considering the hunting phenomenon.

It may be seen that most of the test data available from railroad industry for comparison with the analytical results obtained in this work lack sufficient details, especially for the stochastic case. It is recommended that such tests be undertaken and results made available so that proper understanding of the behavior of the freight car system due to the random part of the track irregularities can be obtained.

The detailed analyses presented in this thesis for determining the probabilistic responses and subsequent optimization, when the system is acted upon by stochastic inputs, can be applied to other similar nonlinear mechanical systems including locomotives and high speed transportation systems. However, for the case of high-speed vehicles, in addition to the random track irregularities, the significant effects of the stochastic aerodynamic forces must also be included. These topics are expected to form the main thrust of any future investigation in this vital field of engineering.

REFERENCES

REFERENCES

1. McConnell, D.P., "Directions in Track Structure Research," ASME Paper No. 74-WA/APM-24, Nov. 1974.

2. Kenn, A.D., "The Stress and Stability Analysis of Railroad Track," Trans. ASME, Journal of Applied Mechanics, No. 41, Dec. 1974, pp. 841-848.

3. Ahlbeck, D.R., Harrison, H.D. and Noble, S.L., "An Investigation of Factors Contributing to Wide Gage on Tangent Railroad Track," ASME Paper No. 75-WA/RT-1, Nov. 1975.

4. Marta, H.A. and Mels, K.D., "Wheel Rail Adhesion," Journal of Engineering for Industry, Trans. ASME, No. 91, Series B, Aug. 1969, pp. 839-854.

5. Vermuelen, P.J. and Johnson, K.L., "Contact of Nonspherical Elastic Bodies Transmitting Tangential Forces," Trans. ASME, Journal of Applied Mechanics, No. 31, 1964, pp. 338-340.

6. Wickens, A.H., "General Aspects of the Lateral Dynamics of Railway Vehicles," ASME Paper No. 68-WA/RR-3, Dec. 1968.

7. Clark, J.W. and Law, E.H., "Investigation of the Truck Hunting Instability Problem of High-Speed Trains," ASME Paper No. 67-TRAN-17, Aug. 1976.

8. Cooperrider, N.K., "The Hunting Behavior of Conventional Railway Trucks," ASME Paper No. 70-WA/RR-2, Dec. 1970.

9. Law, E.H. and Brand, R.S., "Analysis of the Nonlinear Dynamics of a Railway Vehicle Wheelset," Trans. ASME, Journal of Dynamic Systems, Measurement, and Control, Vol. 95, Series G, No. 2, March 1973, pp. 28-35.

10. Law, E.H., "Nonlinear Wheelset Dynamic Response to Random Lateral Rail Irregularities," Trans. ASME, Journal of Engineering of Industry, Vol. 96, Series B, No. 1, Nov. 1974, pp. 1168-1176.

11. Leffler, B.R., "The Relation Between the Swaying of Hopper Car and Stagger of Rail Joint in Track," AREA Proceeding, Vol. 27, 1926.

12. Manos, W.P. and Shang, J.C., "Dynamic Analysis of Rolling Freight Cars," ASME, Anthology of Rail Vehicle Dynamics, Vol. 2, 1972, pp. 135-145.

13. "Harmonic Roll Series," Track Train Dynamics Project Report, Assoc. Amer. Railroads, 1975.

14. Wiebe, D., "The Effects of the Lateral Instability of High Center of Gravity Freight Cars," Trans. ASME, Vol. 90B, No. 4, Nov. 1968, pp. 727-736.

15. "Computer Simulation of the Response of 70 Ton Box Cars," A Stucki Company Report, Pittsburgh, PA., 1970.

16. Henderson, K.A. and Johnson, J., "A Criterion for the Control of 100-Ton Hopper Car Roll Motion," Trans. ASME, Vol. 90B, No. 4, Nov. 1968, pp. 717-724.

17. Scott, J.F., Johnson, J., and Charenko, A., "Roll Motion of 100-Ton Hopper Cars," Summary of Test Work, Canadian National Railways, Montreal, Sept. 1969.

18. Reynolds, D.J., and Blank, R.W., "A Car Rocking Mechanism," ASME Paper No. 77-WA/RT-11, Nov. 1977.

19. Liepins, A.A., "Digital Computer Simulation of Railraod Freight Car Rocking," Trans. ASME, Vol. 90B, No. 4, 1968, pp. 701-707.

20. Mecham, H.C. and Ahlbeck, D.R., "A Computer Study of Dynamic Loads Caused by Vehicle-Track Interaction," Trans. ASME, Journal of Engineering for Industry, Aug. 1969, pp. 808-816.

21. Emerson, G., "Freight Car Rocking Dynamics Using Analog Simulation," Dissertation, Massachusetts Institute of Technology, 1975.

22. Platin, B.E. and Beaman, J.J., "Computational Methods to Predict Rail Car Response to Track Cross-Level Variation," DOT Final Report 1976, No. FR-OR and D-76-293.

23. Willis, T. and Shum, K., "A Nonlinear Mathematical Model of the Dynamics of a Railroad Freight Car/Freight Element," ASME Paper No. 76-DE-42, April 1976.

24. Willis, T., "Nonlinear Analysis of Rail Vehicle Dynamics Survey of Rail Vehicle Dynamics Research," I.I.T. Chicago, Report No. Ill-60616, 1976.

25. Healy, M.J., "A Computer Method for Calculating Dynamic Responses of Nonlinear Flexible Rail Vehicles," ASME Paper No. 76-RT-5, April 1976.

26. Seireg, A., "A Survey of Optimization of Mechanical Design," Trans. ASME, Journal of Engineering for Industry, Vol. 94, Series B, No. 1, May 1972, pp. 495-499.

27. Den Hartog, J.P., "Mechanical Vibrations," 4th Ed., McGraw-Hill, New York, 1956.

28. Seireg, A. and Howard, L., "An Approximate Normal-Mode Method for Damped Lumped-Parameter Systems," Trans. ASME, Journal of Engineering for Industry, Series B, Vol. 89, No. 4, Nov. 1967, pp. 597-604.

29. Liber, T. and Sevin, E., "Optimal Shock Isolation Synthesis," The Shock and Vibration Bulletin, No. 35, Part 5, 1966.

30. McMunn, J.C., "Multi-Parameter Optimum Damping in Linear Dynamical Systems," Ph.D. Thesis, University of Minnesota, 1967.

31. Nelson, J.A. and Hapemann, M.J., "A New Transient Propulsion Unit Suspension - Proved on Northeast Carridor High-Speed Test Cars," Trans. ASME, Journal of Engineering for Industry, Vol. 91B, No. 3, Aug. 1966, pp. 897-907.

32. Elmaraghy, W.H., Dokainish, M.A. and Siddall, J.N., "Minimax Optimization of Railway Vehicle Suspension," ASME Paper No. 74-WA/RT-3, Nov.1974.

33. Sewall, J.L., Parrish, R.V. and Durling, B.J., "Rail Vehicle Dynamic Studies," Shock Vibration Bulletin, No. 40, Part 6, U.S. Department of Defence, Dec. 1969, pp. 109-126.

34. Sevin, E. and Pilkey, W.D., "Optimum Shock and Vibration Isolation," Shock and Vibration Information Center, U.S. Department of Defence, No. SVM6, 1971, pp. 105-114.

35. Kemper, J., "Optimum Damping in Nonlinear System Subjected to Shock Load," Ph.D. Thesis, University of Colorado, 1969.

36. Hedrick, J.K., Billington, G.F. and Dreesbach, D.A., "Analysis Design, and Optimization of High Speed Vehicle Suspension Using State Variable Techniques," Trans. ASME, Journal of Dynamic Systems, Measurement, and Control, Vol. 96G, No. 2, June 1974, pp. 193-203.

37. Jacoby, S.L.S., Kowalik, J.S. and Pizzo, J.T., "Iterative Methods for Nonlinear Optimization Problems," Prentice-Hall, New Jersey, 1972, pp. 71-79.

38. Kowalik, J. and Osborne, M.R., "Methods for Unconstrained Optimization Problems," American Elsevier, New York, 1968, pp. 22-24.

39. Corbin, J.C. and Kaufman, W.M., "Classifying Track by Power Spectral Density, Proceedings of ASME Symposium on Mechanics of Transportation Suspension Systems, AMD-Vol. 15, Dec. 1975, pp. 1-20.

40. Sayers, M. and Hedrick, J.K., "Railroad Track Description," Modified excerpt for a Final Report for a U.S. D.O.T. Office of University Research Contract DOT-OS-50107.

41. Osman, M.O.M. and Sankar, T.S., "Short-Time Acceptance Test for Machine Tools Based on the Random Nature of the Cutting Forces," Trans. ASME Journal of Engineering for Industry, Series B, Vol. 94, No. 4, Nov. 1972, pp. 1020-1024.

42. Sankar, T.S., "A Reliability Estimate for Machine Tool Spindles Subjected to Random Forces," Journal of Mechanism and Machine Theory, Vol. 10, 1975, pp. 131-138.

43. Lapidus, L. and Seinfeld, J.H., "Numerical Solution of Ordinary Differential Equations", Academic Press, New York, 1971, pp. 39-150.

44. Milne, W.E., "Numerical Solution of Differential Equations," John Wiley & Sons Inc., New York, 1962, pp. 72-93.

45. Lin, Y.K., "Probabilistic Theory of Structural Dynamics," McGraw-Hill, New York, 1967, pp. 164-172.

46. Atalik, T.S. and Utku, S., "Stochastic Linearization of Multi-degree-of-freedom Nonlinear Systems," Journal of Earthquake Engineering and Structural Dynamics, Vol. 4, 1976, pp. 411-420.

47. Caughey, T.K., "Derivation and Application of the Fokker-Planck Equation to Discrete Nonlinear Dynamic Systems Subjected to White Random Excitation," Journal of the Acoustical Society of America, Vol. 35, No. 11, Nov. 1963, pp. 1683-1692.

48. Ariaratnam, S.T., "Random Vibrations of Nonlinear Suspensions," Journal of Mechanical Engineering Science, Vol. 2, No. 3, 1960, pp. 195-201.

49. Caughey, T.K., "Equivalent Linearization Techniques," Journal of the Acoustical Society of America, Vol. 35, No. 11, Nov. 1963, pp. 1706-1711.

50. Crandall, S.T., "Perturbation Techniques for Random Vibration of Nonlinear Systems," Journal of the Acoustical Society of America, Vol. 35, No. 11, Nov. 1963, pp. 1700-1705.

51. Foster, E.T., "Semilinear Random Vibrations in Discrete Systems," Trans. ASME, Journal of Applied Mechanics, No. 3, Vol. 90, Series E, Sept. 1968, pp. 560-564.

52. Yang, I.M., "Stationary Random Response of Multidegree-of-Freedom Systems," Ph.D. Thesis, California Institute of Technology, June 1970.

53. Iwan, W.D. and Yang, I.M., "Application of Statistical Linearization Techniques to Nonlinear Multidegree-of-Freedom Systems," ASME Paper No. 71-WA/APM-5.

54. Gresch, W., "Mean-Square Responses in Structural Systems," Journal of the Acoustical Society of America, Vol. 48, No. 1, Part 2, July 1970, pp. 403-413.

55. Yang, I.M. and Iwan, W.D., "Calculation of Correlation Matrices for Linear Systems Subjected to Nonwhite Excitation," ASME Paper No. 71-APMW-10.

56. Davison, E.J. and Man, F.T., "The Numerical Solution of $A^TQ + QA = -C$," Transactions on Automatic Control, IEEE, Vol. AC-13, Aug. 1968, pp. 448-449.

57. Cooperrider, N.K., Cox, J.J. and Kedrick, J.K., "Lateral Dynamics Optimization of a Conventional Rail Car," Trans. ASME, Journal of Dynamics Systems, Measurement, and Control, September 1975, pp. 293-299.

58. Wilson, J.T., "Response Behavior of Vehicle Systems Subjected to Random Excitation," M.Eng. Thesis, McGill University, 1969, pp. 28-30.

59. Hausner, A., "Analog and Analog/Hybrid Computer Programming," Prentice-Hall, 1971, pp. 121-149.

60. McKeown, F.S., "Report American Steel Foundries Participation in A.A.R./R.P.I./F.R.A. Track-Train Dynamic Program," Section I, 1974.

APPENDIX I

THE EQUATIONS OF MOTION OF THE MULTICONFIGURATION MODEL

APPENDIX I

THE EQUATIONS OF MOTION OF THE MULTICONFIGURATION MODEL

In Chapter 4, the equations of motion corresponding to each of the different configurations of the freight car system given in Fig. 4.1(b) were derived. The equations were expressed in a matrix form as:

$$\underset{\sim}{M}\ddot{\underset{\sim}{X}} + \underset{\sim}{C}\dot{\underset{\sim}{X}} + \underset{\sim}{K}\underset{\sim}{X} + \underset{\sim}{S}(\dot{\underset{\sim}{Y}}^{(1)}) + \underset{\sim}{G} = \underset{\sim}{F}(t) \qquad \text{(I.1)}$$

In this appendix, the complete set of equations including all the expressions associated with each configuration are presented for clarification.

Configuration 1

$$n = 3 \qquad \underset{\sim}{X}^T = [Z_c, Y_c, \theta_c]$$

$$\underset{\sim}{M} = \begin{bmatrix} M_s & 0 & 0 \\ 0 & M_s & M_t C_v \\ 0 & M_t C_v & I_s \end{bmatrix}, \quad \underset{\sim}{C} = \begin{bmatrix} 2C_s & 0 & 0 \\ 0 & 0 & 0 \\ 0 & 0 & 2f^2 C_s \end{bmatrix} \quad \underset{\sim}{K} = \begin{bmatrix} 2K & 0 & 0 \\ 0 & K_h & K_h(C_v-h) \\ 0 & K_h(C_v-h) & K_s \end{bmatrix}$$

and

$$\underset{\sim}{G}^T = [M_s g, 0, 0]$$

$$\underset{\sim}{S}^T(\dot{\underset{\sim}{Y}}^{(1)}) = [F_t(s_1+s_2), F_t s_4, F_t f s_1 - F_t f s_2 + 2F_t f s_3 + F_t(C_v-h)s_4]$$

$$\underset{\sim}{F}^T(t) = [2C_s\dot{Z}_v + 2K Z_v, K_h Y, 2C_s f\dot{Z}_{cr} + 2Kf Z_{cr} + K_h Y(C_v-h)]$$

Configurations 2a, 2b

$$n = 4 \quad , \qquad \underset{\sim}{X}^T = [Z_c, Y_c, \theta_c, \theta_t]$$

In this case:

$$\underset{\sim}{M} = \begin{bmatrix} M_s & 0 & \mp M_t d & \pm M_t d \\ 0 & M_s & M_t b_1 & M_t C_1 \\ \mp M_t d & M_t b_1 & I_{s_1} & I_{s_2} \\ \pm M_t d & M_t C_1 & I_{s_2} & I_{s_3} \end{bmatrix}, \quad \underset{\sim}{C} = \begin{bmatrix} 2C_s & 0 & \mp 2C_t d & \pm 2C_t d \\ 0 & 0 & 0 & 0 \\ \mp 2C_t d & 0 & C_{s_1} & -2C_t d^2 \\ \pm 2C_t d & 0 & -2C_t d^2 & C_{s_2} \end{bmatrix}$$

$$\underset{\sim}{K} = \begin{bmatrix} 2K & 0 & \mp 2Kd & \pm 2Kd \\ 0 & K_h & K_h b_1 & K_h(C_1 - h) \\ \mp 2Kd & K_h b_1 & K_{s_1} & K_{s_2} \\ \pm 2Kd & K_h(C_1 - h) & K_{s_2} & K_{s_3} \end{bmatrix}, \quad \underset{\sim}{G}^T = [(M_c + M_t)g, 0, \mp M_t g d, \pm M_t g d]$$

$$\underset{\sim}{S}^T(\dot{\underset{\sim}{Y}}^{(1)}) = [F_t(s_1 + s_2), F_t s_4, \mp F_t d(s_1 + s_2) + 2F_c f s_3 + F_t b_1 s_4,$$
$$\pm F_t d(s_1 + s_2) + F_t f(s_1 - s_2) + F_t(C_1 - h)s_4]$$

$$\underset{\sim}{F}^T(t) = [2C_s \dot{Z}_v + 2KZ_v, K_h Y, 2C_c f \dot{Z}_{cr} \mp 2C_t d \dot{Z}_v \mp 2KdZ_v + K_h b_1 Y,$$
$$\pm 2C_t d \dot{Z}_v + 2C_t f \dot{Z}_{cr} \pm 2KdZ_v + 2KfZ_{cr} + K_h Y C_v]$$

Configurations 3a, 3b

$$n = 3 \quad , \qquad \underset{\sim}{X}^T = [Z_c, Y_c, \theta_c]$$

For configurations 3a and 3b, the terms in Equation (I.1) are the same as those given for Configuration 1 except for the vector $\underset{\sim}{G}$ of constant forces due to the introduction of terms involving ϵ in the constraint Equations (4.1.3a) and (4.1.3b). $\underset{\sim}{G}$ in this case is given by:

$$\underset{\sim}{G}^T = [M_s g - 2Kd\varepsilon/(e-d), \mp K_h(C_1-h)\varepsilon/(e-d), -2Kf^2\varepsilon/(e-d) - K_h(C_v-h)\varepsilon(C_1-h)/(e-d)]$$

Configurations 4a, 4b

$$n = 4 \quad , \qquad \underset{\sim}{X}^T = [Z_c, Y_c, \theta_c, \theta_t]$$

A comparison of the constraint equations (Equations (4.1.2a) and (4.1.2b)) for Configuration 2 with those given for Configuration 4, Equations (4.1.4a) and (4.1.2b) shows that, because of the introduction of the constant terms involving ε in Configuration 4, its $\underset{\sim}{G}$ vector should be changed. Also from this comparison, it appears that the values of d, C_1 and b_1 in equations of Configuration 2 should be replaced by e, C_2 and b_2 respectively for the Configuration 4 equations. $\underset{\sim}{G}$ in this case is given by:

$$\underset{\sim}{G}^T = [2K\varepsilon + M_s g, 0, \mp 2K\varepsilon e \mp mge, \pm 2K\varepsilon e \pm mge]$$

In all the above equations corresponding to each rocking configuration, the following expressions were used for simplification:

$$M_s = M_t + M_c, \quad I_{s_3} = I_c + I_t + M_t C_v^2 , \quad C_v = C_1 + b_1$$

$$C_s = C_t + C_c, \quad K_s = 2Kf^2 + K_h(C_v-h)^2$$

$$K_{s_1} = 2Kd^2 + K_h b_1^2, \quad K_{s_2} = -2Kd^2 + K_h b_1(C_1-h)$$

$$K_{s_3} = 2Kd^2 + 2Kf^2 + K_h(C_1-h)^2, \quad C_{s_1} = 2C_c f^2 + 2G_t d^2$$

$$C_{s_2} = 2C_t(d^2 + f^2) , \quad I_{s_1} = I + M_t d^2 + M_t b_1^2$$

$$I_{s_2} = -M_t d^2 + M_t b_1 C_1, \quad I_{s_3} = I_t + M_t d^2 + M_t C_1^2 .$$

APPENDIX II

LISTING OF THE COMPUTER PROGRAM

FOR THE TIME RESPONSE

APPENDIX II

LISTING OF THE COMPUTER PROGRAM FOR THE TIME RESPONSE

```
      PROGRAM MATH(INPUT,OUTPUT)
C
C
C     PROGRAM TO EVALUATE THE TIME RESPONSES OF A LARGE CAPACITY RAILROAD
C     FREIGT VEHICLE WHEN IT IS SUBJECTED TO PURELY PERIDIC EXCITATIONS
C     FROM THE TRACK IRREGULARITIES.
C
C
      REAL I1,M1,K,KH,L,I,M,L1,L2,L3,L4,L5
      DIMENSION Y(12),F(12),AY(12),AK(4,12),ZXY(121,XF(12)
      DIMENSION IY(120)
      DATA IXL/1H-/
C
C
C     DEFINITION OF THE SYSTEM PARAMETERS
C
C
      I1=3400
      M1=5.12
      F1=39.5
      H=2.7
      G=384
      B1=70
      B2=65.7
      C1=6.7
      C2=11.
      EPS=.25
      D=7
      E=25
      W8=28.5
      H1=28.3
      I=1860000
      M=615
      W=20000
      TF=20
      L=.0025
      T1=0
      I3=1
      K=45200
      KH=40000
      XXX=35000
      TF=13.1
      FC=0.
      CC=0.
      FT=8000
      CT=200
      DO1372 J=1,80
 1372 IY(J)=IXL
      PRINT 3452
 3452 FORMAT(1H1)
      PRINT 1472,(IY(J),J=1,78)
      PRINT 2354
 2354 FORMAT(7X,*I*,2X,*TIME (SEC)*,5X,*I*,5X,*PLOT OF CAR ROCK *,
     1*ANGLE*,9X,*I*,1X,*CAR ROCK ANGLE (RAD)*,    *I*)
      PRINT 1472,(IY(J),J=1,78)
 1472 FORMAT(7X,78A1)
C
```

```
C
C     THE SOLUTION STARTS ASSUMING THE VEHICLE IN CONFIGURATION 1
C     TO DETERMINE THE STATE VARIABLES VECTOR I.E. POSITION AND
C     VELOCITY FIELD OF THE CAR AND TRUCKS
C
C
   10 DO 70 J=1,12
      F(J)=0
   70 AY(J)=0
   27 DO 20 J=7,12
   20 AY(J)  =Y(J)
      DO 40 M2=1,4
      CALL FUN(T1,Y,F1,H,ZR,ZL,XY,DZR,DZL,DXY,S1,S2,S3,S4,DS,SK,K,
     1RR,RL,KH)
      F(12)=Y(11)
      F(11)=(-2*(CT+CC)*Y(11)-2*K*Y(12)
     1+(CT+CC)*(DZR+DZL)+K*(ZR+ZL)
     1-(M1+M)*G-(S1+S2)*FT)/(M1+M)
      F(8)=Y(7)
      F(7)=(-M1*(C1+B1)*F(9)-2*F1*F1*(CT+CC)*Y(7)-(2*K*F1*F1+
     1KH*((C1+B1-H)**2))*Y(8)-KH*(C1+B1-H)*Y(10)-S1*FT*F1+S2*FT*F1
     1-2*S3*FC*F1-S4*FT*(C1+B1-H)+(CT+CC)*F1*(DZR-DZL)+K*F1*(ZR-ZL)+K
     1H*(C1+B1-H)*XY)/(I+I1+M1*(C1+B1)*(C1+B1))
      F(10)=Y(9)
      F(9)=(M1*(C1+B1)*F(7)-KH*Y(10)-KH*(C1+B1-H)*Y(8)-S4*FT+KH*XY)
     1/(M1+M)
      DO 30 J=7,12
   30 AK(M2,J)=F(J)*L
      IF(M2.EQ.4)GO TO 40
      IF(M2.NE.2)T1=T1+L/2
      IF(M2-3)25,26,25
   26 DO 18 J=7,12
   18 Y(J)=AY(J)+AK(M2,J)
      GO TO 40
   25 DO 400 J=7,12
      Y(J)=AY(J)+AK(M2,J)/2
  400 CONTINUE
   40 CONTINUE
      DO 50 J=7,12
   50 Y(J)=AY(J)+(AK(1,J)+2*AK(2,J)+2*AK(3,J)+AK(4,J))/6
      Y(1)=Y(7)
      Y(2)=Y(8)
      Y(3)=Y(9)+(C1+B1)*Y(7)
      Y(4)=Y(10)+(C1+B1)*Y(8)
      Y(5)=Y(11)
      Y(6)=Y(12)
      F(1)=F(7)
      F(2)=Y(1)
      F(3)=F(9)+(C1+B1)*F(1)
      F(4)=Y(3)
      F(5)=F(11)
      F(6)=Y(5)
C
C
C     EVALUATION OF THE FOLLOWING FORCES
C        CENTER PLATE
C        SIDE BEARINGS
```

```
C          WHEEL-RAIL
C
C
  100 DR=-CC*(Y(11)+F1*Y(7)-DZR)
      DL=-CC*(Y(11)-F1*Y(7)-DZL)
      RR=-K*(Y(6)+F1*Y(2)-ZR)-S1*FT-CT*(Y(5)+F1*Y(1)-DZR)
      RL=-K*(Y(6)-F1*Y(2)-ZL)-S2*FT-CT*(Y(5)-F1*Y(1)-DZL)
      RH=-KH*(Y(4)-H*Y(2)-XY)-S4*FT
      IF(T1.GT.TF)GO TO 200
      L1=(DL*(F1-D)+M*(G+F(11))*D+I*F(7)-DR*(F1+D)
     1+2*F1*FC*S3-M*B1*F(9))/(2*D)
      L2=M*(F(11)+G)-(DL+DR)-L1
      L5=M*F(9)
C
C
C     SEARCH PROCEDURE TO FIND THE MODEL CONFIGURATION
C     AT NEXT TIME INSTANT THAT SATISFY GEOMETRIC AND FORCES
C     COMPATIBILITY
C
C
      IF(L1.GT.XXX  )GO TO 20003
      IF(L2.LT.XXX  )GO TO 1076
      GO TO 1004
20003 IF(L2.GT.XXX  )GO TO 1001
      GO TO 1005
 1076 IF(Y(8).LT.0)GO TO 1007
      IF(Y(8).GT.0)GO TO 1006
C
C     CONFIGURATION *1*
C
 1001 L1=(DL*(F1-D)+M*(G+F(11))*D+I*F(7)-DR*(F1+D)
     1+2*F1*FC*S3-M*B1*F(9))/(2*D)
      L2=M*(F(11)+G)-(DL+DR)-L1
      L5=M*F(9)
      L4=0
      L3=0
      OM=0
      I3=1
      IF(RR.LT.0)RR=0
      IF(RL.LT.0)RL=0
      IF(Y(8).GT.0)GO TO 1257
      RMO=(RL*2*WB+RH*28.3+I1*F(7)+900*11+L3*(E-WB))/
     1(W*WB+M1*F(3)*(H1-C1)+M1*(G+F(5))*WB+L4*(WB+E)+L1*(WB-D)+OM+L2*
     1(WB+D)+L4*(WB+E)+L5*H1+900*67+1500*57+2510*28.5)
      GO TO 1352
 1257 RMO=(RR*2*WB+L5*H1+M1*F(3)*(H1-C1)+L4*(E-WB)+OM+900*11)/
     1(W*WB+I1*F(7)+M1*(G+F(5))*WB+L1*WB+D)+L2*(WB-D)
     1+L3*(WB+E)+900*67+1500*57+2510*28.5+RH*24.3)
 1352 JIXY=JIXY+1
      CALL PLOT (T1,Y,RMO,L2,L1,RR,RL,I3,JIXY,EPSI,L4,SDR,E1,E2,
     1RH,L3,L5)
      GO TO 1
C
C     CONFIGURATION *2A*
C
 1002 L2=M*(G+F(11))-(DL+DR)
      L5=M*F(9)
```

```
      L4=0
      L1=0
      L3=0
      OM=(DL*(F1-D)-DR*(F1+D)+M*(G+F(12))*D+I*F(8)-M*B1*F(10)+2*F1*FC*
     1S3)
      IF(L2.LE.XXX   )GO TO 1006
      I3=2
      IF(RR.LT.0)RR=0
      IF(RL.LT.0)RL=0
      RMO=(RR*2*WB+L5*H1+M1*F(3)*(H1-C1)+L4*(E-WB)+OM+900*11)/
     1(W*WB+I1*F(7)*M1*(G+F(5))*WB+L1*(WB+D)+L2*(WB-D)
     1+L3*(WB+E)+900*67+1500*57+2510*28.5+RH*24.3)
      JIXY=JIXY+1
      CALL PLOT (T1,Y,RMO,L2,L1,RR,RL,I3,JIXY,EPSI,L4,SDR,E1,E2,
     1RH,L3,L5)
      GO TO 2
C
C     CONFIGURATION *28*
C
 1003 L1=M*(G+F(11))-(DL+DR)
      L5=M*F(9)
      L3=0
      L2=0
      L4=0
      OM=(DL*(F1-D)-DR*(F1+D)+M*(G+F(12))*D+I*F(8)-M*B1*F(10)+2*F1*FC*
     1S3-L1*2*D)
      IF(L1.LT.XXX   )GO TO 1007
      I3=3
      IF(RR.LT.0)RR=0
      IF(RL.LT.0)RL=0
      RMO=(RL*2*WB+RH*28.3+I1*F(1)+900*11+L3*(E-WB))/
     1(W*WB+M1*F(3)*(H1-C1)+M1*(G+F(5))*WB+L4*(WB+E)+L1*(WB-D)+OM+L2*
     1(WB+D)+L4*(WB+E)+L5*H1+900*67+1500*57+2510*28.5)
      JIXY=JIXY+1
      CALL PLOT (T1,Y,RMO,L2,L1,RR,RL,I3,JIXY,EPSI,L4,SDR,E1,E2,
     1RH,L3,L5)
      GO TO 3
C
C     CONFIGURATION *3A*
C
 1004 L4=(DR*(F1+D)+M*F(9)*B1-I*F(7)-M*(G+F(11))*D-DL*(F1-D)
     1-2*F1*FC*S3)/(E-D)
      L2=M*(F(11)+G)-(DL+DR)-L4
      L5=M*F(9)
      L1=0
      L3=0
      OM=0
      IF(RR.LT.0)RR=0
      IF(RL.LT.0)RL=0
      IF(L4.LT.XXX   .AND.ABS(L2).LT.ABS(L4))GO TO 1005
      IF(L4.LE.XXX   )GO TO 1002
      IF(L2.LT.XXX   )GO TO 1006
      I3=4
      RMO=(RR*2*WB+L5*H1+M1*F(3)*(H1-C1)+L4*(E-WB)+OM+900*11)/
     1(W*WB+I1*F(1)+M1*(G+F(5))*WB+L1*(WB+D)+L2*(WB-D)
     1+L3*(WB+E)+900*67+1500*57+2510*28.5+RH*24.3)
      JIXY=JIXY+1
```

```
      CALL PLOT (T1,Y,RMO,L2,L1,RR,RL,I3,JIXY,EPSI,L4,SDR,E1,E2,
     1RH,L3,L5)
      GO TO 4
C
C     CONFIGURATION *3B*
C
 1005 L3=(DL*(F1+D)+I*F(7)-M*F(9)*B1-M*(G+F(11))*D+DR*(F1-D)
     1+2*W1*FC*S3)/(E-D)
      L1=M*(F(11)+G)-(DL+DR)-L3
      L5=M*F(9)
      L2=0
      L4=0
      OM=0
      IF(L3.LT.XXX   .AND.ABS(L1).LT.ABS(L3))GO TO 1004
      IF(L3.LE.XXX   )GO TO 1003
      IF(L1.LE.XXX   )GO TO 1007
      I3=5
      IF(RR.LT.0)RR=0
      IF(RL.LT.0)RL=0
      RMO=(RL*2*WB+RH*28.3+I1*F(1)+900*11+L3*(E-WB))/
     1(W*W8+M1*F(3)*(H1-C1)+M1*(G+F(5))*WB+L4*(WB+E)+L1*(WB-D)+OM+L2*
     1(WB+D)+L4*(WB+E)+L5*H1+900*67+1500*57+2510*28.5)
      JIXY=JIXY+1
      CALL PLOT (T1,Y,RMO,L2,L1,RR,RL,I3,JIXY,EPSI,L4,SDR,E1,E2,
     1RH,L3,L5)
      GO TO 5
C
C     CONFIGURATION *4A*
C
 1006 L4=M*(G+F(11))-(DL+DR)
      L5=M*F(9)
      L1=0
      L2=0
      L3=0
      OM=(DL*(F1-E)-DR*(F1+E)+M*(G+F(12))*E+I*F(8)-M*B2*F(10)
     1+2*F1*FC*S3)
      IF(L4.LT.XXX   )GO TO 1
      IF(RR.LT.0)RR=0
      IF(RL.LT.0)RL=0
      I3=6
      RMO=(RR*2*WB+L5*H1+M1*F(3)*(H1-C1)+L4*(E-WB)+OM+900*11)/
     1(W*W8+I1*F(7)+M1*(G+F(5))*WB+L1*(WB+D)+L2*(WB-D)
     1+L3*(WB+E)+900*67+1500*57+2510*28.5+RH*24.3)
      JIXY=JIXY+1
      CALL PLOT (T1,Y,RMO,L2,L1,RR,RL,I3,JIXY,EPSI,L4,SDR,E1,E2,
     1RH,L3,L5)
      GO TO 6
C
C     CONFIGURATION *4B*
C
 1007 L3=M*(G+F(11))-(DL+DR)
      L5=M*F(9)
      L1=0
      L2=0
      L4=0
      OM=(DL*(F1-E)-DR*(F1+E)+M*(G+F(12))*E+I*F(8)-M*B2*F(10)
     1+2*F1*FC*S3-L4*2*E)
```

```
      IF(L3.LE.XXX  )GO TO 1
      I3=7
      IF(RR.LT.0)RR=0
      IF(RL.LT.0)RL=0
      RMO=(RL*2*WB+RH*28.3+I1*F(1)+900*11+L3*(E-WB))/
     1(W*W8+M1*F(3)*(H1-C1)+M1*(G+F(5))*WB+L4*(WB+E)+L1*(WB-O)+OM+L2*
     1(WB+O)+L4*(W8+E)+L5*H1+900*67+1500*57+2510*28.5)
      JIXY=JIXY+1
      CALL PLOT (T1,Y,RMO,L2,L1,RR,RL,I3,JIXY,EPSI,L4,SDP,E1,E2,
     1RH,L3,L5)
      GO TO 7
C
C
C     SOLUTION OF THE EQUATION OF MOTION OF CONFIGURATION *1*
C     BY INTEGRATING THE EQUATIONS OF MOTION NUMERICALLY
C
C
    1 N=6
      I3=1
      DO 201 J=7,12
  201 AY(J)=Y(J)
      DO 401 M2=1,4
      CALL FUN(T1,Y,F1,H,ZR,ZL,XY,DZR,DZL,DXY,S1,S2,S3,S4,OS,SK,K,
     1RR,RL,KH)
      F(12)=Y(11)
      F(11)=(-2*(CT+CC)*Y(11)-2*K*Y(12)
     1+(CT+CC)*(DZR+DZL)+K*(ZR+ZL)
     1-(M1+M)*G-(S1+S2)*FT)/(M1+M)
      F(8)=Y(7)
      F(7)=(-M1*(C1+B1)*F(9)-2*F1*F1*(CT+CC)*Y(7)-(2*K*F1*F1+
     1KH*((C1+B1-H)**2))*Y(8)-KH*(C1+B1-H)*Y(10)-S1*FT*F1+S2*FT*F1
     1-2*S3*FC*F1-S4*FT*(C1+B1-H)+(CT+CC)*F1*(DZR-DZL)+K*F1*(ZR-ZL)+K
     1H*(C1+B1-H)*XY)/(I+I1+M1*(C1+B1)*(C1+B1))
      F(10)=Y(9)
      F(9)=(M1*(C1+B1)*F(7)-KH*Y(10)-KH*(C1+B1-H)*Y(8)-S4*FT+KH*XY)
     1/(M1+M)
      DO 301 J=7,12
  301 AK(M2,J)=F(J)*L
      IF(M2.EQ.4)GO TO 401
      IF(M2.NE.2)T1=T1+L/2
      IF(M2-3)251,261,251
  261 DO 181J=7,12
  181 Y(J)=AY(J)+AK(M2,J)
      GO TO 401
  251 DO 4010 J=7,12
      Y(J)=AY(J)+AK(M2,J)/2
 4010 CONTINUE
  401 CONTINUE
      DO 501 J=7,12
  501 Y(J)=AY(J)+(AK(1,J)+2*AK(2,J)+2*AK(3,J)+AK(4,J))/6
      Y(1)=Y(7)
      Y(2)=Y(8)
      Y(3)=Y(9)+(C1+B1)*Y(7)
      Y(4)=Y(10)+(C1+B1)*Y(8)
      Y(5)=Y(11)
      Y(6)=Y(12)
      F(1)=F(7)
```

```
      F(2)=Y(1)
      F(4)=Y(3)
      F(3)=F(9)+(C1+B1)*F(1)
      F(5)=F(11)
      F(6)=Y(5)
      GO TO 100
C
C
C     SOLUTION OF THE EQUATION OF MOTION OF CONFIGURATION *2A*
C     BY INTEGRATING THE EQUATIONS OF MOTION NUMERICALLY
C
C
    2 N=12
      I3=2
      DO 202 J=1,N
  202 AY(J)=Y(J)
      DO 402 M2=1,4
      CALL FUN(TI,Y,F1,H,ZR,ZL,XY,DZR,DZL,DXY,S1,S2,S3,S4,DS,SK,K,
     1RR,RL,KH)
      F(12)=Y(11)
      F(11)=(M1*D*(F(7)-F(1))-2*(CT+CC)*Y(11)+2*CT*D*(Y(7)-Y(1))
     1-2*K*Y(12)+2*K*D*(Y(8)-Y(2))-(M1+M)*G-(S1+S2)*FT+(CC+CT)*(DZR+D
     1ZL)+K*(ZR+ZL))/(M1+M)
      F(10)=Y(9)
      F(9)=(-M1*B1*F(7)-M1*C1*F(1)-KH*Y(10)-KH*B1*Y(8)
     1-KH*(C1-H)*Y(2)-S4*FT+KH*XY)/(M1+M)
      F(8)=Y(7)
      F(7)=((M1*D*D-M1*C1*B1)*F(1)+M1*D*F(11)-M1*B1*F(9)
     1+2*CT*D*Y(11)-2*CC*F1*F1*Y(7)-2*CT*D*D*Y(7)+2*CT*D*D*Y(1)+2*K
     1*Y(12)-2*K*D*D*(Y(8)-Y(2))-KH*B1*Y(10)
     1-KH*B1*B1*Y(8)-KH*(C1-H)*B1*Y(2)+M
     11*G*D+FT*D*(S1+S2)-2*S3*FC*F1-S4*FT*B1+(CC*F1-CT*D)*(DZR+DZL)
     1-K*D*(ZR+ZL)+KH*B1*XY)/(I+M1*(D*D+B1*B1))
      F(6)=Y(5)
      F(5)=F(11)-D*(F(7)-F(1))
      F(4)=Y(3)
      F(3)=F(9)+B1*F(7)+C1*F(1)
      F(2)=Y(1)
      F(1)=(M1*D*D*F(7)-M1*D*F(11)-M1*C1*B1*F(7)-M1*C1*F(9)
     1-2*K*D*Y(12)+2*K*D*D*(Y(8)-Y(2))-2*K*F1*F1*Y(2)
     1-2*CT*D*Y(11)+2*CT*D*D*Y(7)-2*CT*D*D*Y(1)-2*CT*F1*F1*Y(1)
     1-KH*(C1-H)*(Y(10)+B1*Y(8))-KH*(C1-H)*(C1-H)*Y(2)
     1-M1*G*D-(S1+S2)*FT*D-(S1-S2)*FT*F1-S4*FT*(C1-H)+CT*D*(DZR+DZL
     1)+CT*F1*(DZR-DZL)+K*D*(ZR+ZL)+K*F1*(ZR-ZL)+KH*(C1-B1)*XY
     11/(I1+M1*(D*D+C1*C1))
      DO 302 J=1,N
  302 AK(M2,J)=F(J)*L
      IF(M2.EQ.4)GO TO 402
      IF(M2.NE.2)T1=T1+L/2
      IF(M2-3)252,262,252
  262 DO 182 J=1,N
  182 Y(J)=AY(J)+AK(M2,J)
      GO TO 402
  252 DO 4020 J=1,N
      Y(J)=AY(J)+AK(M2,J)/2
 4020 CONTINUE
  402 CONTINUE
```

```
      DO 502 J=1,N
  502 Y(J)=AY(J)+(AK(1,J)+2*AK(2,J)+2*AK(3,J)+AK(4,J))/6
      GO TO 100
C
C
C     SOLUTION OF THE EQUATION OF MOTION OF CONFIGURATION *28*
C     BY INTEGRATING THE EQUATIONS OF MOTION NUMERICALLY
C
C
    3 N=12
      I3=3
      DO 203 J=1,N
  203 AY(J)=Y(J)
      DO 403 M2=1,4
      CALL FUN(T1,Y,F1,H,ZR,ZL,XY,DZR,DZL,DXY,S1,S2,S3,S4,OS,SK,K,
     1RR,RL,KH)
      F(12)=Y(11)
      F(11)=(M1*D*(F(1)-F(7))-2*(CT+CC)*Y(11)-2*CT*D*(Y(7)-Y(1))
     1-2*K*Y(12)-2*K*D*(Y(8)-Y(2))-(M1+M)*G-(S1+S2)*FT+(CC+CT)*(DZR+D
     1ZL)+K*(ZR+ZL))/(M1+M)
      F(10)=Y(9)
      F(9)=(-M1*B1*F(7)-M1*C1*F(1)-KH*Y(10)-KH*B1*Y(8)
     1-KH*(C1-H)*Y(2)-S4*FT+KH*XY)/(M1+M)
      F(8)=Y(7)
      F(7)=((M1*D*D-M1*C1*B1)*F(1)-M1*D*F(11)-M1*B1*F(9)
     1-2*CT*D*Y(11)-2*CC*F1*F1*Y(7)-2*CT*D*D*Y(7)+2*CT*D*D*Y(1)-2*K
     1*Y(12)-2*K*D*D*(Y(8)-Y(2))-KH*B1*Y(10)
     1-KH*B1*B1*Y(8)-KH*(C1-H)*B1*Y(2)-M
     11*G*D-FT*D*(S1+S2)-2*S3*FC*F1-S4*FT*B1+(CC*F1+CT*D)*(DZR+DZL)
     1+K*D*(ZR+ZL)+KH*B1*XY)/(I+M1*(D*D+B1*B1))
      F(2)=Y(1)
      F(1)=(M1*D*D*F(7)+M1*D*F(11)-M1*C1*B1*F(7)-M1*C1*F(9)
     1+2*K*D*Y(12)+2*K*D*D*(Y(8)-Y(2))          -2*K*F1*F1*Y(2)
     1+2*CT*D*Y(11)+2*CT*D*D*Y(7)-2*CT*D*D*Y(1)-2*CT*F1*F1*Y(1)
     1-KH*(C1-H)*(Y(10)+B1*Y(8))-KH*(C1-H)*(C1-H)*Y(2)
     1+M1*G*D+(S1+S2)*FT*D-(S1-S2)*FT*F1-S4*FT*(C1-H)-CT*D*(DZR+DZL
     11)+CT*F1*(DZR-DZL)-K*D*(ZR+ZL)+K*F1*(ZR-ZL)+KH*(C1-B1)*XY
     11)/(I1+M1*(D*D+C1*C1))
      F(6)=Y(5)
      F(5)=F(11)-D*(F(7)-F(1))
      F(4)=Y(3)
      F(3)=F(9)+B1*F(7)+C1*F(1)
      DO 303 J=1,N
  303 AK(M2,J)=F(J)*L
      IF(M2.EQ.4)GO TO 403
      IF(M2.NE.2)T1=T1+L/2
      IF(M2-3)253,263,253
  263 DO 183 J=1,N
  183 Y(J)=AY(J)+AK(M2,J)
      GO TO 403
  253 DO 4030 J=1,N
      Y(J)=AY(J)+AK(M2,J)/2
 4030 CONTINUE
  403 CONTINUE
      DO 503 J=1,N
  503 Y(J)=AY(J)+(AK(1,J)+2*AK(2,J)+2*AK(3,J)+AK(4,J))/6
      GO TO 100
```

```
C
C
C     SOLUTION  F TH EEQUATION OF MOTION OF CONFIGURATION *3A*
C     BY INTEGRATING THE EQUATIONS OF MOTION NUMERICALLY
C
C
    4 N=6
      I3=4
      DO 204 J=7,12
  204 AY(J)=Y(J)
      DO 404 M2=1,4
      CALL FUN(T1,Y,F1,H,ZR,ZL,XY,DZR,DZL,DXY,S1,S2,S3,S4,OS,SK,K,
     1RR,RL,KH)
      F(12)=Y(11)
      F(11)=(-2*(CT+CC)*Y(11)-2*K*(Y(12)-(D*EPS/(E-D)))-(M+M1)*G
     1-(S1+S2)*FT+(CT+CC)*(DZR+DZL)+K*(ZR+ZL))/(M1+M)
      F(10)=Y(9)
      F(9)=(-M1*(C1+B1)*F(7)-KH*Y(10)-KH*(B1+C1-H)*Y(8)+KH*(C1-H)*
     1(EPS/(E-D))-S4*FT+KH*XY)/(M1+M)
      F(8)=Y(7)
      F(7)=(-M1*(C1+B1)*F(9)-2*F1*F1*(CT+CC)*Y(7)-2*K*F1*F1*Y(8)
     1-KH*(B1+C1-H)*Y(10)-KH*((B1+C1-H)**2)*Y(8)+2*K*F1*F1*((EPS/(E-D)))
     1+KH*(B1+C1-H)*(C1-H)*(EPS/(E-D))-(S1-S2)*FT*F1-2*S3*FC*F1-S4*FT*(B
     11+C1-H)+(CT+CC)*F1*(DZR-DZL)+K*F1*(ZR-ZL)+KH*XY*(B1+C1-H))/
     1(I+I1+M1*((C1+B1)**2))
      DO 374 J=7,12
  374 AK(M2,J)=F(J)*L
      IF(M2.EQ.4)GO TO 404
      IF(M2.NE.2)T1=T1+L/2
      IF(M2-3)254,264,254
  264 DO 184 J=7,12
  184 Y(J)=AY(J)+AK(M2,J)
      GO TO 404
  254 DO 4040 J=7,12
      Y(J)=AY(J)+AK(M2,J)/2
 4040 CONTINUE
  404 CONTINUE
      DO 504 J=7,12
  504 Y(J)=AY(J)+(AK(1,J)+2*AK(2,J)+2*AK(3,J)+AK(4,J))/6
      Y(6)=Y(12)-D*EPS/(E-D)
      Y(2)=Y(8)-EPS/(E-D)
      Y(4)=Y(10)+(B1+C1)*Y(8)-C1*EPS/(E-D)
      GO TO 100
C
C     SOLUTION  F TH EEQUATION OF MOTION OF CONFIGURATION *3B*
C     BY INTEGRATING THE EQUATIONS OF MOTION NUMERICALLY
C
    5 N=6
      I3=5
      DO 205 J=7,12
  205 AY(J)=Y(J)
      DO 405 M2=1,4
      CALL FUN(T1,Y,F1,H,ZR,ZL,XY,DZR,DZL,DXY,S1,S2,S3,S4,OS,SK,K,
     1RR,RL,KH)
      F(12)=Y(11)
      F(11)=(-2*(CT+CC)*Y(11)-2*K*(Y(12)-(D*EPS/(E-D)))-(M+M1)*G
     1-(S1+S2)*FT+(CT+CC)*(DZR+DZL)+K*(ZR+ZL))/(M1+M)
```

```
      F(10)=Y(9)
      F(9)=(-M1*(C1+B1)*F(7)-KH*Y(10)-KH*(B1+C1-H)*Y(8)-KH*(C1-H)*
     1(EPS/(E-D))-S4*FT+KH*XY)/(M1+M)
      F(8)=Y(7)
      F(7)=(-M1*(C1+B1)*F(9)-2*F1*F1*(CT+CC)*Y(7)-2*K*F1*F1*Y(8)
     1-KH*(B1+C1-H)*Y(10)-KH*((B1+C1-H)**2)*Y(8)-2*K*F1*F1*((EPS/(E-D)))
     1-KH*(B1+C1-H)*(C1-H)*(EPS/(E-D))-(S1-S2)*FT*F1-2*S3*FC*F1-S4*FT*(B
     11+C1-H)+(CT+CC)*F1*(DZR-DZL)+K*F1*(ZR-ZL)+KH*XY*(B1+C1-H))/
     1(I+I1*M1*((C1+B1)**2))
      DO 375 J=7,12
  375 AK(M2,J)=F(J)*L
      IF(M2.EQ.4)GO TO 405
      IF(M2.NE.2)T1=T1+L/2
      IF(M2-3)255,265,255
  265 DO 185 J=7,12
  185 Y(J)=AY(J)+AK(M2,J)
      GO TO 405
  255 DO 4050 J=7,12
      Y(J)=AY(J)+AK(M2,J)/2
 4050 CONTINUE
  405 CONTINUE
      DO 505 J=7,12
  505 Y(J)=AY(J)+(AK(1,J)+2*AK(2,J)+2*AK(3,J)+AK(4,J))/6
      Y(6)=Y(12)-D*EPS/(E-D)
      Y(2)=Y(8)-EPS/(E-D)
      Y(4)=Y(10)+(B1+C1)*Y(8)-C1*EPS/(E-D)
      GO TO 100
C
C
C     SOLUTION  F TH EEQUATION OF MOTION OF CONFIGURATION *4A*
C     BY INTEGRATING THE EQUATIONS OF MOTION NUMERICALLY
C
C
    6 N=12
      I3=6
      D=21
      C1=11
      B1=65.7
      DO 206 J=1,N
  206 AY(J)=Y(J)
      DO 406 M2=1,4
      CALL FUN(T1,Y,F1,H,ZR,ZL,XY,DZR,DZL,DXY,S1,S2,S3,S4,DS,SK,K,
     1RR,RL,KH)
      F(12)=Y(11)
      F(11)=(M1*D*(F(7)-F(1))-2*(CT+CC)*Y(11)+2*CT*D*(Y(7)-Y(1))
     1-2*K*Y(12)+2*K*D*(Y(8)-Y(2))-(M1+M)*G-(S1+S2)*FT+(CC+CT)*(DZR+D
     1ZL)+K*(ZR+ZL)-2*K*EPS)/(M1+M)
      F(10)=Y(9)
      F(9)=(-M1*B1*F(7)-M1*C1*F(1)-KH*Y(10)-KH*B1*Y(8)
     1-KH*(C1-H)*Y(2)-S4*FT+KH*XY)/(M1+M)
      F(8)=Y(7)
      F(7)=((M1*D*D-M1*C1*B1)*F(1)+M1*D*F(11)-M1*B1*F(9)
     1+2*CT*D*Y(11)-2*CC*F1*F1*Y(7)-2*CT*D*D*Y(7)+2*CT*D*D*Y(1)+2*K
     1*Y(12)-2*K*D*D*(Y(8)-Y(2))-KH*B1*Y(10)
     1-KH*B1*B1*Y(8)-KH*(C1-H)*B1*Y(2)+M
     11*G*D+FT*D*(S1+S2)-2*S3*FC*F1-S4*FT*B1+(CC*F1-CT*D1*(DZR+DZL)
     1-K*D*(ZR+ZL)+KH*B1*XY+2*K*E*EPS)/(I+M1*(D*D+B1*B1))
```

```
      F(6)=Y(5)
      F(5)=F(11)-D*(F(7)-F(1))
      F(4)=Y(3)
      F(3)=F(9)+B1*F(7)+C1*F(1)
      F(2)=Y(1)
      F(1)=(M1*D*D*F(7)-M1*D*F(11)-M1*C1*B1*F(7)-M1*C1*F(9)
     1-2*CT*D*Y(11)+2*CT*D*D*Y(7)-2*CT*D*D*Y(1)-2*CT*F1*F1*Y(1)
     1-2*K*D*Y(12)+2*K*D*D*(Y(8)-Y(2))-2*K*E*EPS-2*K*F1*F1*Y(2)
     1-KH*(C1-H)*(Y(10)+B1*Y(8))-KH*(C1-H)*(C1-H)*Y(2)
     1-M1*G*D-(S1+S2)*FT*D-(S1-S2)*FT*F1-S4*FT*(C1-H)+CT*D*(DZR+DZL
     1)+CT*F1*(DZR-DZL)+K*D*(ZR+ZL)+K*F1*(ZR-ZL)+KH*(C1-B1)*XY
     1)/(I1+M1*(D*D+C1*C1))
      DO 306 J=1,N
  306 AK(M2,J)=F(J)*L
      IF(M2.EQ.4)GO TO 406
      IF(M2.NE.2) T1=T1+L/2
      IF(M2-3)256,266,256
  266 DO 186 J=1,N
  186 Y(J)=AY(J)+AK(M2,J)
      GO TO 406
  256 DO4060J=1,N
      Y(J)=AY(J)+AK(M2,J)/2
 4060 CONTINUE
  406 CONTINUE
      DO 506 J=1,N
  506 Y(J)=AY(J)+(AK(1,J)+2*AK(2,J)+2*AK(3,J)+AK(4,J))/6
      D=7
      C1=6.7
      B1=70
      GO TO 100
    7 N=12
C
C
C     SOLUTION, F TH EEQUATION OF MOTION OF CONFIGURATION *48*
C     BY INTEGRATING THE EQUATIONS OF MOTION NUMERICALLY
C
C
      I3=7
      B1=65.7
      C1=11
      D=21
      DO 207 J=1,N
  207 AY(J)=Y(J)
      DO 407 M2=1,4
      CALL FUN(T1,Y,F1,H,ZR,ZL,XY,DZR,DZL,DXY,S1,S2,S3,S4,DS,SK,K,
     1RR,RL,KH)
      F(12)=Y(11)
      F(12)=Y(11)
      F(11)=(M1*D*(F(1)-F(7))-2*(CT+CC)*Y(11)-2*CT*D*(Y(7)-Y(1))
     1-2*K*Y(12)-2*K*D*(Y(8)-Y(2))-(M1+M)*G-(S1+S2)*FT+(CC+CT)*(DZR+D
     1ZL)+K*(ZR+ZL))/(M1+M)
      F(10)=Y(9)
      F(9)=(-M1*B1*F(7)-M1*C1*F(1)-KH*Y(10)-KH*B1*Y(8)
     1-KH*(C1-H)*Y(2)-S4*FT+KH*XY)/(M1+M)
      F(8)=Y(7)
      F(7)=((M1*D*D-M1*C1*B1)*F(1)-M1*D*F(11)-M1*B1*F(9)
     1-2*CT*D*Y(11)-2*CC*F1*F1*Y(7)-2*CT*D*D*Y(7)+2*CT*D*D*Y(1)-2*K
```

```
     1*Y(12)-2*K*D*D*(Y(8)-Y(2))-KH*B1*Y(10)
     1-KH*B1*B1*Y(8)-KH*(C1-H)*B1*Y(2)-M
     11*G*D-FT*D*(S1+S2)-2*S3*FC*F1-S4*FT*B1+(CC*F1+CT*D)*(DZR+DZL)
     1+K*D*(ZR+ZL)+KH*B1*XY-2*K*E*EPS)/(I+M1*(D*D+B1*B1))
      F(2)=Y(1)
      F(1)=(M1*D*D*F(7)+M1*D*F(11)-M1*C1*B1*F(7)-M1*C1*F(9)
     1+2*K*D*Y(12)+2*K*D*D*(Y(8)-Y(2))+2*K*E*EPS-2*K*F1*F1*Y(2)
     1+2*CT*D*Y(11)+2*CT*D*D*Y(7)-2*CT*D*D*Y(1)-2*CT*F1*F1*Y(1)
     1-KH*(C1-H)*(Y(10)+B1*Y(8))-KH*(C1-H)*(C1-H)*Y(2)
     1+M1*G*D+(S1+S2)*FT*D-(S1-S2)*FT*F1-S4*FT*(C1-H)-CT*D*(DZR+DZL
     1)+CT*F1*(DZR-DZL)-K*D*(ZR+ZL)+K*F1*(ZR-ZL)+KH*(C1-B1)*XY
     1)/(I1+M1*(D*D+C1*C1))
      F(6)=Y(5)
      F(5)=F(11)-D*(F(7)-F(1))
      F(4)=Y(3)
      F(3)=F(9)+B1*F(7)+C1*F(1)
      DO 307 J=1,N
  307 AK(M2,J)=F(J)*L
      IF(M2.EQ.4)GO TO 407
      IF(M2.NE.2)T1=T1+L/2
      IF(M2-3)257,267,257
  267 DO 187 J=1,N
  187 Y(J)=AY(J)+AK(M2,J)
      GO TO 407
  257 DO4070J=1,N
      Y(J)=AY(J)+AK(M2,J)/2
 4070 CONTINUE
  407 CONTINUE
      DO 507 J=1,N
  507 Y(J)=AY(J)+(AK(1,J)+2*AK(2,J)+2*AK(3,J)+AK(4,J))/6
      D=7
      C1=6.7
      B1=70
      GO TO 100
  200 STOP
      END
```

```
      SUBROUTINE FUN(T1,Y,F1,H,ZR,ZL,XY,DZR,DZL,DXY,S1,S2,S3,S4,OS,SK,K,
     1RR,RL,KH)
C
C
C
C       THIS SUBROUTINE IS TO EVALUATE THE FORCING FUNCTIONS ACTING ON
C      THE MODEL IN THE FORM OF RECTIFIED SIN WAVE IT ALSO CHECKS FOR THE
C      GIB STOP AND THE FRICTION DAMPING FORCES
C      DIFFERENT VEHICLE NONLINEARITY EFFECTS LIKE THE WHEEL LIFT
C
C
C
      REAL K,KH
      DIMENSION Y(12),A(5)
      XKH=40000
      OS=3.9
      B1=70
      C1=6.7
C
C      GIB STOP EFFECT
C
      YGIB=Y(4)-2.7*Y(2)-XY
      IF(ABS(YGIB).LT..375)GO TO 2112
      KH=197000
      GO TO 2113
C
 2112 KH=XKH
C
C       FORCING FUNCTION EVALUATION
C
2113  ZR=.3183-.2121*(COS(OS*T1))-.04244*COS(2*OS*T1)-.01818*COS(3*OS*T1
     1)
      ZL=.3183+.2121*(COS(OS*T1))-.04244*COS(2*OS*T1)+.01818*COS(3*OS*T1
     1)
      DZR=.2121*OS*SIN(OS*T1)+.04244*2*OS*SIN(2*OS*T1)+
     1.01818*3*OS*SIN(3*OS*T1)
      DZL=-.2121*OS*SIN(OS*T1)+.04244*2*OS*SIN(2*OS*T1)-.01818*
     13*OS*SIN(3*OS*T1)
      XY=.00+.1*COS(OS*T1)*.5
      DXY=.1*OS*SIN(OS*T1)*.5*(-1)
      XY=2*XY
      DXY=2*DXY
      ZR=1.5*ZR
      ZL=1.5*ZL
      DZR=1.5*DZR
      DZL=1.5*DZL
C
C      WHEEL LIFT EFFECT
C
      IF(RR.LT.0.OR.RL.LT.0)GO TO 3737
      GO TO 5353
 3737 IF(RR.LT.0)GO TO 3355
      IF(RL.LT.0)GO TO 4466
 3355 ZR=0
      DZR=0
      GO TO 5353
 4466 ZL=0
```

```
      DZL=0
      GO TO 5353
C
C     SGN OF THE FRICTION DAMPING FORCES
C
 5353 IF(Y(5)+F1*Y(1)-DZR)301,302,303
  401 IF(Y(5)-F1*Y(1)-DZL)304,305,306
  402 IF(2*F1*Y(7)-DZR+DZL)310,311,312
  403 IF(Y(3)-H*Y(1)-DXY)307,308,309
  301 S1=-1
      GO TO 401
  302 S1=0
      GO TO 401
  303 S1=1
      GOTO 401
  304 S2=-1
      GO TO 402
  305 S2=0
      GO TO 402
  306 S2=1
      GO TO 402
  310 S3=-1
      GO TO 403
  311 S3=0
      GO TO 403
  312 S3=1
      GO TO 403
  307 S4=-1
      RETURN
  308 S4=0
      RETURN
  309 S4=1
      RETURN
      END
```

```
      SUBROUTINE PLOT (T1,Y,RMO,L2,L1,RR,RL,I3,JIXY,EPSI,L4,SOR,E1,E2,
     1RH,L3,L5)
C
C
C     SUBROUTINE TO PLOT THE CAR ROCKING RESPONSE
C
C
C
      REAL L4,L1,L2,L3,L5
      DIMENSION IY(120),Y(12)
      DATA IBLK,II,IFST/1H ,1HI,1H*/
      IF(JIXY.LT.80 )RETURN
      DO 1110 I=1,101
 1110 IY(I)=IBLK
      IY(8)=II
      IY(26)=II
      IY(45)=II
      IY(64)=II
      IY(65)=II
      IF(Y(8).GT..20)GO TO 1278
      JY=14+(Y(8)*10000+500)/45
      IY(JY)=IFST
      PRINT 1202 ,T1,(IY(K),K=1,45),Y(8)
 1202 FORMAT(7X,*I*,F10.3,45A1,3X,G14.7,4X,*I*)
      JIXY=0
 1278 RETURN
      END
```

BEFORE RESONANCE

TIME (SEC)	PLOT OF CAR ROCK ANGLE	CAR ROCK ANGLE (RAD)
.200	* I	-.2064241E-02
.400	* I	-.5460687E-02
.600	* I	-.3182022E-02
.800	*	.5750679E-02
1.000	I*	.1246360E-01
1.200	I*	.1068412E-01
1.400	* I	-.2265972E-02
1.600	* I	-.1512607E-01
1.800	* I	-.2044399E-01
2.000	* I	-.1059295E-01
2.200	*	.6698884E-02
2.400	I *	.1569699E-01
2.600	I *	.1420941E-01
2.800	*I	.1701068E-02
3.000	* I	-.6107023E-02
3.200	* I	.7526204E-02
3.400	*I	-.3969375E-03
3.600	*I	.1939021E-02
3.800	* I	-.1475783E-02
4.000	* I	-.6602443E-02
4.200	* I	-.6636832E-02
4.400	*I	-.4800175E-03
4.600	*	.7779755E-02
4.800	I*	.9898755E-02
5.000	*	.5840278E-02
5.200	* I	-.6614876E-02
5.400	* I	-.1174263E-01
5.600	* I	-.1347586E-01
5.800	* I	-.1242591E-02
6.000	I*	.1109388E-01
6.200	I*	.1250110E-01
6.400	*I	.3856697E-02
6.600	* I	-.8461267E-02
6.800	* I	-.1167846E-01
7.000	* I	-.7761136E-02
7.200	*	.5990002E-02
7.400	I*	.1134689E-01
7.600	I*	.9030572E-02
7.800	* I	-.3612667E-02
8.000	* I	-.1029038E-01
8.200	* I	-.9297874E-02
8.400	*I	-.1864640E-02
8.600	I*	.9054903E-02
8.800	*	.7413705E-02
9.000	* I	-.3008758E-02
9.200	* I	-.8261648E-02
9.400	* I	-.6555203E-02
9.600	*I	.3581472E-02
9.800	*	.8285148E-02
10.000	*	.7354657E-02
10.200	* I	-.2074406E-02
10.400	* I	-.8462462E-02
10.600	* I	-.8401967E-02
10.800	*I	.2903224E-03
11.000	*	.8385654E-02
11.200	I*	.9182257E-02
11.400	*I	.2371032E-02
11.600	* I	-.8036100E-02
11.800	* I	-.1001989E-01
12.000	* I	-.4653184E-02

AT RESONANCE

TIME (SEC)	PLOT OF CAR ROCK ANGLE	CAR ROCK ANGLE (RAD)
.200	*	-.2162784E-02
.400	*	-.6749163E-02
.600	*	-.6537427E-02
.800	*	.1338798E-02
1.000	*	.1392574E-01
1.200	*	.1977394E-01
1.400	*	.1478094E-01
1.600	*	-.2060071E-02
1.800	*	-.1726199E-01
2.000	*	-.2676801E-01
2.200	*	-.1929117E-01
2.400	*	-.1662860E-02
2.600	*	.1772333E-01
2.800	*	.2844053E-01
3.000	*	.2175731E-01
3.200	*	-.1345484E-02
3.400	*	-.2308850E-01
3.600	*	-.3347691E-01
3.800	*	-.2450355E-01
4.000	*	.5128061E-02
4.200	*	.3103552E-01
4.400	*	.4271833E-01
4.600	*	.2098257E-01
4.800	*	-.1413040E-01
5.000	*	-.4249003E-01
5.200	*	-.5538825E-01
5.400	*	-.3805768E-01
5.600	*	-.3589290E-03
5.800	*	.3476965E-01
6.000	*	.5647838E-01
6.200	*	.5215393E-01
6.400	*	.1802136E-01
6.600	*	-.2314834E-01
6.800	*	-.5278658E-01
7.000	*	-.5703942E-01
7.200	*	-.3398737E-01
7.400	*	.1102196E-01
7.600	*	.5151385E-01
7.800	*	.6788751E-01
8.000	*	.4415129E-01
8.200	*	-.9959426E-03
8.400	*	-.4226081E-01
8.600	*	-.6762236E-01
8.800	*	-.5283144E-01
9.000	*	-.1117674E-02
9.200	*	.4476010E-01
9.400	*	.7341405E-01
9.600	*	.5982125E-01
9.800	*	.1240397E-01
10.000	*	-.4010407E-01
10.200	*	-.6985634E-01
10.400	*	-.5411855E-01
10.600	*	-.6297022E-02
10.800	*	.4318582E-01
11.000	*	.7276183E-01
11.200	*	.6010853E-01
11.400	*	.1695017E-01
11.600	*	-.3224047E-01
11.800	*	-.6196225E-01
12.000	*	-.5030381E-01
12.200	*	-.9177469E-02
12.400	*	.3595558E-01
12.600	*	.6391833E-01
12.800	*	.6127503E-01
13.000	*	.3141252E-01

AFTER RESONANCE

TIME (SEC)	PLOT OF CAR ROCK ANGLE	CAR ROCK ANGLE (RAD)
.200	*	-.2133991E-02
.400	*	-.7435080E-02
.600	*	-.8380400E-02
.800	*	-.1640747E-02
1.000	*	.1191504E-01
1.200	*	.1947341E-01
1.400	*	.2185205E-01
1.600	*	.1178391E-01
1.800	*	-.6761217E-02
2.000	*	-.2017635E-01
2.200	*	-.2717208E-01
2.400	*	-.2097349E-01
2.600	*	-.2533622E-02
2.800	*	.1479993E-01
3.000	*	.2520775E-01
3.200	*	.2432410E-01
3.400	*	.1242914E-01
3.600	*	-.6372712E-02
3.800	*	-.1809137E-01
4.000	*	-.2451670E-01
4.200	*	-.2018993E-01
4.400	*	-.5761802E-02
4.600	*	.1091617E-01
4.800	*	.1985321E-01
5.000	*	.2225389E-01
5.200	*	.1565019E-01
5.400	*	.7908701E-03
5.600	*	-.1263696E-01
5.800	*	-.1895942E-01
6.000	*	-.1713119E-01
6.200	*	-.7641956E-02
6.400	*	.3567056E-02
6.600	*	.1174464E-01
6.800	*	.1322528E-01
7.000	*	.8961328E-02
7.200	*	.1150190E-02
7.400	*	-.5142659E-02
7.600	*	-.9642449E-02
7.800	*	-.8767551E-02
8.000	*	-.4116235E-02
8.200	*	.5090237E-04
8.400	*	.4773213E-02
8.600	*	.7988984E-02
8.800	*	.7145141E-02
9.000	*	.2655780E-02
9.200	*	-.1588060E-02
9.400	*	-.6192306E-02
9.600	*	-.8398260E-02
9.800	*	-.6028765E-02
10.000	*	-.1620912E-02
10.200	*	.2781560E-02
10.400	*	.7044623E-02
10.600	*	.8294444E-02
10.800	*	.4838027E-02
11.000	*	.5671182E-03
11.200	*	-.3993844E-02
11.400	*	-.7737948E-02
11.600	*	-.7917917E-02
11.800	*	-.3707239E-02
12.000	*	.4604612E-03

APPENDIX III

LISTING OF THE PROGRAM FOR THE SIMULATION SOLUTION

APPENDIX III

LISTING OF THE PROGRAM FOR THE SIMULATION SOLUTION

```
1.001    "RAILROAD FREIGHT VEHICLE MODEL";
1.004    1E003=+(2*K*ZWM)/(MW*ZWDM)/(10*TMSC)/10
1.020    "OFF LINE CHECK":
1.027    1E026=+(R1/IW)*(F9M/TM)
1.030    @NA, XMODE; NORMAL;
1.040    "ESTABLISH VARIABLES"11; 12; 13; 14;
1.050    "COMPUTE THEORETICAL VALUES"
1.060    21;
1.069    1C108=(H*KH*TTM)/(MT*YTDM)/TMSC/10
1.104    2C012=(2*F*TWDM/X3DM)/10
1.207    1E071=+ 01
2.010    "ON-LINE CHECK":
2.020    @WA, XMODE; NORMAL;
2.030    "SET UP CONSOLE"680, CONSOL ; 1, 2, USE; 1, CONSOLE;
2.040    "LIST?"$SSW? 0, CONSOL; 21; 1, CONSOL; HALT;
2.060    "SET POTS"@SP, MODE, 21; @PC, MODE;
2.070    "CHECK POTS" 00002, VERIFY; 21; "POT OK? "; HALT;
2.110    NORMAL; HALT;
3.048    X1DM=500, X2DM=500, X3DM=600, X4DM=400
11.010   "CONSTANTS OF THE PROBLEM"
11.020   MC=615, MT=5.12, MW=40, IC=1860000
11.030   IW=24000, IT=3400, C1=6.7, C2=11, B1=70, B2=65.7, B=65.5
11.040   OS=3.7, F=39.5, E=25
11.050   H=2.7, WB=28.5, D=7, KB=1320000, KP=1320000
11.060   KR=1320000, KL= 50000, G=384
11.070   R2=15, R1=11, KPL=050000, KL=550000
11.080   KP=2640000, KB=2640000, KG=2640000
11.090   KR=6000000
12.010   "PARAMETERS"
12.020   CC=100, FC=1000, CT=400, FT=8000
12.030   K=45200, KH=40000
12.200   CC=0, FC=0, CT=100, FT=8000
13.010   "SCALE FACTORS"
13.020   ZCDM=75, YCDM=150, TCDM=3.5
13.030   ZCM=10, YCM=20, TCM=.25
13.031   ZTDM=75, YTDM=150, TTDM=3 5
13.032   ZTM=10, YTM=20, TTM=.25
13.033   ZWDM=75, YWDM=150, TWDM=3.5
13.034   ZWM=10, YWM=20, TWM=.25
13.035   ZRM=.75, ZLM=.75, XRM=.075, XLM= 075
13.036   GM=384, S1M=1, S2M=1
13.037   S3M=1, S4M=1, F1M=5000000, XM=150000
13.038   F2M=5000000, F3M=5000000, F4M=5000000
13.039   F5M=350000, F6M=8000000, F7M=3000000
13.040   F8M=3000000, F9M=1500000, F10M=1500000
13.041   R1M=86, R2M=320, P1M=64000
13.042   P2M=20, T1M=60, T2M=3750, LM=10000000
13.043   HM=8000000, RM=406, QM=2000000
13.044   PM=65000, SM=150000, YM=75000
13.045   TM=3810, VM=1250, WM=25000
13.046   ZM=12000        , ZRRM=1, ZLLM=1, TMSC=100
13.048   X1DM=500, X2DM=500, X3DM=600, X4DM=400
13.049   Z1M=3.5, Z2M=3.5, Z3M=3.5, Z4M=3.5, Z5M=3.5
13.051   Z6M=3.0, Z7M=2.0, Z8M=2.0, Z9M=2., Z10M=2.
13.053   Z1M=1.75, Z2M=1.75, Z3M=1.75, Z4M=1.75, Z5M=3.5
13.054   Z7M=.50, Z8M=.5
14.010   "INITIAL CONDITIONS"
14.020   ZCD=75, ZTD=75, ZWD=75
14.021   ZC=-10, ZT=-10, ZW=-10
14.030   YCD=150, YTD=150, YWD=150
14.031   YC=-20, YT=-20, YW=-20
14.032   TCD=3.5, TTD=3.5, TWD=3.5
```

```
14.033      TC=-.25, TT=-.25, TW=-.25
14.034      ZRR=-1, ZLL=+1
21.001      "POT SETTINGS"
21.002      1E000=+(2*K*ZTM)/(MT*ZTDM)/(100*TMSC)/10
21.003      1E002=+((KH*H*H+2*K*F*F)*TTM)/(IT*TTDM)/(100*TMSC)/10
21.004      1E003=+(2*K*ZWM)/(MW*ZWDM)/(10*TMSC)/10
21.005      1E004=+(KH/MW)*(YWM/YWDM)/(10*TMSC)
21.006      1E005=+((2*K*F*F+KH*R2*R2)/IW)*(TWM/TWDM)/(10*TMSC),
21.007      1E006=+(R2*KH/MT)*(TWM/YTDM)/(10*TMSC)
21.008      1E007=+(IC/IT)*(R1M/PM)/10
21.009      1E008=+(C1/IT)*(HM/PM)/10
21.011      1E010=(1/MT)*(HM/YTDM)/(10*TMSC)*(+1)/10.5
21.012      1E011=+(2*CC*F*F/IC)*(TWDM/TCDM)/TMSC
21.013      1E012=+(2*CC/MC)/TMSC
21.014      1E013=+(D/IC)*(F2M/R1M)
21.015      1E014=(E/IC)*(F4M/R1M)/10
21.016      1E015=(2*FC*F/IC)*(S3M/TCDM)/TMSC
21.017      1E016=(G/ZCDM)/TMSC
21.018      1E017=+(FT/MT)*(S4M/YTDM)/TMSC/10
21.019      1E018=(FT*F/IT)*(S2M/PM)
21.020      1E019=+(FT*H/IT)*(S4M/PM)
21.021      1E020=+(FT/MW)*(S1M/XM)
21.022      1E021=+(FT/MW)*(S2M/XM)
21.023      1E022=+(1/MW)*(F9M/YM)
21.024      1E023=+(1/MW)*(F10M/YM)
21.025      1E024=+(FT*F/IW)*(S2M/T1M)
21.026      1E025=+(WB/IW)*(F8M/TM)/10
21.027      1E026=+(R1/IW)*(F9M/TM)
21.028      1E027=+(R2/IW)*(F10M/TM)
21.029      1E028=+(R2*KH/IW)*(YWM/VM)/10
21.030      1E029=+(2*K/MW)*(ZTM/WM)
21.031      1E030=+((KH*R2*H+2*K*F*F)/IT)*(TWM/ZM)
21.032      1E031=+(2*CT*F*F/IT)*(TWM /ZM)
21.033      1E032=+(KH*H/IT)*(YWM/ZM)
21.034      1E033=+(ZM/TTDM)/(100*TMSC)
21.035      1E034=+(F1M/LM)/10
21.036      1E035=+(F2M/LM)
21.037      1E036=+(F3M/LM)
21.038      1E037=+(F4M/LM)
21.039      1E038=+LM/(ZCDM*MC)/(10*TMSC)
21.040      1E039=+(QM/ZTDM)/(100*TMSC)/10
21.041      1E040=+(FT/MT)*(S1M/QM)
21.042      1E041=+(FT/MT)*(S2M/QM)
21.043      1E042=+(F5M/HM)
21.044      1E043=+(F6M/HM)
21.045      1E044=(1/MC)*(HM/YCDM)/TMSC
21.046      1E045=+(E/IC)*(F3M/R1M)
21.047      1E046=+(2*CT/MW)*(ZTDM/WM)
21.048      1E047=+(2*CC/MW)*(ZCDM/WM)
21.049      1E048=+(WM/ZWDM)/(10*TMSC)
21.050      1E049=+(1/MW)*(F7M/XM)
21.051      1E050=+(1/MW)*(F8M/XM)/10
21.052      1E051=+(XM/ZWDM)/(10*TMSC)/10
21.053      1E052=+(2*CC*F*F/IW)*(TCDM/VM)
21.054      1E053=+(2*CT*F*F/IW)*(TTDM/VM)
21.055      1E054=+(R2*KH/IW)*(YTM/VM)
21.056      1E055=+(VM/TWDM)/(10*TMSC)
21.057      1E056=+(FT*F/IW)*(S1M/T1M)/10
21.058      1E057=+(2*FC*F/IW)*(S3M/T1M)
21.059      1E058=+(FT*R2/IW)*(S4M/T1M)
21.060      1E059=+(T1M/TM)
21.061      1C100=(2*CT*F*F/IT)/(10*TMSC)/10
```

```
21.062      1C101=2*(CT+CC)/MW/TMSC/10
21.063      1C102=(KH*H/IT)*(YTM/TTDM)/(10*TMSC)/10
21.064      1C103=(KH*R2/MW)*(TWM/YWDM)/TMSC
21.065      1C104=((2*K*F*F+KH*R2*H)/IW)*(TTM/TWDM)/(10*TMSC)/10
21.066      1C105=((2*(CC+CT)*F*F)/IW)*(TWDM/TWDM)/TMSC/10
21.067      1C106=(TM/TWDM)/TMSC/100
21.068      1C107=(WB/IW)*(F7M/TM)/10
21.069      1C108=(H*KH*TTM)/(MT*YTDM)/TMSC/10
21.070      1C109=(YM/YWDM)/TMSC/10
21.071      1C110=(KH/MW)*(YTM/YWDM)/(10*TMSC)
21.072      1C111=(FT/MW)*(S4M/YM)
21.073      1C112=(FT*F/IT)*(S1M/PM)
21.074      1C113=(PM/TTDM)/(10*TMSC)/100
21.075      1C114=(KH/MT)*(YWM/YTDM)/(100*TMSC)
21.076      1C115=(2*CT/MT)*(ZWDM/ZTDM)/(10*TMSC)/10
21.077      1C116=(2*K/MT)*( ZWM/ZTDM)/(100*TMSC)/10
21.078      1C117=(1/MT)*(LM/QM)
21.079      1C118=(RM/TCDM )/(10*TMSC)
21.080      1C119=(R1M/RM)
21.093      2C000=(ZTDM/X1DM)
21.094      2C002=(TTDM*F/X1DM)/10
21.095      2C003=(ZWDM/X1DM)
21.096      2C004=(TWDM*F/X1DM)
21.097      2C005=(ZTDM/X2DM)
21.098      2C006=(TTDM*F/X2DM)/10
21.099      2C007=(ZWDM/X2DM)
21.100      2C008=(TWDM*F/X2DM)
21.101      2C009=(2*F*TCDM/X3DM)/10
21.104      2C012=(2*F*TWDM/X3DM)/10
21.105      2C013=(YTDM/X4DM)/10
21.106      2C014=(H*TTDM/X4DM)
21.107      2C015=(YWDM/X4DM)
21.108      2C016=(R2*TWDM/X4DM)
21.109      2C017=(ZC M/Z1M)/10
21.110      2C018=(D*TCM/Z1M)
21.111      2C019=(ZTM/Z1M)/10
21.112      2C020=(D*TTM/Z1M)
21.113      2C021=(ZCM/Z2M)/10
21.114      2C022=(D*TCM/Z2M)
21.115      2C023=(ZTM/Z2M)/10
21.116      2C024=(D*TTM/Z2M)
21.117      2C025=(KP/F1M)*Z1M
21.118      2C026=(KP/F2M)*Z2M
21.119      2C027=(KPL/F5M)*Z5M
21.120      2C028=(YCM/Z5M)/10
21.121      2C029=(B1*TCM/Z5M)/10
21.122      2C030=(YTM/Z5M)/10
21.123      2C031=(C1*TTM/Z5M)
21.124      2C032=(KR/F7M)*Z7M
21.125      2C033=(ZWM/Z7M)/100
21.126      2C034=(WB*TWM/Z7M)/100
21.127      2C035=(ZRM/Z7M)/100
21.128      2C036=(ZWM/Z8M)/100
21.129      2C037=(WB*TWM/Z8M)/100
21.130      2C038=(ZLM/Z8M)/100
21.131      2C039=(KR/F8M)*Z8M
21.132      2C040=(KL/F9M)*Z9M
21.133      2C041=(YWM/Z9M)/100
21.134      2C042=(TWM*R1/Z9M)/100
21.135      2C043=(XRM/Z9M)/10
21.136      2C044=(KL/F10M)*Z10M
21.137      2C045=(YWM/Z10M)/100
```

```
21. 138      2C046=(R1*TWM/Z10M)/100
21. 139      2C047=(XLM/Z10M)/10
21. 140      2C048=(ZCM/Z3M)/10
21. 141      2C049=(E*TCM/Z3M)/10
21. 142      2C050=(ZTM/Z3M)/10
21. 143      2C051=(E*TTM/Z3M)/100
21. 144      2C052=(ZCM/Z4M)/10
21. 145      2C053=(E*TCM/Z4M)/10
21. 147      2C055=(E*TTM/Z4M)/100
21. 148      2C056=(KB/F3M)*Z3M
21. 149      2C057=(KB/F4M)*Z4M
21. 150      2C058=(KG/F6M)*Z6M
21. 151      2C059=1
21. 152      2C060=1
21. 153      2C061=OS/TMSC
21. 154      2C062=OS/TMSC
21. 155      2C063=1
21. 157      2C065=(YCM/Z6M)/100
21. 158      2C066=(B2*TCM/Z6M)/100
21. 159      2C067=(YTM/Z6M)/100
21. 160      2C068=(C2*TTM/Z6M)/10
21. 161      2C069=1
21. 162      2C070=1
21. 163      2C071=. 0666
21. 164      2C072=. 0666
21. 165      2C073=. 069
21. 166      2C074=. 0666
21. 167      2C075=. 1
21. 168      2C076=. 0666
21. 169      2C077=. 0666
21. 170      2C078=. 069
21. 171      2C079=. 0666
21. 172      2C080=. 1
21. 173      2C100=. 0588
21. 174      2C101=. 0588
21. 175      2C102=. 065
21. 176      2C103=. 0588
21. 177      2C104=. 1
21. 200      1E060=+(KH*H/MW)*(TTM/YWDM)/TMSC
21. 202      1E001=+(KH/MT)*(YTM/YTDM)/(100*TMSC)
21. 206      1E070=(D/IC)*(F1M/R1M)*(+1)
21. 207      1E071=+. 01
21. 208      1E061=-. 3333
21. 209      1E062=-. 25
21. 210      1E063=-. 3333
21. 211      1E064=-. 25
21. 212      1E065=-. 2857
21. 213      1E066=-. 4
21. 214      1E067=-. 3333
21. 215      1E068=-. 25
21. 216      1E069=-. 2
21. 217      1E075=-. 55
21. 218      1E076=-. 2142
21. 219      1E077=-. 3
21. 220      1E078=-. 3333
21. 221      1E079=-. 25
21. 222      1E080=-. 0666
21. 223      1E081=-. 05
21. 224      1E082=-. 1428
21. 225      1E083=-. 2
21. 238      2C064=(B/IC)*(HM/RM)
21. 273      2C081=(FT*F/IT)*(S1M/PM)
```

APPENDIX IV

THE SYSTEM CONSTANTS OF A 100 TON FREIGHT CAR

APPENDIX IV

THE SYSTEM CONSTANTS OF A 100 TON FREIGHT CAR

In Chapter 6, the values of the mechanical parameters of a 100 ton railroad freight vehicle [19,20] were utilized to start the search for the optimum suspension elements. The values of these parameters are given in detail in the following table

b_1 = 70 in(177.8 cm)	h = 2.7 in(6.85 cm)	W_B = 28.25 in(71.75 cm)
b_2 = 65.7 in(166.8 cm)	K = 45200 lb/in (79100 N/cm)	M_c = 615 lb.sec^2/in (107625 kg)
C_1 = 6.7 in (17 cm)	K_h = 40000 lb/in (70000 N/cm)	M_t = 5.12 lb.sec^2/in (896 kg)
C_2 = 11 in (27.94 cm)	$K_p = K_b = K_G$ = 1320000 lb/in (2310 kN/cm)	M_w = 40 lb.sec^2/in (7000 kg)
C_c = 0	K_r = 2640000 lb/in (4620 kN/cm)	ε = 0.25 in(0.635 cm)
C_t = 200 lb.sec/in (350 N.sec/cm)	K_{rL} = 550000 lb/in (962.5 kN/cm)	Z_{cr} = 0.75 in(1.905 cm)
d = 7 in (17.78 cm)	I_c = 18.6x10^5 lb.in.sec^2 (2.1x10^5 kg.m^2)	
e = 25 in (63.5 cm)	I_t = 3400 lb.in.sec^2 (384.2 kg.m^2)	
f = 39.5 in(100.3 cm)	I_w = 24000 lb.in.sec^2 (2712 kg.m^2)	
F_c = 0	r_2 = 15 in(38.1 cm)	
F_t = 8000 lb (35584 N)		
r_1 = 11 in(27.94 cm)		

Table IV.1: The System Constants of a 100 Ton Freight Car.

APPENDIX V

PROOF OF $E[z_k\dot{y}_k] = 0$ AND EXPRESSIONS FOR $E[S_{ik}(\dot{y}_k, z_k)z_j]$ AND $E[S_{ik}(\dot{y}_k, z_k)\dot{y}_j]$

APPENDIX V

PROOF OF $E[z_k\dot{y}_k] = 0$ AND EXPRESSIONS FOR $E[S_{i_k}(\dot{y}_k,z_k)z_j]$ AND $E[S_{i_k}(\dot{y}_k,z_k)\dot{y}_j]$

In Chapter 7, expressions for $E[S_{i_k}(\dot{y}_k,z_k)\dot{y}_j]$ and $E[S_{i_k}(\dot{y}_k,z_k)z_j]$ were stated in Equation (7.10). In this appendix, these expressions are derived and also proved that the displacement z_k of the nonlinear element k is uncorrelated to the velocity $\dot{y}_k$ of the same nonlinear element is given. This proof was used in Equation (7.17) to separate the displacement dependent nonlinear forces from the velocity dependent nonlinear elements. The required proofs are achieved in the following manner.

Given three Gaussian random variablex, X_1, X_2 and X_3, an expression for $E[X_1 f(X_2,X_3)]$ can be given by [52]:

$$E[X_1 f(X_2,X_3)] = \frac{a_{21}a_{33} - a_{23}a_{31}}{a_{22}a_{33} - a_{23}a_{32}} E[X_2 f(X_2,X_3)] - \frac{a_{21}a_{32} - a_{31}a_{22}}{a_{22}a_{33} - a_{23}a_{32}} E[X_3 f(X_2,X_3)] \qquad (V.1)$$

where

$$a_{kj} = E[X_k X_j] \quad , \quad k,j = 1,2 \text{ and } 3$$

For the special case, when only two variables X_1 and X_2 are considered the above expression (V.1) simplifies to:

$$E[X_1 f(X_2)] = \frac{a_{21}}{a_{22}} E[X_2 f(X_2)] \qquad (V.2)$$

Substituting $X_1 = z_k$, $X_2 = y_k$, and $f(X_2) = \frac{d}{dt}(y_k)$ in Equation (V.2)

$$E[z_k \cdot \dot{y}_k] = \frac{E[y_k z_k]}{E[y_k^2]} E[y_k \dot{y}_k] \tag{V.3}$$

But

$$E[y_k \cdot \dot{y}_k] = 0$$

Then (V.3) gives:

$$E[z_k \dot{y}_k] = 0 \tag{V.4}$$

Expression (V.4) shows that the two Gaussian variables z_k and y_k are uncorrelated. This result was used before in Equation (7.17), (7.18) and (7.19).

Now consider the general case of (V.1).

Substituting $X_2 = \dot{y}_k$, $X_3 = z_k$, $f(X_2, X_3) = S_{ik}(\dot{y}_k, z_k)$, and using the result in (V.4)

$$E[X_1 \, S_{ik}(\dot{y}_k, z_k)] = \frac{a_{21}}{a_{22}} E[\dot{y}_k \, S_{ik}(\dot{y}_k, z_k)] + \frac{a_{31}}{a_{33}} E[z_k \, S_{ik}(\dot{y}_k, z_k)] \tag{V.5}$$

Substituting X_1 equal to z_j first and then repeating by setting X_1 equal to $\dot{y}_j$ in (V.5),

$$E[S_{ik}(\dot{y}_k, z_k) z_j] = E[S_{ik}(\dot{y}_k, z_k)\dot{y}_k] \cdot E[\dot{y}_k z_j]/E[\dot{y}_k^2] + E[S_{ik}(\dot{y}_k, z_k) z_k] \cdot E[z_k z_j]/E[z_k^2] \tag{V.6}$$

and

$$E[S_{ik}(\dot{y}_k, z_k)\dot{y}_j] = E[S_{ik}(\dot{y}_k, z_k)\dot{y}_k] \cdot E[\dot{y}_k \dot{y}_j]/E[\dot{y}_k^2] + E[S_{ik}(\dot{y}_k, z_k) z_k] \cdot E[z_k \dot{y}_k]/E[z_k^2] \tag{V.7}$$

The above expressions are needed for use in Equations (7.10).

APPENDIX VI

RELATIONS BETWEEN THE SYSTEM OF COORDINATES $\underset{\sim}{x}$, $\underset{\sim}{y}$ AND $\underset{\sim}{z}$

APPENDIX VI

RELATIONS BETWEEN THE SYSTEM OF COORDINATES $\underset{\sim}{X}$, $\underset{\sim}{y}$ AND $\underset{\sim}{z}$

In Chapter 7, the equations of motion of the single configuration model was given in the matrix form:

$$\underset{\sim}{M}\ddot{\underset{\sim}{X}} + \underset{\sim}{C}\dot{\underset{\sim}{X}} + \underset{\sim}{K}\underset{\sim}{X} + \underset{\sim}{g}_1(\underset{\sim}{y}) + \underset{\sim}{g}_2(\underset{\sim}{z}) = \underset{\sim}{F}_c \qquad \text{(VI.1)}$$

where the relation between the coordinate systems $\underset{\sim}{X}$, $\underset{\sim}{y}$ and $\underset{\sim}{z}$ employed was given by:

$$\underset{\sim}{y} = \underset{\sim}{A}^*\underset{\sim}{X} \quad \text{and} \quad \underset{\sim}{z} = \underset{\sim}{E}\underset{\sim}{X} - \underset{\sim}{b}(t)$$

In this appendix the values of the transformation matrices with constant coefficients $\underset{\sim}{A}^*$ and $\underset{\sim}{E}$ are given. Using the definition of $\underset{\sim}{y}$ in Equation (7.21), $\underset{\sim}{A}^*$ can be given as:

$$\underset{\sim}{A}^* = \begin{bmatrix} 1 & 0 & 0 & 0 & 0 & 0 & 0 & 0 & 0 \\ 0 & 1 & 0 & 0 & 0 & 0 & 0 & 0 & 0 \\ 0 & 0 & 2f & 0 & 0 & 0 & 0 & 0 & -2f \\ 0 & 0 & 0 & 1 & 0 & f & -1 & 0 & -f \\ 0 & 0 & 0 & 0 & 1 & -h & 0 & -1 & r_2 \\ 0 & 0 & 0 & 1 & 0 & -f & -1 & 0 & f \end{bmatrix}$$

and from the definition of $\underset{\sim}{Z}$ in Equation (7.24), $\underset{\sim}{E}$ can be given as:

$$\underset{\sim}{E} = \begin{bmatrix} 1 & 0 & -d & -1 & 0 & d & 0 & 0 & 0 \\ 1 & 0 & d & -1 & 0 & -d & 0 & 0 & 0 \\ 1 & 0 & -e & -1 & 0 & e & 0 & 0 & 0 \\ 1 & 0 & e & -1 & 0 & -e & 0 & 0 & 0 \\ 0 & 1 & b_1 & 0 & -1 & C_1 & 0 & 0 & 0 \\ 0 & 1 & b_2 & 0 & -1 & C_2 & 0 & 0 & 0 \\ 0 & 0 & 0 & 0 & 0 & 0 & 1 & 0 & W_B \\ 0 & 0 & 0 & 0 & 0 & 0 & 1 & 0 & -W_B \\ 0 & 0 & 0 & 0 & 0 & 0 & 0 & -1 & -r_1 \\ 0 & 0 & 0 & 0 & 0 & 0 & 0 & -1 & -r_1 \end{bmatrix}$$

and

$$\underset{\sim}{b}^T(t) = [0,0,0,0,0,0,Z_R,Z_L,-Y_R,-Y_L]$$

APPENDIX VII

EVALUATION OF THE MEAN RESPONSE VECTOR $\underset{\sim}{X}$

APPENDIX VII

EVALUATION OF THE MEAN RESPONSE VECTOR $\underset{\sim}{X}$

In Chapter 7, the equivalent linear stochastic system was described by Equation (7.2) to be in the form:

$$\underset{\sim}{M}\ddot{\underset{\sim}{X}} + (\underset{\sim}{C} + \gamma\underset{\sim}{A}^*)\dot{\underset{\sim}{X}} + (\underset{\sim}{K} + \eta\underset{\sim}{E})\underset{\sim}{X} = \eta\underset{\sim}{b}(t) + \underset{\sim}{F}_c \qquad \text{(VII.1)}$$

In this appendix, the gravitational forces vector with constant coefficient $\underset{\sim}{F}_c$ is used for evaluating the mean vector of the system response $\underset{\sim}{X}$. Thereafter, the effect of $\underset{\sim}{F}_c$ can be neglected while evaluating the instantaneous covariance matrix of the system $\underset{\sim}{P}$ as given in (7.43).

In order to evaluate the mean vector $\underset{\sim}{X}$ the frequency response function $\underset{\sim}{H}(\omega)$ should be described. For the linear system (VII.1), this function is given by the expression:

$$\underset{\sim}{H}(\omega) = (-\omega^2\underset{\sim}{M} + i\omega(\underset{\sim}{C} + \gamma\underset{\sim}{A}^*) + (\underset{\sim}{K} + \eta\underset{\sim}{E}))^{-1} \qquad \text{(VII.2)}$$

For such a linear system, the relation between the input-output mean vectors is given by:

$$\underset{\sim}{m}_x = \underset{\sim}{H}(0)\ \underset{\sim}{m}_f \qquad \text{(VII.3)}$$

where $\underset{\sim}{m}_f$ is the mean vector of the input forcing function. In Equation (VII.1), $\underset{\sim}{b}(t)$ is stationary Gaussian with zero mean and therefore the mean vector of the forcing function in this case is:

$$\underset{\sim}{m}_f = \underset{\sim}{F}_c \qquad \text{(VII.4)}$$

and $\underset{\sim}{H}(0)$ in Equation (VII.3) can be found by substituting $\omega = 0$ in

(VII.2). Then:

$$\underset{\sim}{H}(0) = (K + \eta E)^{-1} \qquad \text{(VII.5)}$$

Now, upon substituting (VII.4) and (VII.5) into (VII.3), the mean vector of the response $\underset{\sim}{X}$ becomes:

$$\underset{\sim}{m}_X = (\underset{\sim}{K} + \eta\underset{\sim}{\sim}E)^{-1}\ \underset{\sim}{F}_c \qquad \text{(VII.6)}$$

Relation (VII.6) describes the only contribution of the vector $\underset{\sim}{F}_c$ to the system response. This is to just shift the response by a constant from a zero mean. Using this result, the system Equation (VII.1) can now be simplified to the form:

$$\underset{\sim}{M}\ddot{\underset{\sim}{X}} + (\underset{\sim}{C} + \gamma\underset{\sim}{\sim}A^*)\dot{\underset{\sim}{X}} + (\underset{\sim}{K} + \eta\underset{\sim}{\sim}E)\underset{\sim}{X} = \eta\underset{\sim}{\sim}b(t) \qquad \text{(VII.7)}$$

The above equation can be used, as shown in Chapter V, to evaluate the instantaneous covariance matrix of the response process.

APPENDIX VIII

LISTING OF THE COMPUTER PROGRAM TO CALCULATE THE RESPONSE SPECTRAL DENSITY

APPENDIX VIII

LISTING OF THE COMPUTER PROGRAM TO CALCULATE THE RESPONSE SPECTRAL DENSITY

```
      PROGRAM MATH(INPUT,OUTPUT)
C
C
C     PROGRAM TO EVALUATE THE POWER SPECTRAL DENSITY RESPONSES OF THE NONLINEAR
C     MODEL OF A RAIL ROAD FREIGHT VEHICLE.THE SYSTEM IS SOLVED UTILIZING
C     THE STATISTICAL LINEARIZATION TECHNIQUE WHEN THE VEHICLE IS SUBJECTED
C     TO RECTIFIED WHITE NOISE EXCITATIOS FROM THE TRACK IRREGULARITIES.
C
C     THE PROGRAM USES THE FOLLOWING LIBRARY SUBROUTINES
C      1-VMULFF TO MULTIPLY MATRICES
C      2-GMTRA TO TRANSPOSE A MATRIX
C      3-LINV1F TO INVERSE A MATRIX
C      4-CBAL,COMHES,COMLR FROM EISPACK PACKAGE TO
C      FIND THE EIGENVALUES OF A GIVEN MATRIX
C
C
      REAL M(9,9),K(9,9),KH,KV,KP,KB,KPL,KBL,MT,MC,IC,IT,H,HS,KT(9,9)
      REAL IW,MW,KR,KL
      COMMON/BLOCK1/A,Q R,Z10,AR,AI,ZETA1,ZETA2,FA5,ZETA11,FA,FA2
      COMMON/BLOCK2/Q,FA4,BI,Q1
      DIMENSION A(27,27),B(27,03),C(9,9),F1(10,3)
      DIMENSION ETA(9,9),CTO(9,9),GAM(9,6),ET(9,10),O(3,3),Q(27,27)
      DIMENSION AS(6,9),SEGXN(27),GAMA(9,9),FA(27,27)
      DIMENSION AR(27,27),AI(27,27),WR(27),WI(27),FV1(27),IV1(27)
      DIMENSION ZETA1(27,27),ZETA2(27,27),SEGMAZ(27),AII(9,9)
      DIMENSION FA4(27,27),FA5(27,27),FA6(27, 3),FA7( 3,27)
      DIMENSIONBV(18,3),BF(9,3),AF(9,9),CF(3,9),OF(3,3),BVCF(9,9)
      DIMENSION ZETA11(27,27),BVOF(9,3),EXI(9,9)
      DIMENSION       E(10,9),AMC(9,9),AMK(9,9),AMF(9,3),BI(27,27)
      DIMENSION     XI( 6,6),FA2(27,27),SEGMAX(27),SEGMAY(27)
      DIMENSION  GMF12(6,6),ETF1(9,9),Q1(27,27)
      DIMENSION QR(27,27),Z10(27,27)
      DO 2 I=1,9
      DO 2J=1,9
      M(I,J)=0
      C(I,J)=0
      K(I,J)=0
      AII(I,J)=0.0
    2 CONTINUE
      DO 1805I=1,10
      DO 1805J=1,3
 1805 F1(I,J)=0
      DO 1806I=1,3
      DO 1806J=1,3
 1806 O(I,J)=0
      DO 1807I=1,9
      DO 1807J=1,10
 1807 ET(I,J)=0
      DO 1808 I=1,9
      DO 1808 J=1,6
 1808 GAM(I,J)=0
      DO 1809 I=1,6
      DO 1809 J=1,9
 1809 AS(I,J)=0
      DO 1905 I=1,10
      DO 1905 J=1,9
 1905 E(I,J)=0.
```

```
      DO 1906 I=1,9
      DO 1906 J=1,9
 1906 AF(I,J)=0
      DO 1907 I=1,9
      DO 1907 J=1,3
 1907 BF(I,J)=0
      DO 1908 I=1,3
      DO 1908 J=1,9
 1908 CF(I,J)=0
      DO 1909 I=1,27
      DO 1909 J=1,27
 1909 A(I,J)=0
      DO 1705 I=1,27
      DO 1705 J=1,3
 1705 B(I,J)=0
      PRINT3657
 3657 FORMAT(1H1,5X,*I*,6X,*FREQUENCY*,6X,*I*,6X,*CAR ROCK PSD*,6X,
     1*I*,2X,*CAR LATERAL DISP. PSD*,2X,*I*)
      PRINT1289
 1289 FORMAT(80X)
C
C     IDENTIFICATION OF THE SYSTEM PARAMETERS
C
      MC=615
      IC=1860000
      MT=5.12
      IT=3400
      F=39.5
      H=2.7
      MW=40
      Iw=24000
      H1=1
      WB=28.5
      R2=15
      R1=11
      D1=7
      E1=25
      B1=70
      B2=65.7
      C1=6.7
      C2=11
      HS=.00001
      KP=1320000
      KB=1320000
      KR=6000000
      KBL=1320000
      KPL=55000
      KL=550000
      V=22.5
      AXY=.0015*V
      AV=.0015*V
      ACR=.0015*V
      Z30=.25
      Z40=.25
      Z60=.375
      FT=8000
      FC=1000
```

```
      CT=300
      CC=100
      KV=45200
      KH=40000
      OMS=.134*V
      OMCR=.2513*V
      OMXY=.2513*V
      OMV =.2513*V
C
C     INITIAL GUESS OF THE MEAN SQUARE RESPONSES FROM THIS THE
C     INITIAL VALUES OF THE EQUEVALENT STIFFNESS AND DAMPING MATRICES
C     ETA AND GAMA ARE EVALUATED
C
      SEGMAX(1)=.26
      SEGMAX(2 )=1.73
      SEGMAX(3 )=.0000545
      SEGMAX(4 )=.26
      SEGMAX(5 )=.617
      SEGMAX(6 )=.0000519
      SEGMAX(7 )=.2589
      SEGMAX(8 )=.219
      SEGMAX(9 )=.00004966
      SEGMAX(10)=1.567
      SEGMAX(11)=3.702
      SEGMAX(12)=.0001347
      SEGMAX(13)=1.567
      SEGMAX(14)=1.089
      SEGMAX(15)=.000129
      SEGMAX(16)=1.5632
      SEGMAX(17)=.1957
      SEGMAX(18)=.0001244
      SEGMAX(19)=0
      SEGMAX(20)=0
      SEGMAX(21)=0
      I4=0.
      GO TO 1800
C
C     EVALUATION OF THE SYSTEM MATRICES
C
    3 I4=I4+1
      DO 31 J=1,27
      DO 31 I=1,27
      AI(I,J)=0
   31 CONTINUE
C
C     ELEMENTS OF THE VEHICLE STATE EQUATION
C
      M(1,1)=1/MC
      M(2,2)=1/MC
      M(3,3)=1/IC
      M(4,4)=1/MT
      M(5,5)=1/MT
      M(6,6)=1/IT
      M(7,7)=1/MW
      M(8,8)=1/MW
```

```
      M(9,9)=1/IW
      C(1,1)=2*CC
      C(3,3)=2*CC*F*F
      C(4,4)=2*CT
      C(6,6)=2*CT*F*F
      C(1,7)=-2*CC
      C(3,9)=-2*CC*F*F
      C(4,4)=2*CT
      C(4,7)=-2*CT
      C(6,9)=-2*CT*F*F
      C(7,1)=-2*CC
      C(7,4)=-2*CT
      C(7,7)=2*(CC+CT)
      C(9,3)=-2*CC*F*F
      C(9,6)=-2*CT*F*F
      C(9,9)=2*(CT+CC)*F*F
      K(4,4)=2*KV
      K(5,5)=KH
      K(5,6)=-H*KH
      K(6,5)=-H*KH
      K(6,6)=2*KV*F*F+KH*H*H
      K(4,7)=-2*KV
      K(5,8)=-KH
      K(5,9)=R2*KH
      K(6,8)=KH*H
      K(6,9)=-2*KV*F*F-KH*R2*H
      K(7,4)=-2*KV
      K(7,7)=2*KV
      K(8,5)=-KH
      K(8,6)=KH*H
      K(8,8)=KH
      K(8,9)=-KH*R2
      K(9,5)=R2*KH
      K(9,6)=K(6,9)
      K(9,8)=K(8,9)
      K(9,9)=2*KV*F*F+KH*R2*R2
C
C     ELEMENTS OF THE TRANSFORMATION MATRICES WITH CONSTANT COEFFECIENTS
C
      AS(1,1)=1
      AS(2,2)=1
      AS(3,3)=2*F
      AS(4,4)=1
      AS(5,5)=1
      AS(6,6)=-F
      AS(4,6)=F
      AS(5,6)=-H
      AS(6,4)=1
      AS(3,9)=-2*F
      AS(4,9)=-F
      AS(4,7)=-1
      AS(5,8)=-1
      AS(5,9)=R2
      AS(6,7)=-1
      AS(6,9)=F
      E(1,1)=1
      E(1,3)=-01
```

```
      E(1,4)=-1
      E(1,6)=D1
      E(2,1)=1
      E(2,3)=D1
      E(2,4)=-1
      E(2,6)=-D1
      E(3,1)=1
      E(3,3)=-E1
      E(3,4)=-1
      E(3,6)=E1
      E(4,1)=1
      E(4,3)=E1
      E(4,4)=-1
      E(4,6)=-E1
      E(5,2)=1
      E(5,3)=B1
      E(5,5)=-1
      E(5,6)=C1
      E(6,2)=1
      E(6,3)=B2
      E(6,5)=-1
      E(6,6)=C2
      E(7,7)=1
      E(7,9)=WB
      E(8,7)=1
      E(8,9)=-WB
      E(9,8)=-1
      E(9,9)=-R1
      E(10,8)=-1
      E(10,9)=-R1
      F1(7,1)=1
      F1(7,2)=1
      F1(8,1)=-1
      F1(8,2)=1
      F1(9,3)=-1
      F1(10,3)=-1
C
C     ELEMENTS OF THE MATRICES OF THE FILTER STATE EQUATION
C
      BF(9,3)=1
      BF(6,2)=1
      BF(3,1)=1
      CF(3,8)=1
      CF(3,7)=OMXY
      CF(2,5)=1
      CF(2,4)=OMV
      CF(1,2)=1
      CF(1,1)=OMCR
      AF(9,9)=-2*H1*OMXY
      AF(6,6)=-2*H1*OMV
      AF(3,3)=-(2*H1*OMCR+OMS)
      AF(3,2)=-(OMCR*OMCR+2*H1*OMS*OMCR)
      AF(8,9)=1
      AF(9,8)=-OMXY*OMXY
      AF(9,7)=-OMXY*OMXY*OMS
      AF(7,8)=1
      AF(5,6)=1
```

```
      AF(6,5)=-OMV*OMV
      AF(6,4)=-OMV*OMV*OMS
      AF(4,5)=1
      AF(1,2)=1
      AF(2,3)=1
      AF(3,1)=-OMS*OMCR*OMCR
      DO 555 I=1,3
      DO 555 J=1,3
  555 DF(I,J)=0
C
C     USE OF THE EVALUATED MEAN SQUARE RESPONSES TO UPDATE  ETA,GAMA MATRICES
C
      CALL VMULFF(GAM,AS,9,6,9,9,6,GAMA,9,IER1)
      CALL VMULFF(ET,E,9,10,9,9,10,ETA,9,IER2)
      DO 4 I=1,9
      DO 4 J=1,9
      CTO(I,J)=C(I,J)+GAMA(I,J)
      KT(I,J)=K(I,J)+ETA(I,J)
    4 CONTINUE
C
C
C     SOLUTION OF THE OVERALL STATE  EQUATION OF THE
C     LINEARISED SYSTEM USING STATE VARIABLES TECHNIQUE.
C
C
      CALL VMULFF(M,CTO ,9,9,9,9,9,AMC,9,IER3)
      CALL VMULFF(M,KT  ,9,9,9,9,9, AMK,9,IER4)
      CALL VMULFF(ET,F1,9,10,3,9,10,ETF1,9,IER5)
      CALL VMULFF(M,ETF1,9,9,3,9,9,AMF,9,IER6)
      DO 313 I=1,9
      DO 313 J=1,3
      BV(I,J)=AMF(I,J)
  313 CONTINUE
      DO 778 I=1,27
      DO 778 J=1,27
  778 A(I,J)=0
      DO 6 I=1,9
      DO 6 J=1,9
      A(I,J)=-AMC(I,J)
      A(I,J+9)=-AMK(I,J)
      AI1(I,J)=0
      AI1(I,I)=1
      A(I+9,J)=AI1(I,J)
      A(I+18,J+18)=AF(I,J)
    6 CONTINUE
      CALL VMULFF(BV,CF,9,3,9,9,3,BVCF,9,IER105)
      DO 5 I=1,9
      DO 5 J=1,9
      A(I,J+18)=BVCF(I,J)
    5 CONTINUE
      CALL VMULFF(BV,DF,9,3,3,9,3,BVDF,9,IER106)
      DO 434 I=1,9
      DO 434 J=1,3
  434 B(I,J)=BVDF(I,J)
      DO 323 I=19,27
      DO 323 J=1,3
  323 B(I,J)=BF(I,J)
```

```
      D(1,1)=8*3.14*ACR*OMCR*OMCR
      D(2,2)=2*3.14*AV*OMV*OMV
      D(3,3)=2*3.14*AXY*OMXY*OMXY
      CALL GMTRA(A,FA,27,27)
      CALL VMULFF(FA,FA,27,27,27,27,27,FA2,27,IER7)
C
C
C     CALCULATION OF THE EIGENVALUES OF MATRIX FA
C
C
      NM=27
      N=27
      DO777 I=1,27
      DO777 J=1,27
      AR(I,J)=FA (I,J)
      AI(I,J)=0.0
  777 CONTINUE
      CALL CBAL(NM,N,AR,AI,IS1,IS2,FV1)
      CALL COMHES(NM,N,IS1,IS2,AR,AI,IV1)
      CALL COMLR(NM,N,IS1,IS2,AR,AI,WR,WI,IERR)
C
C
C     NUMERICAL TECHNIQUE TO SOLVE LIAPUNOV EQUATION
C
C
      DO 7 I=1,27
    7 BI(I,I)=1
      DO 8 I=1,27
      DO 8 J=1,27
      ZETA11(I,J)=
     1          BI(I,J)-(HS/2)*FA(I,J)+(HS*HS/12)*FA2(I,J)
      ZETA2(I,J)=BI(I,J)+(HS/2)*FA(I,J)+(HS*HS/12)*FA2(I,J)
    8 CONTINUE
      CALL LINV1F(ZETA11,27,27,ZETA1,0 ,IER30)
      CALL VMULFF(ZETA1,ZETA2,27,27,27,27,27,FA4,27,IER8)
      CALLGMTRA (B,FA7,27,3)
      EXI(3,3)=D(1,1)
      EXI(6,6)=D(2,2)
      EXI(9,9)=D(3,3)
C
C     EVALUATION OF THE MEAN SQUARE RESPONSES
C
      DO1005 I=1,27
      DO1005 J=1,27
 1005 Q(I,J)=0
      DO 1006 I=1,9
      DO 1006 J=1,9
 1006 QR(I+18,J+18)=EXI(I,J)
      IF(I4.GE. 2)GO TO 56
      DO 9 I=1,27
      DO 9 J=1,27
      Q(I,J)=QR(I,J)*HS
    9 CONTINUE
C
C     NEXT STEP IS TO EVALUATE THE INSTANTANEOUS COVARIANCE MATRIX
C     AND THE MEAN SQUARE RESPONSES OF VECTOR X
```

```
      CALL POWER
      DO 11 I=1,27
      SEGXN(I)=Q1(I,I)
   11 CONTINUE
      DO 18 I=1,27
      SEGMAX(I)=SEGXN(I)
   18 CONTINUE
C
C
C     CALCULATION OF THE MEAN SQUARE RESPONSE OF VECTORS Y1,Z1 FROM X
C
C
 1000 SEGMAY(1)=SEGMAX( 1)
      SEGMAY(2)=SEGMAX( 2)
      SEGMAY(3)=4*F*F*SEGMAX( 3)+4*F*F*SEGMAX( 9)
      SEGMAY(4)=SEGMAX( 4)+F*F*SEGMAX( 6)+SEGMAX( 7)+F*F*SEGMAX( 9)
      SEGMAY(5)=SEGMAX( 5)+H*H*SEGMAX( 6)+SEGMAX( 8)+R2*R2*SEGMAX( 9)
      SEGMAY(6)=SEGMAY(4)
      GAM(3,3)=SQRT(2/3.14)*2*FC*F/SQRT(SEGMAY(3))
      GAM(6,4)=SQRT(2/3.14)*F1*F/SQRT(SEGMAY(4))
      GAM(4,4)=SQRT(2/3.14)*FT   /SQRT(SEGMAY(4))
      GAM(6,5)=-SQRT(2/3.14)*FT*H /SQRT(SEGMAY(5))
      GAM(4,6)=+SQRT(2/3.14)*FT   /SQRT(SEGMAY(6))
      GAM(6,6)=-SQRT(2/3.14)*FT*F /SQRT(SEGMAY(6))
      GAM(5,5)=+SQRT(2/3.14)*FT   /SQRT(SEGMAY(5))
      GAM(7,6)=-GAM(4,6)
      GAM(8,5)=-GAM(5,5)
      GAM(7,4)=-GAM(4,4)
      GAM(9,3)=-GAM(3,3)
      GAM(9,4)=-GAM(6,4)
      GAM(9,5)=GAM(6,5)*(R2/H)
      GAM(9,6)=-GAM(6,6)
      SEGMAZ(1)=SEGMAX(10)+D1*D1*SEGMAX(12)+SEGMAX(13)+
     1D1*D1*SEGMAX(15)
      SEGMAZ(2)=SEGMAZ(1)
      SEGMAZ(3)=SEGMAX(10)+E1*E1*SEGMAX(12)+SEGMAX(13)+
     1E1*E1*SEGMAX(15)
      SEGMAZ(4)=SEGMAZ(3)
      SEGMAZ(5)=SEGMAX(11)+B1*B1*SEGMAX(12)+SEGMAX(14)+C1*C1*SEGMAX(15)
      SEGMAZ(6)=SEGMAX(11)+B2*B2*SEGMAX(12)+SEGMAX(14)+C2*C2*SEGMAX(15)
      SEGMAZ(7)=SEGMAX(16)+WB*WB*SEGMAX(18)
     1+.25*(OMCR*OMCR*SEGMAX(19)+SEGMAX(20)+OMV*OMV*SEGMAX(22)
     1+SEGMAX(23))
      SEGMAZ(8)=SEGMAZ(7)
      SEGMAZ(9)=SEGMAX(17)+R1*R1*SEGMAX(18)+(OMXY*OMXY*SEGMAX(25
     1)+SEGMAX(26))
      SEGMAZ(10)=SEGMAZ(9)
      CALL NAWAL(SEGMAZ,Z30,Z40,Z60,XI)
      ET(1,2)=KP/2
      ET(1,1)=ET(1,2)
      ET(3,1)=-KP*D1/2
      ET(3,2)=-ET(3,1)
      ET(1,4)=(KB/2)+XI(1,3)
      ET(1,3)=ET(1,4)
      ET(3,3)=-(KB*E1/2)+XI(3,3)
      ET(3,4)=(KB*E1/2)+XI(3,3)
      ET(3,5)=KPL*B1/2
```

```
      ET(3,6)=KBL*B2+XI(3,6)*2
      ET(4,1)=-ET(1,1)
      ET(4,2)=-ET(1,2)
      ET(4,3)=-KB/2+XI(4,3)
      ET(4,4)=-KB/2+XI(4,4)
      ET(2,5)=KPL/2
      ET(5,5)=-ET(2,5)
      ET(2,6)=KBL+2*XI(2,6)
      ET(5,6)=-KBL+2*XI(5,6)
      ET(6,1)=-ET(3,1)
      ET(6,2)=-ET(3,2)
      ET(6,3)=(KB*E1/2)+XI(6,3)
      ET(6,4)=-(KB*E1/2)+XI(6,4)
      ET(6,5)=KPL*C1/2
      ET(6,6)=KBL*C2+XI(6,6)*2
      ET(7,7)=KR/2
      ET(7,8)=KR/2
      ET(8,9)=-KL/2
      ET(8,10)=-KL/2
      ET(9,7)=KR/2
      ET(9,8)=-KR/2
      ET(9,9)=-KL/2
      ET(9,10)=-KL/2
      GO TO 3
   56 H1=.05
      AF(9,9)=-2*H1*OMXY
      AF(6,6)=-2*H1*OMV
      AF(3,3)=-(2*H1*OMCR+OMS)
      AF(3,2)=-(OMCR*OMCR+2*H1*OMS*OMCR)
      DO 2256 I=1,9
      DO 2256 J=1,9
      A(I+18,J+18)=AF(I,J)
 2256 CONTINUE
C
C
C     THE NEXT STEP IS TO EVALUATE THE SPECTRAL DENSITY
C     OF THE EQUIVALENT LINEAR SYSTEM
C
C
      CALL ALIA
      END
```

```
      SUBROUTINE POWER
C
C
C     THIS SUBROUTINE IS TO EVALUATE THE INSTANTANEOUS COVARIANCE
C     MATRIX USING DAVISON METHOD
C
C
      COMMON/BLOCK2/Q,ZETA4,ZETA ,Q1
      DIMENSION Q(27,27),QN(27,27)   ,ZETA(27,27),ZETA1(27,27)
      DIMENSION    ZETA3(27,27),ZETA4(27,27),Q1(27,27),ZETA2(27,27)
      DIMENSION QQ(27,27),SZE(27,27)
      I3=0
      DO 5555 I=1,27
      DO 5555J=1,27
      SZE(I,J)=0
      QQ(I,J)=Q(I,J)
 5555 CONTINUE
      CALLVMULFF(ZETA,ZETA4,27,27,27,27,27,27,ZETA1,27,IER9)
      CALL GMTRA(ZETA1,ZETA2,27,27)
      CALLVMULFF(ZETA2,QQ,27,27,27,27,27,27,ZETA3,27,IER10)
      CALL VMULFF(ZETA3,ZETA1,27,27,27,27,27,27,ZETA2,27,IER11)
      DO 5566 I=1,27
      DO 5566 J=1,27
      QQ(I,J)=QQ(I,J)+ZETA2(I,J)
      Q(I,J)=QQ(I,J)
 5566 CONTINUE
   99 CALLVMULFF(ZETA4,ZETA4,27,27,27,27,27,27,ZETA1,27,IER9)
      CALL GMTRA(ZETA1,ZETA2,27,27)
      CALLVMULFF(ZETA2,Q ,27,27,27,27,27,27,ZETA3,27,IER10)
      CALL VMULFF(ZETA3,ZETA1,27,27,27,27,27,27,ZETA2,27,IER11)
      DO 100 I=1,27
      DO 100 J=1,27
      QN(I,J)=ZETA2(I,J)+Q(I,J)
  100 CONTINUE
      IF(I3.GT.20)GO TO 1100
      DO 300 I=1,27
      DO 300 J=1,27
      ZETA4(I,J)=ZETA1(I,J)
  300 Q(I,J)=QN(I,J)
      I3=I3+1
      GO TO 99
 1100 DO 400 I=1,27
      DO 400 J=1,27
  400 Q1(I,J)=QN(I,J)
      RETURN
      END
```

```
      SUBROUTINE NAWAL(SEGMAZ,Z30,Z40,Z60,XI)
C
C     THIS SUBROUTINE IS TO EVALUATE THE ERROR FUNCTION
C     USING SERIES APROXIMATION
C
      DIMENSION SEGMAZ(27),XI( 6, 6),XJ(6,6)
      E1=25
      B2=65.5
      C2=11
      KB=1320000
      KBL=1320000
      IF(Z30/SQRT(SEGMAZ(3)).LT.1)GO TO 9000
      XJ(1,3)=SQRT(SEGMAZ(3))*1.2533*(1-.797*(SQRT(SEGMAZ(3))*EXP(-Z30*
     1Z30/
     12*SEGMAZ(3))/Z30)*(1-SEGMAZ(3)/(Z30*Z30)))
      GO TO 6000
 9000 XJ(1,3)=SQRT(SEGMAZ(3))
     1                *((Z30/SQRT(SEGMAZ(3)))-(1/6)*((Z30/SQRT(
     1SEGMAZ(3)))**3)+(1/40)*((Z30/SQRT(SEGMAZ(3)))**5))
 6000 IF(Z60/SQRT(SEGMAZ(6)).LT.1)GO TO 4000
      XJ(2,6)=SQRT(SEGMAZ(6))*1.2533*(1-.797*(SQRT(SEGMAZ(6))*EXP(-Z60*
     1Z60/
     12*SEGMAZ(6))/Z60)*(1-SEGMAZ(6)/(Z60*Z60)))
      GO TO 6600
 4000 XJ(2,6)=SQRT(SEGMAZ(6))
     1                *((Z60/SQRT(SEGMAZ(6)))-(1/6)*((Z60/SQRT(
     1SEGMAZ(6)))**3)+(1/40)*((Z60/SQRT(SEGMAZ(6)))**5))
 6600 XI(1,4)=KB*XJ(1,3)/2
      XI(2,6)=KBL*XJ(2,6)/2
      XI(1,3)=XI(1,4)
      XI(3,3)=-XI(1,3)*E1
      XI(3,4)=-XI(3,3)
      XI(4,3)=-XI(1,3)
      XI(4,4)=-XI(1,4)
      XI(6,3)=-XI(3,3)
      XI(6,4)=-XI(4,4)
      XI(3,6)=XI(2,6)*B2
      XI(5,6)=-XI(2,6)
      XI(6,6)=XI(2,6)*C2
      RETURN
      END
```

```
      SUBROUTINE ALIA
C
C     THIS SUBROUTINE EVALUATES THE SPECTRAL DENSITY OF THE LINEARIZED SYSTEM
C
      COMMON/BLOCK1/A,R,Y1,XR3,X34,Z6,YR3,Y34,XQ3,XQ4,Z4
      COMMON/BLOCK2/YQ3,YQ4,Y2,Y3
      DIMENSION XR3(27,27),X34(27,27),Z6(27,27),YR3(27,27),Y34(27,27)
      DIMENSION XQ3(27,27),XQ4(27,27),Z4(27,27),YQ3(27,27),YQ4(27,27)
      DIMENSION A(27,27),R(27,27),Y1(27,27),Y2(27,27),Y3(27,27),B(27,27)
      DIMENSION X1(27,27),X2(27,27),Y11(27,27),Y12(27,27),Y13(27,27)
      DIMENSION Y24(27,27),Y23(27,27),Y66(27,27),Y4(27,27)
      DIMENSION Y33(27,27),Y14(27,27),X3(27,27),          Y22(27,27)
      DIMENSION X4(27,27),Y28(27,27)
      OS=1
    3 DO 7778 I=1,27
      DO 7778 J=1,27
      B(I,J)=0.
      B(I,I)=1.
      Y1(I,J)=OS*B(I,J)
      Y2(I,J)=-Y1(I,J)
      X1(I,J)=-A(I,J)
 7778 CONTINUE
      CALL GMTRA(X1,X2,27,27)
      CALL LINV1F(Y1,27,27,Y11,00,IER100)
      CALL VMULFF(X1,Y11,27,27,27,27,27,Y12,27,IER101)
      CALL VMULFF(Y12,X1,27,27,27,27,27,Y13,27,IER101)
      DO 778 I=1,27
      DO 778 J=1,27
      Y33(I,J)=-Y1(I,J)-Y13(I,J)
  778 CONTINUE
      CALL LINV1F(Y33,27,27,Y3,00,IER103)
      CALL VMULFF(Y11,X1,27,27,27,27,27,Y14,27,IER104)
      CALL VMULFF(Y14,Y3,27,27,27,27,27,X3,27,IER105)
      DO 668 I=1,27
      DO 668 J=1,27
      X3(I,J)=-X3(I,J)
  668 CONTINUE
      CALL LINV1F(Y2,27,27,Y22,00,IER106)
      CALLVMULFF(X2,Y22,27,27,27,27,27,Y24,27,IER107)
      CALLVMULFF(Y24,X2,27,27,27,27,27,Y23,27,IER107)
      DO 558 I=1,27
      DO 558 J=1,27
      Y66(I,J)=-Y2(I,J)-Y23(I,J)
  558 CONTINUE
      CALL LINV1F(Y66,27,27,Y4,00,IER109)
      CALL VMULFF(Y22,X2,27,27,27,27,27,Y28,27,IER110)
      CALL VMULFF(Y28,Y4,27,27,27,27,27,X4 ,27,IER110)
      DO 448 I=1,27
      DO 448 J=1,27
      X4(I,J)=-X4(I,J)
  448 CONTINUE
      CALL VMULFF(X3 ,R,27,27,27,27,27,XR3,27,IER80)
      CALLVMULFF(XR3,X4,27,27,27,27,27,X34,27,IER80)
      CALLVMULFF(Y3,  R,27,27,27,27,27,YR3,27,IER80)
      CALLVMULFF(YR3,Y4,27,27,27,27,27,Y34,27,IER80)
      CALL VMULFF(Y3 ,R,27,27,27,27,27,XQ3,27,IER80)
      CALLVMULFF(XQ3,X4,27,27,27,27,27,XQ4,27,IER80)
```

```
      CALL VMULFF(X3,   R,27,27,27,27,27,Y03,27,IER80)
      CALL VMULFF(Y03,Y4,27,27,27,27,27,Y04,27,IER80)
      DO 1550 I=1,27
      DO 1550 J=1,27
      Z6(I,J)=X34(I,J)-Y34(I,J)
      Z4(I,J)=Y04(I,J)+X04(I,J)
 1550 CONTINUE
      PRINT 7563,OS,Z6(12,12),Z6(11,11)
 7563 FORMAT(10X,G15.7,7X,G15.7,10X,G15.7)
      IF(OS.GT.9)GO TO 8
      OS=OS+.2
      GO TO 3
    8 RETURN
      END
```